Application of a Donor-Acceptor Strategy to Intercept Molecular Main Group Element Precursors en Route to Nanodimensional Materials

by

Anindya K. Swarnakar

A thesis submitted in partial fulfilment of the requirement for the degree of

Doctor of Philosophy

Department of Chemistry
University of Alberta

Abstract

The work in this thesis describes the stabilization of reactive and elusive main group entities with the aid of Wittig reagents, transition metal complexes, or *N*-heterocyclic carbenes (NHCs) as donors. Wittig reagents were employed to stabilize various group 14 element dihydrides (EH_2; E = Ge and Sn) within donor-acceptor complexes. Furthermore, traditional hot injection or microwave assisted heating of a GeH_2 donor-acceptor complex yielded surface functionalized Ge nanoparticles. Donor-acceptor complexes of unsaturated mixed group 13/15 hydrides (HB=NH) were also synthesized via Lewis acid-assisted N_2 elimination followed by H^- migration from B to N within carbene-bound azidoborane precursors. The reactivity of such HB=NH complexes was studied in detail including attempts to convert these species into bulk BN. Parallel chemistry with Ga was explored in an attempt to prepare a donor-acceptor complex of HGa=NH; however the high reactivity of the Ga-H bonds in the precursor azidogallane complex NHC•GaH_2N_3 did not permit the isolation of such species. In addition, donor-acceptor complexes of chlorooxoborane (ClBO) featuring very short B=O bonds have been synthesized. These species are found to be active reagents for alkane C-F bond activation and functionalization.

Preface

A portion of the work presented in this thesis has been done in collaboration with the other researchers within the Department of Chemistry, University of Alberta. Crystallographic studies for all the compounds presented in this thesis were performed by Dr. R. McDonald and Dr. M. J. Ferguson including mounting of crystals, operation of the diffractometer, refinement of the structures and preparation of the crystallographic data tables. Elemental analyses and mass spectrometric analyses were performed by Analytical Instrument Laboratory and Mass Spectrometry Laboratory at the Department of Chemistry, University of Alberta. The $^{2}H\{^{1}H\}$, ^{15}N, ^{119}Sn NMR spectra were taken with the help of M. Miskolzie and N. Dabral at the NMR Spectrometry Laboratory, University of Alberta.

In Chapter 2: The chemistry of N- and P-donor ligands (4-dimethylaminopyridine and tricyclohexylphosphine) toward $GeCl_2$ center were studied in collaboration with Sean M. McDonald and Kelsey C. Deutsch. The synthesis and characterization of germanium nanoparticles were performed in collaboration with Dr. Tapas K. Purkait and Prof. Jonathan G. C. Veinot at the Department of Chemistry, University of Alberta. Moreover, the photoluminescence lifetime study of the germanium nanoparticles was accomplished in collaboration with Glenda B. De Los Reyes and Prof. Frank A. Hegmann at the Department of Physics, University of Alberta.

In Chapter 4: The computation calculations were performed in collaboration with Dr. Christian Hering-Junghans.

According to the policy of our research group, each chapter of this thesis is essentially self-contained, and prepared in the form of a paper that is intended for publication in peer-reviewed journals.

A portion of this thesis is previously published and the publications are listed below.

Chapter 2:

1. Swarnakar, A. K.; McDonald, S. M.; Deutsch, K. C.; Choi, P.; Ferguson, M. J.; McDonald, R.; Rivard, E. *Inorg. Chem*. **2014**, *53*, 8662.
2. Purkait, T. K.; Swarnakar, A. K.; De Los Reyes, G. B.; Hegmann, F. A.; Rivard, E.; Veinot, J. G. C. *Nanoscale* **2015**, *7*, 2241.

Chapter 3:

Swarnakar, A. K.; Ferguson, M. J.; McDonald, R.; Rivard, E. *Dalton Trans*. **2016**, *45*, 6071.

Chapter 4:

1. Swarnakar, A. K.; Hering-Junghans, C.; Nagata, K.; Ferguson, M. J.; McDonald, R.; Tokitoh, N.; Rivard, E. *Angew. Chem. Int. Ed.* **2015**, *54*, 10666.
2. Swarnakar, A. K.; Hering-Junghans, C.; Ferguson, M. J.; McDonald, R.; Rivard, E. *Chem. Sci*. **2017**, *8,* 2337.

Chapter 5:

Swarnakar, A. K.; Ferguson, M. J.; McDonald, R.; Rivard, E. *Dalton Trans*. **2017**, *46*, 1406.

Dedicated to my Parents

Sri Ananta K. Swarnakar and Smt. Rina Swarnakar

"The world is ready to give up its secrets if we only know how to knock, how to give it the necessary blow. The strength and force of the blow come through concentration."

–Swami Vivekananda (1863-1902)

Acknowledgement

First and foremost, I would like to express my sincere gratitude to my supervisor, Prof. Eric Rivard for his continuous support and motivation through out my PhD. He always encouraged me to work independently and creatively by giving me the complete freedom while providing constructive feedback and guidance whenever needed. In addition to this, his constant encouragement and immense patience have played a key role in improving my thinking and writing ability and successful accomplishment of this thesis. Lastly, your advice on both research as well as on my career have been invaluable and I could not have imagined having a better advisor and mentor for my PhD study.

Beside my advisor, I also like to thank my supervisory committee members, Prof. Doug Stephan, Prof. Steven Bergens, Prof. Rylan Lundgren, Prof. Jeffrey Stryker, and Prof. Todd Lowary for their valuable time spent in evaluating my thesis work and providing constructive comments and insightful feedback.

I am also thankful to the fellow Rivard group members (past and present) specially, Gang He, Ibrahim Al-Rafia, Chrissy Braun, Matt Roy, Sarah Parke, Melanie Lui, Christian Hering-Junghans, Mike Boone, Paul Lummis, Emanuel Hupf, Bruno Luppi, Jocelyn Sinclair, Ian Watson, William T. Delgado, Alyona Shynkaruk, Kate Powers, Koichi Nagata, Fatemeh Shahin, Nathan Paisley, Patricia Andreiuk, Devon Schatz, Derek Zomerman, Paul Choi and all other Rivard group members I met during my PhD for the productive discussions and cheerful lab environments. I could have not completed this long journey without the help of Dr. Bob McDonald, Dr. Mike Ferguson, Dr. Wayne Moffat, Jennifer Jones, Mark Miskolzie, Nupur

Dabral, Jing Zheng, Anita Weiler, Ryan Lewis and machine shop of chemistry department (University of Alberta).

I gratefully indebted for the funding I received from ATUMS (CREATE fellowship), Collaborative Research Fund and graduate fellowship of Department of Chemistry, University of Alberta to conduct my PhD research.

Finally, I would like to thank my family and friends for their emotional support. First, I appreciate the love and affection I received from my parents and my brothers (Sudipta Swarnakar and Adwaitya Swarnakar). I am beholden to them for their unfailing support and continuous encouragement throughout my life. I would also like to convey my gratitude to Tapas Purkait and his family for their enormous help and support during my stay in Canada.

Last but not the least, I would like to take an opportunity to express my appreciation to all my friends specially, Supriya Ghosh, Bitan Banerjee, Bijaya Dey, Santa Rabina, Achinta Bera, Koyel Paul, Vivek Gandhi, Subir Goswami, Manas Sajjan, Arpan Dandapat, Subrata Biswas, Sandip Kar, Shrawan Kumar, Urmibhusan Bhakta, Raja Mukherjee, Abhoy Karmakar, Narasimha Thota, Prasnata Das, and all the group members of Amader Chemophore and Amader Rannaghar for the moral support and joyous time spent.

Table of Contents

Chapter 3: Transition Metal-Mediated Donor-Acceptor Coordination of Low Valent Group 14 Element Halides

Chapter 4: Stabilization of Inorganic Acetylene, HBNH, Using Flanking Coordinative Interactions and Attempts to Isolate Molecular BN

Chapter 5: Azido- and Amido-substituted Gallium Hydrides Supported by *N*-Heterocyclic Carbenes

Chapter 6: Isolable Oxoborane (RBO) Complexes and their Role in Mediating C-F Bond Activation

List of Figures

List of Schemes

List of Tables

List of Symbols and Abbreviations

Å	Angstrom
Ar	Aryl
Ar^F	3,5-$C_6H_3(CF_3)_2$
avg.	Average
Bbt	2,6-$\{CH(SiMe_3)_2\}_2$-4-$\{C(SiMe_3)_3\}C_6H_2$
br	Broad
Bu_2O	Dibutyl ether
c.a.	Approximately
CAAC	Cyclic(alkyl)(amino)carbene
C_6D_6	Benzene-d_6
$CDCl_3$	Chloroform-d
Cp	Cyclopentadienyl
Cp*	Pentamethylcyclopentadienyl
COD	1,5-Cyclooctadiene
CD_2Cl_2	Dichloromethane-d_2
Cy	Cyclohexyl
d	Doublet
°C	Degree centigrade
δ	Delta (partial charge or chemical shift)
DFT	Density functional theory
diox	dioxane

Dipp	2,6-$^{i}Pr_2C_6H_3$
Dipt	2,6-(2-$^{i}PrC_6H_4)_2C_6H_3$
dppe	1,2-bis(diphenylphosphino)ethane or $Ph_2PCH_2CH_2PPh_2$
EDX	Energy dispersive X-ray analysis
η	Eta (number of atoms of a ligand that coordinate)
Et_2O	Diethyl ether
eV	Electron volt
FTIR	Fourier transform infrared spectroscopy
g	Gram
GeNPs	Germanium nanoparticles
HOMO	Highest occupied molecular orbital
Hz	Hertz
IMes	$(HCNMes)_2C$:
IMe_4	$(MeCNMe)_2C$:
$ImMe_2{}^{i}Pr_2$	$(MeCN^{i}Pr)_2C$:
IPr	$(HCNDipp)_2C$:
^{i}Pr	Isopropyl
$I^{t}Bu$	$(HCN^{t}Bu)_2C$:
K	Kelvin
Kcal	Kilocalorie
$\lambda_{em.}$	Excitation wavelength
$\lambda_{ex.}$	Emission wavelength
LUMO	Lowest unoccupied molecular orbital

Me	Methyl
Mes	Mesityl or 2,4,6-$Me_3C_6H_3$
mg	Milligram
MHz	Megahertz
mL	Milliliter
mmol	Millimole
Mp	Melting point
μ	Mu
^{n}Bu	n-Butyl
NBO	Natural bonding orbital
NHC	*N*-heterocyclic carbene
NHO	*N*-heterocyclic olefin
$^{n}J_{AB}$	n bond coupling constant between A and B
NMR	Nuclear magnetic resonance
NPA	Natural population analysis
ν	Nu (wave number)
OTf	Trifluoromethanesulfonate or triflate
Ph	Phenyl
PhF	Fluorobenzene
PL	Photoluminescence
ppm	Parts per million
π	Pi
ρ	Rho (density)

s	Singlet
^{s}Bu	sec-Butyl
SEM	Scanning electron microscopy
σ	Sigma
SIMes	$(H_2CNMes)_2C$:
SIPr	$(H_2CNDipp)_2C$:
t	Triplet
Tbt	2,4,6-$\{CH(SiMe_3)_2\}_3C_6H_2$
^{t}Bu	tert-Butyl
TEM	Transmission electron microscopy
THF	Tetrahydrofuran
Trip	2,4,6-$^{i}Pr_3C_6H_2$
vide infra	See below
vide supra	See above
vs.	Versus
WBI	Wiberg-bond index
XPS	X-ray photoelectron spectroscopy

Chapter 1: Introduction

1.1 Main Group Element Complexes and Stabilization of Unusual Bonding Environments

The coordination chemistry of p-block elements is fundamentally important due to potential applications in non-precious metal mediated catalysis[1] and for the development of new precursors for semiconducting materials in the electronic industry.[2] Accordingly, the stabilization of reactive main group species in the form of coordination complexes has gained considerable attention in the last few decades. Interest in this area also stems from the discovery of unprecedented bonding motifs which advance our general knowledge of inorganic chemistry.[3]

1.1.1 Kinetic Stabilization

The term "kinetic stabilization" is used when a sterically demanding ligand is employed to stabilize a reactive center or unsaturated bonding environment. The steric shield of the bulky ligand (or ligands) prevents the dimerization or oligomerization of such reactive species.[4] For example, bulky terphenyl ligands were utilized by the Power group to protect inorganic multiple bonds between heavier group 14 elements, such as in the inorganic alkyne analogues Ar′GeGeAr′ [Ar′ = 2,6-$(Dipp)_2C_6H_3$; Dipp = 2,6-$^iPr_2C_6H_3$] (**1**), Ar′SnSnAr′ (**2**) and Ar′′PbPbAr′′ [Ar′′ = 2,6-$(Trip)_2C_6H_3$; Trip = 2,4,6-$^iPr_3C_6H_2$] (**3**).[5] Here the steric bulk of the organic ligands prevents the association of such reactive species to form oligomers or polymers (Figure 1.1).

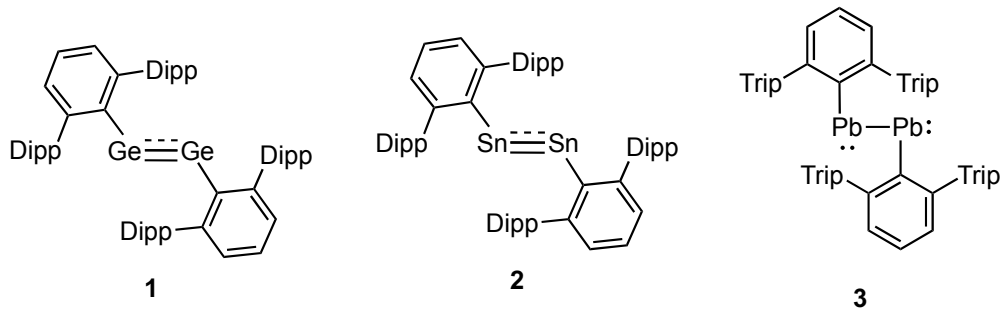

Figure 1.1. Kinetic stabilization of heavier group 14 inorganic alkyne analogues (**1**, **2** and **3**).

1.1.2 Electronic Stabilization

On the other hand, the term "electronic stabilization" is applied when a vacant orbital or a lone pair of a reactive species is stabilized by employing a suitable electron pair donor (Lewis base) or an electron pair acceptor (Lewis acid). For example, the divalent forms of group 14 elements ($:EMe_2$; E = Ge or Sn) are often unstable in the free state due to the presence of a highly reactive vacant p orbital in combination with an adjacent lone pair.[3e] However, by introducing a Lewis acid such as ($Fe(CO)_4$) along with a Lewis base (THF) both $:GeMe_2$ and $:SnMe_2$ can be isolated under ambient conditions as the donor-acceptor complexes, **4** and **5** (Figure 1.2).[6] Furthermore, electronic stabilization of highly elusive B≡B (**6**) and P-P (**7**) units was also possible with the aid of an *N*-heterocyclic carbene, IPr [IPr = $(HCNDipp)_2C$: (Dipp = 2,6-$^{i}Pr_2C_6H_3$)], as an electron donating ligand (Figure 1.2).[7]

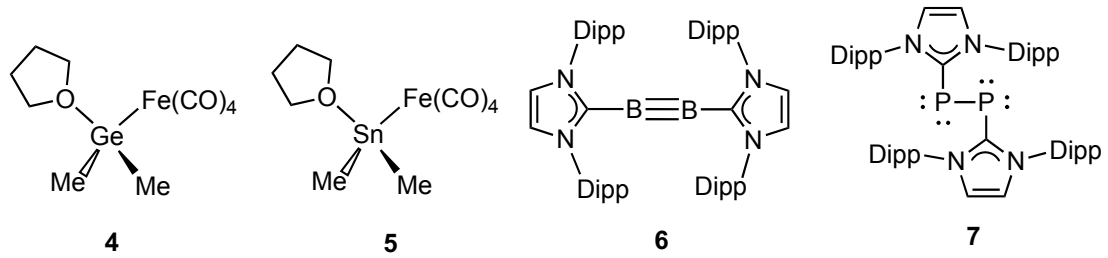

Figure 1.2. Electronic stabilization of reactive main group species: Donor-acceptor stabilization of dimethyl germylene (**4**) and dimethyl stannylene (**5**); donor stabilization of elusive B_2 and P_2 units (**6** and **7**).

1.2 Diverse Ligand Choices for Main Group Element Complexation

The ability to control the reactivity of a metal center within a coordination complex by changing the steric bulk and donor/acceptor properties of a ligand is a central aspect of inorganic chemistry.[8] Moreover, this concept is key to the development of active catalysts. While traditionally N- and P-based ligands have formed the basis of coordination chemistry (*i.e.* amines or phosphines), new donors based on anionic carbon-based ligands, neutral electron donating carbenes, nucleophilic exocyclic olefins and electron rich transition metal complexes are now emerging.[4a,9]

1.2.1 Anionic Carbon-based Donor Ligands

Cyclopentadienyl (Cp) and pentamethylcyclopentadienyl (Cp*) ligands are well-known as 6-electron donors and their metal complexes are referred to as "metallocenes".[10] Moreover Cp and Cp* have been used to generate isolable low valent group 14 element complexes as demonstrated by the preparation of Cp^*_2Si (**8**) and Cp_2Pb (**9**) (Figure 1.3).[11a,b] Cp_2Pb adopts an extended structure in the solid state due to the large size and low electronegativity of Pb,[11a] whereas the tin analogue Cp_2Sn**:** exists as a monomer in the solid state.[11c] Recently, Mo-Ge and W-Ge

multiply bonded complexes were stabilized by Filippou and co-workers with the aid of Cp* as a co-ligand leading to the formation of $Cl(dppe)_2Mo{\equiv}Ge\text{-}Cp^*$ (**10**) and $Cl(dppe)_2W{\equiv}Ge\text{-}Cp^*$ (**11**) (dppe = $Ph_2PCH_2CH_2PPh_2$) (Figure 1.3); in both compounds **10** and **11**, the Cp* ligand binds to the Ge center in an η^1-fashion.[12] Metallocenes of cationic group 13 and group 15 elements are also reported, and examples include $[Cp^*_2B]B(C_6F_5)_4$ (**12**), $[Cp^*_2Al][Cp^*AlCl_3]$ (**13**), $[Cp^*_2As]AlCl_4$ (**14**), and $[Cp^*_2Sb]AlCl_4$ (**15**).[13,14]

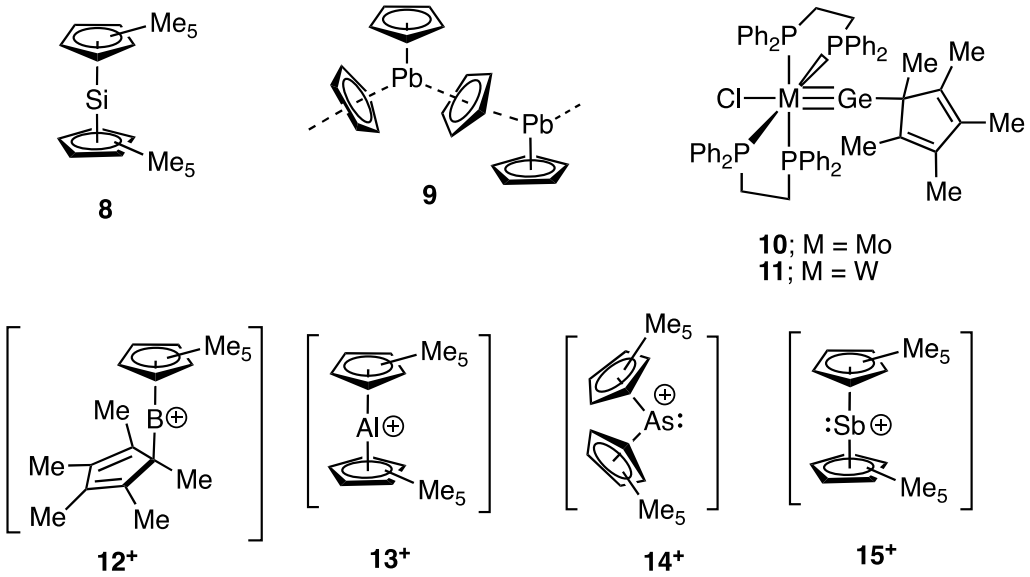

Figure 1.3. Cyclopentadienyl (Cp) and pentamethylcyclopentadienyl (Cp*) as ligands for reactive main group complexes.

Another well-known class of anionic carbon based ligands are terphenyl donors of the general form: 2,6-$Aryl_2C_6H_3$ (Ar′, Ar″ and Ar*; Ar* = 2,6-$(Mes)_2C_6H_3$; Mes = 2,4,6-$Me_3C_6H_2$) (Figure 1.4).[15] Due to the perpendicular orientation of the neighboring aryl groups about the central ring, a concave steric pocket is generated about the ligated atom. As a result, these ligands are highly efficacious in protecting the coordinated reactive unit from associative decomposition processes.

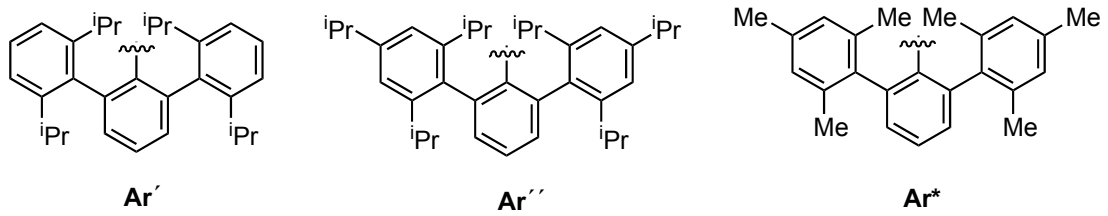

Figure 1.4. Frequently used terphenyl ligands in molecular main group element chemistry.

With the aid of the terphenyl ligand, Ar″, Robinson and co-workers successfully isolated the dianionic salt of the formally Ga-Ga multiply bonded species, Na_2[Ar″GaGaAr″] (**16**) (Figure 1.5).[16] Due to the presence of a somewhat short Ga-Ga bond distance (2.319(3) Å) in **16** relative to standard Ga-Ga single bonds, the Ga-Ga linkage in **16** was originally considered to be a triple bond;[17] however, the Ga-Ga-C angles (125.9(2) and 134.0(2)°) indicated the presence of considerable lone pair character on each Ga center. Later Nagase and Takagi concluded that the central part of the molecule is best regarded as a Na_2Ga_2 cluster with significant covalent character.[18]

A few years later, the Power group reported the isolation of neutral dimetallenes of gallium (**17**) and other heavier group 13 elements (In and Tl) (**18** and **19**) supported by the terphenyl ligand Ar′ (Figure 1.5).[19] As discussed earlier, Power and co-workers prepared a homologous group 14 element dimetallyne series ArEEAr (E = Ge, Sn and Pb; Ar = terphenyl ligand) (Figure 1.1).[5]

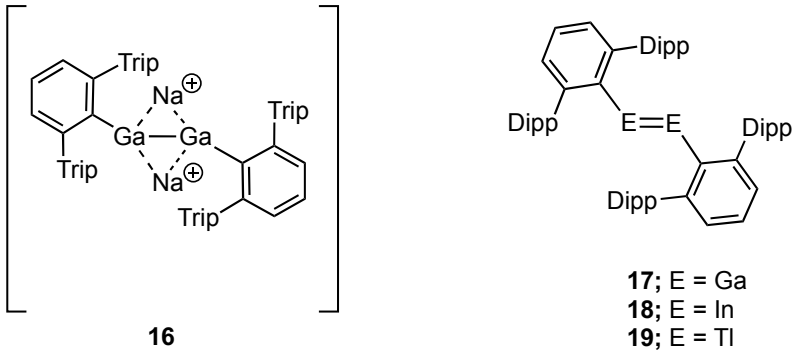

Figure 1.5. Stabilization of a group 13 element dimetyllyne (**16**) and dimetallenes (**17-19**) with the aid of terphenyl ligands.

The related sterically hindered anionic carbon-based ligands are Tbt (Tbt = 2,4,6-{$CH(SiMe_3)_2$}$_3C_6H_2$) and Bbt (Bbt = 2,6-{$CH(SiMe_3)_2$}$_2$-4-{$C(SiMe_3)_3$}C_6H_2) were initially reported by Okazaki, Tokitoh and co-workers (Figure 1.6).[20,21] With the aid of the bulky Tbt and Bbt substituents, Tokitoh reported their seminal work on stabilizing of the heavier group 15 multiply bonded species, Bbt-Sb=Sb-Bbt (**20**) and Tbt-Bi=Bi-Tbt (**21**) (Figure 1.6).[22]

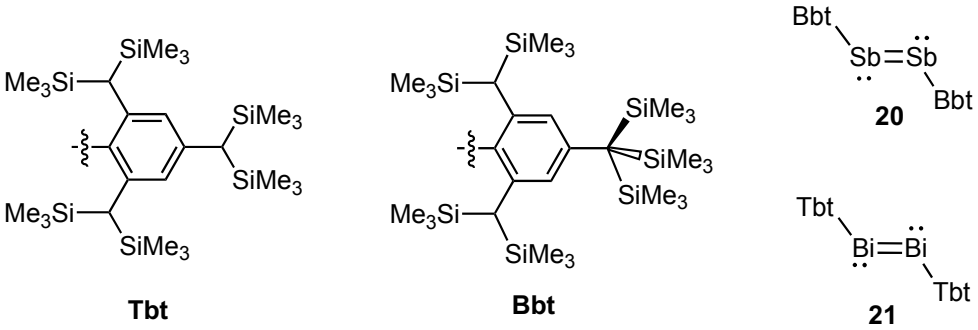

Figure 1.6. Tbt and Bbt ligands and stabilization of heavier group 15 element multiply bonded species.

Apart from preparing homonuclear inorganic multiple bonds, Tbt and Bbt were also employed as ligands for the isolation of reactive mixed group 14/16 element multiple bonds (such as Si=Ch, Ge=Ch or Sn=S; Ch = S and Se), and the

resulting compounds were termed as "heavy ketones".[23,24] Due to the high polarizability and reduced mutual p orbital (π) overlap in relation to C=O linkages, compounds containing these reactive E=Ch bonds are prone toward oligomerization or polymerization when less hindered ligands are present. Later, Goto and co-workers successfully isolated (Tbt)(Trip)Si=S (**23**) (Trip = 2,4,6-$^{i}Pr_3C_6H_2$) via dechalcogenation of a tetrathiosilolane (**22**) (Figure 1.7).[25] Following a similar dechalcogenation methodology (Tbt)(Trip)Ge=S (**24**) and (Tbt)(Trip)Ge=Se (**25**) were also successfully synthesized by the Tokitoh group (Figure 1.7).[26] However, the combined steric bulk of the Tbt and Trip substituents was insufficient to stabilize Sn=S or Sn=Se bonds, and only dimerization products $[(Tbt)(Trip)Sn(Ch)]_2$ (Ch = S and Se) were obtained.[26c] Later, the use of a terphenyl ligand (Ditp; Ditp = 2,6-(2-$^{i}PrC_6H_4)_2C_6H_3$) in concert with Tbt led to the formation of (Tbt)(Ditp)Sn=S (**26**) and (Tbt)(Ditp)Sn=Se (**27**) as stable crystalline solid (Figure 1.7).[27]

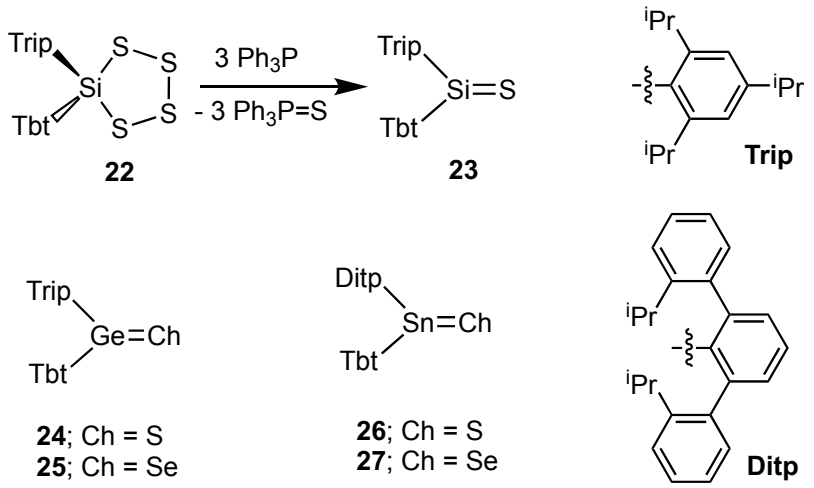

Figure 1.7. Stabilization of heavy ketone analogues with the aid of Tbt, Trip and Ditp ligands

More recently Tamao and co-workers introduced the bulky anionic Eind (Eind = 1,1,3,3,5,5,7,7-octaethyl-s-hydrindacen-4-yl) ligand to the community, and used this symmetric ligand to stabilize the first germanone $(Eind)_2Ge{=}O$ (**28**) containing a Ge=O double bond as the key structural feature (Scheme 1.1).[28] The molecular structure of compound **28** displayed a planar tricoordinated Ge center with a Ge=O bond distance of 1.6468(5) Å, which is 6% shorter than typical Ge(IV)-O single bonds (1.76 Å).[29]

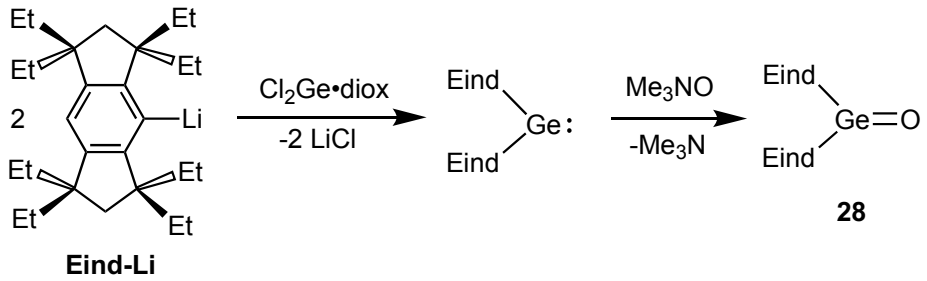

Scheme 1.1. Stabilization of a germanone with the aid of Eind ligands.

1.2.2 Carbenes: Neutral Electron Pair Donors as Ligands

1.2.2.1 Electronic Configurations and Stability of Carbenes

Carbenes are a class of neutral compounds containing a divalent carbon atom with formally six electrons in its valence shell. Due to the presence of an incomplete octet and coordinative unsaturation, they are generally highly unstable species in the free state. The carbene carbon is linked to the two adjacent groups by covalent bonds and the remaining two non-bonding electrons can either adopt parallel spins (triplet state) or anti-parallel spins (singlet state). A schematic representing possible ground state singlet and triplet states of a carbene species is shown in Figure 1.8.

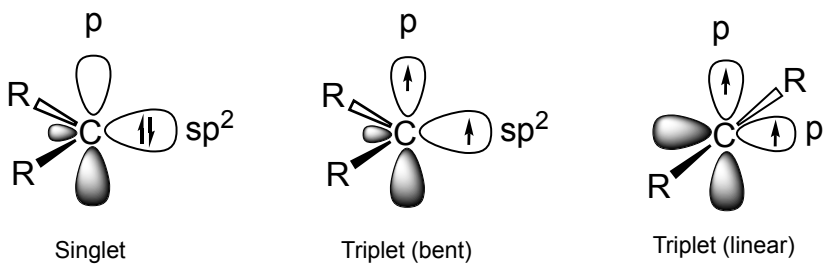

Figure 1.8. Electronic configuration of singlet and triplet carbenes.

A substituent or adjacent atom (R) with an energetically and geometrically available electron pair can stabilize the singlet state of a carbene by delocalizing electron density into the empty p orbital of the carbene carbon. If the energy of the singlet state is sufficiently reduced by such delocalization, then it will be stable and isolable entity. The isolation of an uncoordinated carbene remained elusive until the late 1980s. In 1988 Bertrand and co-workers reported the first isolable carbene **29**, stabilized by adjacent phosphorus- and silicon-based substituents (Scheme 1.2).[30] Compound **29** was synthesized as a red oil from the reaction of $Li[Me_3SiCN_2]$ with $ClP(N^iPr_2)_2$. In compound **29**, the lone pair of the carbene carbon strongly interacts with the neighboring Si substituent; as a result, **29** was found to be a very weak sigma donor. Three years later, Arduengo *et al.* reported the synthesis of the thermally stable carbene, 1,3-diadamantylimidazol-2-ylidene (or IAd (**30**)) as a white crystalline solid; the synthesis of **30** was accomplished by deprotonation of an imidazolium chloride with the strong base NaH (Scheme 1.2).[31]

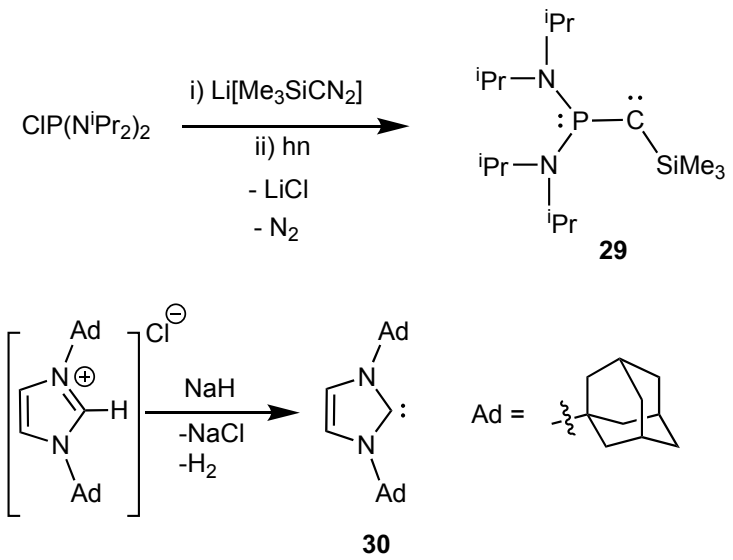

Scheme 1.2. Synthesis of the stable carbene **29** and **30**.

Compound **30** is considered to be the first stable cyclic diamino carbene, termed hereafter as an *N*-heterocyclic carbene (NHC). This was the major breakthrough in the field of carbene chemistry and provided inspiration for later experimental and theoretical studies involving the use of NHCs to stabilize reactive main group species. In compound **30** the bulky adamantyl groups attached to the nitrogen atoms help kinetically stabilize the carbene carbon and prevent it from dimerization to the corresponding alkene. *N*-heterocyclic carbenes also exhibit a singlet ground state and the electronic stabilization from the adjacent N atoms is a key factor. The highest occupied molecular orbital (HOMO) can be best described as the sp^2 hybridized lone pair and lowest unoccupied molecular orbital (LUMO) of the carbene carbon has considerable the π*(N-C) character with a large contribution from C (Figure 1.9). The σ-withdrawing and π-donating characters of the adjacent N atoms stabilize the structure by inductively withdrawing electron density from the HOMO and delocalizing the electron density into carbon-based p orbital. Also the cyclic form

of the NHC leads to a bent N-C-N angle at the carbene carbon (Figure 1.9). This method of carbene stabilization works for almost all classes of NHCs.

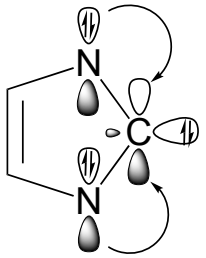

Figure 1.9. Electronic stabilization of an *N*-heterocyclic carbene.

1.2.2.2 Recent Progress in *N*-Heterocyclic Carbene (NHC) Chemistry within the Main Group

The deprotonation of an imidazolium ion or reductive processes, such as reduction of thiourea analogues with sodium or potassium, leads to the formation of a wide range of *N*-heterocyclic carbene donors (Figure 1.10). IPr, SIPr (SIPr = $(H_2CNDipp)_2C$:), IMes (IMes = $[(HCNMes)_2C$:]; Mes = 2,4,6-$Me_3C_6H_2$) or SIMes (SIPr = $(H_2CNMes)_2C$:) are the most commonly used NHCs to stabilize the low valent main group complexes and their structures are summarized in Figure 1.10. Due to the presence of large Dipp or Mes groups, they impart stability and solubility to the target main group element complexes. Other frequently used NHCs are I^tBu (I^tBu = $(HCN^tBu)_2C$:), $ImMe_2{}^iPr_2$ ($ImMe_2{}^iPr_2$ = $(MeCN^iPr)_2C$:), and IMe_4 (IMe_4 = $(MeCNMe)_2C$:) (Figure 1.10).[32]

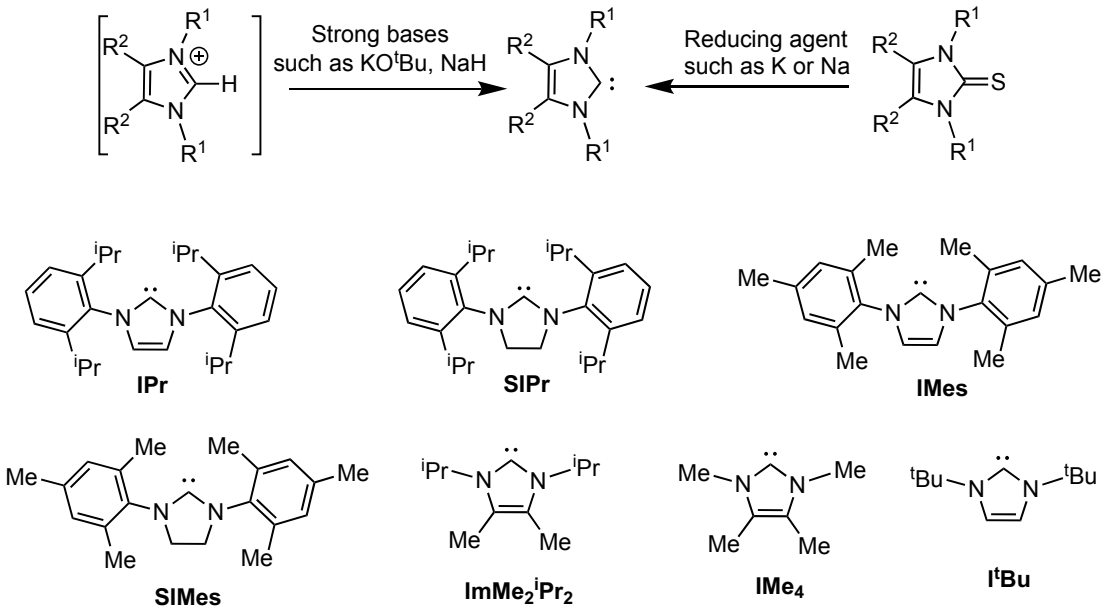

Figure 1.10. Commonly used *N*-heterocyclic carbene ligands used in the main group coordination chemistry.

The use of NHCs to stabilize heavier main group element multiple bonds has gone through a tremendous period of growth over the last two decades. In 2007, the first example of an NHC-stabilized B=B bond IPr•HB=BH•IPr (**31**) was reported by the group of Robinson.[33] This species was prepared by reacting IPr•BBr_3 with excess equivalents of potassium graphite (KC_8) which produced a mixture of IPr•HB=BH•IPr (**31**) and IPr•H_2B-BH_2•IPr (**32**) (Scheme 1.3); the source of the hydrogen atoms is thought to be hydrogen abstraction from the Et_2O solvent. Later, Braunschweig and co-workers isolated IPr•(Br)B=B(Br)•IPr (**33**) via the reduction of a bis carbene adduct of tetrabromodiborane, IPr•Br_2B-BBr_2•IPr, with two equivalents of sodium naphthalenide (Scheme 1.3). By increasing the ratio of reducing agent to four equivalents, they were able to isolate an IPr-supported B≡B triple bond in the form of the green complex, IPr•B≡B•IPr (**6**); this was the first isolable molecule

containing a B≡B triple bond (Figure 1.2 and Scheme 1.3).[7a] The first example of an NHC-stabilized E_2 unit (E = group 14 elements) came from the laboratory of Robinson, where an IPr adduct of $SiCl_4$ (IPr•$SiCl_4$) was reduced with four equivalents of KC_8 to form IPr•Si=Si•IPr (**34**) in low yield, with the simultaneous formation of the ClSiSiCl adduct IPr•(Cl)Si-Si(Cl)•IPr (**35**) as an isolable by-product (Scheme 1.3).[34a] Later, Jones and co-workers successfully isolated Ge_2 and Sn_2 units supported by IPr specially the reaction of IPr•ECl_2 (E = Ge or Sn) with their nacnac Mg(I) dimer ($\{Mg\{[N(Mes)CMe]_2CH\}\}_2$) as a reducing agent led to the formation of IPr•Ge=Ge•IPr (**36**) and IPr•Sn=Sn•IPr (**37**), respectively (Scheme 1.3).[34b,c] Compounds **34**, **36** and **37** can be best described as NHC adducts of doubly bonded :E=E: (E = Si, Ge and Sn) fragments. Moreover, the ^{IPr}C-E=E bond angles in compounds **34**, **36** and **37** are all close to 90° and represent trans-bent geometries in terms of the interaction between the carbon donor in IPr and the central E_2 fragments.

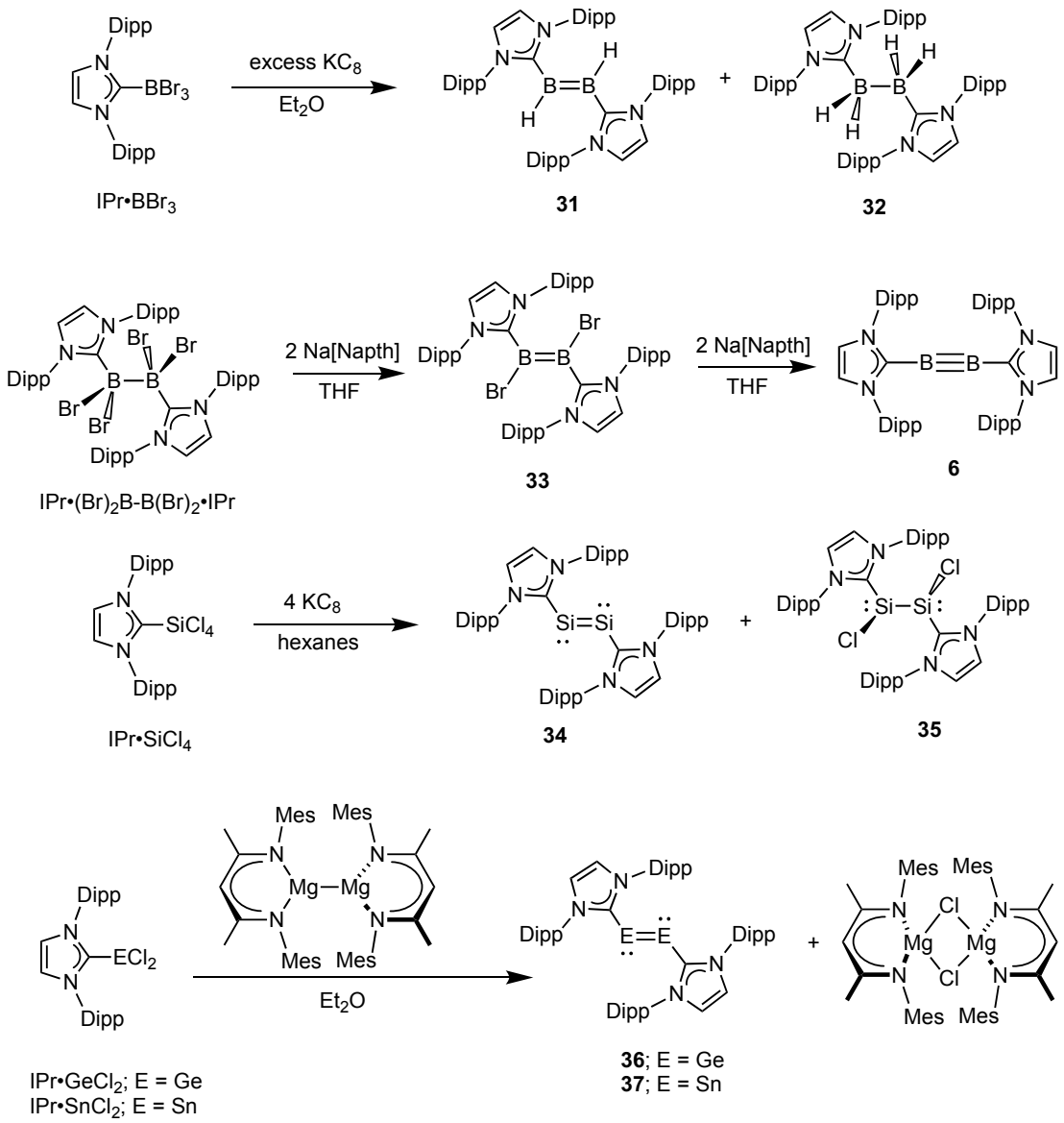

Scheme 1.3. Stabilization of group 14 diatomic allotropes (E_2) with the aid of an *N*-heterocyclic carbene donor, IPr.

1.2.2.3 Recent Progress in Cyclic(alkyl)(amino)carbene (CAAC) Chemistry within the Main Group

Recently cyclic(alkyl)(amino)carbenes (CAACs) have attracted considerable attention as competent donors within inorganic coordination chemistry. CAACs are the mono amino versions of NHCs and were first prepared by the Bertrand group.[35] Since only one adjacent N atom is present, the empty p orbital of the carbene carbon in CAACs is electronically less stabilized and this makes CAACs more electrophilic compared to most NHCs.[36] As a consequence of their better π-accepting properties, CAACs are efficacious ligands for the stabilization of electron rich main group element fragments. The structures of commonly used CAAC ligands (**L1**, **L2**, **L3** and **L4**) are shown in Figure 1.11.

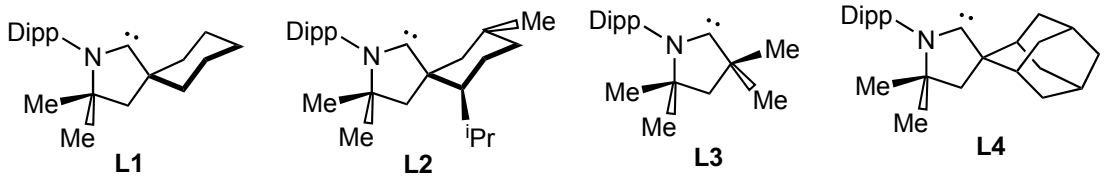

Figure 1.11. Commonly used CAAC ligands in coordination chemistry.

By taking advantage of the enhanced π-accepting character of CAACs, Bertrand and co-workers stabilized the nucleophilic borylene fragment (H-B:) as $(L1)_2B$-H (**38**) (Scheme 1.4).[37] Compound **38** was prepared by the reduction of L1•BBr_3 with five equivalents of KC_8. To confirm the presence of a lone pair on the central boron atom, a reaction of **38** with triflic acid was also performed which gave the expected $[BH_2]^+$ unit supported by two CAAC ligands (Scheme 1.4). Furthermore, utilizing the π-accepting property of the CAAC (**L1**) in combination with the π-accepting nature of the CN groups, Bertrand and co-workers reported the

deprotonation of L1•B(CN)$_2$H (**39**) to form a boryl anion, L1•B(CN)$_2^-$ (**40**) as its potassium salt (Scheme 1.4).[38] Hydrogen atoms attached to the electropositive boron centers are generally hydridic in character ($B^{\delta+}$-$H^{\delta-}$); however in the presence of π-accepting ligands (*e. g.* CAAC and CN) the B-H residue in **39** becomes acidic. As a result, compound **39** readily undergoes deprotonation in the presence of the strong base, potassium bis(trimethylsilyl)amide (KHMDS) (Scheme 1.4).

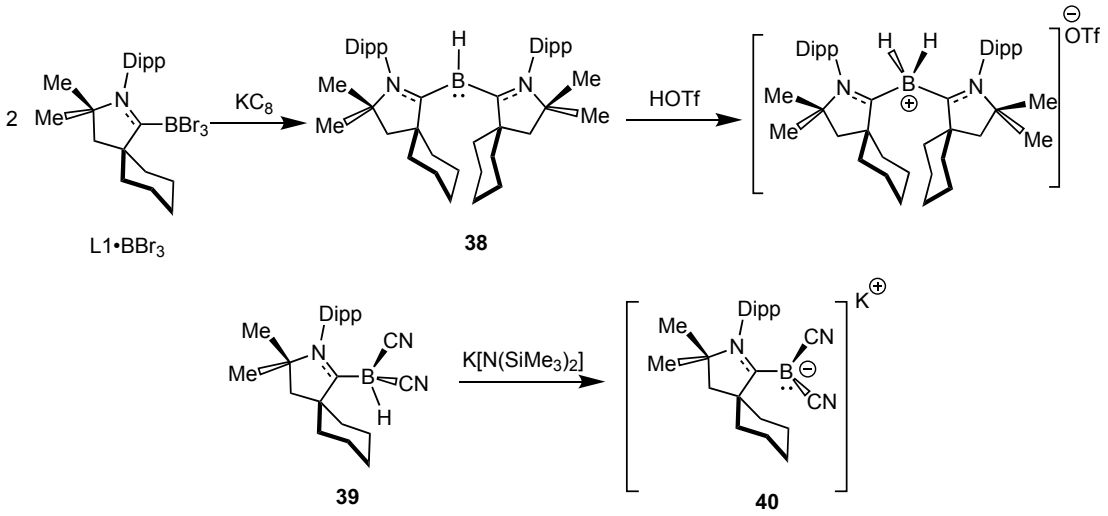

Scheme 1.4. Stabilization of nucleophilic boron (I) centers by CAAC ligands.

CAACs were also employed to stabilize diatomic allotropes of heavier group 15 elements.[39] For example, the reaction of **L1** with white phosphorous (P_4) enabled the isolation of a P_2 unit supported by two CAAC ligands as L1•P-P•L1 (**41**) (Scheme 1.5).[39a] The $^{31}P\{^1H\}$ NMR spectrum of compound **41** displays a resonance at +59.4 ppm and it is largely downfield-shifted compared to that in Robinson's IPr•P-P•IPr (**7**) (-52.4 ppm);[7b] this suggests a more electron deficient P_2 unit in compound **41** and is commensurate with the stronger π-accepting nature of CAAC ligands compared to most NHCs. Moreover, **L1** was found to be an effective ligand for the stabilization of

four different oxidation states (III, II, I or 0) of Sb, as shown by the compound series: L1•$SbCl_3$ [Sb(III)], L1•$SbCl_2$ [Sb(II)] (**42**), L1•SbCl [Sb(I)] (**43**), and L1•Sb-Sb•L1 [Sb(0)] (**44**) (Scheme 1.5).[39b,c]

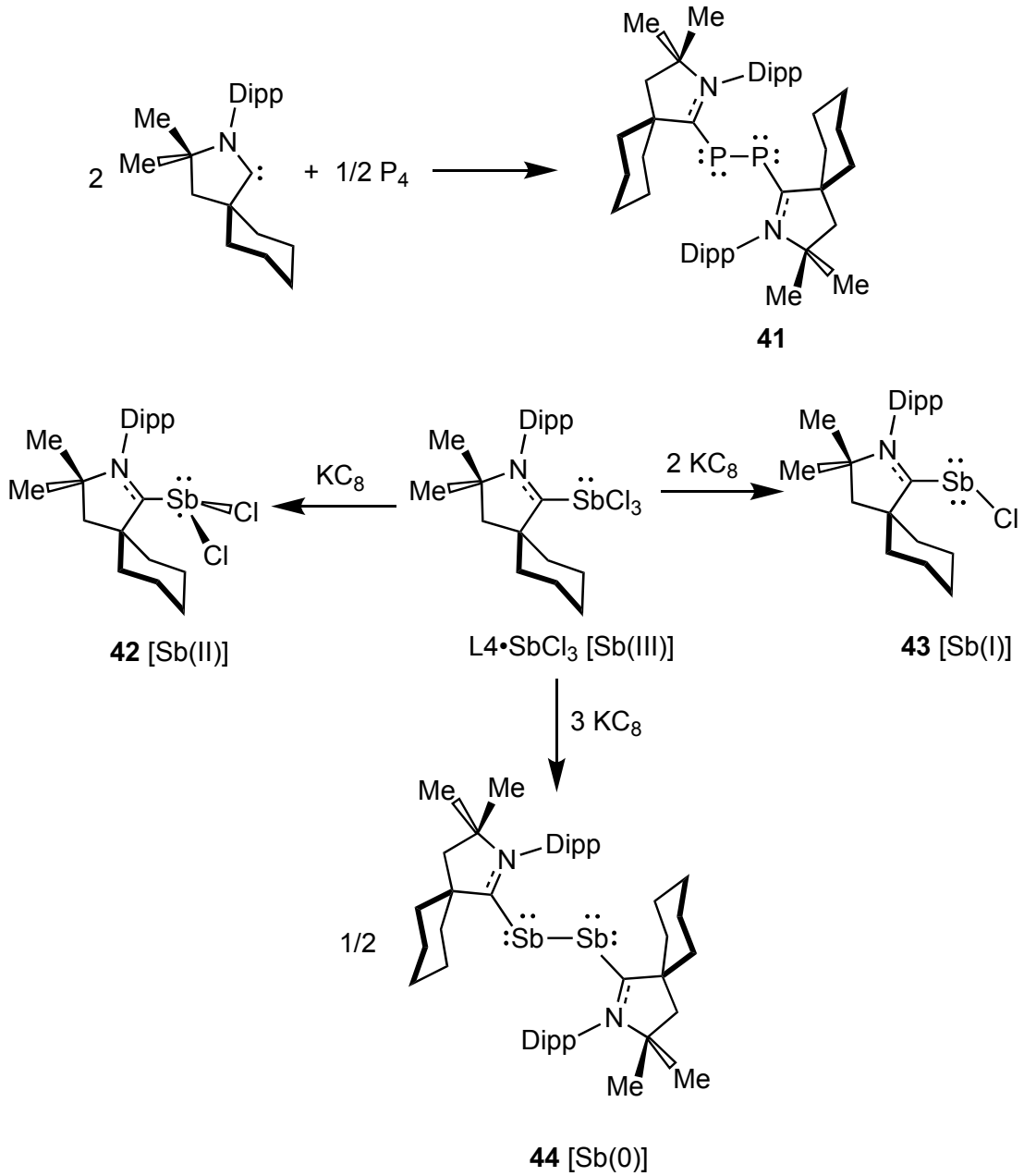

Scheme 1.5. Stabilization of diatomic allotropes of group 15 elements, P_2 (**41**) and Sb_2 (**44**) by CAAC ligands (**L1**).

1.2.3 *N*-Heterocyclic Olefins (NHOs) and Wittig Reagents

1.2.3.1 *N*-Heterocyclic Olefins (NHOs) as Ligands for Main Group Centers

In contrast to NHCs and CAACs, *N*-heterocyclic olefins (NHOs) are relatively unexplored carbon-based ligands within the context of supporting transition metal-mediated catalysis and to intercept reactive main group species. A common structural motif within an NHO involves placement of a terminal CH_2 unit on an NHC fragment to yield NHC=CH_2 species. As shown in Scheme 1.6, the resonance forms of an NHO are in line with the highly polarized nature of the exocyclic C=C double bond and the nucleophilic character of the terminal ligating carbon atom.

$ImMe_4CH_2$ was the first *N*-heterocyclic olefin (NHO) ligand reported, and was prepared in the early 1990s by Kuhn and co-workers.[40] The terminal carbon of the exocyclic double bond in $ImMe_4CH_2$ was found to be sufficiently electron rich to coordinate to transition metal and main group Lewis acidic entities, such as $Mo(CO)_5$ or BH_3 (Scheme 1.6).

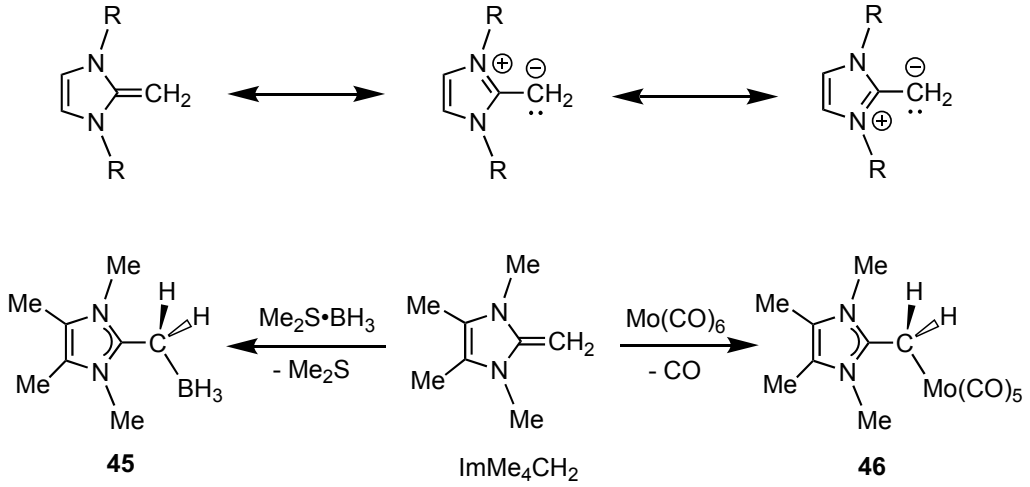

Scheme 1.6. Resonance forms of an *N*-heterocyclic olefin (NHO) (top) and coordination of $ImMe_4$=CH_2 to BH_3 and $Mo(CO)_5$ unit (bottom).

IPr=CH_2 is the most commonly used NHO, initially synthesized by the methylation of IPr followed by the deprotonation of methyl group (Scheme 1.7).[41]

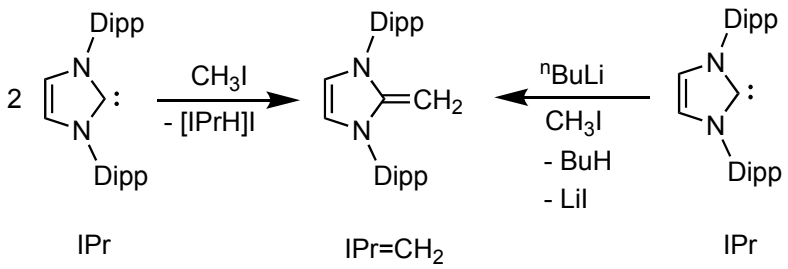

Scheme 1.7. General synthetic strategy used to prepare IPr=CH_2 from IPr.

The Rivard group extensively studied the ligating property of IPr=CH_2 toward various reactive main group element complexes; examples include the isolation of low valent group 14 dihydrides (see section 1.3.3), reduced PN heterocycles and $(GeCl_2)_x$ chains.[41*a*,42]

IPr=CH_2 has also been employed as a ligand for the stabilization of various cationic boron or gallium species.[43] For example Robinson and co-workers reported the activation of THF by IPrCH_2•BBr_3 and the formation of [IPrCH_2•B(OC_4H_8Br)$_2$]Br (**47**), a cationic boron derivative stabilized by IPr=CH_2 (Scheme 1.8).[41*c*] Furthermore, Chiu *et al.* employed IPr=CH_2 as a ligand to stabilize mono and dicationic boron derivatives, as exemplified by the synthesis of [IPrCH_2•BClCp*]$AlCl_4$ (**48**) and [IPrCH_2•BCp*]($AlCl_4$)$_2$ (**49**) (Cp* = η^5-C_5Me_5) (Scheme 1.8).[43*a*]

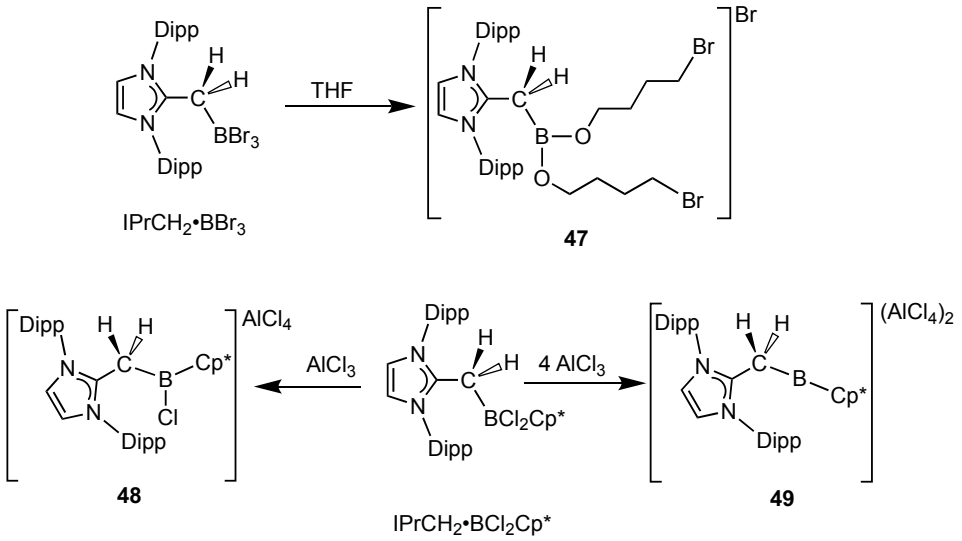

Scheme 1.8. $IPrCH_2$ stabilized cationic boron complexes (**47-49**).

1.2.3.2 Wittig Reagents as Ligands in the Main Group

A surprisingly ignored ligand class in the chemical community are nucleophilic (ylidic) Wittig reagents of the general form $R_3PCR'_2$. Wittig reagents are often used in organic synthesis for the conversion of ketones to alkenes (Scheme 1.9).[44] Wittig reagents of the general form $R_3P{=}CR'_2$ (R = Me or Ph; R′ = H or Me) are usually synthesized via deprotonation of their corresponding phosphonium salts, $[R_3PCHR'_2]X$ (X = Cl, Br or I) with a strong base, such as $^{n}BuLi$. Due to the highly polarized nature of the formal P=C double bond, a significant amount of negative charge is positioned on the terminal carbon atom in a Wittig reagent, leading to the observed nucleophilic character (Scheme 1.9).

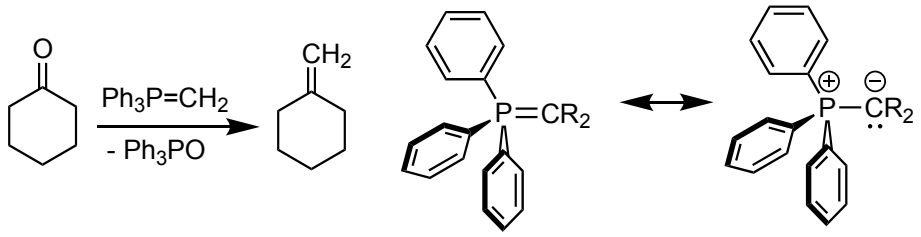

Scheme 1.9. Conversion of a ketone to an alkene with the aid of a Wittig reagent and major canonical forms of a Wittig reagent.

Wittig reagents are to some extent known as ligands for transition metals and actinides;[45] however, the coordination chemistry of these ylides within the main group is almost unknown.[46] In 1958 Hawthrone first reported the Lewis acid-base adduct $Ph_3PCH_2{\bullet}BH_3$ (**50**), synthesized from the reaction of $Ph_3P{=}CH_2$ with diborane (B_2H_6) (Figure 1.12).[47] Another example of a Wittig reagent-main group element adduct was reported by Beletskaya and co-workers; they observed the coordination chemistry of Me_3PCH_2 to a silicon center to give the silafulvene complex **51** (Figure 1.12).[48]

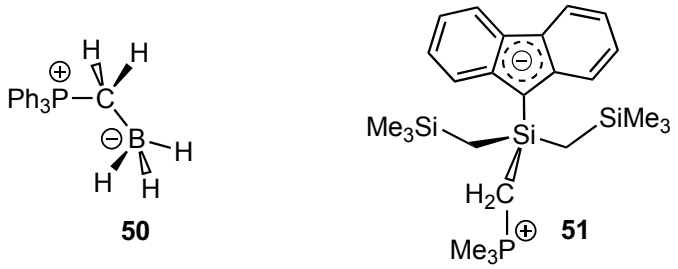

Figure 1.12. Formation of adducts with electron deficient boron (**50**) and silicon (**51**) species.

As discussed in chapter 2 of this thesis, a Wittig reagent ($Ph_3P{=}CMe_2$) was introduced to isolate elusive low valent group 14 element dihydrides, ($:EH_2$; E = Ge and Sn) in combination with a suitable Lewis acidic molecular group (such as metal

carbonyls). This work can be considered as the most recent contribution of a Wittig reagent as a donor in main group element chemistry.[49] Given the ease at which Wittig reagents are prepared (often made in undergraduate teaching labs), it is hoped that such donors will become more prominent in coordination chemistry.

1.2.4 Electron Rich Transition Metal Complexes as Ligands in the Main Group

In addition to the donor systems mentioned already, one can also use the electron rich character of some late transition metal centers to bind/stabilize electron deficient species. In 1964, Nowell and Russell reported the structure of (η^5-C_5H_5)$(CO)_2$Co•$HgCl_2$; the first structural evidence of a dative Lewis acid-base interaction between two metal centers.[50] Thus far, various late transition metal Lewis bases containing Ir, Pt and Rh have been developed.[51] The most common Lewis base metal complexes that have coordinated to main group centers are $Pt(PCy_3)_2$, $Pt(NHC)_2$, $Cp(CO)_2Rh$, $Cp(R_3P)_2Rh$ (R = Me or Et), $Cp(Ph_3P)(CO)Rh$ and $Cp^*(CO)_2Ir$ ($Cp^* = \eta^5$-C_5Me_5) (Figure 1.13).[52]

Electron deficient group 13 element complexes with late transition metal ligands are currently being extensively explored. For example, Braunschweig and co-workers reported a series of aluminium trichloride adducts of a Pt(0) based ligand: [(I^tBu)(Cy_3P)Pt•$AlCl_3$] (**52**), [(SIMes)(Cy_3P)Pt•$AlCl_3$] (**53**), [$(SIMes)_2$Pt•$AlCl_3$] (**54**), [$(Cy_3P)_2$Pt•$AlCl_3$] (**55**) (Figure 1.13).[53] Apart from Pt, other late transition metal centers (such as Rh, Ir and Fe) are also sufficiently electron rich to coordinate to group 13 Lewis acids, forming [$Cp(Me_3P)_2Rh$•$AlMe_3$] (**56**), [Et_4N][$Cp(OC)_2Fe$•$AlPh_3$] (**57**), [$Cp^*(Me_3P)(H)_2Ir$•$AlPh_3$] (**58**),

$Cp^*(Cp^*Ga)_2Rh{\bullet}GaCl_3]$ (**59**), and $[Cp^*Fe(C_7H_8)][Cp^*(OC)_2Fe{\bullet}InCl_3]$ (**60**) (Figure 1.13).[54,55]

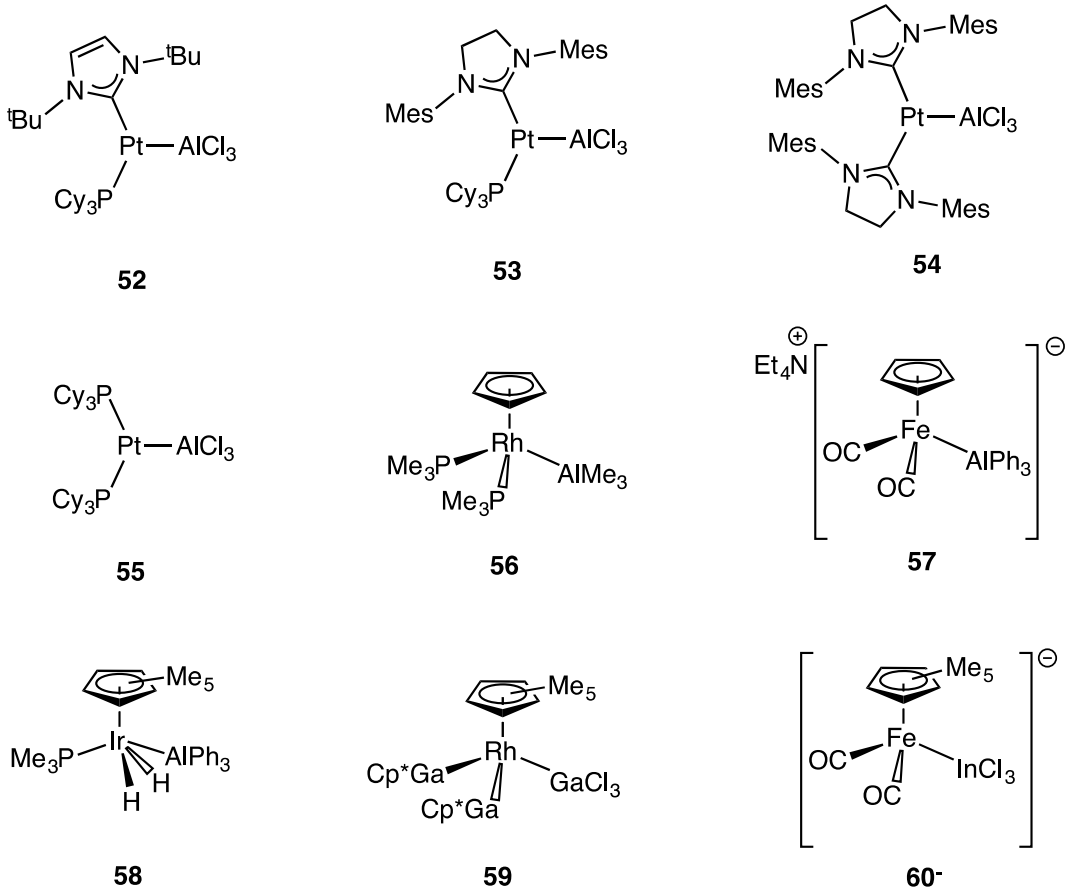

Figure 1.13. Lewis acidic group 13 element adducts with electron rich transition metal complexes.

In some instances, E-X bond activation processes result after the initial formation of a metal Lewis base adduct with main group element (E) species.[56] As a salient example of this transformation, $Pt(PCy_3)_2$ reacts with BX_3 (X = Cl, Br or I) to form the oxidative addition products, **61a**, **61b** and **61c** respectively (Scheme 1.10).[56a,b,c]

Recently, Braunschweig and co-workers used a similar transformation to gain entry to their landmark complex $(Br)(Cy_3P)_2Pt\text{-}BO$ (**62**) featuring a terminal B-O

triple bond (Scheme 1.10). Specifically, compound **62** was synthesized via oxidative addition of $Br_2BOSiMe_3$ to $Pt(PCy_3)_2$, followed by $BrSiMe_3$ elimination.[57] This is the first, and thus far only, example of a BO triple bonded species in molecular form, and thus a major breakthrough in borane chemistry.

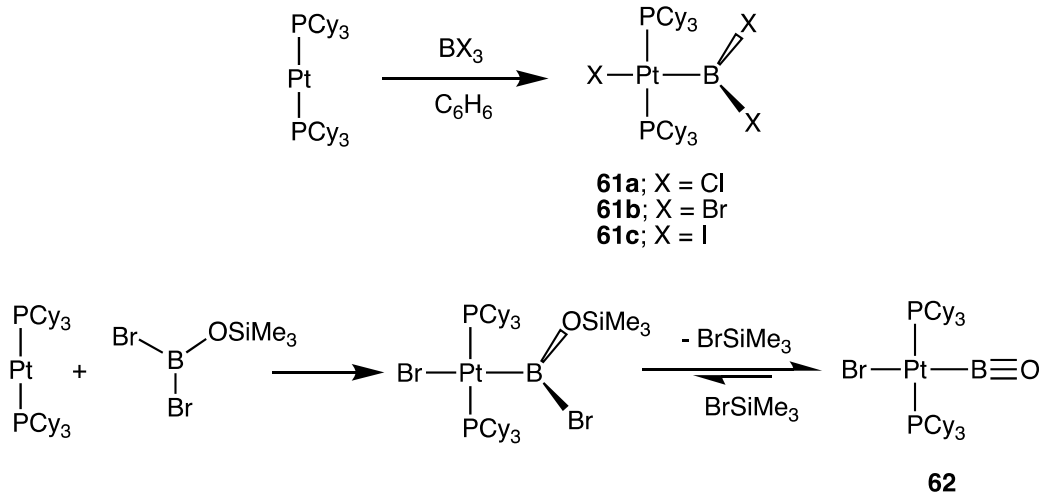

Scheme 1.10. Formal oxidative addition of B-X (X = Cl, Br or I) to $Pt(PCy_3)$ (top), and stabilization of BO triple bonded ligand by a Pt-center (bottom).

In contrast to group 13 elements, fewer examples of metalloligand-element complexes with group 14 elements are known. The groups of Marder and Roulet reported the following $SnCl_2$ bridged complexes of electron rich transition metals: $[\{(Me_3P)_3ClRh\}_2(\mu\text{-}SnCl_2)]$ (**63**) and $[\{(Cy_3P)(CO)(I)Pt\}_2(\mu\text{-}SnCl_2)]$ (**64**) (Figure 1.14).[58] Moreover, Braunschweig, Jones and co-workers isolated coordination complexes of the low valent group 14 element halides $(Cy_3P)_2Pt{\bullet}ECl_2$ (E = Ge, Sn and Pb) (**65**, **66** or **67**) with the aid of $Pt(PCy_3)_2$ as an electron pair donor (Figure 1.14).[59]

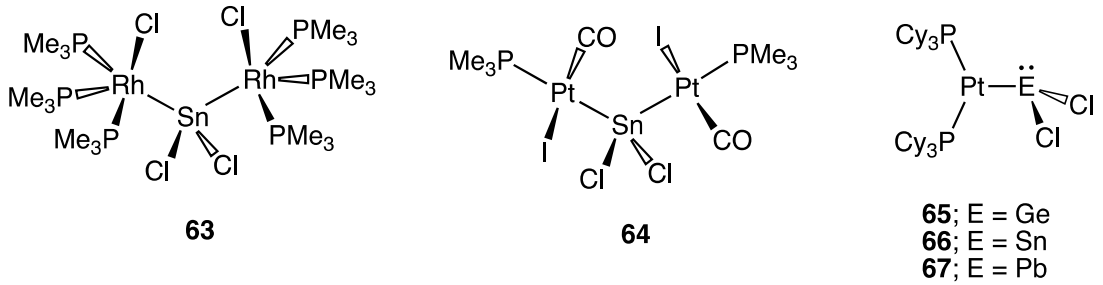

Figure 1.14. Lewis acidic group 14 element adducts with electron rich transition metal complexes.

In the chapter 3 of this thesis, the Lewis acidic behavior of ECl_2•$W(CO)_5$ (E = Ge and Sn) units and $PbCl_2$ toward a cyclopentadienyl rhodium-based complex, $CpRh(PMe_2Ph)_2$ was explored.[60] In addition, the oxidative addition of Ge-Cl and Sn-Cl bonds within ECl_2•$W(CO)_5$ unit (E = Ge and Sn) at $Pt(PCy_3)_2$ is also discussed. The ultimate goal of this work would be to generate binary M_xE_y species by thermal extrusion/elimination of the peripheral $W(CO)_5$ and PCy_3 substituents.

1.3 Stabilization of Low Valent Main Group Complexes by Push-Pull Interactions

1.3.1 Donor-Acceptor Stabilization

A molecular entity with a very small HOMO-LUMO energy gap is often susceptible to self oligomerization or polymerization. However, in the presence of suitable Lewis base (LB) and Lewis acid (LA) capping units one can isolate of such reactive species as a stable molecular complex. Specially, the Lewis base donates an electron pair into the low lying LUMO of the reactive entity, while the Lewis acid concurrently accepts electron density from the HOMO of the reactive unit. This LA/LB combination can shut down possible oligomerization/decomposition processes allowing various

unsaturated synthons to be isolable under ambient conditions (Scheme 1.11). The Marks group was the first to apply this strategy to isolate organogermylene and stannylene derivatives with the aid of a Lewis base (THF) and the strong Lewis acid $Fe(CO)_4$.[6] Here, THF donates electrons into the vacant p orbital of the Ge(II) or Sn(II) centers (in Me_2Ge or Me_2Sn), whereas the lone pair of the low valent group 14 species interacts with the Lewis acidic $Fe(CO)_4$ unit to form the donor-acceptor complexes, THF•EMe_2•$Fe(CO)_4$ (E = Ge and Sn; **4** and **5**) (Figure 1.2 and Scheme 1.11).

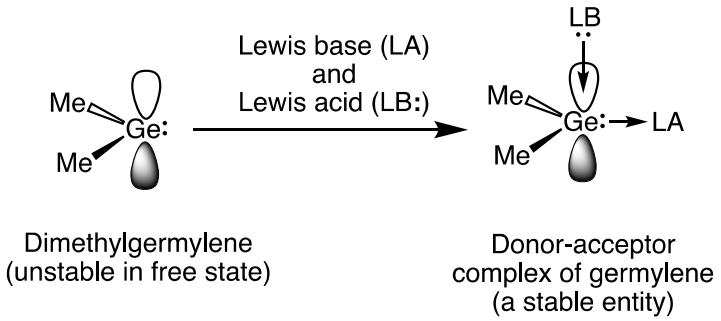

Scheme 1.11. Donor-acceptor stabilization of an organogermylene.

1.3.2 Donor Acceptor Stabilization of Mixed Group 13/15 Element Hydride Complexes

The Scheer group employed donor-acceptor protocol to intercept and stabilize the novel mixed group 13/15 element hydrides, H_2E-E´H_2 (E = B, Al or Ga; E´ = N, P or As).[61] Such mixed hydride complexes could play an important intermediate role in the production of semiconducting materials (such as in the synthesis of GaN),[62] and are promising as hydrogen storage materials and as precursors to inorganic polymers.[61*h*] Due to the presence of low-lying LUMO and highly active electron pair (HOMO) within in the same molecule (*i.e.* dual Lewis acid-base character), H_2E-

E´H_2 species are prone to oligomerization or polymerization; and are thus unstable in the free state under ambient conditions (Scheme 1.12).

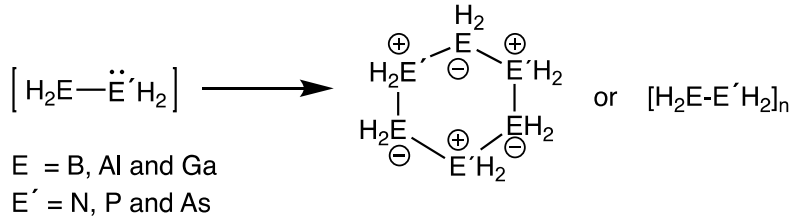

Scheme 1.12. Oligomerization or polymerization of H_2E-E´H_2 species.

In 2001, Scheer and co-workers first isolated mixed hydrides complexes of parent H_2Al-PH_2 and H_2Ga-PH_2 with the aid of Lewis basic Me_3N and Lewis acidic $W(CO)_5$, as capping groups, as demonstrated by the synthesis of Me_3N•H_2Al-PH_2•$W(CO)_5$ (**68**) and Me_3N•H_2Ga-PH_2•$W(CO)_5$ (**69**) (Figure 1.15).[61a] Here, Me_3N stabilizes the empty p orbitals on Al or Ga via electron donation, whereas the Lewis acidic $W(CO)_5$ group interacts with the lone pair on phosphorus. Two years later, a similar LA/LB combination was used to form complexes Me_3N•H_2B-PH_2•$W(CO)_5$ (**70**) and Me_3N•H_2B-AsH_2•$W(CO)_5$ (**71**) (Figure 1.15).[61] The Rivard group also contributed to this field by employing various LA/LB combinations to stabilize the parent amine-borane, H_2B-NH_2 within formal donor-acceptor complexes, such as IPr•H_2B-NH_2•BH_3 (**72**) (Figure 1.15).[63]

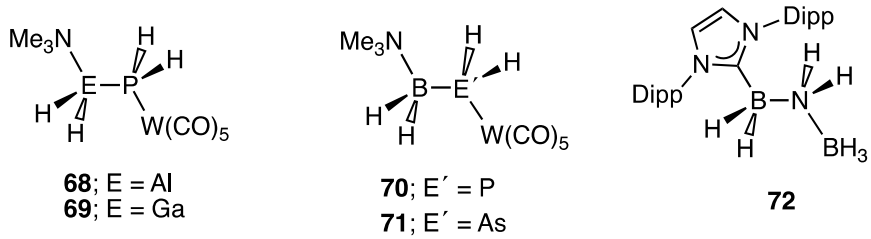

Figure 1.15. Donor-acceptor stabilization of mixed group 13/15 hydride complexes (**68-72**).

Despite these important studies, the lightest unsaturated version of a parent mixed group 13/15 hydride, HBNH, remained elusive and was only identifiable in cryogenic matrices or as a fleeting species in the gas phase.[64,65] HBNH is likely a key intermediate in the laser-induced preparation of nanodimensional boron nitride (BN) from $H_3N{\bullet}BH_3$ dehydrogenation;[66] boron nitride is of great value to the materials community due to its insulating properties and ability to withstand harsh external conditions.[67] As discussed in chapter 4, the Lewis acid (LA) assisted elimination of N_2 followed by H migration from B to N of $LB{\bullet}BH_2N_3$ produced a donor-acceptor complex of HBNH in the form of LB•HB=NH•LA (Scheme 1.13).[68]

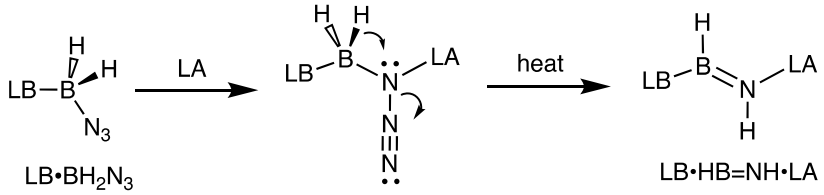

Scheme 1.13. Lewis acid-assisted N_2 elimination from an azidoborane adduct to form a stable HB=NH complex.

A related unsaturated mixed group 13/15 hydride, HGa=NH, could also be a viable building block for the future low temperature deposition of bulk gallium nitride (GaN), a highly valued material for its blue luminescent and semiconducting properties.[69] Therefore, a similar donor-acceptor stabilization approach via Lewis acid-assisted N_2 elimination was applied as in Scheme 1.13 to isolate a HGa=NH donor-acceptor complex. However, the high reactivity of the Ga-H bonds in $IMes{\bullet}GaH_2N_3$ did not permit the isolation of such species as described in chapter 5 of this thesis.[70]

1.3.3 Donor-Acceptor Stabilization of Heavy Group 14 Element Dihydrides

A major research theme within the Rivard group is the use of a donor-acceptor protocol to stabilize low valent group 14 dihydride complexes. Group 14 element dihydrides :EH_2 (E = Si, Ge or Sn) have attracted attention due to their likely presence during the formation of bulk semiconducting materials. For example, SiH_2 was found to be an intermediate during the chemical vapour deposition (CVD) of semiconducting silicon films from the gas phase precursor SiH_4 at very high temperatures (>550 °C) (Scheme 1.14).[3e,71]

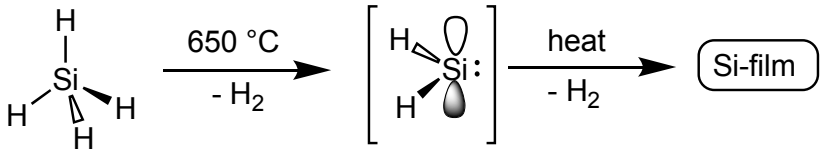

Scheme 1.14. SiH_2 is an intermediate present during the synthesis of Si-film from SiH_4 via high temperature CVD methods.

These elements dihydrides are unstable at room temperature in their free state;[72] however, with the aid of suitable capping Lewis acid and Lewis bases they can be stabilized in the form of donor-acceptor complexes LB•EH_2•LA. The first example appeared in the literature in 2009 wherein a GeH_2 unit was stabilized using IPr as a Lewis base and BH_3 as Lewis acid.[73] Specifically, reaction of IPr•$GeCl_2$ with two equivalents of $LiBH_4$ led to the generation of the stable donor-acceptor complex IPr•GeH_2•BH_3 (**73**) (Scheme 1.15). Herein $LiBH_4$ is both a source of H^- as well as the Lewis acidic BH_3 group. In compound **73**, the *N*-heterocyclic carbene IPr donates an electron pair into the vacant p orbital of the Ge, whereas the lone pair in the GeH_2 unit binds to the Lewis acidic BH_3 group; therefore, a push-pull type interaction enables the isolation of the reactive GeH_2 moiety under ambient temperature.

A similar approach was applied in the attempted isolation of a SnH_2 complex. However treatment of IPr•$SnCl_2$ with $LiBH_4$ only gave IPr•BH_3 as a soluble product, along with the formation of metallic tin as black insoluble precipitate. Later, the use of the highly Lewis acidic $W(CO)_5$ unit enabled the successful isolation of the SnH_2 donor-acceptor complex IPr•SnH_2•$W(CO)_5$ (**74**) (Scheme 1.15).[74] Compound **74** was prepared by treating IPr•$SnCl_2$•$W(CO)_5$ with the H^- source $LiBH_4$ as outlined in Scheme 1.15. This donor-acceptor stabilization strategy was expanded to include an example of a SiH_2 adduct, IPr•SiH_2•BH_3 (**75**) (Scheme 1.15).[75]

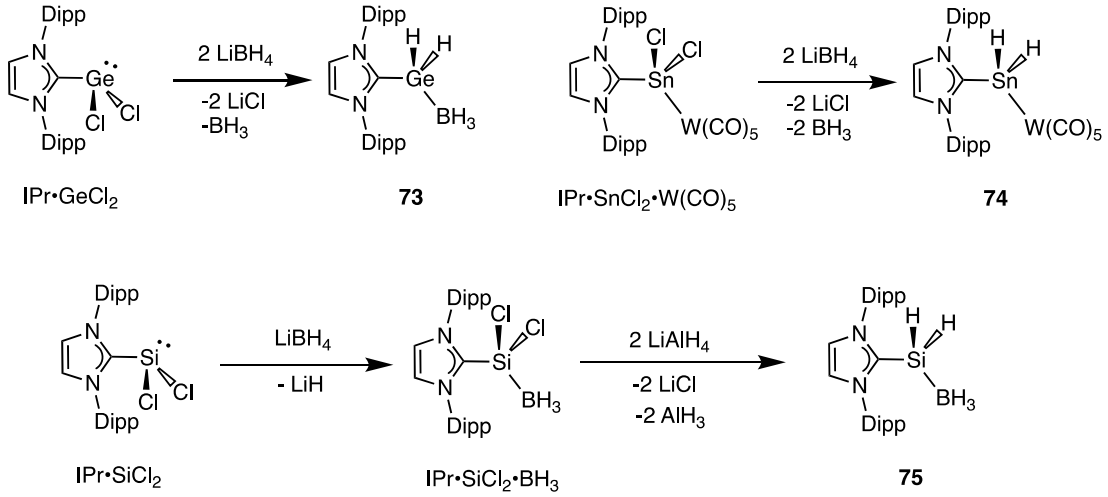

Scheme 1.15. Synthesis of donor-acceptor complexes of GeH_2 (**73**), SnH_2 (**74**) and SiH_2 (**75**).

As already alluded to, the Rivard group also employed *N*-heterocyclic olefins (NHOs), such as IPr=CH_2 as Lewis bases for the stabilization of GeH_2 and SnH_2. As discussed in section 1.2.3.1, due to the presence of a highly polarized exocylic double bond in the NHOs, a considerable amount of negative charge is placed at the terminal carbon of IPrCH_2. Accordingly, the strong donor ability of IPrCH_2 was used to

intercept GeH_2 and SnH_2 units as shown by the formation of $IPrCH_2$•GeH_2•$W(CO)_5$ (**76**) and $IPrCH_2$•SnH_2•$W(CO)_5$ (**77**), respectively (Figure 1.16).[42a]

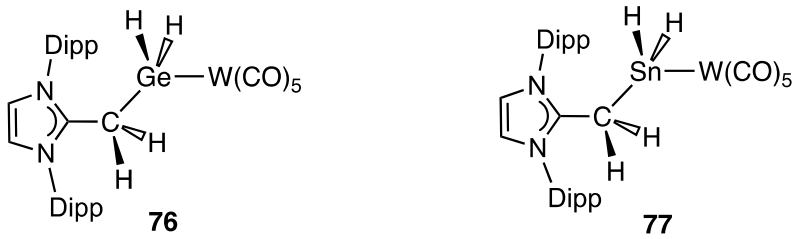

Figure 1.16. Donor-acceptor stabilization of GeH_2 (**76**) and SnH_2 (**77**) complexes with $IPrCH_2$.

A related LB/LA combination was also employed to isolate the heavier inorganic ethylene analogues H_2GeGeH_2, H_2SiGeH_2 and H_2SiSnH_2 in the form of the stable donor-acceptor complexes IPr•H_2Ge-GeH_2•$W(CO)_5$ (**78**), IPr•H_2Si-GeH_2•$W(CO)_5$ (**79**), IPr•H_2Si-SnH_2•$W(CO)_5$ (**80**), respectively (Figure 1.17).[76]

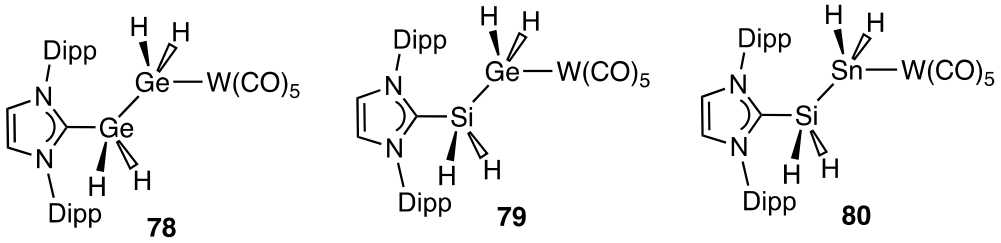

Figure 1.17. Donor-acceptor stabilization of H_2GeGeH_2 (**78**), H_2SiGeH_2 (**79**) and H_2SiSnH_2 (**80**) complexes.

1.4. Germanium Nanoparticles (GeNPs)

1.4.1 Properties and Applications

Germanium nanoparticles (GeNPs) represent a very promising class of main group material with a wide range of possible applications in the areas of optoelectronics, bioimaging and energy conversion/storage.[77] In addition, the large exciton radius (*ca.* 17.7 nm) of GeNPs results in quantum confinement effects within comparatively

large particle sizes.[78] This makes them advantageous for use in solar cells, flash memory devices, field effect transistors, and photodetectors.[79] Moreover, the low toxicity and environment friendly nature of GeNPs in comparison to widely used CdSe quantum dots opens the door for biological and medical applications, and their use as narrow band gap semiconductor nanomaterials.[80]

1.4.2 Known Synthetic Strategies for GeNPs.

Recently, a variety of methods have been explored for the synthesis of GeNPs;[81] however, a mild procedure involving precise control of size, dimension and surface functionality of GeNPs has not yet been achieved. Early reports on the synthesis of GeNPs were based on the reduction of $GeCl_4$ to metallic Ge with strong reducing agents, such as alkali metals or organometallic reagents.[82] Along this theme, Cho and co-workers reported the synthesis of amorphous GeNPs by treating $GeCl_4$ with sodium naphthalenide ($Na[C_{10}H_8]$) in diglyme at room temperature. Later $^{n}BuLi$ was added to isolate butyl-capped nanocrystals with an average diameter of 10 nm (Scheme 1.16).[82*c*] An alternative route to synthesize GeNPs involves the metathesis reaction of germanium zintl salts, such as NaGe, KGe or Mg_2Ge.[83] In this study by Kauzlarich and co-workers chloride-terminated Ge nanoparticles were prepared by refluxing $GeCl_4$ with NaGe in diglyme (Scheme 1.16). The surface chlorides can be replaced by alkyl groups (butyl or octyl) by treatment with the appropriate alkyl lithium reagent. Moreover, the chloride-capped GeNPs can be functionalized with different functional groups, such as acetal and alkoxy-substituents by halogen-ligand replacement chemistry.[83] A frequently used method for the synthesis of hydride-

terminated Ge nanoparticles is the reduction of Ge(II) or Ge(IV) species in the presence of hydride-based reducing agents (Scheme 1.16).[84] For example, Jiang and co-workers reported the synthesis of hydride terminated Ge nanoparticles by reacting $GeCl_4$ with $NaBH_4$ or $LiAlH_4$.[84] Other methods of producing GeNPs involve the high temperature decomposition (> 400 °C) of organogermanes or the reaction of Ge(II) halides (such as GeI_2) with n-butyllithium.[85] All of the above-mentioned routes to GeNPs involve either the use pyrophoric reagents and or harsh reaction conditions, or require very high temperatures.

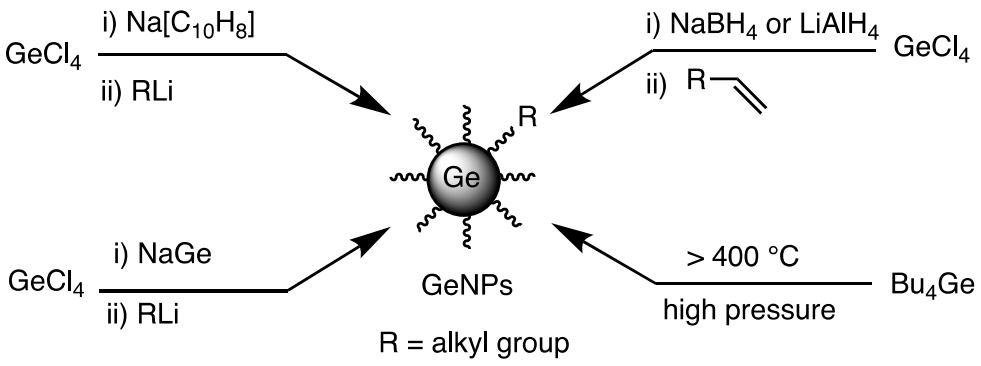

Scheme 1.16. Known synthetic methods for Ge nanoparticles (GeNPs).

As will be discussed in chapter 2 of this thesis, a one-pot method to synthesize GeNPs was developed from the controlled decomposition of the donor-acceptor complex $Ph_3PCMe_2{\bullet}GeH_2{\bullet}BH_3$. Hot injection (HI) and microwave irradiation (MI)-induced degradation of this bottleable precursor in presence of suitable capping ligands was used to access crystalline and comparatively monodisperse luminescent GeNPs at temperature below 200 °C.[49*b*]

1.5 Acknowledgement to the Collaborators

A portion of the work presented in this thesis has been done in collaboration with the other researchers within the Department of Chemistry, University of Alberta. Crystallographic studies for all the compounds presented in this thesis were performed by Dr. R. McDonald and Dr. M. J. Ferguson including mounting of crystals, operation of the diffractometer, refinement of the structures and preparation of the crystallographic data tables. Elemental analyses and mass spectrometric analyses were performed by Analytical Instrument Laboratory and Mass Spectrometry Laboratory at the Department of Chemistry, University of Alberta. The $^{2}H\{^{1}H\}$, ^{15}N, ^{119}Sn NMR spectra were taken with the help of M. Miskolzie and N. Dabral at the NMR Spectrometry Laboratory, University of Alberta.

In Chapter 2: The chemistry of N- and P-donor ligands (4-dimethylaminopyridine and tricyclohexylphosphine) toward $GeCl_2$ center were studied in collaboration with Sean M. McDonald and Kelsey C. Deutsch. The synthesis and characterization of germanium nanoparticles were performed in collaboration with Dr. Tapas K. Purkait and Prof. Jonathan G. C. Veinot at the Department of Chemistry, University of Alberta. Moreover, the photoluminescence lifetime study of the germanium nanoparticles was accomplished in collaboration with Glenda B. De Los Reyes and Prof. Frank A. Hegmann at the Department of Physics, University of Alberta.

In Chapter 4: The computation calculations were performed in collaboration with Dr. Christian Hering-Junghans.

According to the policy of our research group, each chapter of this thesis is essentially self-contained, and prepared in the form of a paper that is intended for publication in peer-reviewed journals.

A portion of this thesis is previously published and the publications are listed below.

Chapter 2:

3. Swarnakar, A. K.; McDonald, S. M.; Deutsch, K. C.; Choi, P.; Ferguson, M. J.; McDonald, R.; Rivard, E. *Inorg. Chem*. **2014**, *53*, 8662.
4. Purkait, T. K.; Swarnakar, A. K.; De Los Reyes, G. B.; Hegmann, F. A.; Rivard, E.; Veinot, J. G. C. *Nanoscale* **2015**, *7*, 2241.

Chapter 3:

Swarnakar, A. K.; Ferguson, M. J.; McDonald, R.; Rivard, E. *Dalton Trans*. **2016**, *45*, 6071.

Chapter 4:

3. Swarnakar, A. K.; Hering-Junghans, C.; Nagata, K.; Ferguson, M. J.; McDonald, R.; Tokitoh, N.; Rivard, E. *Angew. Chem. Int. Ed.* **2015**, *54*, 10666.
4. Swarnakar, A. K.; Hering-Junghans, C.; Ferguson, M. J.; McDonald, R.; Rivard, E. *Chem. Sci*. **2017**, *8,* 2337.

Chapter 5:

Swarnakar, A. K.; Ferguson, M. J.; McDonald, R.; Rivard, E. *Dalton Trans*. **2017**, *46*, 1406.

1.6 Reference

1. (*a*) Welch, G. C.; Juan, R. R. S.; Masuda, J. D.; Stephan, D. W. *Science* **2006**, *314*, 1124; (*b*) Welch, G. C.; Stephan, D. W. *J. Am. Chem. Soc*. **2007**, *129*, 1880; (*c*) McCahill, J. S. J.; Welch, G. C.; Stephan, D. W. *Angew. Chem. Int. Ed.* **2007**, *46*, 4968; (*d*) Chase, P. A.; Jurca, T.; Stephan, D. W. *Chem. Commun.* **2008**, 1701; (*e*) Hounjet, L. J.; Stephan, D. W. *Org. Process Res. Dev.* **2014**, *18*, 385.
2. (*a*) Manasevit, H. M. *Appl. Phys. Lett*. **1968**, *12*, 156; (*b*) Cowley, A. H.; Jones, R. A. *Polyhedron* **1994**, *13*, 1149; (*c*) Maury, F. *Adv. Mater*. **1991**, *3*, 542; (*d*) Thangaraju, B.; Kaliannan, P. *J. Phys. D: Appl. Phys.* **2000**, *33*, 1054; (*e*) Knapp, C. E.; Carmalt, C. J. *Chem. Soc. Rev.* **2016**, *45*, 1036; (*f*) Malik, M. D.; Afzaal, M.; O'Brien, P. *Chem. Rev*. **2010**, *110,* 4817; (*g*) Ekerdt, J. G.; Sun, Y. -M.; Szabo, A.; Szulczewski, G. J.; White, J. M. *Chem. Rev*. **1996**, *96*, 1499 and references therein.
3. (*a*) Power, P. P. *Chem. Rev.* **1999**, *99*, 3463; (*b*) Mizuhata, Y.; Sasamori, T.; Tokitoh, N. *Chem. Rev.* **2009**, *109*, 3479; (*c*) Power, P. P. *Nature* **2010**, *463*, 171; (*d*) Fischer, R. C.; Power, P. P. *Chem. Rev*. **2010**, *810*, 3877; (*e*) Rivard, E. *Chem. Soc. Rev.* **2016**, *45*, 989.
4. (*a*) Rivard, E.; Power, P. P. *Inorg. Chem.* **2007**, *46*, 10047; (*b*) Kays, D. L. *Chem. Soc. Rev.* **2016**, *45*, 1004.
5. (*a*) Stender, M.; Phillips, A. D.; Wright, R. J.; Power, P. P. *Angew. Chem. Int. Ed.* **2002**, *41*, 1785; (*b*) Phillips, A. D.; Wright, R. J.; Olmstead, M. M.; Power, P. P. *J. Am. Chem. Soc.* **2002**, *124*, 5930; (*c*) Pu, L.; Twamley, B.; Power, P. P. *J. Am. Chem. Soc.* **2000**, *122*, 3524.
6. Marks, T. J.; Newman, A. R. *J. Am. Chem. Soc*. **1973**, *95*, 769.

7. (*a*) Braunschweig, H.; Dewhurst, R. D.; Hammond, K.; Mies, J.; Radacki, K.; Vargas, A. *Science* **2012**, *336*, 11420; (*b*) Wang, Y.; Xie, Y.; Wei, P.; King, R. B.; Schaefer III, H. F.; Schleyer, P. v. R.; Robinson, G. H. *J. Am. Chem. Soc.* **2008**, *130*, 14970.
8. Gavrilova, A. L.; Bosnich, B. *Chem. Rev.* **2004**, *104*, 349.
9. (*a*) Wang, Y.; Robinson, G. H. *Inorg. Chem*. **2011**, *50*, 12326; (*b*) Rivard, E. *Dalton Trans.* **2014**, *43*, 8577; (*c*) Soleilhavoup, M.; Bertrand, G. *Acc. Chem. Res.* **2015**, *58*, 256.
10. (*a*) Beswick, M. A.; Palmer, J. S.; Wright, D. S. *Chem. Soc. Rev.* **1998**, *27*, 225; (*b*) Jutzi, P.; Burford, N. *Chem. Rev.* **1999**, *99*, 969.
11. (*a*) Almenningen, A.; Haaland, A.; Motzfeldt, T. *J. Organomet. Chem*. **1967**, *7*, 97; (*b*) Jutzi, P.; Kanne, D.; Kruger, C. *Angew. Chem. Int. Ed. Engl.* **1986**, *25*, 164; (*c*) Panatonni, C.; Bombieri, G.; Croatto, U. *Acta. Crystallogr*. **1966**, *21A*, 823; (*d*) Jutzi, P.; Kohl, F.; Hofman, P.; Kruger, C.; Tsay, Y. –H. *Chem. Ber.* **1980**, *113*, 757; (*e*) Cowley, A. H.; Jutzi, P.; Kohl, F. X.; Lasch, J. G.; Norman, N. C.; Schltiter. E. *Angew. Chem. Int. Ed. Engl.* **1984**, *23*, 616.
12. (*a*) Filippou, A. C.; Philippopoulos, A. I.; Portius, P.; Neumann, D. U. *Angew. Chem. Int. Ed*. **2000**, *39*, 2778; (*b*) Filippou, A. C.; Portius, P.; Philippopoulos, A. I. *Organometallics* **2002**, *21,* 653.
13. (*a*) Voigt, A.; Filipponi, S.; Macdonald, C. L. B.; Gorden, J. D.; Cowley, A. H. *Chem. Commun*. **2000**, 911; (*b*) Dohmeier, C.; Schnockel, H.; Robl, C.; Uwe, S.; Ahlrichs, R. *Angew. Chem. Int. Ed. Engl.* **1993**, *32*, 1655; (*c*) Burns, C. T.; Shapiro, P. J.; Budzelaar, P. H. M.; Willett, R.; Vij, A. *Organometallics* **2000,** *19,* 3361.

14. (*a*) Jutzi, P.; Wippermann, T.; Kruger, C.; Kraus, H. –J. *Angew. Chem. Int. Ed. Engl.* **1983**, *22*, 250; (*b*) Wiacek, R. J.; Jones, J. N.; Macdonald, C. L. B.; Cowley, A. H. *Can. J. Chem*. **2002**, *80*, 1518.

15. (*a*) Schiemenz, B.; Power, P. P. *Organometallics* **1996**, *15*, 958; (*b*) Simons, R. S.; Haubrich, S. T.; Mork, B. V.; Niemeyer, M.; Power, P. P. *Main Group Chem.* **1998**, *2*, 275; (*c*) Du, C. -J. F.; Hart, H.; Ng, D. K. -K. *J. Org. Chem.* **1986**, *51*, 3162; (*d*) Saednya, A.; Hart, H. *Synthesis* **1996**, *12*, 1455.

16. Su, J.; Li, X.-W.; Crittendon, R. C.; Robinson, G. H. *J. Am. Chem. Soc.* **1997**, *119*, 5471.

17. (*a*) Bytheway, I.; Lin, Z. *J. Am. Chem. Soc.* **1998**, *120*, 12133; (*b*) Xie, Y.; Schaefer, H. F.; Robinson, G. H. *Chem. Phys. Lett.* **2000**, *317*, 174.

18. Takagi, N.; Schmidt, M. W.; Nagase, S. *Organometallics* **2001**, *20*, 1646.

19. (*a*) Hardman, N. J.; Wright, R. J.; Phillips, A. D.; Power, P. P. *Angew. Chem. Int. Ed.* **2002**, *41*, 2842; (*b*) Wright, R. J.; Phillips, A. D.; Hardman, N. J.; Power, P. P. *J. Am. Chem. Soc.* **2002**, *124*, 8538; (*c*) Wright, R. J.; Phillips, A. D.; Hino, S.; Power, P. P. *J. Am. Chem. Soc.* **2005**, *127*, 4794.

20. Okazaki, R.; Unno, M.; Inamoto, N. *Chem. Lett.* **1987**, 2293.

21. Tokitoh, N.; Sasamori, T.; Okazaki, R. *Chem. Lett.* **1998**, 725.

22. (*a*) Tokitoh, N.; Arai, Y.; Okazaki, R.; Nagase, S. *Science* **1997**, *277*, 78; (*b*) Sasamori, T.; Takeda, N.; Tokitoh, N. *Chem. Commun*. **2000**, 1353.

23. Tokitoh, N.; Matsumoto, T.; Okazaki, R. *Bull. Chem. Soc. Jpn*. **1999**, *72*, 1165.

24. Okazaki, R.; Tokitoh, N. *Acc. Chem. Res.* **2000**, *33*, 625.

25. Suzuki, H.; Tokitoh, N.; Okazaki, R. Nagase, S.; Goto, M. *J. Am. Chem. Soc.* **1994**, *116*, 11578.

26. (*a*) Tokitoh, N.; Matsumoto, T.; Manmaru, K.; Okazaki, R. *J. Am. Chem. Soc.* **1993**, *115*, 8855; (*b*) Matsumoto, T.; Tokitoh, N.; Okazaki, R. *Angew. Chem. Int. Ed. Engl.* **1994**, *33*, 2316; (*c*) Matsumoto, T.; Tokitoh, N.; Okazaki, R. *J. Am. Chem. Soc.* **1999**, *121*, 8811.

27. Saito, M.; Tokitoh, N.; Okazaki, R. *J. Am. Chem. Soc.* **1997**, *119*, 11124.

28. Li, L.; Fukawa, T.; Matsuo, T.; Hashizume, D.; Fueno, H.; Tanaka, K.; Tamao, K. *Nat. Chem.* **2012**, *4*, 361.

29. Allen, F. H. *Acta Crystallogr.* **2002***, B58*, 380.

30. Igau, A.; Grutzmacher, H.; Baceiredo, A.; Bertrand, G. *J. Am. Chem. Soc*. **1988**, *110*, 6463.

31. Arduengo, A. J.; Harlow, R. L.; Kline, M. A. *J. Am. Chem. Soc.* **1991**, *113*, 361.

32. (*a*) Wang, Y.; Robinson, G. H. *Chem. Commun.* **2009**, 5201; (*b*) Siemeling, U. *Aust. J. Chem.* **2011**, *64*, 1109; (*c*) Martin, D.; Soleilhavoup, M.; Bertrand, G. *Chem. Sci.* **2011**, *2*, 389; (*d*) Wang, Y.; Robinson, G. H. *Dalton Trans.* **2012**, *41*, 337; (*e*) Clyburne, J. A. C.; McMullen, N. *Coord. Chem. Rev.* **2000**, *210*, 73.

33. Wang, Y.; Quillian, B.; Wei, P.; Wannere, C. S.; Xie, Y.; King, R. B.; Schaefer III, H. F.; Schleyer, P. v. R.; Robinson, G. H. *J. Am. Chem. Soc.* **2007**, *129*, 12412.

34. (*a*) Wang, Y.; Xie, Y.; Wei, P.; King, R. B.; Schäfer III, H. F.; Schleyer, P. v. R.; Robinson, G. H. *Science* **2008**, *321*, 1069; (*b*) Sidiropoulos, A.; Jones, C.; Stasch, A.; Klein, S.; Frenking, G. *Angew. Chem. Int. Ed.* **2009**, *48*, 9701; (*c*) Jones, C.;

Sidiropoulos, A.; Holzmann, N.; Frenking, G.; Stasch, A. *Chem. Commun.* **2012**, *48*, 9855.

35. Lavallo, V.; Canac, Y.; Präsang, C.; Donnadieu, B.; Bertrand, G. *Angew. Chem. Int. Ed.* **2005**, *44*, 5705.
36. Back, O.; Henry-Ellinger, M.; Martin, C. D.; Martin, D.; Bertrand, G. *Angew. Chem. Int. Ed.* **2013**, *52*, 2939.
37. (*a*) Kinjo, R.; Donnadieu, B.; Ali Celik, M.; Frenking, G.; Bertrand, G. *Science* **2011**, *333*, 610; (*b*) Ruiz, D. A.; Melaimi, M.; Bertrand, G. *Chem. Commun*. **2014**, *50*, 7837.
38. Ruiz, D. A.; Ung, G.; Melaimi, M.; Bertrand, G. *Angew. Chem. Int. Ed.* **2013**, *52*, 7590.
39. (*a*) Back, O.; Donnadieu, B.; Parameswaran, P.; Frenking, G.; Bertrand, G. *Nat. Chem.* **2010**, *2*, 369; (*b*) Kretschmer, R.; Ruiz, D. A.; Moore, C. E.; Rheingold, A. L.; Bertrand, G. *Angew. Chem. Int. Ed.* **2014**, *53*, 8176; (*c*) Dorsey, C. L.; Mushinski, R. M.; Hudnall, T. W. *Chem. Eur. J.* **2014**, *20*, 8914; (*d*) Back, O.; Celik, M. A.; Frenking, G.; Melaimi, M.; Donnadieu, B.; Bertrand, G. *J. Am. Chem. Soc.* **2010**, *132*, 10262.
40. Kuhn, N.; Bohnen, H.; Kreutzberg, J.; Bläser, D.; Boese, R. *J. Chem. Soc., Chem. Commun.* **1993**, *14*, 1136.
41. (*a*) Al-Rafia, S. M. I.; Malcolm, A. C.; Liew, S. K.; Ferguson, M. J.; McDonald, R.; Rivard, E. *Chem. Commun*. **2011**, *47*, 6987; (*b*) Dumrath, A.; Wu, X. -F.; Neumann, H.; Spannenberg, A.; Jackstell, R.; Beller, M. *Angew. Chem. Int. Ed*. **2010**, *49*, 8988; (*c*) Wang, Y.; Abraham, M. Y.; Gilliard Jr., R. J.; Sexton, D. R.; Wei, P.;

Robinson, G. H. *Organometallics* **2013**, *32*, 6639; (*d*) Powers, K.; Hering-Junghans, C.; McDonald, R.; Ferguson, M. J.; Rivard. E. *Polyhedron* **2016**, *108*, 8.

42. (*a*) Al-Rafia, S. M. I.; Ferguson, M. J.; Rivard, E. *Inorg. Chem.* **2011**, *50*, 10543; (*b*) Al-Rafia, S. M. I.; Momeni, M. R.; McDonald, R.; Ferguson, M. J.; Brown, A.; Rivard, E. *Angew. Chem. Int. Ed*. **2013**, *52*, 6390; (*c*) Berger, C. J.; He, G.; Merten, C.; McDonald, R.; Ferguson, M. J.; Rivard, E. *Inorg. Chem.* **2014**, *53*, 1475.
43. (*a*) Lee, W. -H.; Lin, Y. -F.; Lee, G. -H.; Peng, S. -M.; Chiu. C. -W. *Dalton Trans.* **2016**, *45*, 5937; (*b*) Ghadwal, R. S.; Reichmann, S. O.; Engelhardt, F.; Andrada, D. M.; Frenking, G. *Chem. Commun*. **2013**, *49*, 9440; (*c*) Ghadwal, R. S.; Schurmann, C. J.; Andrada, D. M.; Frenking, G. *Dalton Trans*. **2015**, *44*, 14359; (*d*) Ghadwal, R. S.; Schürmann, C. J.; Engelhardt, F.; Steinmetzger, C. *Eur. J. Inorg. Chem.* **2014**, 4921; (*e*) El-Hellani, A.; Monot, J.; Guillot, R.; Bour, C.; Gandon, V. *Inorg. Chem.* **2013**, *52*, 506.
44. Wittig, G.; Schöllkopf, U. *Chem. Ber*. **1954**, *87*, 1318.
45. (*a*) Pörschke, K. -R.; Wilke, G.; Mynott, R. *Chem. Ber*. **1985**, *118*, 298; (*b*) Fortier, S.; Kaltsoyannis, N.; Wu, G.; Hayton, T. W. *J. Am. Chem. Soc.* **2011**, *133*, 14224.
46. (*a*) Bestmann, H. J.; Sühs, K.; Röder, T. *Angew. Chem. Int. Ed. Engl.* **1981**, *20*, 1038; (*b*) Bestmann, H. J.; Röder, T.; Sühs, K. *Chem. Ber.* **1988**, *121*, 1509; (*c*) Breitsameter, F.; Schrödel, H. -P.; Schmidpeter, A.; Nöth, H.; Rojas-Lima, S. *Z. Anorg. Allg. Chem.* **1999**, *625*, 1293.
47. Hawthorne, F. M. *J. Am. Chem. Soc*. **1958**, *80*, 3480.

48. Borisova, I. V.; Zemlyansky, N. N.; Belsky, V. K.; Kolosova, N. D.; Sobolev, A. N.; Luzikov, Y. N.; Ustynyuk, Y. A.; Beletskaya, I. P. *J. Chem. Soc., Chem. Commun.* **1982**, 1090.

49. (*a*) Swarnakar, A. K.; McDonald, S. M.; Deutsch, K. C.; Choi, P.; Ferguson, M. J.; McDonald, R.; Rivard, E. *Inorg. Chem*. **2014**, *53*, 8662; (*b*) Purkait, T. K.; Swarnakar, A. K.; De Los Reyes, G. B.; Hegmann, F. A.; Rivard, E.; Veinot, J. G. C. *Nanoscale* **2015**, *7*, 2241.

50. Nowell, I. N.; Russell, D. R. *J. Chem. Soc., Chem. Commun*. **1967**, *817.*

51. (*a*) Einstein, F. W. B.; Pomeroy, R. K.; Rushman, P.; Willis, A. C. *Organometallics* **1985**, *4*, 250; (*b*) Usón, R.; Forniés, J.; Espinet, P.; Fortuño, C.; Tomas, M.; Welch, A. J. *J. Chem. Soc., Dalton Trans.* **1988**, 3005.

52. Bauer, J.; Braunschweig, H.; Dewhurst, R. D. *Chem. Rev.* **2012**, *112*, 4329.

53. (*a*) Braunschweig, H.; Gruß, K.; Radacki, K. *Angew. Chem. Int. Ed.* **2007**, *46*, 7782; (*b*) Bauer, J.; Braunschweig, H.; Brenner, P.; Kraft, K.; Radacki, K.; Schwab, K. *Chem. Eur. J.* **2010**, *16*, 11985.

54. (*a*) Mayer, J. M.; Calabrese, J. C. *Organometallics* **1984**, *3*, 1292; (*b*) Burlitch, J. M.; Leonowicz, M. E.; Petersen, R. B.; Hughes, R. E. *Inorg. Chem.* **1979**, *18*, 1097; (*c*) Golden, J. T.; Peterson, T. H.; Holland, P. H.; Bergman, R. G.; Andersen, A. R. *J. Am. Chem. Soc.* **1998**, *120*, 223.

55. Steinke, T.; Fischer, R. A.; Winter, M; Cokoja, M.; Gemel, C. *Dalton Trans*. **2005**, 55; (*b*) Braunschweig, H.; Gruß, K.; Radacki, K. *Inorg. Chem*. **2008**, *47*, 8597; (*c*) Aldridge, S.; Kays, D. L.; Bunn, N. R.; Coombs, N. D. *Main Group Met. Chem*. **2005**, *28*, 201.

56. (*a*) Charmant, J. P. H.; Fan, C.; Norman, N. C.; Pringle, P. G. *Dalton Trans.* **2007**, 114; (*b*) Braunschweig, H.; Brenner, P.; Müller, A.; Radacki, K.; Rais, D.; Uttinger, K. *Chem. Eur. J.* **2007**, *13*, 7171; (*c*) Braunschweig, H.; Radacki, K.; Uttinger, K. *Inorg. Chem.* **2007**, *46*, 8796; (*d*) Braunschweig, H.; Gruss, K.; Radacki, K. *Inorg. Chem.* **2008**, *47*, 8595; (*e*) Braunschweig, H.; Brenner, P.; Cogswell, P.; Kraft, K.; Schwab, K. *Chem. Commun.* **2010**, *46*, 7894.

57. (*a*) Braunschweig, H.; Radacki, K.; Schneider, A. *Science* **2010**, *328*, 345; (*b*) Braunschweig, H.; Radacki, K.; Schneider, A. *Angew. Chem. Int. Ed.* **2010**, *49*, 5993; (*c*) Braunschweig, H.; Radacki, K.; Schneider, A. *Chem. Commun.* **2010**, 46, 6473.

58. (*a*) Chan, D. M. T.; Marder, T. B. *Angew. Chem. Int. Ed. Engl.* **1988**, *27*, 442; (*b*) Beńi, Z.; Ros, R.; Tassan, A.; Scopelliti, R.; Roulet, R. *Dalton Trans*. **2005**, 315.

59. (*a*) Hupp, F.; Ma, M.; Kroll, F.; Jiménez-Halla, J. O. C.; Dewhurst, R. D.; Radacki, K.; Stasch, A.; Jones, C.; Braunschweig, H. *Chem. Eur. J.* **2014**, *20*, 16888; (*b*) Braunschweig, H.; Damme, A.; Dewhurst, R. D.; Hupp, F.; Jiménez-Halla, J. O. C.; Radacki, K. *Chem. Commun.* **2012**, *48*, 10410.

60. Swarnakar, A. K.; Ferguson, M. J.; McDonald, R.; Rivard, E. *Dalton Trans*. **2016**, *45*, 6071.

61. (*a*) Vogel, U.; Timoshkin, A. Y.; Scheer, M. *Angew. Chem. Int. Ed.* **2001**, *40*, 4409; (*b*) Vogel, U.; Hoemensch, P.; Schwan, K. -Ch.; Timoshkin, A. Y.; Scheer, M. *Chem. Eur. J.* **2003**, *9*, 515; (*c*) Schwan, K. -Ch.; Timoshkin, A. Y.; Zabel, M.; Scheer, M. *Chem. Eur. J.* **2006**, *12*, 4900; (*d*) Bodensteiner, M.; Vogel, U.; Timoshkin, A. Y.; Scheer, M. *Angew. Chem. Int. Ed.* **2009**, *48*, 4629; (*e*)

Bodensteiner, M.; Timoshkin, A. Y.; Peresypkina, E. V.; Vogel, U.; Scheer, M. *Chem. –Eur. J.* **2013**, *19*, 957; (*f*) Marquardt, C.; Adolf, A.; Stauber, A.; Bodensteiner, M.; Virovets, A. V.; Timoshkin, A. Y.; Scheer, M. *Chem. –Eur. J.* **2013**, *19*, 11887; (*g*) Marquardt, C.; Thoms, C.; Stauber, A.; Balázs, G.; Bodensteiner, M.; Scheer, M. *Angew. Chem. Int. Ed*. **2014**, *53*, 3727; (*h*) Marquardt, C.; Jurca, T.; Schwan, K.-C.; Stauber, A.; Virovets, A. V.; Whittell, G. R.; Manners, I.; Scheer, M. *Angew. Chem. Int. Ed.* **2015**, *54*, 13782.

62. (*a*) Johnson, J. C.; Choi, H. J.; Knutsen, K. P.; Schaller, R. D.; Yang, P.; Saykally, R. J. *Nat. Mater.* **2002**, *1*, 106; (*b*) Chen, C. C.; Yeh, C. C.; *Adv. Mater.* **2000**, *12*, 738; (*c*) Kim, H. M.; Kim, D. S.; Park, Y. S.; Kim, D. Y.; Kang, T. W.; Chung, K. S. *Adv. Mater.* **2002**, *14*, 991; (*d*) Seryogin, G.; Shalish, I.; Moberlychan, W.; Narayanamurti, V. *Nanotechnology* **2005**, *16*, 2342.
63. Malcolm, A. C.; Sabourin, K. J.; McDonald, R.; Ferguson, M. J.; Rivard, E. *Inorg. Chem.* **2012**, *51*, 12905.
64. (*a*) Lory, E. R.; Porter, R. F. *J. Am. Chem. Soc.* **1973**, *95*, 1766; (*b*) Kawashima, Y.; Kawaguchi, K.; Hirota. E. *J. Chem. Phys*. **1987**, *87*, 6331; (*c*) Thompson, C. A.; Andrews, L. *J. Am. Chem. Soc.* **1995**, *117*, 10125; (*d*) Zhang, F.; Maksyutenko, P.; Kaiser, R. I.; Mebel, A. M.; Gregusova, A.; Perera, S. A.; Bartlett, R. J. *J. Phys. Chem. A* **2010**, *114*, 12148.
65. For selected computational studies on HBNH, see: (*a*) Baird, N. C.; Datta, R. K. *Inorg. Chem.* **1972**, *11*, 17; (*b*) Matus, M. H.; Grant, D. J.; Nguyen, M. T.; Dixon, D. A. *J. Phys. Chem. C* **2009**, *113*, 16553; (*c*) Sundaram, R.; Scheiner, S.; Roy, A. K.; Kar, T. *J. Phys. Chem. C* **2015**, *119*, 3253.

66. Liu, H.; Jin, P.; Xue, Y. -M.; Dong, C.; Li, X.; Tang, C. -C.; Du, X. -W. *Angew. Chem. Int. Ed.* **2015**, *54*, 7051.

67. (*a*) Piane, R. T.; Narula, C. K. *Chem. Rev.* **1990**, *90*, 73; (*b*) Geim, A. K.; Grigorieva, I. V. *Nature* **2013**, *499*, 419; (*c*) Liu, L.; Park, J.; Siegel, D. A.; McCarty, K. F.; Clark, K. W.; Deng, W.; Basile, L.; Idrobo, J. C.; Li, A. P.; Gu, G. *Science* **2014**, *343*, 16.

68. (*a*) Swarnakar, A. K.; Hering-Junghans, C.; Nagata, K.; Ferguson, M. J.; McDonald, R.; Tokitoh, N.; Rivard, E. *Angew. Chem. Int. Ed.* **2015**, *54*, 10666; (*b*) Swarnakar, A. K.; Hering-Junghans, C.; Ferguson, M. J.; McDonald, R.; Rivard, E. *Chem. Sci*. **2017**, *8,* 2337.

69. (*a*) Amano, H.; Sawaki, N.; Akasaki, I.; Toyoda, Y. *Appl. Phys. Lett.* **1986**, *48*, 353; (*b*) Nakamura, S.; Harada, Y.; Seno, M. *Appl. Phys. Lett.* **1991**, *58*, 2021; (*c*) Morkoc, H.; Mohammad, S. N. *Science* **1995**, *267*, 51.

70. Swarnakar, A. K.; Ferguson, M. J.; McDonald, R.; Rivard, E. *Dalton Trans*. **2017**, *46*, 1406.

71. (*a*) Jasinski, J. M.; Gates, S. M. *Acc. Chem. Res.* **1991**, *24*, 9; (*b*) Isobe, C.; Cho, H. -C., Sewell, J. E. *Surf. Sci*. **1993**, *295*, 117.

72. (*a*) Wang, X.; Andrews, L.; Kushto, G. P. *J. Phys. Chem. A* **2002**, *106*, 5809; (*b*) Smith, T. C.; Clouthier, D. J.; Sha, W. Adam, A. G. *J. Chem. Phys.* **2000**, *113*, 9567.

73. Thimer, K. C.; Al-Rafia, S. M. I.; Ferguson, M. J.; McDonald, R.; Rivard, E. *Chem. Commun.* **2009**, 7119.

74. Al-Rafia, S. M. I.; Malcolm, A. C.; Liew, S. K.; Ferguson, M. J.; Rivard, E. *J. Am. Chem. Soc.* **2011**, *133*, 777.

75. Al-Rafia, S. M. I.; Malcolm, A. C.; McDonald, R.; Ferguson, M. J.; Rivard, E. *Chem. Commun.* **2012**, *48*, 1308.

76. (*a*) Al-Rafia, S. M. I.; Momeni, M. R.; Ferguson, M. J.; McDonald, R.; Brown, A.; Rivard, E. *Organometallics* **2013**, *32*, 6658; (*b*) Al-Rafia, S. M. I.; Malcolm, A. C.; McDonald, R.; Ferguson, M. J.; Rivard, E. *Angew. Chem. Int. Ed.* **2011**, *50*, 8354.

77. Kamata, Y. *Mater. Today* **2008**, *11*, 30.

78. Maeda, Y. *Phys. Rev. B: Condens. Matter Mater. Phys.* **1995**, *51*, 1658.

79. (*a*) Pillarisetty, R. *Nature* **2011**, *479*, 324; (*b*) Hekmatshoar, B.; Shahrjerdi, D.; Hopstaken, M.; Fogel, K.; Sadana, D. K. *Appl. Phys. Lett*. **2012**, *101*, 032102; (*c*) Guter, W.; Schone, J.; Philipps, S. P.; Steiner, M.; Siefer, G.; Wekkeli, A.; Welser, E.; Oliva, E.; Bett, A. W.; Dimroth, F. *Appl. Phys. Lett*. **2009**, *94*, 223504; (*d*) Chakraborty, G.; Sengupta, A.; Requejo, F. G.; Sarkar, C. K. *J. Appl. Phys.* **2011**, *109*, 064504; (*e*) Assefa, S.; Xia, F. N. A.; Vlasov, Y. A. *Nature* **2010**, *464*, U80.

80. Lambert, T. N.; Andrews, N. L.; Gerung, H.; Boyle, T. J.; Oliver, J. M.; Wilson, B. S.; Han, S. M. *Small* **2007**, *3*, 691.

81. Vaughn II, D. D.; Schaak, R. E. *Chem. Soc. Rev.* **2013**, *42*, 2861.

82. (*a*) Kornowski, A.; Giersig, M.; Vogel, R.; Chemseddine, A.; Weller, H. *Adv. Mater.* **1993**, *5*, 634; (*b*) Chiu, H. W.; Chervin, C. N.; Kauzlarich, S. M. *Chem. Mater.* **2005**, *17*, 4858; (*c*) Lee, H.; Kim, M. G.; Choi, C. H.; Sun, Y. K.; Yoon, C. S.; Cho, J. *J. Phys. Chem. B* **2005**, *109*, 20719.

83. (*a*) Taylor, B. R.; Kauzlarich, S. M.; Lee, H. W. H.; Delgado, G. R. *Chem. Mater*. **1998**, *10*, 22; (*b*) Tanke, R. S.; Kauzlarich, S. M.; Patten, T. E.; Pettigrew, K. A.; Murphy, D. L.; Thompson, M. E.; Lee, H. W. H. *Chem. Mater*. **2003**, *15*, 1682.

84. (*a*) Wu, H. P.; Liu, J. F.; Wang, Y. W.; Zengand, Y. W.; Jiang, J. Z. *Mater. Lett*. **2006**, *60*, 986; (*b*) Fok, E.; Shih, M. L.; Meldrum, A.; Veinot, J. G. C.; *Chem. Commun*. **2004**, 386; (*c*) Lu, X. M.; Korgel, B. A.; Johnston, K. P. *Chem. Mater*. **2005**, *17*, 6479.

85. (*a*) Henderson, E. J.; Hessel, C. M.; Veinot, J. G. C. *J. Am. Chem. Soc.* **2008**, *130*, 3624; (*b*) Lee, D. C.; Pietryga, J. M.; Robel, I.; Werder, D. J.; Schaller, R. D.; Klimov, V. I. *J. Am. Chem. Soc*. **2009**, *131*, 3436.

Chapter 2: Application of the Donor-Acceptor Concept to Intercept Group 14 Dihydrides Using a Wittig Reagent and One-Pot Synthesis of Germanium Nanoparticles

2.1 Introduction

The use of electron donating ligands to intercept/stabilize reactive inorganic element centers is a widely explored concept in inorganic chemistry. Recently, *N*-heterocyclic carbenes (NHCs) have received considerable attention in this regard due to their ease of synthesis and ability to tune the steric bulk about the ligating carbon centers.[1] A commonly employed NHC in formally low oxidation state main group element chemistry is IPr (IPr = $[(HCNDipp)_2C:]$, Dipp = 2,6-$^{i}Pr_2C_6H_3$), which has been used to access stable complexes of E_2 (E = B, Si, Ge, Sn, P and As)[2] and related species with unusual/novel bonding environments.[3] The Rivard group has also employed IPr in conjunction with suitable Lewis acid (BH_3 and $W(CO)_5$) to prepare various inorganic group 14 element methylene $:EH_2$ and ethylene $H_2EE'H_2$ complexes (E and E′ = Si, Ge and/or Sn) via a general donor-acceptor protocol.[4] In addition, it was shown that many of these parent main group hydrides can be accessed using the ylidic *N*-heterocyclic olefin (NHO) donor, $IPr{=}CH_2$ [$IPr{=}CH_2 = (HCNDipp)_2C{=}CH_2$] in place of IPr.[4e,4f,5] Added interest from this work stems from the implication of $:EH_2$ species, such as the silylene: $:SiH_2$, as key intermediates in the growth of semiconducting films from gas phase precursors (*e.g.* SiH_4; Scheme 1.14).[6]

In this chapter, attempts are made to prepare low oxidation state group 14 element hydride complexes with the aid of common phosphine and pyridine-based donors. In addition, the Wittig reagent $Ph_3P{=}CMe_2$[7] is shown to be an excellent ligand for molecular main group chemistry by virtue of the nucleophilic character of the terminal carbon atom (Scheme 2.1). Furthermore, the ability to rapidly prepare structural variants of this Wittig reagent from inexpensive reagents makes this system advantageous over well-known *N*-heterocyclic carbene-based donors. It should be mentioned that while the use of related Wittig reagents[8] as ligands is known for transition metals and actinides,[9] well-defined coordination chemistry involving R'_3PCR_2 donors within the main group remains a largely untouched area.[10] Here it is also shown that mild heating of the GeH_2 precursor, stabilized by Wittig reagent, $Ph_3P{=}CMe_2$, yields crystalline germanium nanoparticles (GeNPs) *via* hot injection (HI) and

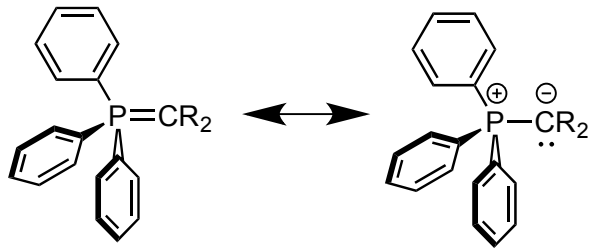

Scheme 2.1. Representative resonance forms for Ph_3PCR_2.

2.2 Results and Discussions

While carbon-based donors are known to bind/stabilize main group element polyhydrides,[3a,4,5a,11] the donor-acceptor protocol was verified by including phosphine and pyridine-based Lewis bases (LBs) to yield new adducts of the general form, LB•EH_2•LA (LA = Lewis acid). A motivation for such studies would be to later study the controlled thermolysis of these complexes to generate group 14 metal coatings and/or nanoparticles.[4g] It should be mentioned that nanomaterials are often capped with phosphorus- or nitrogen-containing ligands to engender solubility and to prevent quenching of luminescence by surface reactive sites.[12] Moreover the use of amines and phosphines within the context of low oxidation state group 14 coordination chemistry has precedence.[13]

First, Ge(II) dihalide adducts of the widely explored donors, 4-dimethylaminopyridine (DMAP) and tricyclohexylphosphine (Cy_3P) were synthesized. Specifically, these adducts were obtained by combining either DMAP or Cy_3P with Cl_2Ge•dioxane in toluene to afford the respective Ge(II) dichloride complexes DMAP•$GeCl_2$ (**1**) and Cy_3P•$GeCl_2$ (**2**)[14] as air-sensitive (yet thermally stable) colorless solids (Scheme 2.2). While the synthesis of the DMAP adduct, **1** proceeded in a quantitative fashion, the synthesis of Cy_3P•$GeCl_2$ (**2**) routinely yielded a $[Cy_3PH]^+$ containing by-product (presumably as a $GeCl_3^-$ salt).[15] So further purification was necessary to afford pure **2** by fractional crystallization from toluene/hexanes. Both compounds **1** and **2** have been structurally authenticated by X-ray crystallography (Figure 2.1) and, as expected, pyramidalized Ge centers are

present with an angle sum at Ge (ΣGe) for compound **1** of 280.83(7)° [ΣGe for compound **2** = 284.33(4)°].

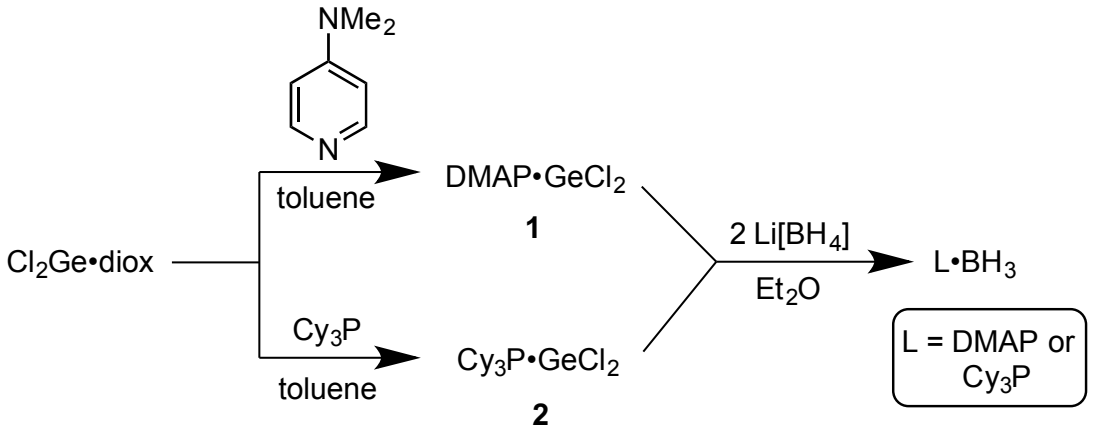

Scheme 2.2. Synthesis of DMAP and Cy_3P adducts of $GeCl_2$ (**1** and **2**) and interaction of these species with excess $Li[BH_4]$.

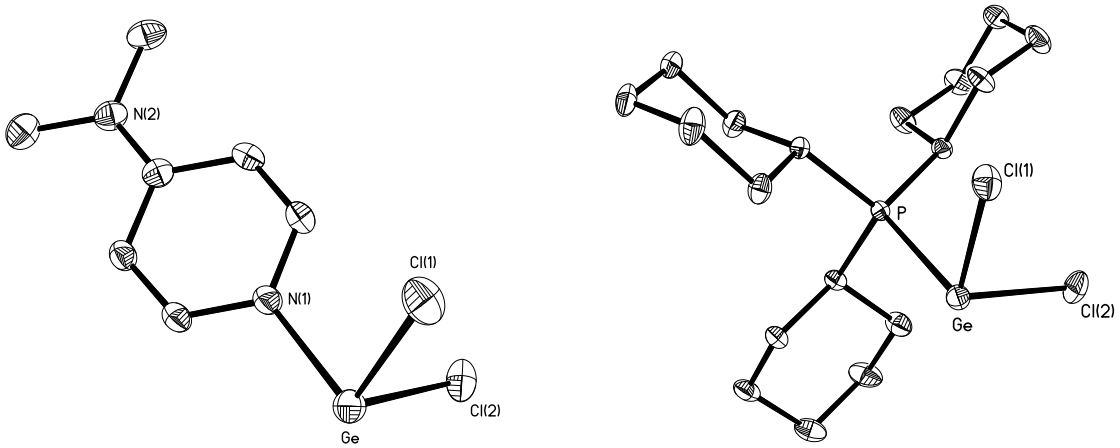

Figure 2.1. Molecular structures of DMAP•$GeCl_2$ (**1**) (left) and Cy_3P•$GeCl_2$ (**2**) (right) with thermal ellipsoids at the 30 % probably level. All hydrogen atoms have been omitted for clarity. Selected bond lengths [Å] and angles [°]: *Compound 1*: Ge-N(1) 2.028(2), Ge-Cl(1) 2.2881(8), Ge-Cl(2) 2.2907(9); N-Ge-Cl(1) 93.03(7), N-Ge-Cl(2) 92.49(7), Cl(1)-Ge-Cl(2) 95.31(3). *Compound 2*: Ge-P 2.5087(7), Ge-Cl(1) 2.2782(7), Ge-Cl(2) 2.2723(7); P-Ge-Cl(1) 93.96(3), P-Ge-Cl(2) 93.21(2), Cl(1)-Ge-Cl(2) 97.16(2).

In order to obtain donor-acceptor complexes of GeH_2, both the compounds, DMAP•$GeCl_2$ (**1**) and Cy_3P•$GeCl_2$ (**2**) were treated with a soluble hydride source. However, when **1** and **2** were separately combined with two equivalents of lithium borohydride Li[BH_4] in ether, the only spectroscopically identifiable products were the known adducts DMAP•BH_3 and Cy_3P•BH_3, respectively; these reactions also afforded copious amounts of grey precipitate which is assumed to be the elemental germanium (Scheme 2.2). These observations are in contrast to what was found with the strongly donating *N*-heterocyclic carbene IPr, which yields IPr•GeH_2•BH_3 under similar reaction conditions as an isolable colorless solid.[4a]

This study was motivated by the structural parallels that exist between Wittig reagents and *N*-heterocyclic olefins (such as IPr=CH_2) due to the mutual presence of ylidic bonding, leading to significant electron density being positioned at a terminal carbon atom (Scheme 2.1).[5] Prior studies with the donor Ph_3P=CH_2 revealed a potential ligand degradation pathway wherein deprotonation of a terminal methylene unit occurs in the presence of electron deficient main group compounds to yield R_xE-CH=PPh_3 species.[16] Accordingly, I focused on the phosphorus ylide Ph_3P=CMe_2 (**3**)[7] which does not contain any acidic hydrogen atoms adjacent to the carbon ligation site. Fortunately the methylated donor Ph_3P=CMe_2 (**3**)[7] can be conveniently prepared in high yield as a moisture-sensitive red solid by treating the commercially available phosphonium salt [Ph_3PCHMe_2]I with ^nBuLi in toluene, followed by removal of the LiI by-product by filtration. Crystals of **3** were also analyzed by single-crystal X-ray crystallography and the resulting molecular structure is shown in Figure 2.2.

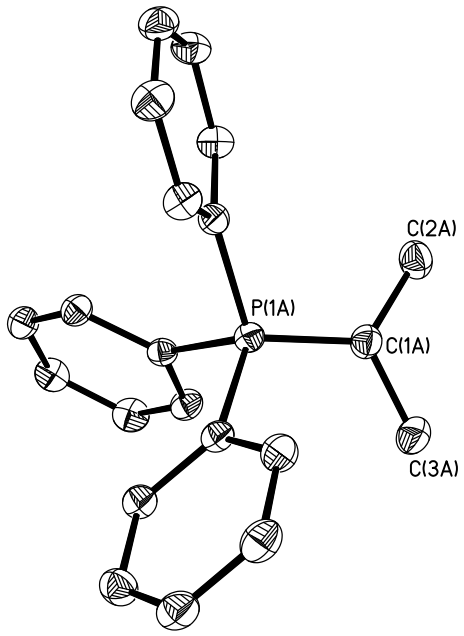

Figure 2.2. Molecular structure of Ph_3PCMe_2 (**3**) with thermal ellipsoids at the 30 % probability level. All hydrogen atoms have been omitted for clarity. Selected bond lengths (Å) and angles (°): P-C(1A) 1.6785(18), C(2A)-C(1A)-P(1A) 122.07(14), C(3A)-C(1A)-P(1A) 120.12(14), C(2A)-C(1A)-C(3A) 114.13(16).

The formation of the stable Ge(II) dihalide adduct Ph_3PCMe_2•$GeCl_2$ (**4**) was accomplished by combining equimolar amounts of $Ph_3P{=}CMe_2$ (**3**) and Cl_2Ge•dioxane in toluene solvent (eqn. 2.1). Compound **4** can be obtained in analytically pure form via re-crystallization from CH_2Cl_2/hexanes and the crystallographically determined structure of this species is presented as Figure 2.3. The binding of the Wittig reagent **3** to a $GeCl_2$ unit (to form **4**) is accompanied by a significant ^{31}P NMR shift from 9.8 to 37.0 ppm. The methyl substituents within the Ph_3PCMe_2 donor in **4** appear as a doublet resonance at 1.77 ppm in the ^{1}H NMR spectrum, and this signal is shifted upfield in comparison to the methyl resonance within the free ligand **3** (2.17 ppm). Ph_3PCMe_2•$GeCl_2$ exhibits a pyramidal geometry about germanium [ΣGe = 287.42(8)°] consistent with the presence of a lone pair at

Ge (Figure 2.3). As will be seen in all complexes of Ph_3PCMe_2 in this study, the binding of the nucleophilic carbon center in Ph_3PCMe_2 to a $GeCl_2$ unit results in elongation of the intraligand P-C bond (from 1.6785(18) Å in free Ph_3PCMe_2 (**3**) to 1.807(2) Å in Ph_3PCMe_2•$GeCl_2$ (**4**)); this effect can be rationalized by a reduction in C(p)→P-C(σ*) hyperconjugative interactions once **3** participates in adduct formation. Also, the contraction of P-C^{Ph} bonds in Ph_3PCMe_2•$GeCl_2$ (**4**) was observed compared to the free ligand, Ph_3PCMe_2 (**3**) (the average P-C^{Ph} bond distance in **3** is 1.827 (2) Å, whereas it is found to be 1.806(2) Å in compound **4**). This observation also suggests that the reduction of C(p)→P-C(σ*) donation occurs upon binding to the Ge center. The formally dative C-Ge bond length in Ph_3PCMe_2•$GeCl_2$ (**4**) [2.1535(19) Å] is slightly elongated with respect to the corresponding distance in IPr•$GeCl_2$ [2.112(2) Å];[4a] direct structural comparison of **4** with the ylide adduct IPrC[illegible]

crys[illegible]

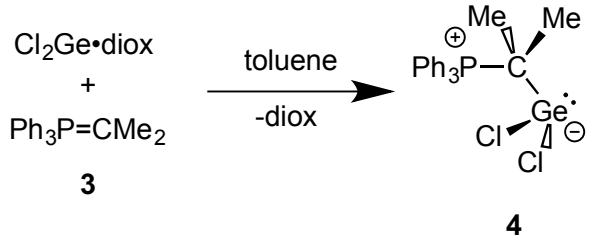

(2.1)

Interestingly, when Ph_3PCMe_2•$GeCl_2$ (**4**) was treated with two equivalents of $Li[BH_4]$ in diethyl ether, clean Cl/H exchange transpired to yield the isolable germanium dihydride-borane adduct Ph_3PCMe_2•GeH_2•BH_3 (**5**) (eqn. 2.2). The successful installation of hydride functionality at the germanium atom in **5** was evidenced by ^{1}H NMR spectroscopy, which revealed the presence of a new broad

resonance at 4.63 ppm for the Ge-*H* protons. In addition, IR spectroscopy clearly displayed a Ge-H stretching band at 1975 cm^{-1} which is similar in value as the vibration at 1987 cm^{-1} belonging to a GeH_2 moiety in IPr•GeH_2•BH_3.[4a]

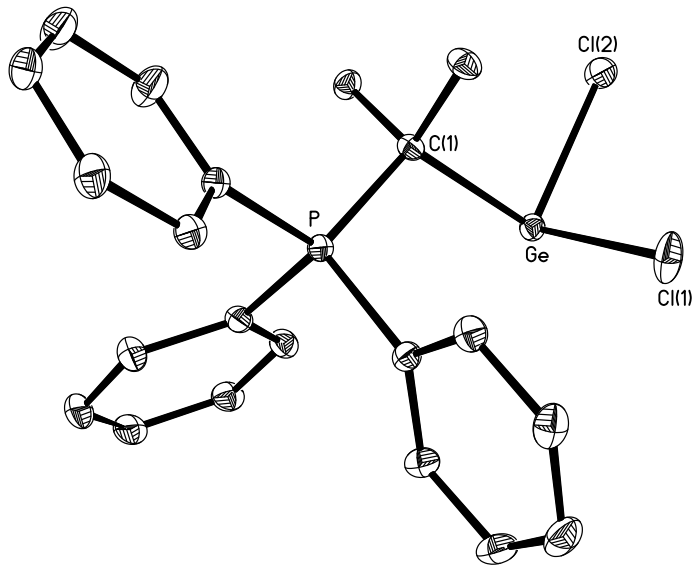

Figure 2.3. Molecular structure of Ph_3PCMe_2•$GeCl_2$ (**4**) with thermal ellipsoids at the 30 % probability level. All hydrogen atoms have been omitted for clarity. Selected bond lengths (Å) and angles (°): Ge–Cl (1) 2.2735(6), Ge-Cl (2) 2.3106(6), Ge-C (1) 2.1535(19); C(1)-Ge-Cl(1) 99.07(6), C(1)-Ge-Cl(2) 93.25(5), Cl(1)-Ge-Cl(2) 95.10(2).

Compound **5** gave a ^{11}B NMR spectrum with a quartet resonance at -39.4 ppm (in C_6D_6; $^1J_{BH}$ = 95.4 Hz) that was assigned to the terminal BH_3 unit, which is comparable with the ^{11}B NMR resonances observed previously for IPr•GeH_2•BH_3 (-40.0 ppm;

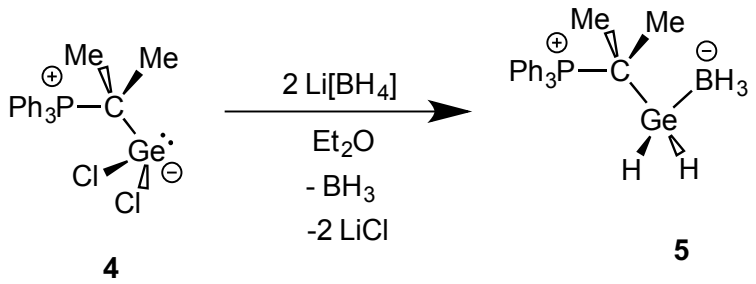

(2.2)

As shown in Figure 2.4, Ph_3PCMe_2•GeH_2•BH_3 (**5**) exhibits a tetrahedral coordination environment at Ge with crystallographically determined Ge-H bond distances of 1.477(18) and 1.46(2) Å. The adjacent Ge-B and Ge-C bond lengths are 2.0786(17) and 2.0406(13) Å, respectively, which are elongated by *ca.* 0.03 Å in comparison to the related distances found in the *N*-heterocyclic carbene adduct IPr•GeH_2•BH_3 [Ge-B = 2.053(3) Å; Ge-C = 2.011(2)Å]. Therefore, the metrical data suggests that Ph_3PCMe_2 is a weaker donor than the *N*-heterocyclic carbene, IPr (*vide infra*).

The deutero analogue of **5**, Ph_3CMe_2•GeD_2•BD_3 (**5D**) was also synthesized by combining two mole ratios of Li[BD_4] with **4** in Et_2O. As expected, the $^2H\{^1H\}$ NMR spectrum of **5D** consisted of broad peaks positioned at 4.63 and 1.56 ppm, corresponding to GeD_2 and BD_3 units, respectively.

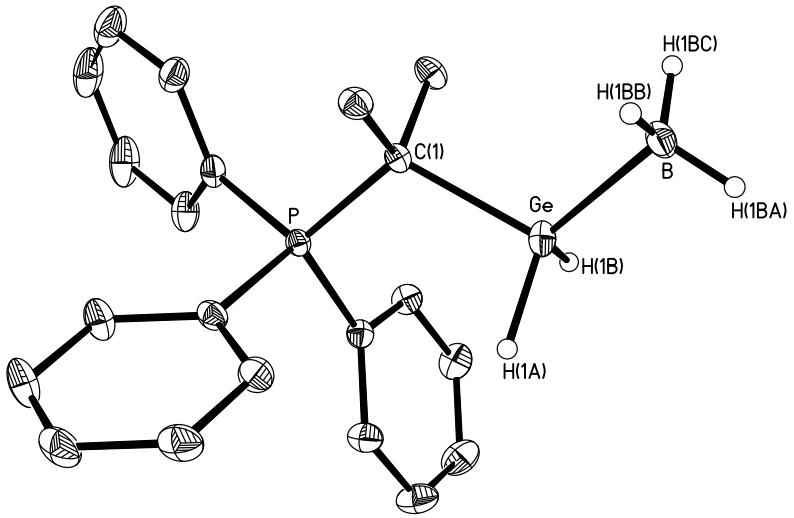

Figure 2.4. Molecular structure of Ph_3PCMe_2•GeH_2•BH_3 (**5**) with thermal ellipsoids at the 30 % probability level. All carbon-bound hydrogen atoms and THF solvate have been omitted for clarity. Selected bond lengths (Å) and angles (°): Ge–B 2.0786(17), Ge-C (1) 2.0406(13), Ge–H(1A) 1.477(18), Ge–H(1B) 1.46(2); C(1)–

Ge–B 111.26(6), C(1)–Ge–H(1A) 103.5(7), C(1)-Ge–H(1B) 100.8(8), H(1A)-Ge-H(1B) 103.4(11), H-B-H 116.7(8) to 118.9(7).

The Wittig reagent-appended germanium (II) dihydride complex Ph_3PCMe_2•GeH_2•BH_3 (**5**) showed similar thermal stability in solution in relation to IPr•GeH_2•BH_3. For example, a toluene-d_8 solution of Ph_3PCMe_2•GeH_2•BH_3 (**5**) was heated in a J-Young NMR tube at 100 °C for 24 hrs which led to the decomposition of **5** to afford Ph_3P•BH_3[17] (> 95 % yield by ^{31}P NMR spectroscopy; δ = 21.7 ppm); for comparison, IPr•GeH_2•BH_3 decomposes in hot toluene to yield IPr•BH_3.[4a] ^{11}B{^{1}H} NMR spectroscopy on the product mixture formed when **5** is heated also confirmed the presence of Ph_3P•BH_3 (d, δ = 42.1 ppm, $^1J_{BP}$ = 43.7 Hz) with the accompanying formation of a volatile product at *ca.* 80 ppm which is tentatively assigned as being the triorganoborane $^iPr_3B$ (literature ^{11}B NMR shift = 83.7 ppm in C_6D_6).[18] One possible route for this decomposition process is hydride transfer[19] from an E-H group (E = Ge or B) to a *C*Me_2 carbon atom of the Wittig donor, leading to population of a C-P σ* orbital and release of PPh_3, which is later trapped by liberated BH_3 to form Ph_3P•BH_3. The insoluble precipitate which formed during the thermolysis of Ph_3PCMe_2•GeH_2•BH_3 (**5**) in toluene was identified as elemental germanium according to EDX analysis (Figure 2.5); in addition, this solid was imaged by SEM which revealed the formation of bulk materials with globular morphology as shown in Figure 2.6.

It appears that Ph_3P=CMe_2 is a weaker electron pair donor than the carbene IPr, as Ph_3PCMe_2•GeH_2•BH_3 (**5**) rapidly reacts with a stoichiometric amount of IPr to

afford IPr•GeH_2•BH_3 and free $Ph_3P{=}CMe_2$ via a Lewis base exchange reaction, as determined by NMR spectroscopy.

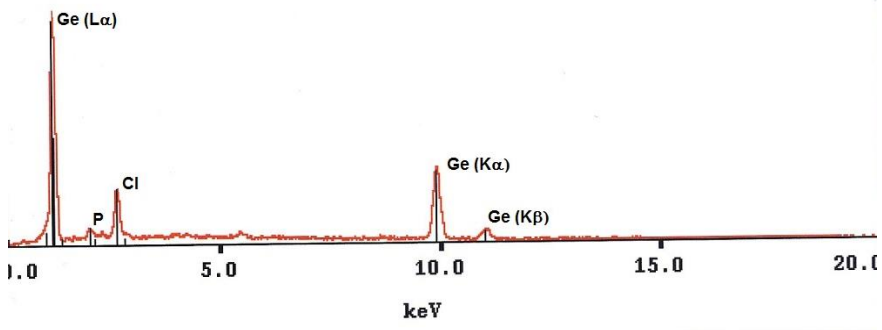

Figure 2.5. EDX spectrum of the insoluble precipitate (germanium metal) formed from the thermolysis of Ph_3PCMe_2•GeH_2•BH_3 (**5**)

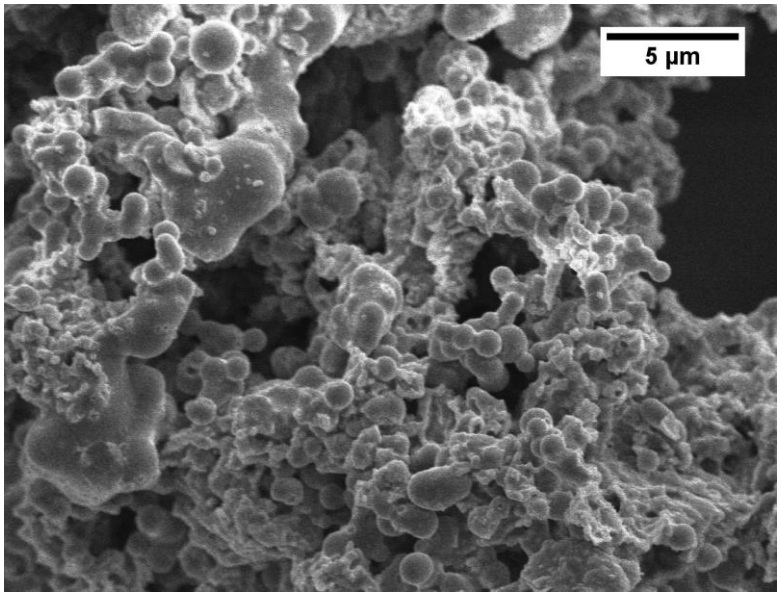

Figure 2.6: SEM of Ge metal formed from the thermolysis of Ph_3PCMe_2•GeH_2•BH_3

Of note, previous attempts to form IPrCH_2•GeH_2•BH_3 led to loss of germanium metal and the isolation of IPrCH_2•BH_3 as the sole donor-containing product.[5a] Thus Ph_3PCMe_2 is likely a stronger donor than the *N*-heterocyclic olefin IPrCH_2 and the previously discussed Lewis bases Cy_3P and DMAP. The mechanism

by which LB•GeH_2•BH_3 complexes (LB = Lewis base) degrade to yield the boranes LB•BH_3 is unknown at this time. Either LB-Ge or Ge-B bond scission (or even hydride transfer from Ge[19]) could be involved as the key step in the decomposition process.

Synthesis of Ge(II) hydride complex Ph_3PCMe_2•GeH_2 was also attempted by treating the $GeCl_2$ adduct **4** with the milder reducing agent K[HB^{s}Bu$_3$]. It was hoped that hydride delivery would occur to yield the less acidic and more hindered borane, ^{s}Bu$_3$B, as a by-product; this could inhibit adduct formation between the borane and the Ge center.[4a] However Ph_3PCMe_2•$GeCl_2$ (**4**) reacts with two equivalents of K[HB^{s}Bu$_3$] to yield free PPh_3 and ^{s}Bu$_3$B[20] according to ^{31}P and ^{11}B NMR spectroscopy, along with the formation of grey precipitate (presumably elemental Ge).

Analogous coordination and hydride transfer chemistry was explored between the Wittig reagent $Ph_3P{=}CMe_2$ and Sn(II) halides. As a start, the Sn(II) halide adduct Ph_3PCMe_2•$SnCl_2$ (**6**) was prepared from the direct reaction of $Ph_3P{=}CMe_2$ and $SnCl_2$ in a toluene/THF mixture (Scheme 2.3). This reaction proceeds to high yield if conducted over a short time frame of 3 hrs. Ph_3PCMe_2•$SnCl_2$ (**6**) was also characterized by single-crystal X-ray crystallography and the molecular structure of this adduct is found in Figure 2.7. The most salient metrical parameters of **6** include a Sn-C bond length of 2.3518(14) Å and a sum of the bond angles at Sn of 273.61(6)°; this latter value is substantially smaller than in the Ge congener **4** [287.42(8)°] as is expected for an increase in s-character within the sterochemically active Sn lone pair in Ph_3PCMe_2•$SnCl_2$ (**6**).

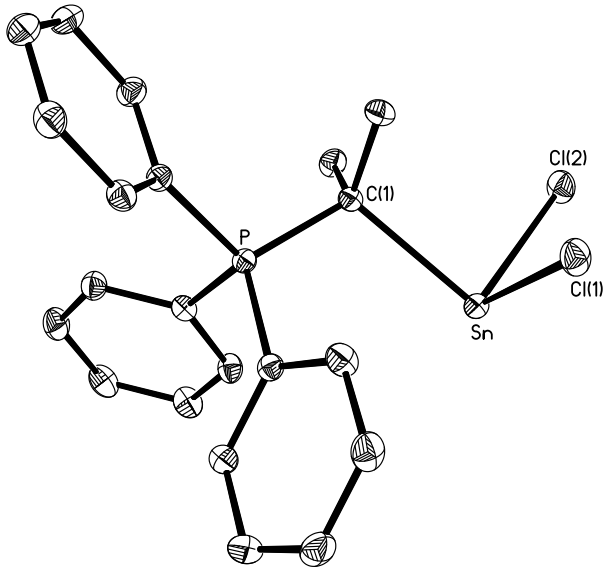

Figure 2.7. Molecular structure of Ph_3PCMe_2•$SnCl_2$ (**6**) with thermal ellipsoids at the 30 % probability level. All hydrogen atoms have been omitted for clarity. Selected bond lengths (Å) and angles (°): Sn-C(1) 2.3518(4), Sn-Cl(1) 2.4854(4), Sn-Cl(2) 2.4852(4), P-C(1) 1.8036(15); Cl(1)-Sn-Cl(2) 87.828(15), C(1)-Sn-Cl(1) 94.87(4), C(1)-Sn-Cl(2) 90.91(4).

If this reaction is allowed to proceed for longer periods (> 24 hrs), formation of the phosphonium salt, $[Ph_3PCHMe_2]SnCl_3$ transpires as evidenced by the emergence of a new ^{31}P signal at 30.9 ppm. The by-product, $[Ph_3PCHMe_2][SnCl_3]$ was also characterized by single crystal X-ray crystallography and the molecular structure of this salt is shown in Figure 2.8. In an attempt to synthesize a SnH_2 complex, Ph_3PCMe_2•$SnCl_2$ (**6**) was reacted with the hydride source, $Li[BH_4]$. However, when **6** was treated with two equivalents of $Li[BH_4]$ in Et_2O, the formation of Ph_3PCMe_2•BH_3 (**7**) along with a black precipitate (presumably metallic tin) was observed (Scheme 2.3). Compound **7** was reported previously by Bestmann and co-workers.[10*a*]

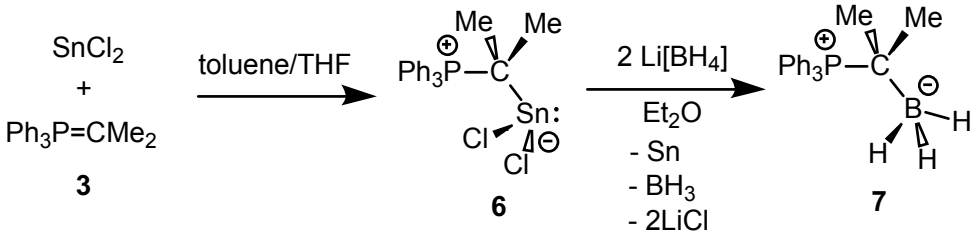

Scheme 2.3. Synthesis of Ph_3PCMe_2•$SnCl_2$ (**6**) and its conversion to Ph_3PCMe_2•BH_3 (**7**).

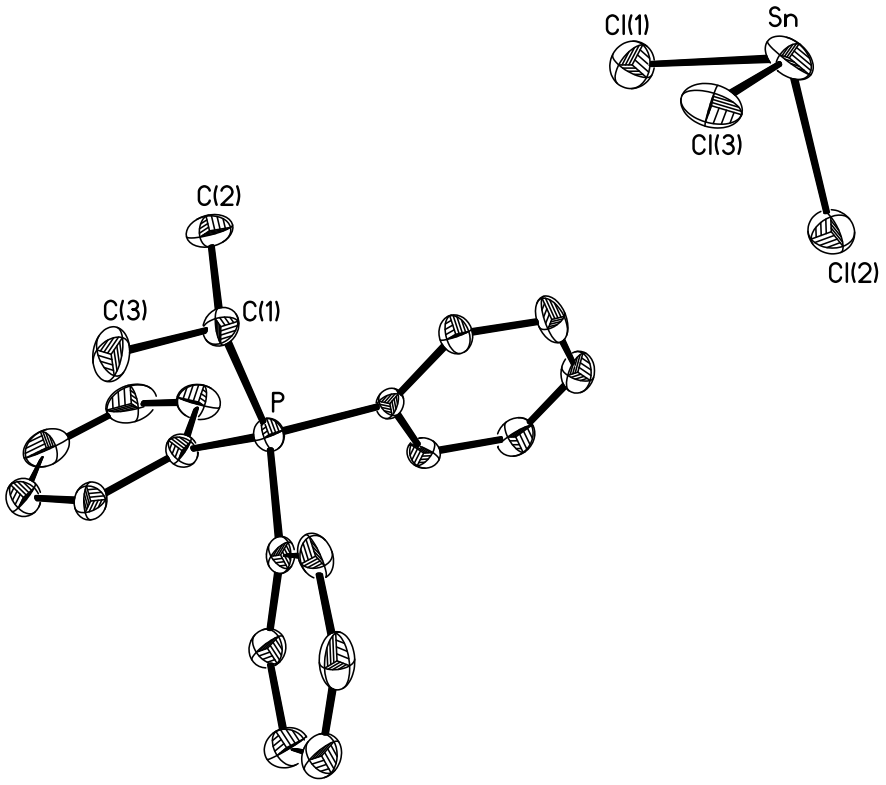

Figure 2.8. Molecular structure of $[Ph_3PCHMe_2][SnCl_3]$ with thermal ellipsoids at the 30 % probability level. All hydrogen atoms and toluene molecule have been omitted for clarity. Selected bond lengths (Å) and angles (°): P-C(1) 1.822(6), Sn-Cl(1) 2.449(3), Sn-Cl(2) 2.472(2), Sn-Cl(3) 2.485(3) ,C(2)-C(1)-P 109.6(5), C(3)-C(1)-P 111.5(5), Cl(1)-Sn-Cl(2) 93.55(9), Cl(1)-Sn-Cl(3) 95.48(8), Cl(2)-Sn-Cl(3) 95.08(8).

An independent synthesis of **7** was accomplished from the reaction of Ph_3PCMe_2 and THF•BH_3 in order to obtain structural characterization by X-ray crystallography (Figure 2.9). It is known from prior studies, and confirmed above, that the synthesis of Sn(II) dihydride (SnH_2) complexes is a more challenging endeavor than GeH_2 adducts as a result of decreased Lewis acidic and basic character at Sn, leading to weaker coordinative interactions.[4g]

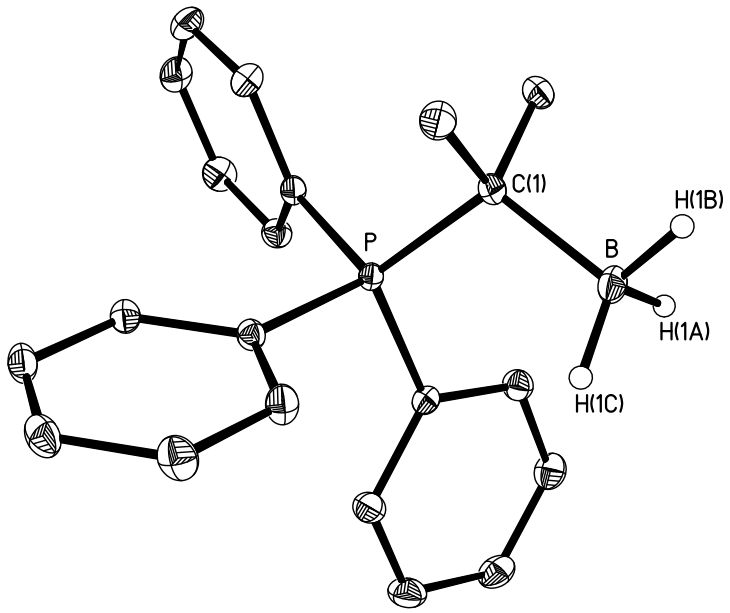

Figure 2.9. Molecular structure of Ph_3PCMe_2•BH_3 (**7**) with thermal ellipsoids at the 30 % probability level. All hydrogen atoms have been omitted for clarity. Selected bond lengths (Å) and angles (°): P-C(1) 1.8205(11), C(1)-B 1.6631(18), B-H(1A) 1.153(16), B-H(1B) 1.146(17), B-H(1C) 1.132(17), C(2)-C(1)-P 109.71(8), C(3)-C(1)-P 109.30(8), P-C(1)-B 109.60(8), H(1A)-B-H(1B) 108.6(12), H(1A)-B-H(1C) 110.0(12), H(1B)-B-H(1C) 110.6(12).

In order to increase the eventual Lewis acidity of a coordinated SnH_2 unit, a highly electron deficient $W(CO)_5$ group was introduced as the acceptor moiety within the donor-acceptor protocol; a related approach worked well for the isolation of the formal Sn(II) dihydride adducts, IPr•SnH_2•$W(CO)_5$ and IPrCH_2•SnH_2•$W(CO)_5$.[4b,5a]

The requisite $SnCl_2$ precursor to a tin hydride-Wittig reagent complex, Ph_3PCMe_2•$SnCl_2$•$W(CO)_5$ (**8**), was prepared in nearly quantitative yield as a colorless solid by a THF solvent displacement reaction between the known tin chloride tungsten pentacarbonyl adduct $(THF)_2$•$SnCl_2$•$W(CO)_5$[21] and the two-electron Wittig donor Ph_3PCMe_2 (**3**) (eqn. 2.3). The formation of Ph_3PCMe_2•$SnCl_2$•$W(CO)_5$ (**8**) was accompanied by a large change in chemical shift in the ^{31}P NMR spectrum relative to the free $Ph_3P{=}CMe_2$ (9.8 ppm) to yield a singlet resonance at 38.2 ppm with flanking tin satellites ($^3J_{PSn}$ = 44.5 Hz). The IR spectrum of **8** shows two resolvable stretching bands at 1930 and 2060 cm^{-1} consistent with a LB•$W(CO)_5$ environment (LB = Lewis base), while a ^{119}Sn NMR resonance, located at 131.3 ppm, is similar as the resonance observed for Ph_3PCMe_2•$SnCl_2$ (**6**) (113.3 ppm), despite the change in coordination number at tin. The related *N*-heterocyclic carbene adduct IPr•$SnCl_2$•$W(CO)_5$ has a ^{119}Sn resonance positioned at -71.3 ppm,[4b] while the ylidic *N*-heterocyclic olefin complex $IPrCH_2$•$SnCl_2$•$W(CO)_5$ yields a resonance at -96 ppm.[5a]

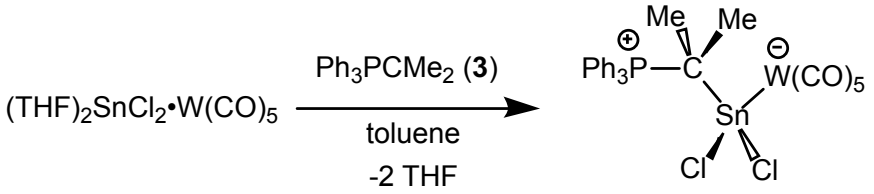

(2.3)

8

The molecular structure of Ph_3PCMe_2•$SnCl_2$•$W(CO)_5$ (**8**) is presented in Figure 2.10. As discussed earlier for related adducts, binding of the $Ph_3P{=}CMe_2$ ligand to a $SnCl_2$•$W(CO)_5$ unit leads to considerable elongation of the Ph_3*P*-*C*Me_2 P-C bond length (from 1.6785(18) Å in the free ligand to 1.8174(18) Å in **8**). The

adjacent C-Sn bond length in **8** is 2.2660(18) Å and is similar in value as the C-Sn interaction in the *N*-heterocyclic olefin bound Sn(II) complex $IPrCH_2$•$SnCl_2$•$W(CO)_5$ [2.2435(5) Å *avg.*].[5a] The Sn-W distance in **8** is 2.73047(15) Å and is slightly shorter than the corresponding distances in the structurally authenticated adducts Cy_3P•$SnCl_2$•$W(CO)_5$ [2.7438(2) Å][4e] and $IPrCH_2$•$SnCl_2$•$W(CO)_5$ [2.758(4) Å *avg.*].[5a] As expected, a localized C_{4v} coordination environment exists about the tungsten center in **8** with a nearly co-linear Sn-W-C(1) array [177.02(7)°] and Sn-W-C(2-5) bond angles involving the remaining CO groups that approach orthogonal geometries [83.98(7) to 96.07(6)°].

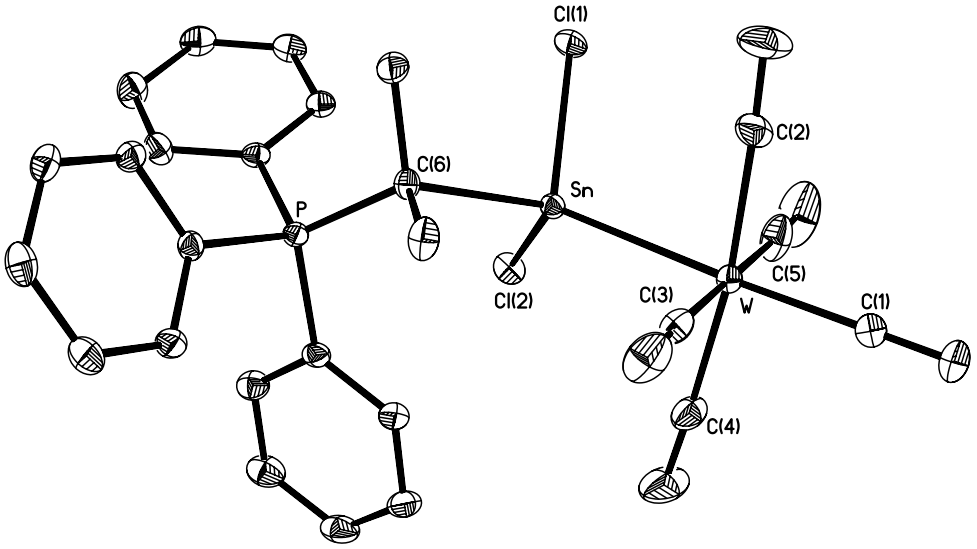

Figure 2.10. Molecular structure of Ph_3PCMe_2•$SnCl_2$•$W(CO)_5$ (**8**) with thermal ellipsoids presented at a 30 % probability level. All hydrogen atoms have been omitted for clarity. Selected bond lengths (Å) and angles (°): C(6)-Sn 2.2660(18), P-C(6) 1.8174(18), Sn-Cl(1) 2.4217(5), Sn-Cl(2) 2.4018(5), Sn-W 2.73047(15), W-C(1) 2.002(2), W-C(2-5) 2.025(2) to 2.038(2); C(6)-Sn-W 123.82(5), Cl(1)-Sn-Cl(2) 93.901(18), Sn-W-C(1) 177.02(7), Sn-W-C(2-5) 83.98(7) to 96.07(6).

With the successful installation of a Lewis acidic $W(CO)_5$ group and a Wittig electron pair donor at Sn to give Ph_3PCMe_2•$SnCl_2$•$W(CO)_5$ (**8**), this compound was then combined with the soluble borohydride salt, $Li[BH_4]$, in Et_2O (eqn. 2.4). The resulting mixture contained the target Sn(II) dihydride adduct Ph_3PCMe_2•SnH_2•$W(CO)_5$ (**9**) which could be isolated as a brown solid after crystallization from a diethyl ether/hexanes mixture at -35 °C. Compound **9** was readily identified by the emergence of a new characteristic singlet resonance at 6.66 ppm in the ^1H NMR spectrum which displayed a set of resolvable tin satellites ($^1J_{H-119Sn}$ = 1030 Hz, $^1J_{H-117Sn}$ = 991 Hz) as expected for the formation of a tin (II) hydride with terminally-positioned hydrogen atoms.[3a,4b,5a,22] Moreover, a triplet resonance at -49.8 ppm was noted in the ^{119}Sn NMR spectrum of **9** with a $^1J_{Sn-H}$ coupling constant which mirrored the value obtained from ^1H NMR spectroscopy. Sn-H IR vibrations were also located at 1740 cm^{-1} with proximal bands from 1891 to 2040 cm^{-1} due to ν(CO) stretches within the $W(CO)_5$ unit. The A_1^1 ν(CO) stretching band at 2040 cm^{-1} in Ph_3PCMe_2•SnH_2•$W(CO)_5$ (**9**) is positioned at a lower wavenumber in relation to the $SnCl_2$ adduct Ph_3PCMe_2•$SnCl_2$•$W(CO)_5$ (**8**) (2060 cm^{-1}) consistent with a higher degree of electron donation to $W(CO)_5$ from the electron-rich SnH_2 unit in **9**. The analogous complex $IPrCH_2$•SnH_2•$W(CO)_5$ affords a ν(Sn-H) band in the IR spectrum at 1758 cm^{-1} with a high frequency CO stretching band at 2043 cm^{-1}, each of which are close in value as in Ph_3PCMe_2•SnH_2•$W(CO)_5$ (**9**), reflecting the similar donating ability of the Wittig and NHO donors in this system.[5a]

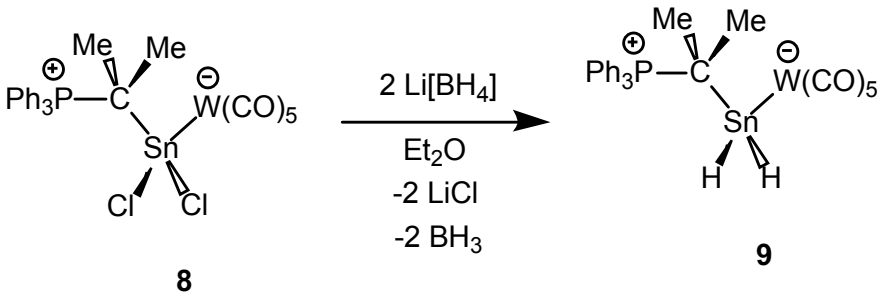

(2.4)

The molecular structure of $Ph_3PCMe_2{\bullet}SnH_2{\bullet}W(CO)_5$ (**9**) is presented in Figure 2.11 and confirms the successful isolation of a new member of the SnH_2 adduct series. By virtue of the hydridic character (and enhanced electron density) of the hydrogen atoms at tin ($Sn^{\delta+}$-$H^{\delta-}$) that facilitates X-ray scattering, these atoms could be located in the electron difference map. Accordingly, Sn-H distances of 1.73(4) and 1.71(3) Å in **9** were determined. The Sn-W distance in $Ph_3PCMe_2{\bullet}SnH_2{\bullet}W(CO)_5$ (**9**) is elongated [2.7833(2) Å] in relation to the Sn-W bond length in the $SnCl_2$ adduct $Ph_3PCMe_2{\bullet}SnCl_2{\bullet}W(CO)_5$ (**8**) [2.73407(15) Å], despite the anticipated increase of electron density at the SnH_2 center in relation to $SnCl_2$ (which bears electron withdrawing Cl atoms). The Wittig carbon-tin interaction in $Ph_3PCMe_2{\bullet}SnH_2{\bullet}W(CO)_5$ (**9**) is the same within experimental error [2.269(2) Å] as the C-Sn bond length in the halogenated congener 8 [2.2660(18) Å]. The intraligand P-C distance involving the CMe_2 unit in **9** is 1.808(2) Å and matches well the adjacent P-C bond distances within the Ph_3P array [1.802(2) to 1.807(2) Å] indicating the presence of single bonds in each case.

Our investigations into the thermal stability of Ph_3PCMe_2•SnH_2•$W(CO)_5$ (**9**) show that this Wittig complex is less stable than the corresponding carbene-supported adduct IPr•SnH_2•$W(CO)_5$ reported by our group in 2011.[4b] Compound **9** melts with decomposition to generate black insoluble product(s) upon heating to 80-81 °C under

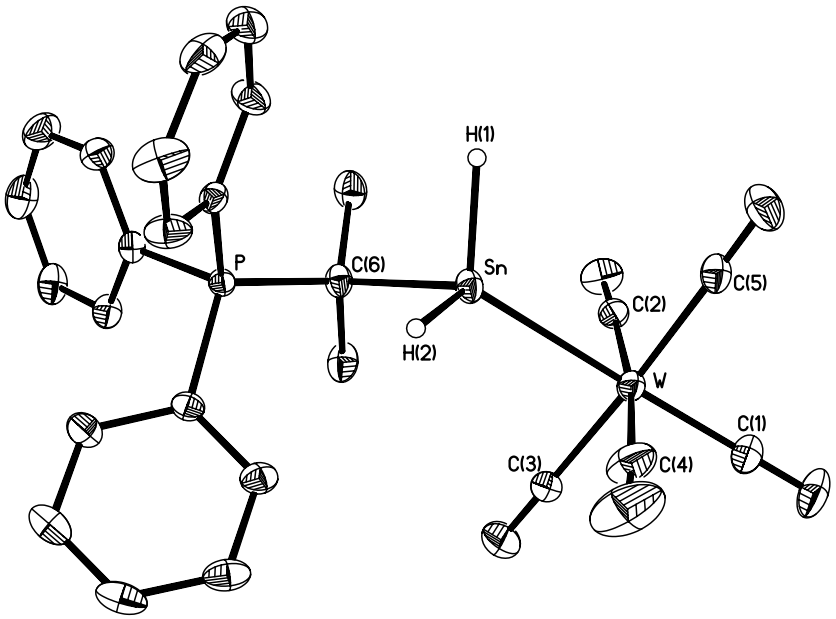

Figure 2.11. Molecular structure of Ph_3PCMe_2•SnH_2•$W(CO)_5$ (**9**) with thermal ellipsoids at a 30 % probability level. All carbon-bound hydrogen atoms and diethyl ether solvate have been omitted for clarity. Selected bond lengths (Å) and angles (°): C(6)-Sn 2.269(2), P-C(6) 1.808(2), Sn-H(1) 1.73(4), Sn-H(2) 1.71(3), Sn-W 2.7833(2), W-C(1) 2.019(3), W-C(2-5) 2.026(3) to 2.043(3); C(6)-Sn-W 117.03(6), H(1)-Sn-H(2) 100.3(17), Sn-W-C(1) 174.66(8), Sn-W-C(2-5) 82.77(10) to 92.66(8).

an atmosphere of nitrogen. In addition, compound **9** is stable for a few hours in C_6D_6 solution at room temperature, however if solutions of **9** are allowed to stand for greater than 24 hours, the complete decomposition of **9** into a black metallic precipitate (containing either Sn metal, Sn/W clusters or both) and free Ph_3P occurs, as determined by ^{31}P NMR spectroscopy; notably, IPr•SnH_2•$W(CO)_5$ is stable under

similar conditions. One possible method by which compound **9** decomposes is via C-Sn bond cleavage leading to the production of free $Ph_3P{=}CMe_2$ (**3**) and the generation of unstable $H_2Sn{\bullet}W(CO)_5$. In order to further evaluate the relative binding affinity of Ph_3PCMe_2, $IPrCH_2$ and IPr, the Wittig analogue $Ph_3PCMe_2{\bullet}SnH_2{\bullet}W(CO)_5$ (**9**) was combined with stoichiometric amounts of IPr or $IPrCH_2$ in toluene at room temperature. These reactions led to the full decomposition of $Ph_3PCMe_2{\bullet}SnH_2{\bullet}W(CO)_5$ before any discernable reactivity (Lewis base exchange) with either IPr or $IPrCH_2$ was detected.

An attempt was also made to prepare the germastannene adduct $Ph_3PCMe_2{\bullet}Cl_2Ge\text{-}SnCl_2{\bullet}W(CO)_5$ by combining the nucleophilic Ge(II) adduct $Ph_3PCMe_2{\bullet}GeCl_2$ (**4**) with the known stannylene complex, $(THF)_2{\bullet}SnCl_2{\bullet}W(CO)_5$.[21] However as noted previously within the IPr adduct series,[4f] $SnCl_2/GeCl_2$ exchange at tungsten transpired to afford the thermally stable germylene complex, $Ph_3PCMe_2{\bullet}GeCl_2{\bullet}W(CO)_5$ (**10**) (eqn. 2.5).

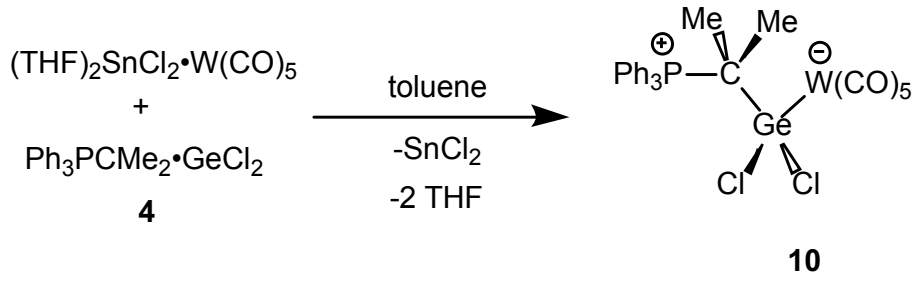

(2.5)

Compound **10** was also characterized by a single-crystal X-ray diffraction study (Figure 2.12) and the geometric parameters about the Ge center in **10** are similar to those found in the NHO adduct $IPrCH_2{\bullet}GeCl_2{\bullet}W(CO)_5$, with a slightly elongated Ge-C dative linkage in 10 [2.0826(15) Å] observed relative to in the $IPrCH_2$ adduct [2.053(2) Å].[5a]

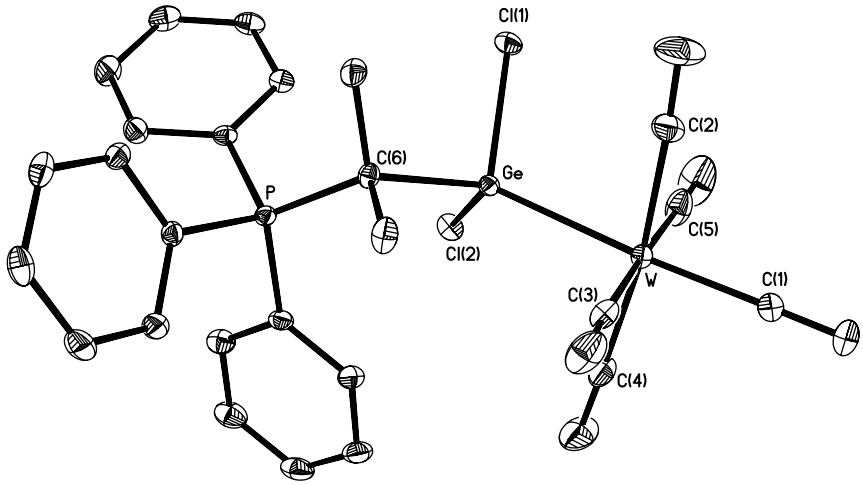

Figure 2.12. Molecular structure of Ph_3PCMe_2•$GeCl_2$•$W(CO)_5$ (**10**) with thermal ellipsoids presented at a 30 % probability level. All hydrogen atoms have been omitted for clarity. Selected bond lengths (Å) and angles (°): C(6)-Ge 2.0826(15), P-C(6) 1.8315(16), Ge-Cl(1) 2.2588(4), Ge-Cl(2) 2.2369(4), Ge-W 2.59459(17), W-C(1) 2.0072(18), W-C(2-5) 2.0293(19) to 2.0397(18); C(6)-Ge-W 124.17(4), Cl(1)-Ge-Cl(2) 94.679(17), Ge-W-C(1) 175.25(5), Ge-W-C(2-5) 82.75(6) to 99.11(5).

After showing that the donating ability of the *C*-methylated Wittig reagent $Ph_3P{=}CMe_2$ (**3**) is sufficient to obtain reactive hydrides, such as GeH_2 and SnH_2, I decided to explore the thermal decomposition chemistry of the GeH_2-Wittig adduct, Ph_3PCMe_2•GeH_2•BH_3 (**5**) in more controlled conditions to yield germanium nanoparticles (GeNPs). Germanium nanopatricles (GeNPs) are promising materials for optoelectronic applications such as solar cells, flash memory devices, and lithium-ion batteries.[23,24] In addition, as a result of its large exciton radius (*ca.* 17.7 nm) and possible involvement of quantum confinement in light emission, GeNPs could also display tunable size-dependent photoluminescence (PL) spanning the visible and infrared regions of the electromagnetic spectrum.[25-29] Moreover, GeNPs are

biocompatible/non-toxic making them attractive as biological imaging and therapeutic agents.[26] Recently, Vaughn and Schaak presented a comprehensive review outlining known methods for preparing colloidal GeNPs.[28] A variety of approaches have been explored including: solution-phase precursor reduction, metathesis of Ge Zintl phases, thermally induced organogermane decomposition, co-reduction of GeI_2 and GeI_4, *etc.*[23,25,30-44] However precise control of NC dimension and surface chemistry has not yet been achieved. In this regard, methods for preparing well-defined GeNPs are of paramount importance to the future growth of this field.

As mentioned earlier, mild heating of the GeH_2-Wittig adduct Ph_3PCMe_2•GeH_2•BH_3 (**5**) in toluene to *ca.* 100 °C yields elemental germanium and soluble byproducts. Positing that Ge particle growth could be controlled to enable nanoparticles formation, the requisite germanium (II) dihydride precursor, **5**, was subjected to hot injection (HI) or microwave irradiation (MI) protocols at predefined temperatures (*i.e.*, 100, 150, 190, and 250 °C; see experimental section). To synthesize hydrophobic dodecyl-terminated GeNPs (Scheme 2.4), HI or MI of **5** were performed in a 1:1 (v:v) solution of diphenyl ether and 1-dodecene. Whereas, hydrophilic GeNPs bearing surface bonded 3-dimethylamino-1-propene moieties (*i.e.*, Me_2N-GeNPs) were generated by subjecting **5** to MI in 3-dimethylamino-1-propyne; this alkyne adopts the dual role of capping ligand and microwave absorber. Unfortunately, the comparatively low boiling point (*i.e.*, 81 °C) of this alkyne precluded its application in HI syntheses. Surface functionalized GeNPs were freed from reaction by-products (*e.g.*, Ph_3P•BH_3) upon sonication in appropriate

solvent/antisolvent mixtures followed by centrifugation (see experimental section). The initial attempts to prepare hydrophobic GeNPs at 100 and 150 °C *via* HI or MI thermolysis of **5** in 1-dodecene/diphenyl ether yielded only trace product. Bright field transmission electron microscopy (TEM) images of the NPs synthesized *via* MI of 5 at 150 °C showed sparse polydisperse particles of ca. 3-5 nm dimensions (Figure 2.13); HRTEM highlights their crystallinity, however limited yield prevented further characterization.

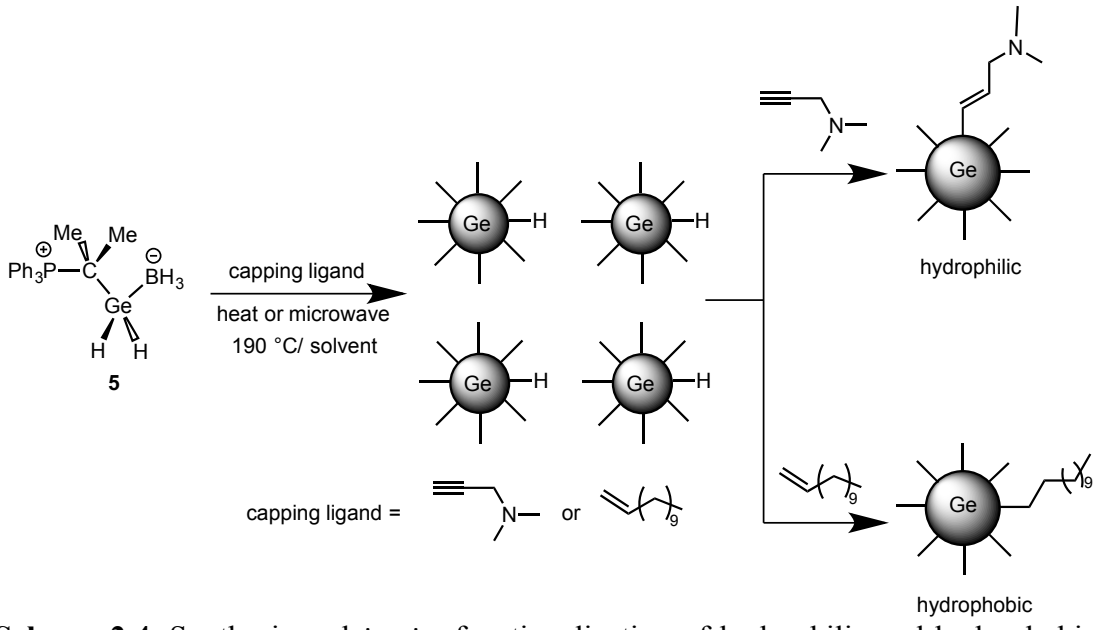

Scheme 2.4. Synthesis and *in-situ* functionalization of hydrophilic and hydrophobic GeNPs upon thermal or microwave irradiation induced decomposition of $Ph_3PCMe_2{\bullet}GeH_2{\bullet}BH_3$ (**5**).

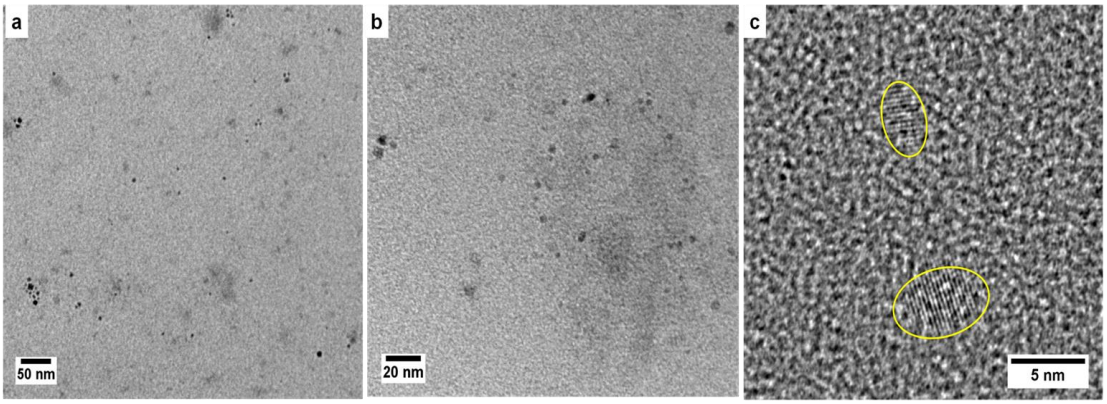

Figure 2.13. Representative brightfield TEM and HRTEM images of dodecyl-GeNPs obtained from MI decomposition of **5** at 30 mg/ 5mL at 150 °C in 1:1 (v:v) dodecene/diphenyl ether.

GeNP size and yield increased with HI and MI reaction temperatures. TEM images (Figure 2.14) of dodecyl-GeNPs synthesized by HI at 190 °C show pseudospherical particles with average diameters (d_{avg}) of 10.1±1.7 nm. Dodecyl- and Me_2N-terminated GeNPs (Figures 2.14b, c) synthesized *via* MI at 190 °C are smaller (*i.e.*, d_{avg} = 5.35 ± 0.96 nm, dodecyl-GeNPs; d_{avg} = 5.41 ± 0.85 nm, Me_2N-GeNPs). In all cases HRTEM images show d-spacings of 0.33 nm that are readily attributed to the Ge(111) plane of diamond-structured Ge.[40]

To evaluate the role of precursor concentration on NP size, MI induced decomposition of **5** was performed at concentrations of 10 and 20 mg/5 mL in 1:1 (v:v) 1-dodecene/diphenyl ether. A clear trend emerges that sees smaller particles produced with decreased precursor concentration (Figures 2.15 and 2.16).

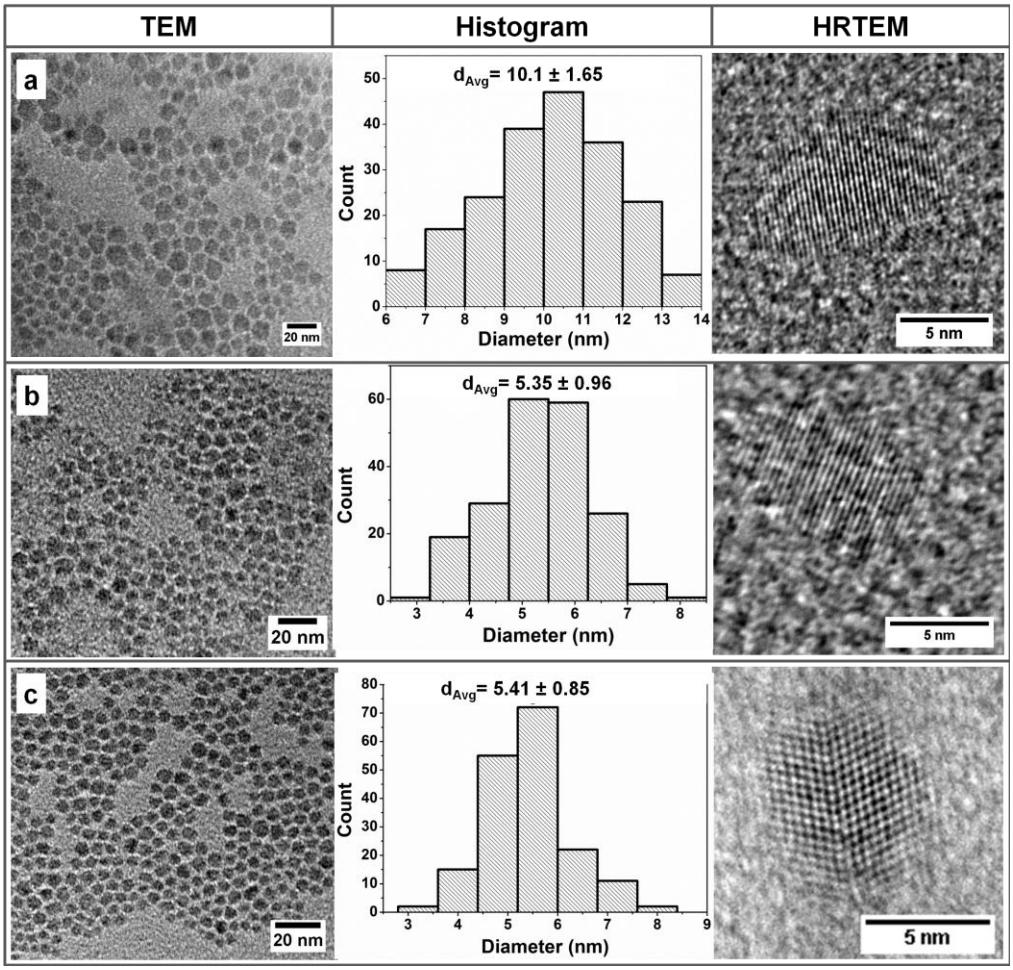

Figure 2.14. Representative TEM evaluation of GeNPs obtained from decomposition of **5** at 30 mg/mL at 190 °C. (a) Dodecyl-GeNPs obtained from HI. (b) Dodecyl-GeNPs and (c) Me_2N-GeNPs synthesized by MI.

The FTIR spectra (Figures 2.17a, 2.17b) of dodecyl-terminated GeNPs synthesized by HI and MI methods show absorptions attributable to NC surface coverage by alkyl functionalities. Specifically, absorptions present at 2800-3000 cm^{-1} are attributed to C-H stretching within a saturated hydrocarbon residue, while accompanying C-H bending appears at 1475 and 1365 cm^{-1}. The FTIR spectrum of the Me_2N-GeNPs (Figure 2.17c) shows features consistent with surface-bonded 3-dimethylamino-1-propene moieties.

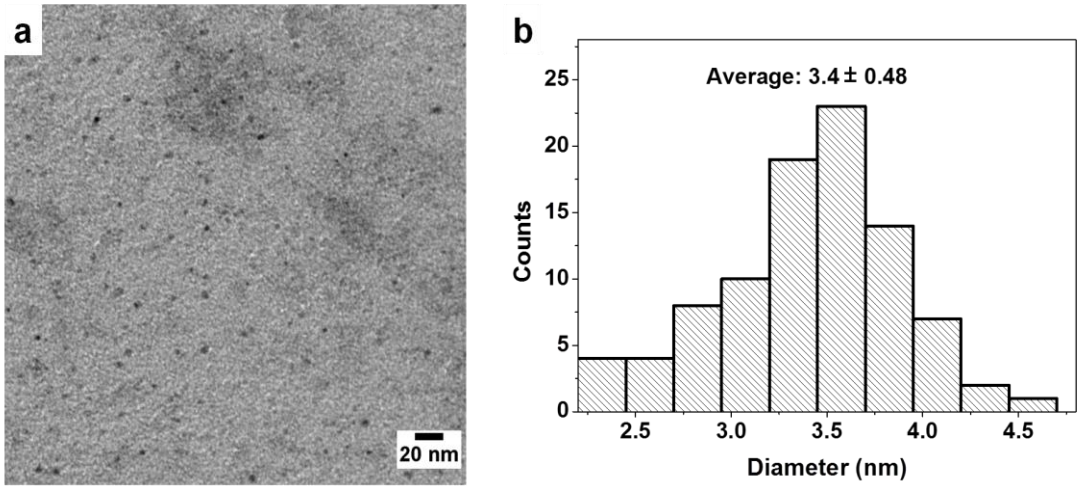

Figure 2.15. Representative brightfield TEM image and size-distribution of dodecyl-GeNPs obtained from MI decomposition of **5** at 10 mg/ 5mL at 190 °C in 1:1 (v:v) dodecene/diphenyl ether.

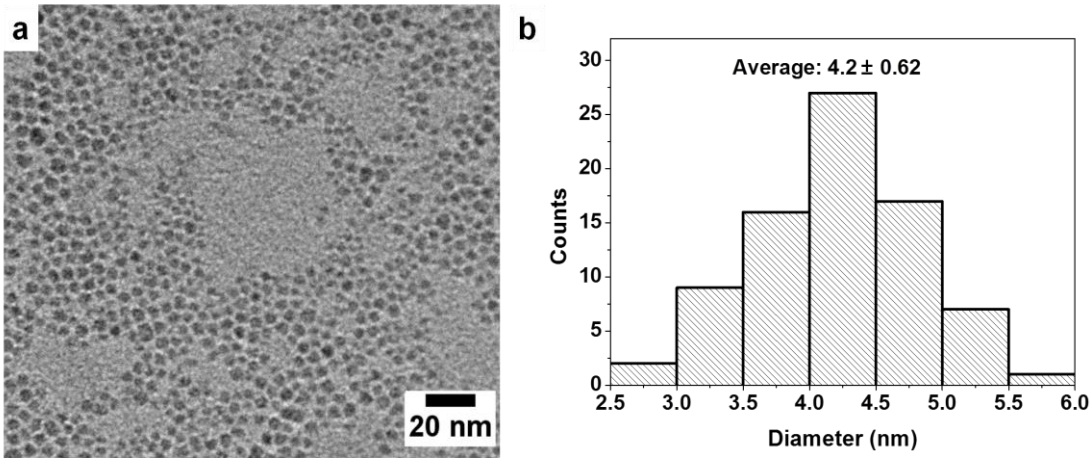

Figure 2.16. Representative brightfield TEM image and size-distribution of dodecyl-GeNPs obtained from MI decomposition of **5** at 20 mg/5 mL at 190 °C in 1:1 (v:v) dodecene/diphenyl ether.

The identity of the surface species on Me_2N-GeNPs was further confirmed by direct comparison of the IR spectra obtained for Me_2N-GeNPs and neat 3-dimethylamino-1-propene (Figure 2.18). These IR data are consistent with the HI and MI induced decomposition of **5** yielding hydride-terminated GeNPs that are subsequently

functionalized *via* hydrogermylation of 1-dodecene (dodecyl-GeNPs) or 3-dimethylamino-1-propyne (Me_2N-GeNPs). The hydrogermylation reaction yields substitutionally inert Ge-C bonds on the NP surface while the terminal alkyl chains and dimethylamino groups impart hydrophobicity and hydrophilicity, respectively.

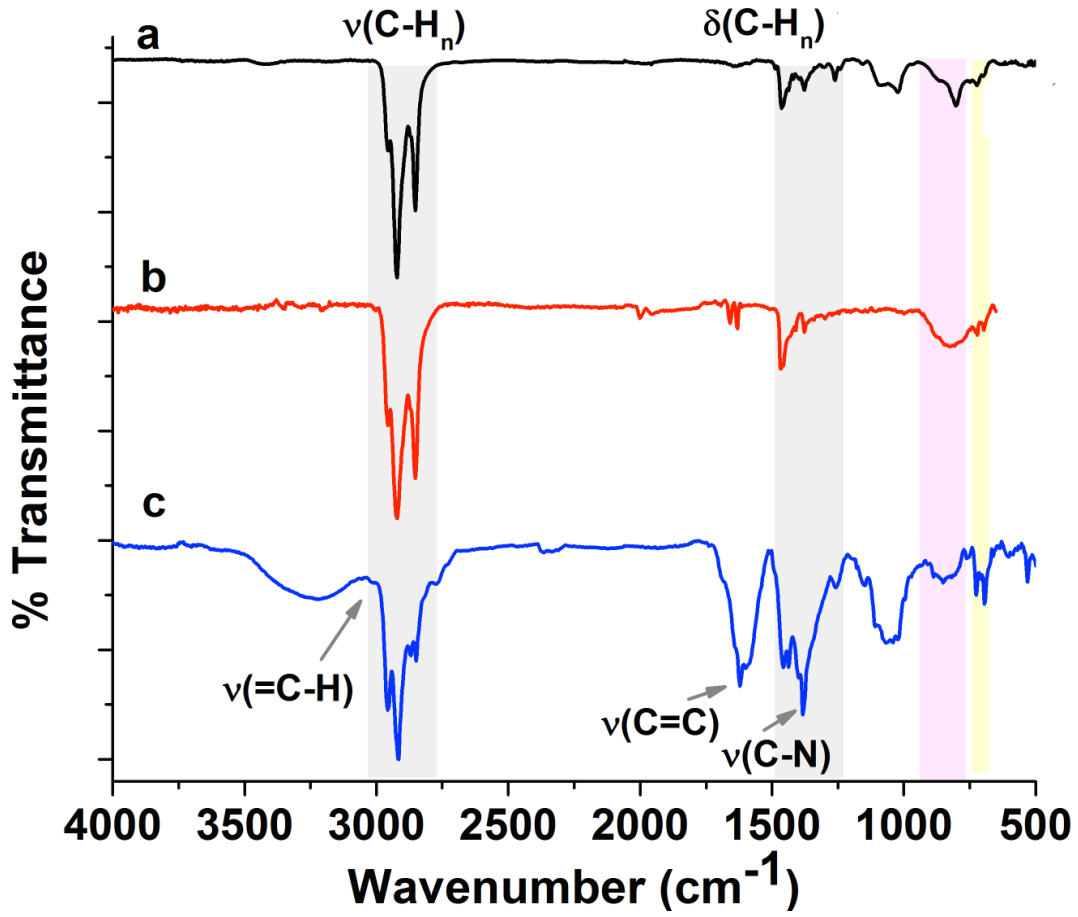

Figure 2.17. FTIR spectra of GeNPs obtained from decomposition of **5** at 30 mg/mL at 190 °C. (a) Dodecyl-GeNPs synthesized by HI. (b) Dodecyl-GeNPs and (c) Me_2N-GeNPs synthesized by MI.

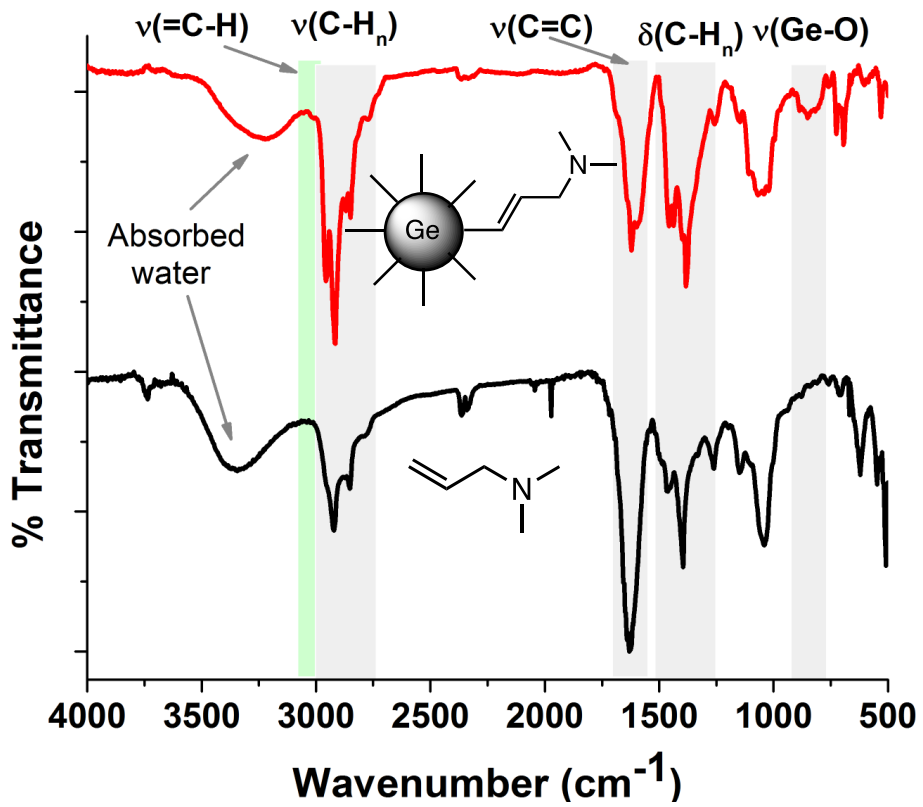

Figure 2.18. FTIR spectra of NMe_2-GeNPs (Top) and neat 3-dimethylamino-1-propene (Bottom).

To gain insight into the elemental composition and speciation of the GeNPs obtained from the solution-phase decomposition of **5**, X-ray photoelectron spectroscopy (XPS) was performed.[45] Survey spectra of all dodecyl-GeNPs confirm only Ge, C, and O are present at the sensitivity of the XPS technique (Figure 2.19). The relative atomic compositions are Ge (19.6%), C (62.7%), O (17.7%) and Ge (21.3%), C (61.5%), O (17.2%) for NPs prepared using HI and MI, respectively. Similarly, survey spectra indicate the relative atomic composition of NMe_2-GeNPs is N (5.2%), Ge (12.5%), C (63.6%) and O (18.7%) (Figure 2.19). The carbon content detected in the present samples arises from surface bonded moieties on the NPs, omnipresent adventitious carbon, and potential impurities. It is non-trivial to account

for the contributions of these carbon components, however a survey spectrum of commercial Ge powder (not shown) provides a baseline estimate of ca. 37% adventitious carbon content. Based upon this value, the N:C ratio found for Me_2N-GeNPs is *ca.* 0.2 and is in excellent agreement with the composition of the expected 3-dimethylamino-1-propene surface termination; from this it can be concluded that the present NPs contain negligible C contamination. Similar compositional analyses for dodecyl-GeNPs are not possible because of the lack of a heteroatom (*i.e.*, N), however it is reasonable the contribution from C impurities is negligible.

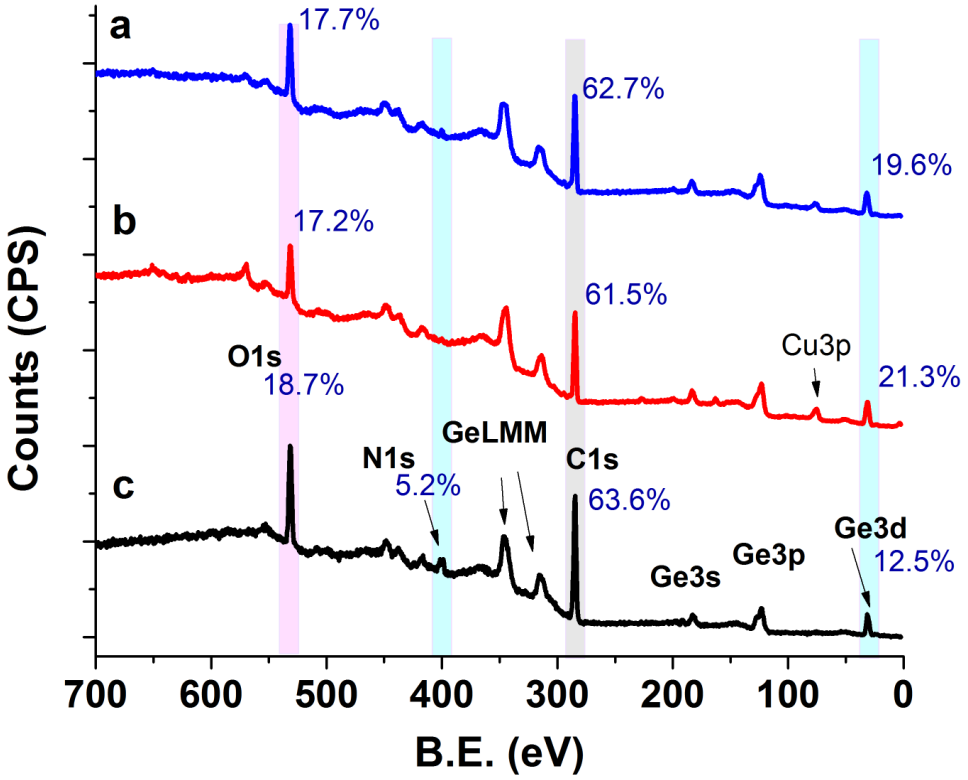

Figure 2.19. Survey XP spectra of: (a) Dodecyl-GeNPs prepared by HI (190 ºC) induced decomposition of **5** at 30 mg/mL in 1:1 (v:v) dodecene/diphenyl ether. (b) Dodecyl-GeNPs and (c) Me_2N-GeNPs synthesized by MI (190 °C) induced decomposition of **5** at 30 mg/ 5 mL in 1:1 (v:v) dodecene/diphenyl ether.

The oxygen content in the presented NPs is consistent with the complexities of Ge surface chemistry. It can be reasonably attributed to the hydrolysis and oxidation of residual Ge-H surface functionalities during work up and/or high temperature reaction with the diphenyl ether solvent.[27,35,46] The origin of these oxygen-based species is the subject of ongoing investigation. The Ge 3d region of the high resolution XP spectra (Figure 2.20) show a broad emission centered at ca. 30.5 eV that is can be fit to components at 29.0, 29.8, 30.8, 31.6, and 32.4 eV. The emission at 29.0 eV is characteristic of core Ge atoms; surface atoms bonded to alkyl and alkenyl groups, as well as surface suboxides account for higher oxidation state components.

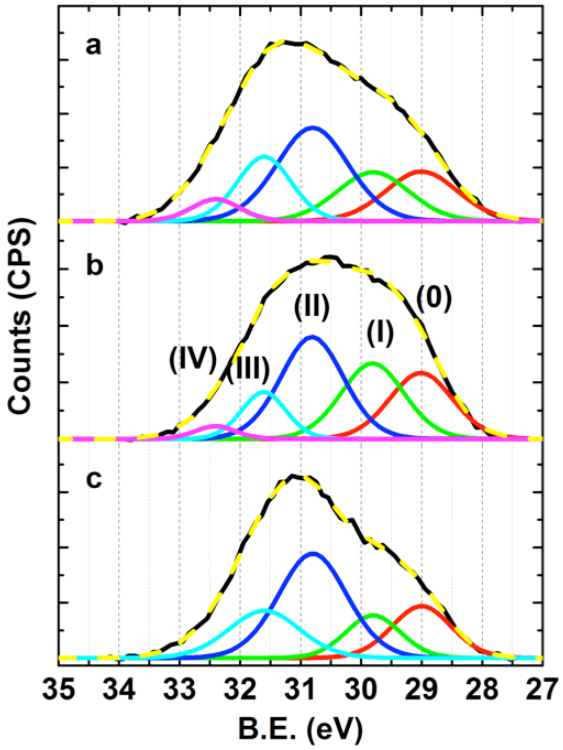

Figure 2.20. High-resolution XP spectra of the Ge 3d region for GeNPs obtained from decomposition of **5** at 30 mg/mL at 190 °C. (a) Dodecyl-GeNPs synthesized by HI. (b) Dodecyl-GeNPs and (c) Me_2N-GeNPs synthesized by MI. Ge $3d_{3/2}$ fitting components have been omitted for clarity.

Many Ge nanoparticles synthesized *via* solution-phase routes show photoluminescence (PL) in the visible spectral region with blue-light emission often being reported.[31,34,47] The appearance of blue emission is not readily explained in the context of quantum confinement; in fact, the effective-mass approximation predicts GeNPs of this dimension should emit in the near-IR or IR regions.[48,49]

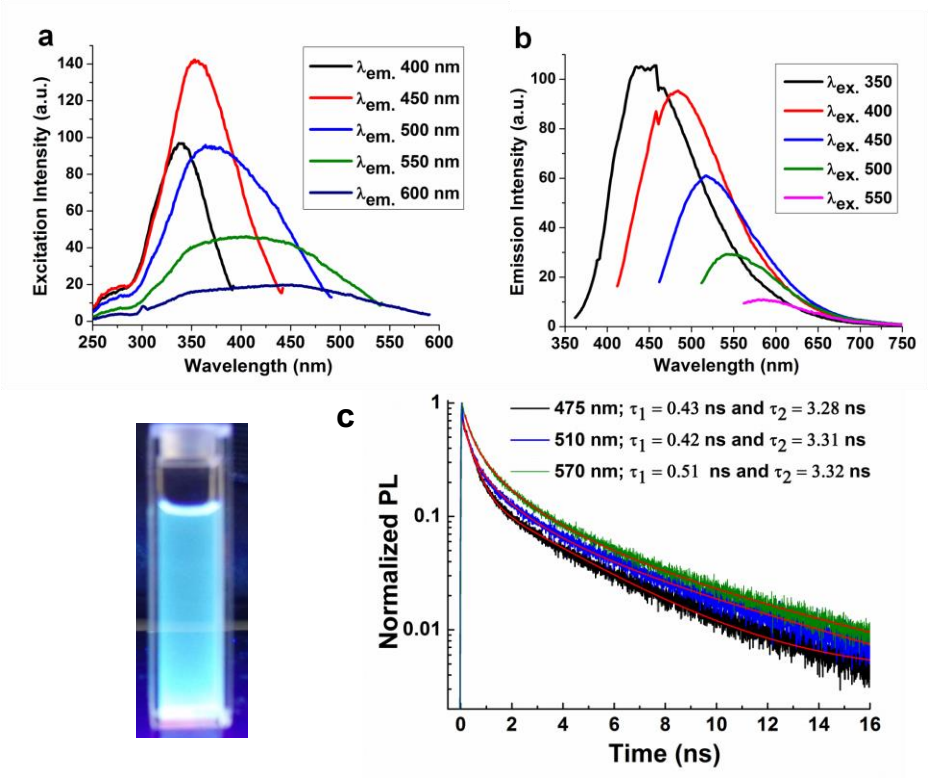

Figure 2.21. Photoluminescent properties of Me_2N-GeNPs obtained from MI induced decomposition of **5** at 30 mg/mL at 190 °C. (a) Excitation spectra obtained while monitoring emission at the indicated wavelengths. (b) Emission spectra obtained upon excitation at the indicated wavelengths. (c) PL decay at indicated emission wavelengths for Me_2N-GeNPs. (Solid red lines show the two component fits of the exponential decays).

Figure 2.21a and 2.21b show the PL excitation and PL spectra of Me_2N-GeNPs. Upon excitation at 365 nm blue luminescence is observed. Similar to other reports of blue/green- emitting GeNPs, [31,34,47] it was noted that the PL maximum shifts with excitation wavelength (Figure 2.21b). The PL quantum yield was determined to be *ca.* 1.8 % for Me_2N-GeNPs (Figure 2.22). PL lifetimes of the Me_2N-GeNPs (Figure 2.21c) at predefined emission wavelengths were obtained using time-correlated single photon counting methods. The short-lived lifetime components (*i.e.*, 0.42 ns and 3.31 ns) at $\lambda_{em.}$ = 510 nm are consistent with previous reports of GeNPs with faster recombination decay.[40,47] The origin of excitation wavelength dependent PL is currently unclear and may result from preferential excitation of NPs of specific sizes, or surface state emission.[50] The direct measurements of the band gap of individual NCs with different sizes were also studied in detail.[51]

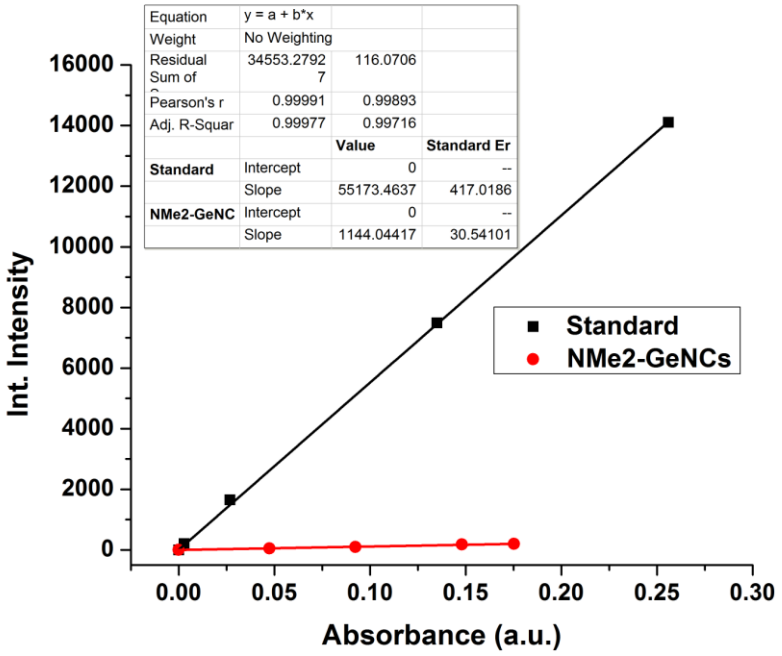

Figure 2.22. PL quantum yield determination for Me_2N-GeNPs.

2.3 Conclusions

It is shown that reactive targets such as GeH_2 and SnH_2 could be generated/intercepted with the aid of a readily available Wittig donor, while parallel chemistry with the commonly used ligands Cy_3P and DMAP was unsuccessful (presumably due to their weaker donating ability in relation to carbon-based ligands). Given the ability to access a wide scope of Wittig donors of the general form $R_3PCR'_2$ in a rapid fashion from inexpensive precursors, it is anticipated that these Lewis bases will be used more actively in the domain of synthetic inorganic main group chemistry in the future. Thus one can view Wittig reagents as competent synthetic analogues to ubiquitous *N*-heterocyclic carbene donors, with their potential use to access new inorganic bonding motifs via coordination chemistry and to advance inorganic element-mediated catalysis envisioned.

In addition, a facile method that provides surface functionalized GeNPs *via* one-pot hot injection or microwave-irradiation induced decomposition of a "bottleable" GeH_2-based precursor was developed. While hot injection and microwave irradiation provided GeNPs, the microwave-initiated method is particularly advantageous as it gives access to GeNPs of different sizes through variation of precursor concentration as well as surface modification using volatile capping ligands. Adding to the appeal of the presented approach, surface Ge-H residues afford sites for incorporating hydrophobic or hydrophilic groups on the periphery of the nanoparticle *via* hydrogermylation. Furthermore, GeNPs of near identical dimension that differ only in surface functionality were prepared and they exhibit very different optical properties. These observations may arise from surface

doping and could open the door to future tailoring of electronic and optical response and are the subject of ongoing investigations.

2.4 Experimental Details

2.4.1 Materials and Instrumentation. All reactions were performed using standard Schlenk line techniques under an atmosphere of nitrogen or in an inert atmosphere glove box (Innovative Technology, Inc.). Solvents were dried using a Grubbs-type solvent purification system[52] manufactured by Innovative Technology, Inc., degassed (freeze-pump-thaw method) and stored under an atmosphere of nitrogen prior to use. $Li[BH_4]$, $Li[BD_4]$, $^{n}BuLi$ (2.5 M solution in hexanes), H_3B•THF (1.0 M solution in THF), $K[HB^{s}Bu_3]$ (1.0 M solution in THF), $[Ph_3P\text{-}CH_3]I$, Cl_2Ge•dioxane, DMAP and Cy_3P were purchased from Aldrich and used as received. 3-Dimethylamino-1-propyne, 1-dodecene and diphenyl ether were purchased from Aldrich, dried over CaH_2 and distilled under nitrogen prior to use. $(THF)_2SnCl_2$•$W(CO)_5$ was prepared according to a literature procedure.[21] ^{1}H, $^{2}H\{^{1}H\}$, ^{11}B, $^{13}C\{^{1}H\}$ and ^{119}Sn NMR spectra were recorded on a Varian iNova-400 spectrometer and referenced externally to $SiMe_4$ (^{1}H and $^{13}C\{^{1}H\}$), $Si(CD_3)_4$ ($^{2}H\{^{1}H\}$), F_3B•OEt_2 (^{11}B), and $SnMe_4$ (^{119}Sn) respectively. Elemental analyses were performed by the Analytical and Instrumentation Laboratory at the University of Alberta. Infrared spectra were recorded on a Nicolet IR100 FTIR spectrometer as Nujol mulls between NaCl plates. Melting points were measured in sealed glass capillaries under nitrogen using a MelTemp apparatus and are uncorrected. Scanning electron microscopy (SEM) images were recorded in a Field Emission Scanning Electron Microscope,

JEOL 6301F. Toluene dispersion samples were deposited on cleaned silicon wafer which was attached with aluminium stubs using double sided carbon tape. Conductive coatings of chrome was applied on the samples using Xenosput XE200 sputter coaters before loading them into SEM holder. Images were recorded using secondary electron imaging with an accelerating voltage of 5.0 kV. Transmission electron microscopy (TEM) images were taken with a JOEL 2011TEM with LaB_6 electron gun using an accelerating voltage of 200 kV. TEM samples were prepared by depositing a droplet of dilute toluene suspension of functionalized Ge nanoparticles (GeNPs) onto a holey carbon coated copper grid and the solvent was removed under vacuum. The nanoparticle size was averaged for no fewer than 200 particles using Gatan Digital Micrograph software (Version 2.02.800.0). High-resolution (HR) TEM images were obtained from Hitachi-9500 electron microscope with an accelerating voltage of 300 kV. The HRTEM images were processed using Gatan Digital Micrograph software (Version 2.02.800.0). Photoluminescence (PL) emission and PL excitation spectra of functionalized GeNPs in 100% ethanol were taken using Carry Eclipse spectrophotometer.

2.4.2 X-ray Crystallography. Crystals of suitable quality for X-ray diffraction studies were removed from a vial in a glove box and immediately covered with a thin layer of hydrocarbon oil (Paratone-N). A suitable crystal was selected, mounted on a glass fiber and quickly placed in a low temperature stream of nitrogen on an X-ray diffractometer.[53] All data were collected at the University of Alberta using a Bruker APEX II CCD detector/D8 diffractometer using Mo Kα ($Cy_3P{\bullet}GeCl_2$ (**2**),

Ph_3PCMe_2•$GeCl_2$ (**4**), Ph_3PCMe_2•GeH_2•BH_3 (**5**), Ph_3PCMe_2•$SnCl_2$ (**6**), Ph_3PCMe_2•BH_3 (**7**), Ph_3PCMe_2•$SnCl_2$•$W(CO)_5$ (**8**), Ph_3PCMe_2•SnH_2•$W(CO)_5$ (**9**), Ph_3PCMe_2•$GeCl_2$•$W(CO)_5$ (**8**)) or Cu Kα (DMAP•$GeCl_2$ (**1**), Ph_3PCMe_2 (**3**)) radiation with the crystals cooled to -100 °C. The data were corrected for absorption through Gaussian integration from the indexing of the crystal faces.[54] Structures were solved using the direct methods program SHELXS-97[55] (compounds **1**, **3**-**6**), Patterson search/structure expansion facilities within the DIRDIF-2008 program suite[56] (compounds **2**, **6**, **8** and **10**), or intrinsic phasing SHELXT[55] (compounds **7** and **9**); structure refinement was accomplished using either SHELXL-97 or SHELXL-2013.[55] All carbon-bound hydrogen atoms were assigned positions based on the sp^2 or sp^3 hybridization geometries of their attached carbon atoms, and were given thermal parameters 20 % greater than those of their parent atoms. A tabular listing of the crystallographic data for compounds 1-10 can be found in Tables 2.1-2.5.

Special Refinement Conditions. *Compound **9***: The O-C and C-C distances within the disordered Et_2O solvent molecule were restrained to be 1.43(1) and 1.50(1) Å, respectively.

2.4.3 Synthetic Procedures

Synthesis of DMAP•$GeCl_2$ (1). To a mixture of DMAP (0.069 g, 0.56 mmol) and Cl_2Ge•dioxane (0.130 g, 0.56 mmol) was added 12 mL of toluene. The reaction mixture was stirred overnight to give a colorless solution. The volatiles were then removed under vacuum to give **1** as a white solid (0.147 g, 98 %). Crystals of suitable quality for X-ray crystallography were grown from a toluene/hexanes mixture at -35

°C. ^{1}H NMR (500 MHz, C_6D_6): δ = 1.85 (s, 6H, N(C*H*$_3$)$_2$), 5.46 (d, $^3J_{HH}$ = 7.5 Hz, 2H, Ar*H*), 8.05 (d, $^3J_{HH}$ = 7.0 Hz, 2H, Ar*H*). ^{13}C{^{1}H} NMR (126 MHz, C_6D_6): δ = 38.2 (N(*C*H$_3$)$_2$), 106.6 (Ar*C*), 143.9 (Ar*C*), 155.6 (Ar*C*). Anal. Calcd. for $C_7H_{10}Cl_2GeN_2$: C, 31.64; H, 3.79; N, 10.54. Found: C, 31.90; H, 3.80; N. 10.26. Mp (°C): 132-136.

Synthesis of Cy_3P•$GeCl_2$ (2).[14] Cy_3P (83 mg, 0.29 mmol) and Cl_2Ge•dioxane (69 mg, 0.29 mmol) were combined in 12 mL of toluene. The reaction mixture was stirred overnight to give a white slurry. The mixture was filtered and the resulting filtrate was concentrated to 7 mL, and 2.5 mL of hexanes was carefully layered ontop. This mixture was cooled to -35 °C for 12 hrs to yield white microcrystalline solid, containing **2** and a co-product tentatively identified as a [Cy_3PH]$GeCl_3$,[15] which was separated from the mother liquor. The solvent was removed from the mother liquor to yield **2** as a white powder (70 mg, 55 %). Crystals of suitable quality for X-ray crystallography were subsequently grown from a toluene/hexanes mixture at -35 °C. ^{1}H NMR (500 MHz, C_6D_6): δ = 0.91-1.05 (m, 9H, Cy*H*), 1.37-1.60 (m, 15H, Cy*H*), 1.93-1.96 (m, 6H, Cy*H*), 2.25-2.30 (m, 3H, Cy*H*). ^{13}C{^{1}H) NMR (126 MHz, C_6D_6): δ = 26.3 (s, Cy*C*), 27.4 (d, J_{CP} = 10.0 Hz, Cy*C*), 29.7 (s, Cy*C*), 31.9 (d, J_{CP} = 3.8 Hz, Cy*C*). ^{31}P{^{1}H) NMR (162 MHz, C_6D_6): δ = 1.8 (s). Anal. Calcd. for $C_{18}H_{33}Cl_2GeP$: C, 50.99; H, 7.85. Found: C, 51.03; H, 7.99. Mp (°C): 177-180.

Synthesis of Ph_3P=CMe_2 (3). *n*-BuLi (0.96 mL, 2.5 M solution in hexanes, 2.4 mmol) was added to a 10 mL toluene solution of isopropyltriphenylphosphonium

iodide (1.01 g, 2.3 mmol) and the mixture was stirred for overnight to yield a dark red slurry. The reaction mixture was filtered and the solvent was then removed from the filtrate under vacuum to give **3** as a red powder (0.58 g, 84 %). Crystals suitable for single-crystal X-ray diffraction were grown from a concentrated hexanes solution at -35 °C. ^{1}H NMR (400 MHz, C_6D_6): δ = 2.17 (d, $^{3}J_{HP}$ = 16.4 Hz, 6H, C(C*H*$_3$)$_2$), 7.03-7.15 (m, 9H, Ar*H*), 7.60-7.66 (m, 6H, Ar*H*). ^{13}C{^{1}H} NMR (100.5 MHz, C_6D_6): δ = 9.2 (d, J_{PC} = 123.0 Hz, *C*(CH$_3$)$_2$), 20.9 (d, J_{CP} = 13.6 Hz, *C*H$_3$), 130.5 (s, Ar*C*), 133.2 (s, Ar*C*), 133.9 (d, J_{CP} = 8.8 Hz, Ar*C*); the ipso C atoms on the Ph rings could not be located. ^{31}P{^{1}H} NMR (161.8 MHz, C_6D_6): δ = 9.8 (s). Anal. Calcd. for $C_{21}H_{21}Cl_2GeP$: C, 82.87; H, 6.95. Found: C, 82.00; H, 6.84. Mp (°C): 115-118.

Synthesis of Ph$_3$PCMe$_2$•GeCl$_2$ (4). To a mixture of Ph$_3$P=CMe$_2$ (0.42 g, 1.4 mmol) and GeCl$_2$•dioxane (0.32 g, 1.4 mmol) was added 5 mL of toluene and the mixture was stirred for one hour at room temperature to give an orange slurry. The resulting precipitate was separated from the mother liquor and dried under vacuum. The precipitate was then purified by crystallization from CH$_2$Cl$_2$/hexanes at -35 °C to give X-ray quality crystals of **4** (0.29 g, 46 %). ^{1}H NMR (500 MHz, C_6D_6): δ = 1.88 (d, $^{3}J_{HP}$ = 20.9 Hz, 6H, C(C*H*$_3$)$_2$), 6.88-6.92 (m, 6H, Ar*H*), 6.98-7.02 (m, 3H, Ar*H*), 7.41-7.46 (m, 6H, Ar*H*). ^{31}P{^{1}H} NMR (161.8 MHz, C_6D_6): δ = 37.5 (s). ^{1}H NMR (500 MHz, CD$_2$Cl$_2$): δ = 1.77 (d, $^{3}J_{HP}$ = 20.4 Hz, 6H, C(C*H*$_3$)$_2$), 7.58-7.63 (m, 6H, Ar*H*), 7.68-7.77 (m, 9H, Ar*H*). ^{13}C{^{1}H} NMR (125.3 MHz, CD$_2$Cl$_2$): δ = 22.1 (s, *C*H$_3$), 29.9 (d, J_{PC} = 24.1, *C*(CH$_3$)$_2$), 120.9 (d, J_{CP} = 80.5 Hz, Ar*C*), 129.9 (d, J_{CP} = 11.3 Hz, Ar*C*), 134.2 (s, Ar*C*), 135.1 (d, J_{CP} = 8.8 Hz, Ar*C*). ^{31}P{^{1}H} NMR (161.8

MHz, CD_2Cl_2): δ = 37.4 (s). Anal. Calcd. for $C_{21}H_{21}Cl_2GeP$: C, 56.31; H, 4.73. Found: C, 55.85; H, 4.63. Mp (°C): 103-105.

Synthesis of Ph_3PCMe_2•GeH_2•BH_3 (5). To a mixture of Ph_3PCMe_2•$GeCl_2$ (62 mg, 0.14 mmol) and Li[BH_4] (6 mg, 0.3 mmol) was added 5 mL of Et_2O, followed by stirring for 3 hrs at room temperature to give a white slurry. The volatiles were then removed under vacuum and the crude product was dissolved in 10 mL of CH_2Cl_2 and the mixture was filtered. The solvent was removed from the filtrate to yield **5** as a white powder (43 mg, 80 %). Crystals of X-ray quality were grown from a saturated THF solution at -35 °C. ^{1}H NMR (500 MHz, C_6D_6): δ = 1.73 (br quartet, $^1J_{BH}$ = 94.8 Hz, 3H, B*H*$_3$), 1.66 (d, $^3J_{HP}$ = 20.4 Hz, 6H, C(C*H*$_3$)$_2$), 4.64 (br, 2H, Ge*H*$_2$), 6.86-6.93 (m, 6H, Ar*H*), 6.97-7.16 (m, 3H, Ar*H*), 7.48-7.51 (m, 6H, Ar*H*). ^{13}C{^{1}H} NMR (125.3 MHz, C_6D_6): δ = 17.4 (d, $^1J_{CP}$ = 23.3 Hz, *C*(CH$_3$)$_2$), 26.5 (s, *C*H$_3$), 121.9 (d, J_{CP} = 81.0 Hz, Ar*C*), 129.3 (d, J_{CP} = 11.4 Hz, Ar*C*), 133.4 (s, Ar*C*), 134.8 (d, J_{CP} = 8.3 Hz, Ar*C*). ^{31}P{^{1}H} NMR (161.8 MHz, C_6D_6): δ = 38.8 (s). ^{11}B NMR (159.8 MHz, C_6D_6): δ = -39.4 (quartet, $^1J_{BH}$ = 95.4 Hz, *B*H$_3$). IR (cm^{-1}): 1975 (m, υ_{Ge-H}) and 2343 (w, υ_{B-H}). Anal. Calcd. for $C_{21}H_{26}BGeP$: C, 64.20; H, 6.67. Found: C, 64.63; H, 6.81. Mp (°C): 110-113.

Synthesis of Ph_3PCMe_2•GeD_2•BD_3 (5D). To a mixture of Ph_3PCMe_2•$GeCl_2$ (68 mg, 0.15 mmol) and Li[BH_4] (9 mg, 0.34 mmol) was added 5 mL of Et_2O, followed by stirring for 3 hrs at room temperature to give a white slurry. The volatiles were then removed under vacuum and the crude product was dissolved in 10 mL of CH_2Cl_2 and

the mixture was filtered. The solvent was removed from the filtrate to yield **5D** as a white powder (52 mg, 87 %). ^{1}H NMR (500 MHz, C_6D_6): Similar as Ph_3PCMe_2•GeH_2•BH_3 with very low intensity peaks due to residual GeHD and GeH_2 isotopologues (< 8 %). ^{2}H{^{1}H} NMR (61.39 MHz, C_6H_6) δ = 1.56 (br, BD_3), 4.63 (s, GeD_2). ^{11}B NMR (159.8 MHz, C_6D_6): δ = -39.4 (br). IR (cm^{-1}): 1377 (m, υ_{Ge-D}), 1754 (w, υ_{B-D}) and low intensity peaks for Ge-H and B-H at 1975 and 2330 respectively.

Synthesis of Ph_3PCMe_2•$SnCl_2$ (6). $Ph_3P{=}CMe_2$ (113 mg, 0.37 mmol) and $SnCl_2$ (70 mg, 0.37 mmol) were combined in a 5 mL toluene/ 1 mL THF mixture, followed by stirring for 3 hrs. The solvent was removed under vacuum to yield **6** as a white powder (153 mg, 83 %). Crystals of X-ray quality were grown from a CH_2Cl_2/hexanes solution at -35 °C. ^{1}H NMR (400 MHz, CD_2Cl_2): δ = 1.87 (d, $^3J_{HP}$ = 21.2 Hz, 6H, C(C*H*$_3$)$_2$), 7.61-7.76 (m, 15H, Ar*H*). ^{13}C{^{1}H} NMR (125.3 MHz, CD_2Cl_2): δ = 21.6 (s, *C*H$_3$), 32.3 (d, $^1J_{CP}$ = 24.8 Hz, *C*(CH$_3$)$_2$), 121.8 (d, $^1J_{CP}$ = 81.0 Hz, Ar*C*), 130.1 (d, J_{CP} = 11.4 Hz, Ar*C*), 134.2 (s, Ar*C*), 134.7 (d, J_{CP} = 8.5 Hz, Ar*C*). ^{31}P{^{1}H} NMR (161.8 MHz, CD_2Cl_2): δ = 36.9 (s, satellites: $^2J_{P\text{-}Sn}$ = *ca.* 89 Hz). ^{119}Sn{^{1}H} NMR (149 MHz, CD_2Cl_2): δ = 113.3 (br). Anal. Calcd. for $C_{21}H_{21}Cl_2PSn$: C, 51.06; H, 4.28. Found: C, 49.86; H, 4.28. Mp (°C): 165-167 (turns black 155-157).

Synthesis of Ph_3PCMe_2•BH_3 (7).[10a] To a solution of $Ph_3P{=}CMe_2$ (213 mg, 0.70 mmol) in 5 mL of Et_2O was added a solution of THF•BH_3 (701 µL, 1.0 M solution in THF, 0.70 mmol) dropwise. The reaction mixture was then stirred overnight at room temperature and the solvent was then removed under vacuum. The resulting solid was

washed with hexanes (3×5 mL) and dried to afford **7** as a white solid (0.154 g, 69 %). Crystals suitable for X-ray crystallography were grown from hexanes/CH_2Cl_2 at -35 °C. ^{1}H NMR (400 MHz, C_6D_6): δ = 1.74 (d, 6H, $^3J_{PH}$ = 21.2 Hz, C(C*H*$_3$)), 2.33 (q, 3H, $^1J_{BH}$ = 90 Hz, B*H*$_3$), 6.89-7.01 (m, 9H, Ar*H*), 7.81-7.85 (m, 6H, Ar*H*). ^{13}C{^{1}H} NMR (125 MHz, C_6D_6): δ = 30.5 (s, *C*H$_3$), 124.7 (d, J_{CP} = 77.0, Ar*C*), 128.7 (d, J_{CP} = 10.8, Ar*C*), 132.4 (d, J_{CP} = 2.3, Ar*C*), 135.4 (d, J_{CP} = 7.8, Ar*C*); the ylidic *C*Me$_2$ carbon could not be located. ^{11}B NMR (128 MHz, C_6D_6): δ = -19.4 (q, $^1J_{BH}$ = 85.7 Hz, *B*H$_3$). ^{31}P{^{1}H} NMR (161 MHz, C_6D_6): δ = 39.4 (s).

Synthesis of Ph_3PCMe_2•$SnCl_2$•$W(CO)_5$ (8). Ph_3P=CMe_2 (49 mg, 0.17 mmol) and $(THF)_2SnCl_2$•$W(CO)_5$ (110 mg, 0.167 mmol) were combined in 10 mL of toluene and stirred for 3 hrs at room temperature to give a yellow slurry. The volatiles were removed under vacuum to afford **8** as a pale yellow powder (130 mg, 94 %). Crystals of X-ray quality were grown from CH_2Cl_2/hexanes at -35 °C. ^{1}H NMR (400 MHz, C_6D_6): δ = 1.61 (d, $^3J_{HP}$ = 20.4 Hz, 6H, C(C*H*$_3$)$_2$; satellites: $^3J_{HSn}$ and/or $^4J_{HW}$ = *ca.* 66 Hz), 6.92-7.08 (m, 9H, Ar*H*), 7.32-7.37 (m, 6H, Ar*H*). ^{13}C{^{1}H} NMR (125.3 MHz, C_6D_6): δ = 24.6 (s, *C*H$_3$), 32.3 (d, J_{CP} = 27.5 Hz, *C*(CH$_3$)$_2$), 120.1 (d, J_{CP} = 82.7 Hz, Ar*C*), 129.8 (d, J_{CP} = 11.6 Hz, Ar*C*), 134.2 (s, Ar*C*), 134.8 (d, J_{CP} = 8.8 Hz, Ar*C*), 198.8 (s, satellites: $^1J_{CW}$ = 123.4 Hz, eq. *C*O), 201.2 (s, ax. *C*O). ^{31}P{^{1}H} NMR (161.8 MHz, C_6D_6): δ = 38.2 (s, satellites: $^2J_{P\text{-}Sn}$ = 44.5 Hz). ^{119}Sn{^{1}H} NMR (149.1 MHz, C_6D_6): δ = 131.3 (d, $^2J_{Sn\text{-}P}$ = 48.5 Hz). IR (Nujol, cm^{-1}): 1930 (br, υ_{CO}) and 2060 (m, υ_{CO}). Anal. Calcd. for $C_{26}H_{21}Cl_2O_5PSnW$: C, 38.18; H, 2.59. Found: C, 38.35; H, 2.65. Mp (°C): 178-180.

Synthesis of Ph_3PCMe_2•SnH_2•$W(CO)_5$ (9). To a mixture of Ph_3PCMe_2•$SnCl_2$•$W(CO)_5$ (78 mg, 0.095 mmol) and $Li[BH_4]$ (4.5 mg, 0.21 mmol) was added 5 mL of Et_2O, followed by stirring for 4 hrs at room temperature to yield a brown slurry. The volatiles were removed under vacuum and the product was extracted with 10 mL toluene and the resulting mixture was filtered. The solvent was then removed under vacuum from the filtrate to yield **9** as a red-brown powder (72 mg, 76 %). Crystals of X-ray quality were grown from Et_2O/hexanes at -35 °C. ^{1}H NMR (500 MHz, C_6D_6): δ = 1.61 (d, $^3J_{HP}$ = 20.4 Hz, 6H, C(C*H*$_3$)$_2$; satellites: $^3J_{HSn}$ and/or $^4J_{HW}$ = *ca.* 60 Hz), 6.66 (s, 2H, Sn*H*$_2$; satellites: $^1J_{H\text{-}119Sn}$ = 1030 Hz, $^1J_{H\text{-}117Sn}$ = 991 Hz), 6.87-7.06 (m, 9H, Ar*H*), 7.29-7.36 (m, 6H, Ar*H*). ^{13}C{^{1}H} NMR (125.3 MHz, C_6D_6): δ = 12.9 (d, J_{CP} = 27.5 Hz, *C*(CH$_3$)$_2$), 27.8 (s, *C*H$_3$), 121.7 (d, J_{CP} = 81.6 Hz, Ar*C*), 129.4 (d, J_{CP} = 11.5 Hz, Ar*C*), 133.6 (s, Ar*C*), 134.5 (d, J_{CP} = 8.3 Hz, Ar*C*), 202.8 (s, eq. *C*O), 205.1 (s, ax. *C*O). ^{31}P{^{1}H} NMR (161.8 MHz, C_6D_6): δ = 38.3 (s; satellites: $^2J_{P\text{-}Sn}$ = 36.3 Hz). ^{119}Sn{^{1}H} NMR (149.1 MHz, C_6D_6): δ = -49.8 (d, $^2J_{Sn\text{-}P}$ = 37.4 Hz). ^{119}Sn NMR (149.1 MHz, C_6D_6): δ = -49.8 (t, $^1J_{Sn\text{-}H}$ = ~1074 Hz; the expected t of d pattern was not resolved due to decomposition of **9** during prolonged time period in solution). IR (Nujol, cm^{-1}): 1740 (s, $\upsilon_{sn\text{-}H}$) and 1891 (w, υ_{CO}), 1959 (s, υ_{CO}), 2040 (m, υ_{CO}). Anal. Calcd. for $C_{26}H_{23}O_5PSnW$: C, 41.69; H, 3.10. Found: C, 42.72; H, 3.63. Mp (°C): 80-82 (turns black 70-75 °C).

Synthesis of Ph_3PCMe_2•SnD_2•$W(CO)_5$ (9D). To a mixture of Ph_3PCMe_2•$SnCl_2$•$W(CO)_5$ (130 mg, 0.16 mmol) and $Li[BD_4]$ (9 mg, 0.3 mmol) was added 5 mL of Et_2O, followed by stirring for 4 hrs at room temperature to yield a

brown slurry. The volatiles were removed under vacuum and the product was extracted with 10 mL toluene and the resulting mixture was filtered. The solvent was then removed under vacuum from the filtrate to yield **9D** as a red-brown powder (73 mg, 61 %). ^{1}H NMR (500 MHz, C_6D_6): same as Ph_3PCMe_2•SnH_2•$W(CO)_5$ with very low intensity peaks due to residual SnHD and SnH_2 isotopomers (< 9 %). ^{2}H{^{1}H} NMR (61.39 MHz, C_6H_6) δ = 6.66 (s, SnD_2). IR (cm^{-1}): 1975 (m, υ_{CO}) and 2343 (w, υ_{CO}), 1254 (υ_{Sn-D}); very low intensity υ_{Sn-H} peak at 1746 cm^{-1}.

Synthesis of Ph_3PCMe_2•$GeCl_2$•$W(CO)_5$ (10). Ph_3PCMe_2•$GeCl_2$ (43 mg, 0.096 mmol) and $(THF)_2$•$SnCl_2$•$W(CO)_5$ (63 mg, 0.096 mmol) were combined in 10 mL of toluene and stirred for 24 hrs at room temperature to give a pale yellow slurry. The volatiles were removed from the reaction mixture and 15 mL of CH_2Cl_2 was added. The resulting solution was filtered and the solvent was removed from the filtrate to give **10** as a white powder (73 mg, 94 %). Crystals of suitable quality for X-ray analysis were grown from CH_2Cl_2/hexanes at -35 °C. ^{1}H NMR (500 MHz, C_6D_6): δ = 1.49 (d, $^{3}J_{HP}$ = 19.9 Hz, 6H, C(C*H*$_3$)$_2$), 6.89-6.94 (m, 6H, Ar*H*), 6.97-7.03 (m, 3H, Ar*H*), 7.38-7.44 (m, 6H, Ar*H*). ^{13}C{^{1}H} NMR (125.3 MHz, C_6D_6): δ = 26.2 (s, *C*H$_3$), 32.4 (d, J_{CP} = 25.5 Hz, *C*(CH$_3$)$_2$), 120.4 (d, J_{CP} = 82.1 Hz, Ar*C*), 129.3 (d, J_{CP} = 6.5 Hz, Ar*C*), 133.8 (s, Ar*C*), 135.5 (d, J_{CP} = 8.8 Hz, Ar*C*), 199.5 (s, eq. *C*O), 202.0 (s, ax. *C*O). ^{31}P{^{1}H} NMR (161.8 MHz, C_6D_6): δ = 38.8 (s). IR (Nujol, cm^{-1}): 1924 (br, υ_{CO}) and 2063 (m, υ_{CO}). Anal. Calcd. for $C_{26}H_{21}Cl_2O_5PGeW$: C, 40.46; H, 2.74. Found: C, 40.44; H, 2.72. Mp (°C): 188-192.

Reaction of DMAP•$GeCl_2$ (1) with Li[BH_4]. To a mixture of the DMAP•$GeCl_2$ (126 mg, 0.47 mmol) and Li[BH_4] (22 mg, 0.99 mmol) was added 5 mL of diethyl ether. Upon addition of the solvent a rapid reaction ensued as evidenced by the formation of (presumably) elemental Ge. Analysis of the soluble fraction after 12 hrs of stirring revealed the clean presence of DMAP•BH_3,[57] which was identified by comparision of the ^{11}B NMR spectroscopic data with those found in the literature.[57] In order to isolate DMAP•BH_3, the solvent was removed from the reaction mixture and 6 mL of CH_2Cl_2 was added. The resulting mixture was filtered and the volatiles were removed from the filtrate to yield DMAP•BH_3 as a white powder as DMAP•BH_3 (51 mg, 79 %).

Reaction of Cy_3P•$GeCl_2$ (2) with Li[BH_4]. Following an identical procedure as listed for the reaction of DMAP•$GeCl_2$ with Li[BH_4], a mixture of the Cy_3P•$GeCl_2$ (38 mg, 0.089 mmol) and Li[BH_4] (5 mg, 0.2 mmol) were combined in 5 mL of Et_2O. The resulting mixture containing (presumably) elemental Ge and Cy_3P•BH_3[58] was purified by removing the voltailes, followed by extraction of Cy_3P•BH_3 with 6 mL of CH_2Cl_2. The isolated white solid from the soluble extract (23 mg, 87 %) was identified as Cy_3P•BH_3 by comparision of the ^{11}B and ^{31}P NMR spectroscopic data with those found in the literature.[58]

Reaction of Ph_3PCMe_2•$SnCl_2$ (6) with Li[BH_4]. To a mixture of the Ph_3PCMe_2•$SnCl_2$ (99 mg, 0.20 mmol) and Li[BH_4] (10 mg, 0.44 mmol) was added 5 mL of diethyl ether. The resulting slurry was stirred for 2 hrs to form a shiny black

precipitate (presumably metallic tin) with the formation of $Ph_3PCMe_2{\bullet}BH_3$ (**7**) as the sole soluble product, as evidenced by ^1H, ^{11}B and ^{31}P NMR spectroscopy.

Reaction of $Ph_3PCMe_2{\bullet}GeH_2{\bullet}BH_3$ (5) with IPr. To a mixture of $Ph_3PCMe_2{\bullet}GeH_2{\bullet}BH_3$ (**5**) (63 mg, 0.16 mmol) and IPr (62 mg, 0.16 mmol) 10 mL toluene was added. The reaction mixture was stirred for overnight. The volatiles were removed under vacuum to yield a brown powder. The ^1H, ^{31}P and ^{11}B NMR spectra were received without further purification. These spectroscopic methods show the formation of $IPr{\bullet}GeH_2{\bullet}BH_3$[4a], Ph_3PCMe_2 (**3**), PPh_3, an unidentified product ($^{31}P\{^1H\}$ NMR (161.8 MHz, C_6D_6): δ = 31.7) and minor amount of the starting material $Ph_3PCMe_2{\bullet}GeH_2{\bullet}BH_3$ (**5**).

Thermolysis of $Ph_3PCMe_2{\bullet}GeH_2{\bullet}BH_3$ (5). Compound **5** (40 mg, 0.10 mmol) was dissolved in 10 mL of toluene and the solution was heated to reflux. Within 4 hrs a grey suspension was formed. The reflux was continued for 24 hrs to obtain grayish black slurry. The reaction mixture was filtered and the solvent was removed from the filtrate to yield a white solid which was identified by ^1H, ^{11}B, ^{31}P NMR spectroscopy. The different NMR spectroscopic methods suggest the formation of $Ph_3P{\bullet}BH_3$[18] (> 95 % yield by ^{31}P NMR spectroscopy; $^{31}P\{^1H\}$ NMR (161.8 MHz, C_6D_6): δ = 21.7 ppm. ^{11}B NMR (159.8 MHz, C_6D_6): δ = 42.1 ppm, $^1J_{BP}$ = 43.7 Hz). Another peak in ^{11}B NMR at 80 ppm which is tentatively assigned as being the triorganoborane $^iPr_3B$ (literature ^{11}B NMR shift = 83.7 ppm in C_6D_6). The precipitate was studied by EDX and SEM techniques.

Decomposition study on Ph_3PCMe_2•SnH_2•$W(CO)_5$ (9). Compound **9** (45 mg, mmol) was dissolved in 10 mL of toluene and stirred at room temperature for 24 hrs to yield a brown solution with black precipitate. The solvent was removed under vacuum. The solid was studied by different spectroscopic techniques. ^{31}P NMR suggests the formation of PPh_3 as one of the decomposition product.

Synthesis of hydrophilic GeNPs with NMe_2 surface groups. Ph_3PCMe_2•GeH_2•BH_3 (**5**) (30 mg, 0.076 mmol) and 5 mL of 3-dimethylamino-1-propyne were transferred into a 5 mL microwave vial in a nitrogen filled glovebox. The microwave vial was sealed inside the glovebox and sonicated for 5 min before placing it into a Biotage Initiator microwave reactor. The mixture was irradiated for 2 hours at 190 °C to give a dark red solution. The volatiles were removed from the resulting mixture using a rotary evaporator and the crude product was redispersed in 8 mL of toluene with sonication, followed by addition of *ca.* 30 mL of hexane. This mixture was centrifuged at 14000 rpm to afford a red solid that was separated from the supernatant and isolated. The resulting pellet was redispersed in 40 mL of toluene/hexanes (1:4) with sonication. The cloudy mixture was centrifuged at 14000 rpm to yield a red solid and the procedure was repeated two more times to afford the GeNPs as a red solid. The hydrophilic NPs are soluble in protic solvent such as alcohols as well as aprotic solvents such as DMSO, DMF, and THF. They are also soluble in aqueous alcohol. Yield: 7 mg.

Preparation of dodecyl-capped GeNPs via microwave irradiation. Ph_3PCMe_2•GeH_2•BH_3 (**5**) (30 mg, 0.076 mmol), 2.5 mL of 1-dodecene and 2.5 mL of diphenyl ether were transferred into a 5 mL microwave vial under atmosphere of nitrogen. The microwave vial was sealed inside the glovebox and sonicated for 5 min. before placing it into a Biotage Initiator microwave reactor. The reaction mixture was irradiated for 1 hr at predetermined temperatures (*i.e.*, 100, 150, 190, and 250 °C). A mixture of toluene/methanol (1:4; 40 mL) was added to the mixture followed by centrifugation at 14000 rpm to provide a red solid. The supernatant was decanted and discarded. The pellet was redispersed in 40 mL of toluene/methanol (1:4) mixture with sonication. The cloudy mixture was centrifuged at 14000 rpm to yield a red solid and the procedure was repeated two more times to afford the GeNPs as a red solid. Hydrophobic GeNPs were soluble in hydrophobic solvents such as toluene, $CHCl_3$, and THF. Yield: 9.5 mg for 190 °C. Lower concentrations (*i.e.*, 10 and 20 mg/5 mL) of 1 in 1:1 (v:v) 1-dodecene/diphenyl ether were used to produce various sizes dodecyl-GeNPs.

Synthesis of dodecyl-capped GeNPs via hot-injection method. Ph_3PCMe_2•GeH_2•BH_3 (**5**) (60 mg, 0.16 mmol) in 1.5 mL diphenyl ether was injected into a hot stirring solvent mixture of 1-dodecene (5 mL) and diphenyl ether (4 mL) at 100, 150, and 190 °C under an argon atmosphere. The reaction mixture turned from colorless to yellow with the formation of a gas. After heating for 1 hour the reaction mixture turned to light yellow (100 °C), yellow (150 °C), and red (190 °C). The reaction mixtures were quenched upon addition of 10 mL dry cold toluene.

Subsequently, 40 mL of toluene/methanol (1:4) was added, followed by centrifugation at 14000 rpm to provide a yellow (for 100 and 150 °C) or red (for 190 °C) solid. The supernatant was decanted and discarded. The pellet was redispersed in 40 mL of toluene/methanol (1:4) with sonication. The cloudy mixture was centrifuged at 14000 rpm to yield a red solid and the procedure was repeated two more times to afford the GeNPs as a red solid. Yield: 15.2 mg at 190 °C. Reactions at 100 and 150 °C yielded trace quantities of GeNPs.

GeNPs Characterization Details:

Photoluminescence (PL) Lifetimes: Nanosecond (ns) lifetime measurements were performed using an excitation pulse of a 400-nm second harmonic signal from a BBO crystal pumped by 800-nm pulses from a Ti: Sapphire laser (Coherent RegA900 with 65 fs pulse width and 250 kHz repetition rate) with average excitation power of 5.28 mW. Time-resolved PL was recorded using a time-correlated single-photon-counting (TCSPC) unit (Picoharp 300, Picoquant) equipped with a single-photon avalanche photodiode (SPAD, PDM Series by Micro Photon Devices) and coupled to a monochromator (Acton SP2500, Princeton Instruments). The TCSPC system has a time resolution of 50 ± 4 ps. A 435-nm long pass filter (Edmund optics) was placed at the entrance of the spectrometer to block scattered laser pulses. For microsecond carrier recombination lifetime measurements, 1 kHz frequency-doubled 400 nm pulses from another Ti: Sapphire laser (Coherent Legend Elite, 45 fs pulse width) were used to excite the PL at an average excitation power of 4.8 mW, however, no microsecond PL component was observed. A fast silicon photodiode (Thorlabs,

PDA36A, rise time 20.6 ns) coupled to a 300 MHz oscilloscope (Tektronix) was used to measure the microsecond carrier recombination lifetime. The photodiode was placed at a path perpendicular to the excitation beam and 10-nm bandpass filters (Edmund Optics) were used to select a particular emission wavelength. The carrier recombination lifetimes were accurately fitted by double exponential decay:

$$y(t) = Ae^{-t/\tau_1} + Be^{-t/\tau_2} + y_0$$

where τ_1 and τ_2 are the decay times and A and B are the respective amplitudes of the decay components. The constant offset term, y_0 was insignificant compared to the coefficients A and B.

Quantum yield (QY) determination: Background subtracted UV-vis absorption spectra and solvent corrected PL emission spectra of predefined dilutions of NMe_2-GeNPs solution (in ethanol) and standard (in cyclohexane) were collected at excitation wavelength 350 nm. The integrated intensities (from 360 – 600 nm) were determined from the solvent corrected PL spectra and plotted vs. respective absorbance at 350 nm. QY was determined using the relationship noted below; where $Slope_{GeNPs}$ and $Slope_{Std}$ were determined from the plot in Fig. S10 and n is refractive index of the solvent.[59] The PL standard of choice for the present study was 9,10-diphenylanthracene (QY = 97%).[60] QY of NMe_2-GeNPs,

$$\mathbf{\Phi}_{GeNPs} = \mathbf{\Phi}_{Std} \frac{Slope_{GeNPs}}{Slope_{Std}} \left(\frac{n_{ethanol}}{n_{cyclohexane}} \right)^2$$

$= 0.97 \times (1144.04/55173.46) \times (1.361/1.4266)^{\wedge 2} = 0.018 = 1.8\ \%$

2.5 Crystallographic Data

Table 2.1: Crystallographic data for **1** and **2**.

Compound	**1**	**2**
Formula	$C_7H_{10}Cl_2P_2GeN_2$	$C_{18}H_{33}Cl_2GeP_2$
Formula weight	256.66	423.90
Crystal system	monoclinic	orthorhombic
Space group	$P2_1/n$	$Pca2_1$
a (Å)	7.3784(2)	15.158(5)
b (Å)	10.6075(3)	9.974(3)
c (Å)	13.2845(3)	13.629(11)
α (deg)	90	90
β (deg)	90.1560(10)	90
γ (deg)	90	90
V(Å^3)	1039.73(5)	2060.5(11)
Z	4	4
ρ (g/cm^3)	1.697	1.366
abs coeff (mm^{-1})	8.330	1.820
T (K)	173(1)	173(1)
$2\theta_{max}$ (°)	137.42	54.98
total data	6480	16583
unique data(R_{int})	1889 (0.0366)	4664 (0.0204)
Obs data [I>2($\sigma(I)$]	1664	4527
Params	111	199
R_1 [$I>2\sigma(I)$][a]	0.0313	0.0189
wR_2 [all data][a]	0.0850	0.0510
max/min $\Delta\rho$ (e$^-$ Å^{-3})	0.497/-0.412	0.530/-0.254

[a] $R_1 = \sum||F_o| - |F_c||/\sum|F_o|$; $wR_2 = [\sum w(F_o^2 - F_c^2)^2/\sum w(F_o^4)]^{1/2}$

Table 2.2: Crystallographic data for **3** and **4**.

Compound	**3**	**4**
Formula	$C_{21}H_{21}P$	$C_{21}H_{21}Cl_2GeP$
Formula weight	304.35	447.84
Crystal system	triclinic	orthorhombic
Space group	$P\bar{1}$	$Pna2_1$
a (Å)	10.0042(2)	12.0720(3)
b (Å)	10.1516(2)	9.3272(3)
c (Å)	18.8977(4)	17.8199(5)
α (deg)	104.8757(15)	90
β (deg)	93.2352(13)	90
γ (deg)	112.6166(12)	90
V(Å^3)	1686.16(6)	2006.48(10)
Z	4	4
ρ (g/cm^3)	1.199	1.482
abs coeff (mm^{-1})	1.372	1.874
T (K)	173(1)	173(1)
$2\theta_{max}$ (°)	142.50	55.02
total data	11431	16975
unique data (R_{int})	6200 (0.0173)	4572 (0.0159)
Obs data [I>2($\sigma(I)$)]	5443	4472
Params	401	226
R_1 [I>2$\sigma(I)$]^a	0.0379	0.0164
wR_2 [all data]^a	0.1020	0.0435
max/min $\Delta\rho$ (e$^-$ Å^{-3})	0.423/-0.207	0.287/-0.185

^{a} $R_1 = \sum||F_o| - |F_c||/\sum|F_o|$; $wR_2 = [\sum w(F_o^2 - F_c^2)^2/\sum w(F_o^4)]^{1/2}$

Table 2.3: Crystallographic data for **5** and **6**.

Compound	**5**•THF	**6**
Formula	$C_{25}H_{34}BGeOP$	$C_{21}H_{21}Cl_2PSn$
Formula weight	464.89	493.94
Crystal system	monoclinic	monoclinic
Space group	*C*2/*c*	*C*2/*c*
a (Å)	34.2302(9)	12.9507(4)
b (Å)	7.9115(2)	14.5477(4)
c (Å)	23.0344(6)	22.1627(6)
α (deg)	90	90
β (deg)	128.5873(3)	103.1066(3)
γ (deg)	90	90
V(Å^3)	4876.0(2)	4066.7(2)
Z	8	8
ρ (g/cm^3)	1.267	1.613
abs coeff (mm^{-1})	1.335	1.599
T (K)	173(1)	173(1)
$2\theta_{max}$ (°)	56.49	54.93
total data	22028	17697
unique data (R_{int})	5986 (0.0188)	4658 (0.0144)
Obs data [I>2($\sigma(I)$)]	5317	4367
Params	284	228
R_1 [I>2$\sigma(I)$]^a	0.0264	0.0180
wR_2 [all data]^a	0.0735	0.0466
max/min $\Delta\rho$ (e$^-$ Å^{-3})	0.858/-0.394	0.438/-0.198

^{a} $R_1 = \sum||F_o| - |F_c||/\sum|F_o|$; $wR_2 = [\sum w(F_o^2 - F_c^2)^2/\sum w(F_o^4)]^{1/2}$

Table 2.4: Crystallographic data for **7** and **8**.

Compound	**7**	**8**
Formula	$C_{21}H_{24}BP$	$C_{26}H_{21}Cl_2O_5PSnW$
Formula weight	318.18	817.84
Crystal system	triclinic	monoclinic
Space group	$P\bar{1}$	$I2/a$
a (Å)	9.7208(4)	14.4711(6)
b (Å)	9.9807(4)	12.6086(5)
c (Å)	10.0913(4)	31.0557(13)
α (deg)	99.4355(4)	90
β (deg)	92.3567(5)	96.8451(4)
γ (deg)	113.1114(4)	90
V(Å^3)	882.28(6)	5626(4)
Z	2	8
ρ (g/cm^3)	1.198	1.931
abs coeff (mm^{-1})	0.153	5.254
T (K)	173(1)	173(1)
$2\theta_{max}$ (°)	57.87	56.66
total data	8248	25310
unique data (R_{int})	4297 (0.0128)	6879 (0.0151)
Obs data [I>2($\sigma(I)$)]	3890	6540
Params	222	326
R_1 [I>2$\sigma(I)$]^a	0.0348	0.0154
wR_2 [all data]^a	0.0928	0.0387
max/min $\Delta\rho$ (e$^-$ Å^{-3})	0.426/-0.235	0.876/-0.359

^{a} $R_1 = \sum||F_o| - |F_c||/\sum|F_o|$; $wR_2 = [\sum w(F_o^2 - F_c^2)^2/\sum w(F_o^4)]^{1/2}$

Table 2.5: Crystallographic data for **9** and **10**.

Compound	**9**•0.5 Et_2O	**10**
Formula	$C_{28}H_{28}O_{5.5}PSnW$	$C_{26}H_{21}Cl_2GeO_5PW$
Formula weight	786.01	771.74
Crystal system	triclinic	monoclinic
Space group	$P\bar{1}$	$I2/a$
a (Å)	10.7586(6)	14.2653(4)
b (Å)	11.9138(7)	12.4535(3)
c (Å)	12.7748(8)	31.0261(3)
α (deg)	79.1297(6)	90
β (deg)	89.4825(7)	97.2299(2)
γ (deg)	64.8919(6)	90
V(Å^3)	1451.45(15)	5468.1(2)
Z	2	8
ρ (g/cm^3)	1.798	1.875
abs coeff (mm^{-1})	4.911	5.592
T (K)	173(1)	173(1)
$2\theta_{max}$ (°)	52.79	55.11
total data	30449	24150
unique data (R_{int})	5932 (0.0168)	6334 (0.0122)
Obs data [I>2($\sigma(I)$)]	5850	6063
Params	335	325
R_1 [I>2$\sigma(I)$]^a	0.0167	0.0129
wR_2 [all data]^a	0.0425	0.0311
max/min $\Delta\rho$ (e$^-$ Å^{-3})	1.019/-0.738	0.518/-0.391

^{a} $R_1 = \sum||F_o| - |F_c||/\sum|F_o|$; $wR_2 = [\sum w(F_o^2 - F_c^2)^2/\sum w(F_o^4)]^{1/2}$

2.6 References

1. (*a*) Arduengo, A. J. III; Harlow, R. L.; Kline, M. *J. Am. Chem. Soc.* **1991,** *113*, 361; (*b*) Kuhn, N.; Kratz, T. *Synthesis* **1993**, 561; (*c*) Dröge, T.; Glorius, F. *Angew. Chem. Int. Ed.* **2010**, *49*, 6940; (*d*) Diéz-González, S.; Nolan, S. P. *Coord. Chem. Rev.* **2007**, *251*, 874; For related carbene-based donors, see: (*e*) Martin, D.; Melaimi, M.; Soleilhavoup, M.; Bertrand, G. *Organometallics* **2011**, *30*, 5304; (*f*) Crabtree, R. H. *Coord. Chem. Rev.* **2013**, *257*, 755.
2. (*a*) Braunschweig, H.; Dewhurst, R. D.; Hammond, K.; Mies, J.; Radacki, K.; Vargas, A. *Science* **2012**, *336*, 1420; (*b*) Wang, Y.; Xie, Y.; Wei, P.; King, R. B.; Schaefer, H. F. III; Schleyer, P. v. R.; Robinson, G. H. *Science* **2008**, *321*, 1069; (*c*) Sidiropoulos, A.; Jones, C.; Stasch, A.; Klein, S.; Frenking, G. *Angew. Chem. Int. Ed.* **2009**, *48*, 9701; (*d*) Jones, C., Sidiropoulos, A.; Holzmann, N.; Frenking, G.; Stasch, A. *Chem. Commun.* **2012**, *48*, 9855; (*e*) Wang, Y.; Xie, Y.; Wei, P.; King, R. B.; Schaefer, H. F. III; Schleyer, P. v. R.; Robinson, G. H. *J. Am. Chem. Soc.* **2008**, *130*, 14970; (*f*) Abraham, M. Y.; Wang, Y.; Xie, Y.; Wei, P.; Schaefer, H. F. III; Schleyer, P. v. R.; Robinson, G. H. *Chem. Eur. J.* **2010**, *16*, 432.
3. For recent examples with IPr and related NHC donors, see: (*a*) Sindlinger, C. P.; Wesemann, L. *Chem. Sci.* **2014**, *5,* 2739; (*b*) Filippou, A.; Baars, B.; Chernov, O.; Lebedev, Y. N.; Schnakenburg, G. *Angew. Chem. Int. Ed.* **2014**, *53*, 565; (*c*) Wang, Y.; Xie, Y.; Wei, P.; Schaefer, H. F. III; Schleyer, P. v. R.; Robinson, G. H. *J. Am. Chem. Soc.* **2013**, *135*, 19139; (*d*) Xiong, Y.; Yao, S.; Inoue, S.; Epping, J. D.; Driess, M. *Angew. Chem., Int. Ed.* **2013**, *52*, 7147; (*e*) Mondal, K. C.; Samuel, P. P.; Tretiakov, M.; Sing, A. P.; Roesky, H. W.; Stückl, A. C.; Niepötter, B.; Carl,

E.; Wolf, H.; Herbst-Irmer, R.; Stalke, D. *Inorg. Chem.* **2013**, *52*, 4736; (*f*) Al-Rafia, S. M. I.; Momeni, M. R.; McDonald, R.; Ferguson, M. J.; Brown, A.; Rivard, E. *Angew. Chem. Int. Ed.* **2013**, *52*, 6390; (*g*) Jana, A.; Huch, V.; Scheschkewitz, D. *Angew. Chem. Int. Ed.* **2013**, *52*, 12179.

4. (*a*) Thimer, K. C.; Al-Rafia, S. M. I.; Ferguson, M. J.; McDonald, R.; Rivard, E. *Chem. Commun.* **2009**, 7119; (*b*) Al-Rafia, S. M. I.; Malcolm, A. C.; Liew, S. K.; Ferguson, M. J.; Rivard, E. *J. Am. Chem. Soc.* **2011**, *133*, 777; (*c*) Al-Rafia, S. M. I.; Malcolm, A. C.; McDonald, R.; Ferguson, M. J.; Rivard, E. *Angew. Chem. Int. Ed.* **2011**, *50*, 8354; (*d*) Al-Rafia, S. M. I.; Malcolm, A. C.; McDonald, R.; Ferguson, M. J.; Rivard, E. *Chem. Commun.* **2012**, *48*, 1308; (*e*) Al-Rafia, S. M. I.; Shynkaruk, O.; McDonald, S. M.; Liew, S. K.; Ferguson, M. J.; McDonald, R.; Herber, R. H.; Rivard, E. *Inorg. Chem.* **2013**, *52*, 5581; (*f*) Al-Rafia, S. M.; Momeni, M. R.; Ferguson, M. J.; McDonald, R.; Brown, A., Rivard, E. *Organometallics* **2013**, *32*, 6658; (*g*) For a recent review of this field, see: Rivard, E. *Dalton. Trans.* **2014**, *43*, 8577.

5. (*a*) Al-Rafia, S. M. I.; Malcolm, A. C.; Liew, S. K.; Ferguson, M. J.; McDonald, R.; Rivard, E. *Chem. Commun.* **2011**, *47*, 6987; For related studies involving NHOs, see: (*b*) Kuhn, N.; Bohnen, H.; Kreutzberg, J.; Bläser, D.; Boese, R. *J. Chem. Soc., Chem. Commun.* **1993**, 1136. (*c*) Fürstner, A.; Alcarazo, M.; Goddard, R.; Lehmann, C. W. *Angew. Chem. Int. Ed.* **2008**, *47*, 3210; (*d*) Dumrath, A.; Wu, X. -F.; Neumann, H.; Spannenberg, A.; Jackstell, R.; Beller, M. *Angew. Chem. Int. Ed.* **2010**, *49*, 8988; (*e*) Malcolm, A. C.; Sabourin, K. J.; McDonald, R.; Ferguson, M. J.; Rivard, E. *Inorg. Chem.* **2012**, *51*, 12905; (*f*) Wang, Y.; Abraham, M. Y;

Gilliard, R. J. Jr.; Sexton, D. R.; Wei, P.; Robinson, G. H. *Organometallics* **2013**, *32*, 6639; (*g*) Berger, C. J.; He, G.; Merten, C.; McDonald, R.; Ferguson, M. J.; Rivard, E. *Inorg. Chem.* **2014**, *53*, 1475.

6. (*a*) Jasinski, J. M.; Gates, S. M. *Acc. Chem. Res.* 1991, *24*, 9; (*b*) Isobe, C.; Cho, H.-C.; Sewell, J. E. *Surf. Sci*. **1993**, *295*, 117.
7. Bestmann, H. J.; Kratzer, O. *Chem. Ber.* **1963**, *96*, 1899.
8. (*a*) Wittig, G.; Schöllkopf, U. *Chem. Ber.-Rec.* **1954**, *87*, 1318; (*b*) Beedham, I.; Micklefield, J. *Curr. Org. Syn.* **2005**, *2*, 231; (*c*) Xu, S.; He, Z. *RSC Adv.* **2013**, *3*, 16885.
9. For selected examples, see: (*a*) Pörschke, K. –R.; Wilke, G.; Mynott, R. *Chem. Ber*. **1985**, *118*, 298; (*b*) Fortier, S.; Kaltsoyannis, N.; Wu, G.; Hayton, T. W. *J. Am. Chem. Soc.* **2011**, *133*, 14224.
10. (*a*) Bestmann, H. J.; Sühs, K.; Röder, T. *Angew. Chem. Int. Ed. Engl.* **1981**, *20*, 1038; (*b*) Borisova, I. V.; Zemlyansky, N. N.; Belsky, V. K.; Kolosova, N. D.; Sobolev, A. N.; Luzikov, Y. N.; Ustynyuk, Y. A.; Beletskaya, I. P. *J. Chem. Soc., Chem. Commun.* **1982**, 1090; (*c*) Bestmann, H. J.; Röder, T.; Sühs, K. *Chem. Ber.* 1988, *121*, 1509. (*d*) Breitsameter, F.; Schrödel, H.-P.; Schmidpeter, A.; Nöth, H.; Rojas-Lima, S. *Z. Anorg. Allg. Chem.* **1999**, *625*, 1293.
11. (*a*) Prabusankar, G.; Sathyanarayana, A.; Suresh, P.; Babu, C. N.; Srinivas, K.; Metla, B. P. R. *Coord. Chem. Rev.* **2014**, *269*, 96; (*b*) Inoue, S.; Eisenhut, C. *J. Am. Chem. Soc.* **2013**, *135*, 18315; (*c*) Abraham, M. Y.; Wang, Y.; Xie, Y.; Wei, P.; Schaefer, H. F. III; Schleyer, P. v. R.; Robinson, G. H. *J. Am. Chem. Soc.* **2011**, *133*, 8874; (*d*) Al-Rafia, S. M. I.; McDonald, R.; Ferguson, M. J.; Rivard, E. *Chem.*

Eur. J. **2012**, *18*, 13810; (*e*) Kinjo, R.; Donnadieu, B.; Celik, M. A.; Frenking, G.; Bertrand, G. *Science* **2011**, *333*, 610; (*f*) Bonyhady, S. J.; Collis, D.; Frenking, G.; Holzmann, N.; Jones, C.; Stasch, A. *Nat. Chem.* **2010**, *2*, 865.

12. (*a*) Chen, M.; Feng, Y.-G.; Wang, X.; Li, T.-C.; Zhang, J.-Y.; Qian, D.-J. *Langmuir* **2007**, *23,* 5296; (*b*) Nyamen, L. D.; Revaprasadu, N.; Pullabhotla, R. V. S. R.; Nejo, A. A.; Ndifon, P. T.; Malik, M. A.; O'Brien, P. *Polyhedron* **2013**, *56,* 62; (*c*) Hines, D. A.; Kamat, P. V. *ACS Appl. Mater. Interfaces* **2014**, *6*, 3041.

13. (*a*) King, R. B. *Inorg. Chem.* **1963**, *2*, 199; (*b*) Jutzi, P.; Hoffman, J.; Brauner, D. J.; Krüger, C. *Angew. Chem. Int. Ed. Engl.* **1973**, *12*, 1002; (*c*) du Mont, W.-W.; Neudert, B.; Rudolph, C.; Schumann, H. *Angew. Chem. Int. Ed. Engl.* **1976**, *15*, 308; (*d*) Ando, W.; Sekiguchi, A.; Hagiwara, K.; Sakakibara, A.; Yoshida, H. *Organometallics* **1988**, *7*, 558; (*e*) Pu, L.; Twamley, B.; Power, P. P. *Organometallics* **2000**, *19*, 2874; (*f*) Hadlington, T. J.; Hermann, M.; Li, J.; Frenking, G.; Jones, C. *Angew. Chem. Int. Ed.* **2013,** *52*, 10199; (*g*) See also: Mizuhata, Y.; Sasamori, T.; Tokitoh, N. *Chem. Rev.* 2009, *109*, 3479.

14. For a prior report involving the preparation of $Cy_3P{\bullet}GeCl_2$, see: Doddi, A.; Gemel, C.; Winter, M.; Fischer, R. A.; Goedecke, C.; Rzepa, H. S.; Frenking, G. *Angew. Chem. Int. Ed.* **2013**, *52*, 450.

15. The identification of the $[HPCy_3]^+$ salt by-product formed in the reaction of Cy_3P with $Cl_2Ge{\bullet}$dioxane was accomplished by ^{31}P NMR spectroscopy (δ = 20.2 ppm) and the detection of a characteristic doublet ^1H NMR resonance for the P-H residue at 7.12 ($^1J_{PH}$ = 488 Hz) in C_6D_6; this latter resonance collapsed to a single resonance in the $^1H\{^{31}P\}$ spectrum. Phosphonium salts of $GeCl_3^-$ ($[HPR_3]GeCl_3$)

have been reported in the literature: (*a*) du Mont, W.-W.; Rudolph, G. *Chem. Ber.* **1976**, *109*, 3419; (*b*) Dal Canto, R. A.; Roskamp, E. J. *J. Org. Chem.* **1992**, *57*, 406; (*c*) Davis, M. F.; Levason, W.; Reid, G.; Webster, M. *Dalton Trans.* **2008**, 2261.

16. (*a*) Kolodiazhnyi, O. I. *Tetrahedron* **1996**, *52*, 1855; (*b*) Cristau, H.-J. *Chem. Rev.* **1994**, *94*, 1299; (*c*) Bestmann, H. J.; Arenz, T. *Angew. Chem. Int. Ed. Engl.* **1986**, *25*, 559.
17. Rajendran, K. V.; Gilheany, D. G. *Chem. Commun*. **2012**, *48*, 817.
18. Papp, R.; Somoza Jr., F. B.; Sieler, J.; Blaurock, S.; Hey-Hawkins, E. *J. Organomet. Chem.* **1999**, *585*, 127.
19. For related studies involving hydride transfer to carbene donor sites (followed by ring-expansion), see: (*a*) Arrowsmith, M.; Hill, M. S.; Kociok-Köhn, MacDougall, D. J.; Mahon, M. F. *Angew. Chem. Int. Ed.* **2012**, *51*, 2098; (*b*) Schmidt, D.; Berthel, J. H. J.; Pietsch, S.; Radius, U. *Angew. Chem. Int. Ed.* **2012**, *51*, 8881; (*c*) ref 11*d*. (*d*) Momeni, M. R.; Rivard, E.; Brown, A. *Organometallics* **2013**, *32*, 6201; (*e*) Iversen, K. J.; Wilson, D. J. D.; Dutton, J. L. *Organometallics* **2013**, *32*, 6209; (*f*) Fang, R.; Yang, L.; Wang, Q. *Organometallics* **2014**, *33*, 53.
20. Brown, H. C.; Krishnamurthy, S.; Hubbard, J. L.; Coleman, R. A. *J. Organometal. Chem.* **1979**, *166*, 281.
21. Balch, A. L.; Oram, D. E. *Organometallics* **1988**, *7*, 155.
22. For related low oxidation state Sn(II) hydrides compounds, see: (*a*) Eichler, B. E.; Power, P. P. *J. Am. Chem. Soc.* **2000**, *122*, 8785; (*b*) Ding, Y.; Hao, H.; Roesky, H. W.; Noltemeyer, M.; Schmidt, H. –G. *Organometallics* **2001**, *20*, 4806; (*c*) Rivard,

E.; Fischer, R. C.; Wolf, R.; Peng, Y.; Merrill, W. A.; Schley, N. D.; Zhu, Z.; Pu, L.; Fettinger, J. C.; Teat, S. J.; Nowik, I.; Herber, R. H.; Takagi, N.; Nagase, S.; Power, P. P. *J. Am. Chem. Soc.* **2007**, *129*, 16197.

23. Gresback, R.; Holman, Z.; Kortshagen, U. *Appl. Phys. Lett.* **2007**, *91*, 093119.
24. Yuan, F. –W.; Tuan, H. –Y. *Chem. Mater.* **2014**, *26*, 2172.
25. Wilcoxon, J. P.; Provencio, P. P.; Samara, G. A. *Condens. Matter* **2001**, *64*, 035417.
26. Lambert, T. N.; Andrews, N. L.; Gerung, H.; Boyle, T. J.; Oliver, J. M.; Wilson, B. S.; Han, S. M. *Small* **2007**, *3*, 691.
27. Henderson, E. J.; Seino, M.; Puzzo, D. P.; Ozin, G. A. *ACS Nano* **2010**, *4*, 7683.
28. Vaughn II, D. D.; Schaak, R. E. *Chem. Soc. Rev.* **2013**, *42*, 2861.
29. Martienssen, W.; Warliomont, H. *Springer Handbook of Condensed Matter and Materials Data*; *Springer GmbH* **2005**.
30. Taylor, B. R.; Kauzlarich, S. M.; Lee, H. W. H.; Delgado, G. R. *Chem. Mater.* **1998**, *10*, 22.
31. Taylor, B. R.; Kauzlarich, S. M.; Delgado, G. R.; Lee, H. W. H. *Chem. Mater.* **1999**, *11*, 2493.
32. Ma, X.; Wu, F.; Kauzlarich, S. M. *J. Solid State Chem.* **2008**, *181*, 1628.
33. Lu, X.; Ziegler, K. J.; Ghezelbash, A.; Johnston, K. P.; Korgel, B. A. *Nano Lett.* **2004**, *4*, 969.
34. Fok, E.; Shih, M.; Meldrum, A.; Veinot, J. G. C. *Chem. Comm.* **2004**, 386.
35. Chiu, H. W.; Chervin, C. N.; Kauzlarich, S. M. *Chem. Mater.* **2005**, *17*, 4858.
36. Stoldt, C. R.; Haag, M. A.; Larsen, B. A. *Appl. Phys. Lett.* **2008**, *93*, 043125.

37. Kortshagen, U.; Anthony, R.; Gresback, R.; Holman, Z.; Ligman, R.; Liu, C.-Y.; Mangolini, L.; Campbell, S. A. *Pure Appl. Chem.* **2008**, *80*, 1901.

38. Gerung, H.; Bunge, S. D.; Boyle, T. J.; Brinker, C. J.; Han, S. M. *Chem. Commun.* **2005**, 1914.

39. Warner, J. H.; Tilley, R. D. *Nanotechnology* **2006**, *17*, 3745.

40. Prabakar, S.; Shiohara, A.; Hanada, S.; Fujioka, K.; Yamamoto, K.; Tilley, R. D. *Chem. Mater.* **2010**, *22*, 482.

41. Henderson, E. J.; Hessel, C. M.; Veinot, J. G. C. *J. Am. Chem. Soc.* **2008**, *130*, 3624.

42. Chou, N. H.; Oyler, K. D.; Motl, N. E.; Schaak, R. E. *Chem. Mater.* **2009**, *21*, 4105.

43. Muthuswamy, E.; Iskandar, A. S.; Amador, M. M.; Kauzlarich, S. M. *Chem. Mater.* **2013**, *25*, 1416.

44. Muthuswamy, E.; Zhao, J.; Tabatabaei, K.; Amador, M. M.; Holmes, M. A.; Osterloh, F. E.; Kauzlarich, S. M. *Chem. Mater.* **2014**, *26*, 2138.

45. Lu, X.; Korgel, B. A.; Johston, K. P. *Chem. Mater.* **2005**, *17*, 6479.

46. Buriak, J. M. *Chem. Rev*. **2002**, *102*, 1271.

47. Shirahata, N.; Hirakawa, D.; Masuda, Y.; Sakka, Y. *Langmuir* **2013**, *29*, 7401.

48. Lee, D. C.; Pietryga, J. M.; Robel, I.; Werder, D. J.; Schaller, R. D.; Klimov, V. I. *J. Am. Chem. Soc.* **2009**, *131*, 3436.

49. Wheeler, L. M.; Levij, L. M.; Kortshagen, U. R. *J. Phys. Chem. Lett.* **2013**, *4*, 3392.

50. Niquet, Y. M.; Allan, G.; Delerue, C.; Lannoo, M. *Appl. Phys. Lett.* **2000**, *77*, 1182.

51. Millo, O.; Balberg, I., Azulay, D.; Purkait, T. K.; Swarnakar, A. K.; Rivard, E.; Veinot, J. G. C. *J. Phys. Chem. Lett.* **2015**, *6*, 3396.

52. Pangborn, A. B.; Giardello, M. A.; Grubbs, R. H.; Rosen, R. K.; Timmers, F. J. *Organometallics* **199**6, *15*, 1518.

53. Hope, H. *Prog. Inorg. Chem.* **1994**, *41*, 1.

54. Blessing, R. H. *Acta Crystallogr.* **1995**, *A51*, 33.

55. Sheldrick, G. M. *Acta Crystallogr.* **2008**, *A64*, 112.

56. Beurskens, P. T.; Beurskens, G.; de Gelder, R.; Smits, J. M. M.; Garcia-Garcia, S.; Gould, R. O. *DIRDIF-2008*; Crystallography Laboratory, Radboud University: Nijmegen, The Netherlands **2008**.

57. Lesley, M. J. G.; Woodward, A.; Taylor, N. J.; Marder, T. B.; Cazenobe, I.; Ledoux, I.; Zyss, J.; Thornton, A.; Bruce, D. W.; Kakkar, A. K. *Chem. Mater.* **1998**, *10,* 1355.

58. Blumenthal, A.; Bissinger, P.; Schmidbaur, H. J. *J. Organomet. Chem.* **1993**, *462*, 107.

59. Williams, A. T. R.; Winfield, S. A.; Miller, J. N. *Analyst* **1983**, *108*, 1067.

60. Suzuki, K.; Kobayashi, A.; Kaneko, S.; Takehira, K.; Yoshihara, T.; Ishida, H.; Shiina, Y.; Oishi, S.; Tobita, S. *Phys. Chem. Chem. Phys.* **2009**, *11*, 9850.

Chapter 3: Transition Metal-Mediated Donor-Acceptor Coordination of Low Valent Group 14 Element Halides

3.1 Introduction

A central concept in synthetic inorganic chemistry is the use of electron-donating ligands to bind/stabilize reactive inorganic species with unusual bonding environments. In this regard *N*-heterocyclic carbenes (NHCs) such as IPr ([(HCNDipp)$_2$C:]; Dipp = 2,6-^{i}Pr$_2$C$_6$H$_3$) and their structural analogues have been used to intercept novel main group species such as B_2 and the homologous ditetrelene series :E=E: (E = Si, Ge and Sn).[1,2] Also of relevance to this chapter is the use of NHCs in conjunction with various Lewis acidic capping units to coordinate the inorganic methylene analogues :EH$_2$ (E = Si, Ge, and Sn) via a general donor-acceptor approach (*e.g.* IPr•GeH$_2$•BH$_3$).[3] In addition, this protocol was extended to include EH$_2$ complexes supported by the *N*-heterocyclic olefin (NHO) IPr=CH$_2$, and the Wittig reagent Ph$_3$P=CMe$_2$.[4] Interest in these complexes stems from the formation of EH$_2$ as intermediates en route to bulk semi-conductors and metals via tetrelane (EH$_4$) degradation.[5] Moreover, it was demonstrated in the previous chapter that luminescent Ge nanoparticles could be prepared from the mild, one pot, decomposition of the donor-acceptor GeH$_2$ complex Ph$_3$PCMe$_2$•GeH$_2$•BH$_3$.[6] Thus finding new ways to stabilize low oxidation state main group hydrides is of importance.

Metal centered Lewis bases (MLBs), wherein an electron rich metal center acts as a formal two-electron donor, are being increasingly investigated within the

context of supporting low-oxidation state main group element chemistry.[7] A possible advantage of MLBs over traditional organic-based donors is the ability to dramatically alter the coordination properties of a MLB via co-ligand modification and/or by changing the metal entirely. Since Nowell and Russell's synthesis of [(η^5-C_5H_5)$(CO)_2$Co→$HgCl_2$] in 1964,[8] various late metal MLBs based on Ir, Pt and Rh have been developed.[9] Moreover metal centered Lewis bases can readily form stable coordinative interactions with electron deficient group 13 (B, Al and Ga)[10] and group 14 (Ge, Sn and Pb)[11] compounds. Herein, the ability of the half sandwich complex $CpRh(PMe_2Ph)_2$ (Cp = η^5-C_5H_5)[12] and the nucleophilic Pt(0) donor, $Pt(PCy_3)_2$ to interact with divalent group 14 species is explored. An ultimate goal would be to generate mixed metal donor-acceptor complexes of EH_2 units (E = Ge, Sn and Pb) for the later preparation of binary E_xM_y (M = metal) bulk or nanomaterials.[13]

3.2 Results and Discussions

This study began with an attempt to synthesize a $GeCl_2$ donor-acceptor complex using $CpRh(PMe_2Ph)_2$ as a Lewis base and $W(CO)_5$ as a capping Lewis acid. However, when $THF{\bullet}GeCl_2{\bullet}W(CO)_5$ was combined with $CpRh(PMe_2Ph)_2$ in toluene for 12 hrs, the resulting deep yellow solid gave spectroscopic signatures consistent with C-H bond activation of the cyclopentadienyl ligand. Specifically, a highly upfield-positioned doublet of triplet resonance was found at -11.98 ppm in the ^1H NMR spectrum in CD_2Cl_2 ($^2J_{H\text{-}P}$ = 29.9 Hz and $^1J_{H\text{-}Rh}$ = 19.9 Hz), indicating that hydrogen migration to yield a terminal Rh-H group transpired. Moreover, two distinct Cp-H resonances of equal intensity were noted at 5.40 and 5.75 ppm, respectively, consistent with a mono-functionalized Cp unit. X-ray crystallography later confirmed that hydrogen migration/Cp ring activation did occur to form the Rh(III) product $[(CO)_5W{\bullet}GeCl_2(\eta^5\text{-}C_5H_4)]RhH(PMe_2Ph)_2$ (**1**) (eqn. 3.1, Figure 3.1).

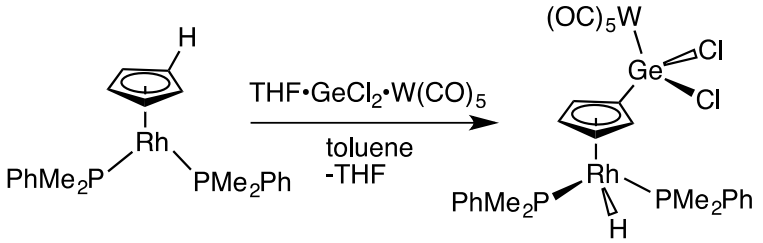

(3.1)

1

A related hydride migration/Cp activation process was noted when $CpRh(PMe_3)_2$ was treated with the bulky alkyl halides ^{t}BuI or ^{i}PrI, affording the alkylated-cyclopentadienyl rhodium salts $[(\eta^5\text{-}C_5H_4R)RhH(PMe_3)_2]I$ (R = ^{t}Bu or ^{i}Pr).[14] It is likely that the high electrophilicity of the $GeCl_2{\bullet}W(CO)_5$ unit promotes attack at the Cp ring in $CpRh(PMe_2Ph)_2$, followed by proton transfer to the basic Rh center.

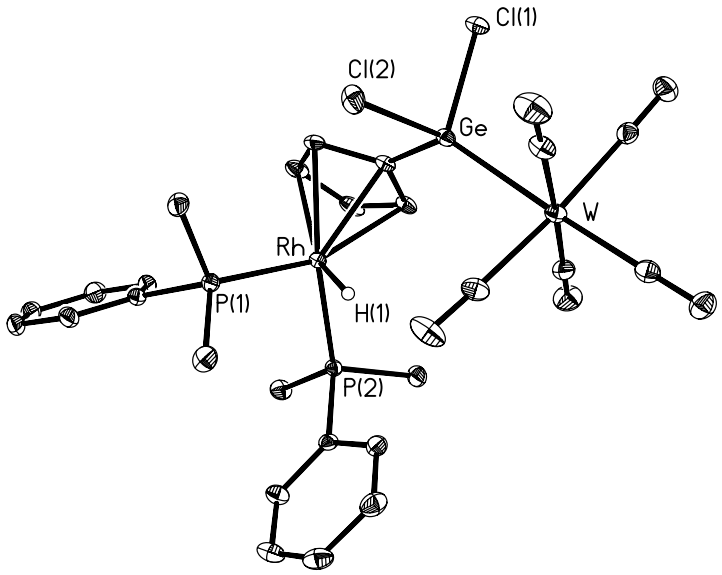

Figure 3.1. Molecular structure of $[(CO)_5W{\bullet}GeCl_2(\eta^5\text{-}C_5H_4)]RhH(PMe_2Ph)_2$ (**1**) with thermal ellipsoids presented at a 30 % probability level. All carbon-bound hydrogen atoms have been omitted for clarity. Selected bond lengths (Å) and angles (deg): Rh-H(1) 1.51(3), Ge-C(6) 1.9709(19), Ge-Cl(1) 2.2464(5), Ge-Cl(2) 2.2324(5), Ge-W 2.5820(2); Cl(1)-Ge-Cl(2) 96.62(2), C(6)-Ge-W 129.52(6), Ge-C(6)-Rh 123.82(9), Ge-C(6)-Rh 123.82(9).

As shown in Figure 3.1, $[(CO)_5W{\bullet}GeCl_2(\eta^5\text{-}C_5H_4)]RhH(PMe_2Ph)_2$ (**1**) has a $GeCl_2{\bullet}W(CO)_5$ group directly attached to a Cp ring with a Ge-C bond distance of 1.9709(19) Å; this value is similar to the covalent Ge-C bond length found within Power's aryl(halo)digermene $Ar^{Mes}Ge(Cl)Ge(Cl)Ar^{Mes}$ [2.000(6) Å] (Ar^{Mes} = 2,6-$Mes_2C_6H_3$; Mes = 2,4,6-$Me_3C_6H_2$).[15] The Ge-W interaction in **1** is 2.5820(2) Å and is the same within experimental error as the average Ge-W distance of 2.5833(16) Å in $IPr{\bullet}GeCl_2{\bullet}W(CO)_5$.[16] The hydride bound to the Rh center in **1** could be located in the electron difference map and the refined Rh-H bond length [1.51(3) Å] is of similar value as in $Cp_2Zr(CH_2PPh_2)_2Rh(H)(PPh_3)$ [1.51(4) Å].[17]

A different reactivity profile was noted when $CpRh(PMe_2Ph)_2$ was combined with the Sn(II) dihalide adduct $(THF)_2SnCl_2{\bullet}W(CO)_5$. In this case the resulting yellow-

orange solid did not yield any spectroscopic evidence for Rh-H bond formation. The ^{1}H NMR spectrum of the product in $CDCl_3$ contained two virtual triplet resonances assigned to two methyl groups within the phosphine ligands (at 1.92 and 2.08 ppm), while one Cp environment was present, as evidenced by a singlet resonance at 5.25 ppm. Crystals of suitable quality for X-ray analysis were subsequently obtained and conclusively identified the product as the expected Lewis acid-base adduct $CpRh(PMe_2Ph)_2$•$SnCl_2$•$W(CO)_5$ (**2**) (eqn. 3.2). The molecular structure of **2** (Figure 3.2) shows a Rh-Sn single bond distance of 2.6152(5) Å, which is comparable to the terminal Rh-Sn linkage reported within *mer*-[{$Rh(CNC_8H_9)_3(SnCl_3)(\mu\text{-}SnCl_2)$}$_2$] [2.606(1) Å].[18] The Rh-Sn bond in **2** is however shorter compared to the Rh-Sn bonds within Marder's Sn(II) bis-adduct $Cl_2Sn[Rh(PMe_3)_3Cl]_2$ [2.712(1) Å].[11a]

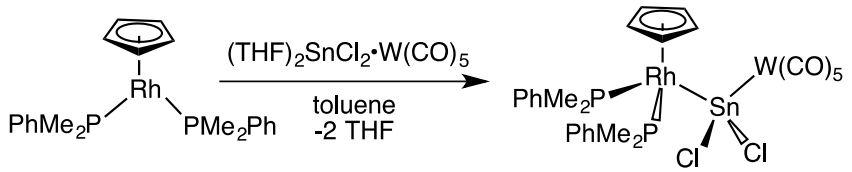

(3.2)

2

Following a related protocol as discussed above, the clean formation of the metal only Lewis pair $CpRh(PMe_2Ph)_2$•$PbCl_2$ (**3**) was accomplished by combining an equimolar amount of $PbCl_2$ with $CpRh(PMe_2Ph)_2$ in toluene (eqn. 3.3). Two broad methyl resonances from the PMe_2Ph ligands were located at 1.42 and 1.62 ppm in the ^{1}H NMR spectrum of **3** in CD_2Cl_2, while the corresponding $^{31}P\{^1H\}$ NMR spectrum afforded a doublet signal at 8.2 ppm with a $^1J_{Rh\text{-}P}$ constant of 170 Hz.

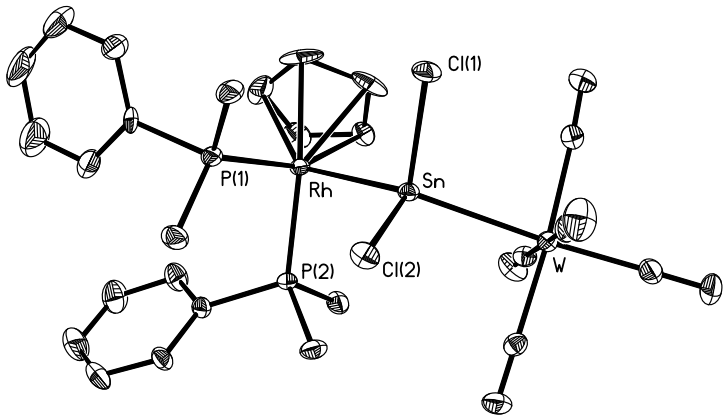

Figure 3.2. Molecular structure of $CpRh(PMe_2Ph)_2 \bullet SnCl_2 \bullet W(CO)_5$ (**2**) with thermal ellipsoids presented at a 30 % probability level. All hydrogen atoms have been omitted for clarity. Selected bond lengths (Å) and angles (deg): Rh-Sn 2.6152(5), Sn-Cl(1) 2.4544(14), Sn-Cl(2) 2.4685(15), Sn-W 2.7736(4); Rh-Sn-W 134.438(17), Cl(1)-Sn-Cl(2) 91.60(6).

The crystallographically determined structure of compound **3** is shown in Figure 3.3, and displays a highly pyramidalized lead center [Σ° at Pb (*avg.*) = 296.7°] with a Rh-Pb bond length of 2.7561(7) Å; this is, to my knowledge, the first structural characterization of such a bond type.

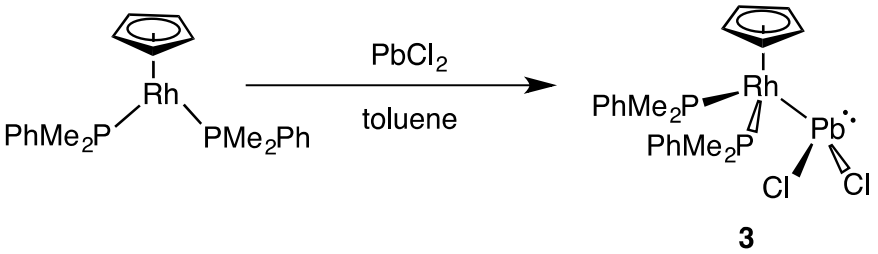

(3.3)

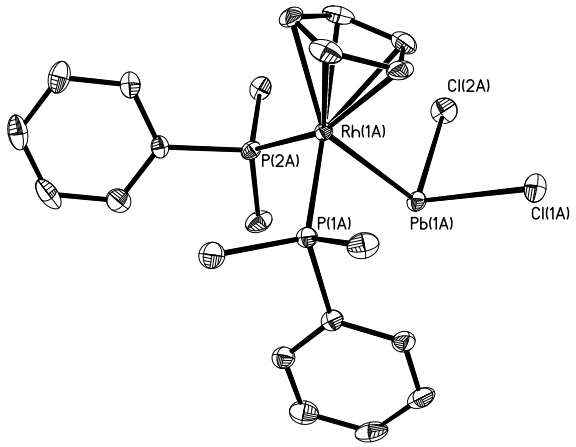

Figure 3.3. Molecular structure of $CpRh(PMe_2Ph)_2 \bullet PbCl_2$ (**3**) with thermal ellipsoids presented at a 30 % probability level. All hydrogen atoms have been omitted for clarity. Selected bond lengths (Å) and angles (deg) with parameters associated with a second molecule in the asymmetric unit listed in square brackets: Rh(1A)-Pb(1A) 2.7561(7) [2.7530(7)], Pb(1A)-Cl(1A) 2.6314(16) [2.6540(16)], Pb(1A)-Cl(2A) 2.6515(16) [2.6489(16)]; Cl(1A)-Pb(1A)-Cl(2A) 95.65(6) [98.91(6)], Rh(1A)-Pb(1A)-Cl(1A) 99.78(4) [111.8(2)], Rh(1A)-Pb(1A)-Cl(2A) 101.25(4) [97.48(4)].

Later, compounds **1**-**3** were reacted with various hydride sources to possibly gain access to new metal-supported EH_2 complexes (E = Ge, Sn or Pb). Motivated by prior successes with using $Li[BH_4]$ to generate donor-acceptor complexes of group 14 dihydrides (*e.g.* $Ph_3PCMe_2 \bullet SnH_2 \bullet W(CO)_5$),[4b] $CpRh(PMe_2Ph)_2 \bullet SnCl_2 \bullet W(CO)_5$ (**2**) was treated with two equivalents of $Li[BH_4]$ in Et_2O. The resulting reaction proceeds with the immediate formation of an insoluble black precipitate, presumably consisting of metallic tin and/or tin-tungsten clusters; the only product found in the colorless supernatant was the known phosphine-borane adduct, $PhMe_2P \bullet BH_3$.[19] The formation of $PhMe_2P \bullet BH_3$ likely occurs via $PhMe_2P$ decomplexation from rhodium and coordination to the Lewis acidic by-product BH_3 that is generated from $Li[BH_4]$ during Cl^-/H^- exchange. As a result, $Li[BH_4]$ was not used further as a hydride source for the related adducts **1** and **3**.

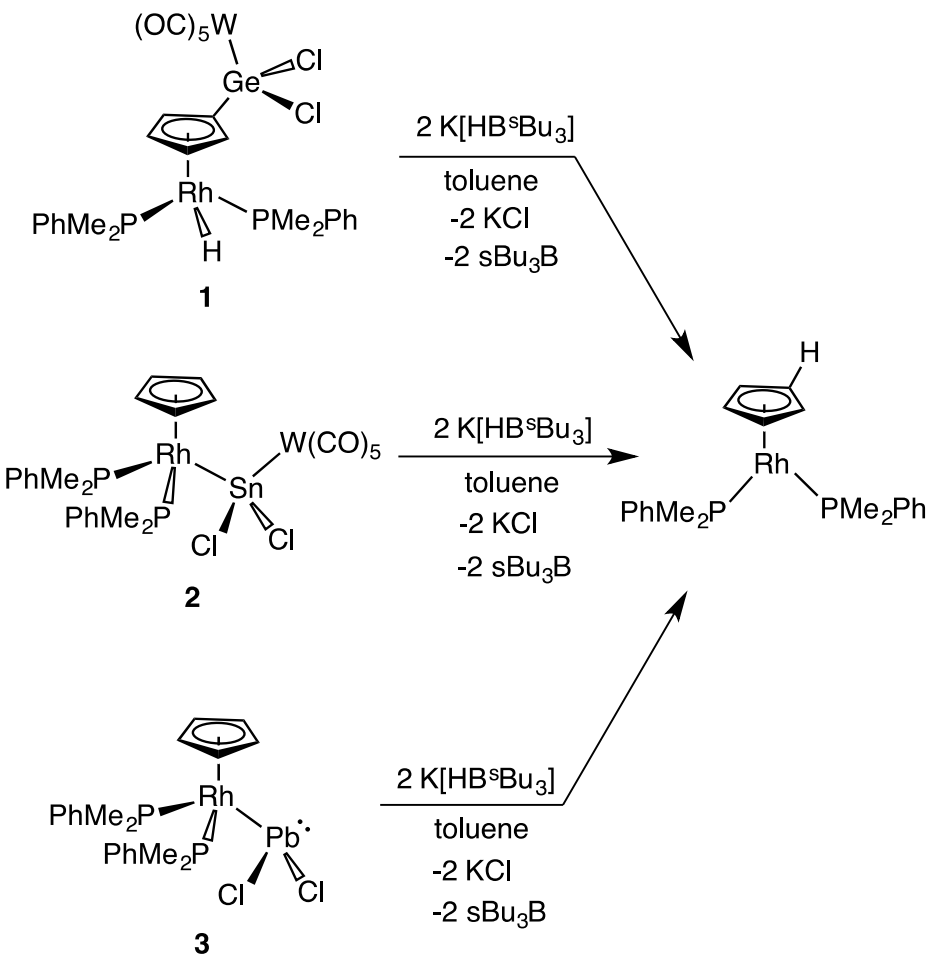

Scheme 3.1. Reactivity of compounds **1-3** with K[HB^{s}Bu$_3$]. The fate of the W(CO)$_5$ units and tetrel elements (Ge and Sn) in these reactions is unknown.

In order to obviate phosphine dissociation from Rh, the alkylated borate salt K[HB^{s}Bu$_3$] was selected as a hydride delivery agent for H^-/Cl^- exchange, the resulting by-product, ^{s}Bu$_3$B, is a hindered borane of low Lewis acidity.[20] However when compounds **1-3** were separately treated with two equivalents of K[HB^{s}Bu$_3$], the regeneration of free CpRh(PMe$_2$Ph)$_2$ occurred in all three cases (Scheme 3.1). Of note, when [(CO)$_5$W•GeCl$_2$(η^5-C$_5$H$_4$)]RhH(PMe$_2$Ph)$_2$ (**1**) was treated with K[HB^{s}Bu$_3$], the formal transfer of a hydrogen atom from Rh back to the Cp ring was

noted, along with the cleavage of a C(Cp)-Ge bond, leading to the formation of $CpRh(PMe_2Ph)_2$.

Positing that the soft-soft coordinative Rh-Pb interactions in **3** might still support the formation of a Pb(II) hydride complex at a later stage, $CpRh(PMe_2Ph)_2$•$PbCl_2$ (**3**) was treated with different Lewis acids in an attempt to form the Pb(II) dihalide precursors $CpRh(PMe_2Ph)_2$•$PbCl_2$•LA (LA = Lewis acid). Initially, compound **3** was reacted with an equimolar amount of THF•$GeCl_2$•$W(CO)_5$ with the goal of producing the formal tetrahalodimetallene complex $CpRh(PMe_2Ph)_2$•Cl_2Pb-$GeCl_2$•$W(CO)_5$. However, when **3** was treated with one equivalent of THF•$GeCl_2$•$W(CO)_5$, the clean formation of the previously synthesized Cp-ring activation product $[(CO)_5W$•$GeCl_2(\eta^5\text{-}C_5H_4)]RhH(PMe_2Ph)_2$ (**1**) transpired along with the expulsion of $PbCl_2$ from the coordination sphere of rhodium (Scheme 3.2). The noted inability of the Pb center in **3** to bind to $W(CO)_5$ is likely due to the lower nucleophilicity of Pb(II) centers in relation to Sn(II) (*i.e.* the inert pair effect).[3e] In another effort to obtain a donor-acceptor complex of $PbCl_2$, the bulky fluorinated arylborane ($BAr^F{}_3$) (Ar^F = 3,5-$(F_3C)_2C_6H_3$) was combined with compound **3**. Interestingly, this reaction afforded a new product with a Rh-H ^{1}H NMR resonance at -11.58 ppm in C_6D_6 (doublet of triplet pattern), consistent with related C-H bond activation occurring as in the formation of **1**. Furthermore, the presence of two distinct Cp resonances in the ^{1}H NMR spectrum and an accompanying ^{11}B NMR signal in the region expected for four-coordinate boron (-10.1 ppm), suggested that electrophilic attack at Cp by $BAr^F{}_3$ occurred. Fortunately colorless crystals of the product could be obtained and X-ray crystallography confirmed the formation of the

Cp ring-activated Rh(III) complex [η^5-$C_5H_4BAr^F{}_3$]RhH(PMe_2Ph)$_2$ (**4**) (Scheme 3.2, Figure 3.4). An independent synthesis of **4** was also accomplished by combining an equimolar mixture of CpRh(PMe_2Ph)$_2$ and $BAr^F{}_3$ in toluene. The molecular structure (Figure 3.4) of compound **4** shows a Rh-H bond distance of 1.50(3) Å, which is of similar value as the Rh-H bond length in compound **1**. The C(Cp)-B bond distance in **4** was found to be 1.636(3) Å which is elongated in comparison to the C(Cp)-B interaction of 1.545(3) Å in [(C_6F_5)$_2$B(η^5-C_5H_4)]$TiCl_3$.[21]

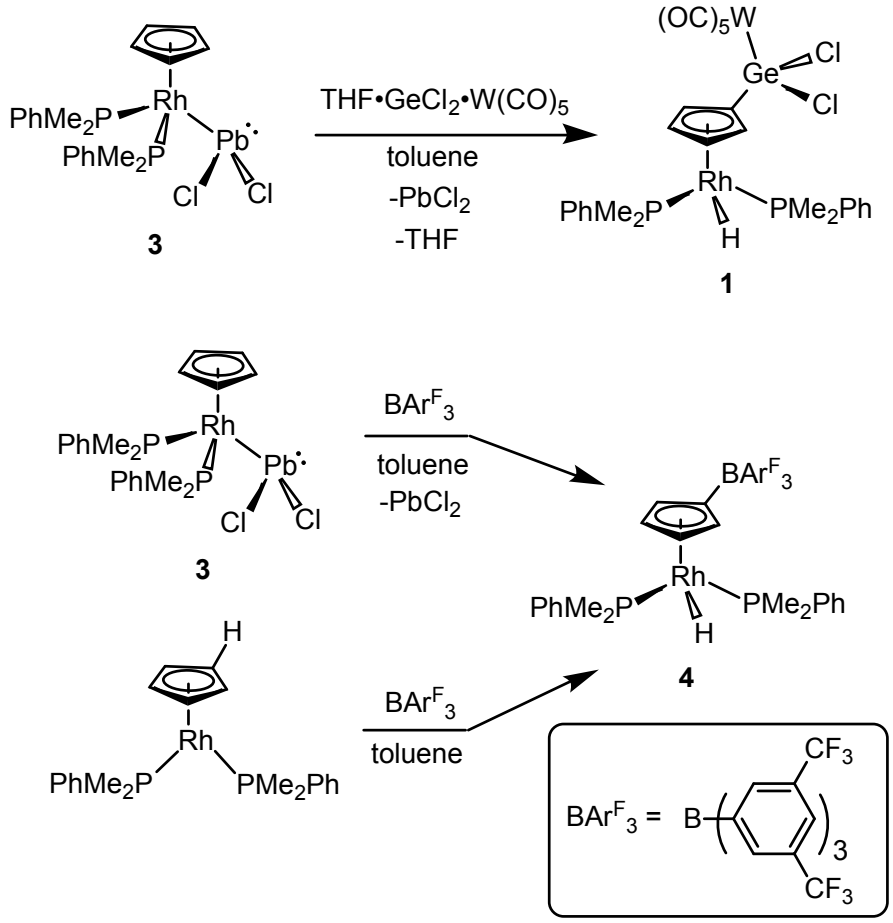

Scheme 3.2. Reactivity of **3** with different Lewis acids, leading to C-H bond activation.

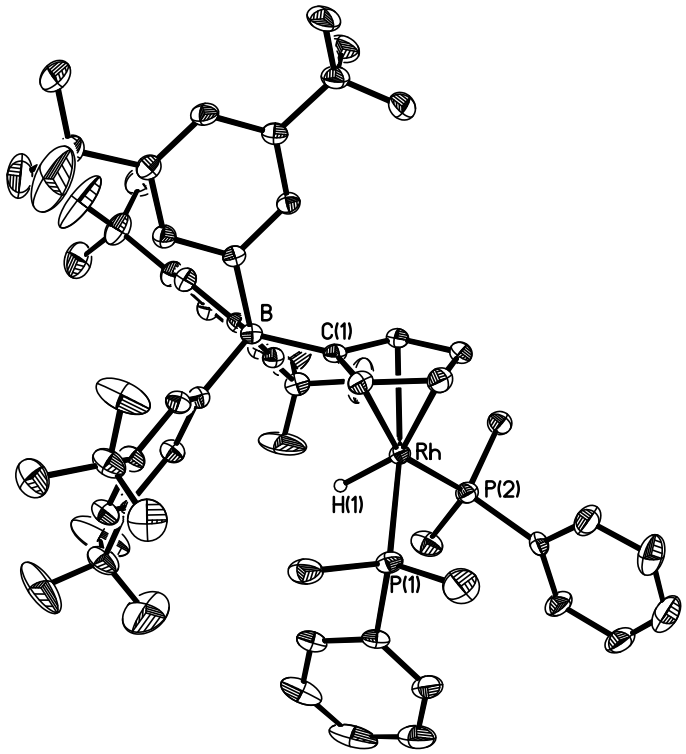

Figure 3.4. Molecular structure of $[\eta^5\text{-}C_5H_4BAr^F{}_3]RhH(PMe_2Ph)_2$ (**4**) with thermal ellipsoids presented at a 30 % probability level. All carbon-bound hydrogen atoms have been omitted for clarity. Selected bond lengths (Å) and angles (deg): B-C(1) 1.636(3), Rh-H 1.50(3); B-C(1)-Rh 132.18(13), average C(1)-B-C(Ar^F) = 109.5(3).

Apart from the use of $CpRh(PMe_2Ph)_2$ in the syntheses of donor-acceptor complexes of group 14 elements, the chemistry of another metal centered Lewis base $Pt(PCy_3)_2$[22] towards group 14 dihalide complexes was also briefly explored in this chapter. First, $Pt(PCy_3)_2$ was treated with THF•$GeCl_2$•$W(CO)_5$ in toluene. In place of 1:1 adduct formation, oxidative addition of the Ge-Cl bond at Pt occurs affording $ClPt(PCy_3)_2Ge(Cl)$•$W(CO)_5$ (**5**) as a yellow, moisture-sensitive solid. Recently Braunschweig, Jones and co-workers reported the formation of the Lewis acid-base adduct, $(Cy_3P)_2Pt$•$GeCl_2$ from the direct interaction of $Pt(PCy_3)_2$ with Cl_2Ge•dioxane.[11*d*] However the presence of a Lewis acidic $W(CO)_5$ unit at the Ge(II)

center facilitates Ge-Cl bond oxidative addition to form **5** (eqn. 3.4). Similar oxidative additions involving Lewis acidic BX_3 (X = Cl, Br or I),[23] GaX_3 (X = Br or I),[24] and $BiCl_3$[25] to Pt(0) complexes are known. The crystal structure of **5** is presented in Figure 3.5 and shows a Pt-Ge bond distance of 2.3526(5) Å, which is somewhat contracted in length in comparison to the Pt-Ge distance in $(PCy_3)_2Pt{\bullet}GeCl_2$ [2.397(1) Å].[11*d*] The overall geometry at Pt is square planar, consistent with a Pt(II) formal oxidation state, while the proximal Ge center adopts a distorted T-shaped geometry with a stereochemically active lone pair (*e.g.* Pt-Ge-Cl(2) angle = 104.87(2)°). The $^{31}P\{^1H\}$ NMR spectrum of **5** in C_6D_6 yields a resonance at 16.9 ppm with resolvable platinum satellites ($^1J_{P\text{-}Pt}$ = 2412 Hz).

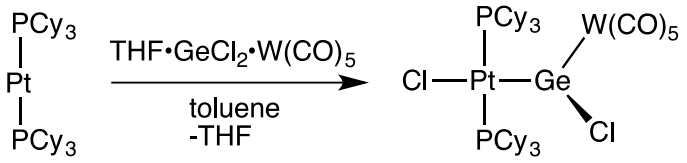

(3.4)

5

Compound **5** was also combined with two equivalents of the hydride source, $K[HB^sBu_3]$ with the intention of yielding a stable Ge(II) hydride complex. However, upon hydride addition, the only species identified in the $^{31}P\{^1H\}$ NMR spectrum of the resulting product mixture was free PCy_3; the formation of $^sBu_3B$ was also confirmed by ^{11}B NMR spectroscopy.

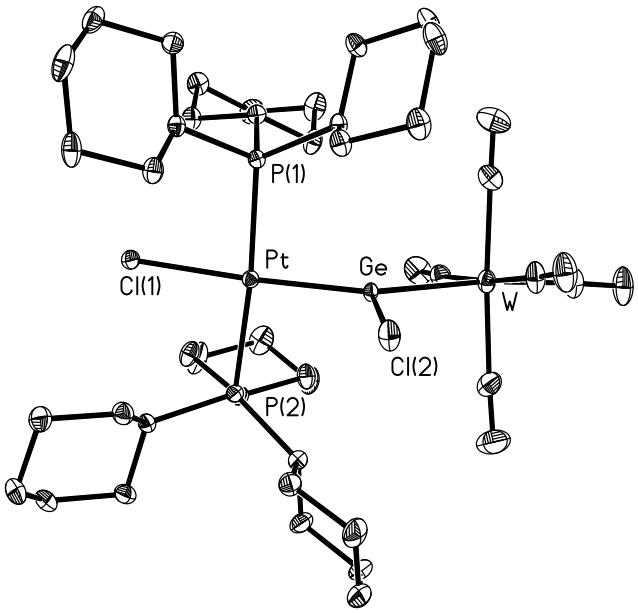

Figure 3.5. Molecular structure of $ClPt(PCy_3)_2Ge(Cl)\bullet W(CO)_5$ (**5**) with thermal ellipsoids presented at a 30 % probability level. All hydrogen atoms have been omitted for clarity. Selected bond lengths (Å) and angles (deg): Pt-Ge 2.3526(5), Ge-Cl(2) 2.2489(9), Pt-Cl(1) 2.4176(8), Ge-W 2.5745(5); Cl(1)-Pt-Ge 176.20(2), Pt-Ge-Cl(2) 104.87(2), Pt-Ge-W 147.463(10).

The bis(phosphine) complex $Pt(PCy_3)_2$ was then mixed with one equivalent of $(THF)_2SnCl_2\bullet W(CO)_5$, resulting in the formation of two different $Pt(PCy_3)_2$-containing products by $^{31}P\{^1H\}$ and $^{195}Pt\{^1H\}$ NMR spectroscopy. Specifically, the $^{31}P\{^1H\}$ NMR spectrum of the product mixture afforded two resonances in a 7:3 ratio with resolvable ^{195}Pt satellites at 26.1 ($^1J_{P\text{-}Pt}$ = 2392 Hz) and 47.4 ($^1J_{P\text{-}Pt}$ = 3063 Hz) ppm. Whereas the $^{195}Pt\{^1H\}$ NMR spectrum gave two different triplets at -3725 ($^1J_{P\text{-}Pt}$ = 2395 Hz) and -4543 ($^1J_{P\text{-}Pt}$ = 3056 Hz) ppm. Unfortunately, these two products could not be separated from each other; a crystal of one of the products, $ClPt(PCy_3)_2Sn(Cl)\bullet W(CO)_5$ (**6**), was selected from the product mixture and identified by X-crystallography (Figure 3.6). Compound **6** likely forms via the oxidative addition of a Sn-Cl bond to a Pt(0) center, in similar fashion as for the Ge congener,

5. The molecular structure of **6** shows a square planar Pt environment with a Pt-Sn bond distance of 2.5061(3) Å, which is shorter than the reported dative Pt-Sn bond in $(Cy_3P)_2Pt{\bullet}SnCl_2$ [2.599(1) Å].[11d] It is likely that the other species present in the abovementioned reaction mixture is the non-activated adduct $(Cy_3P)_2Pt{\bullet}SnCl_2{\bullet}W(CO)_5$.

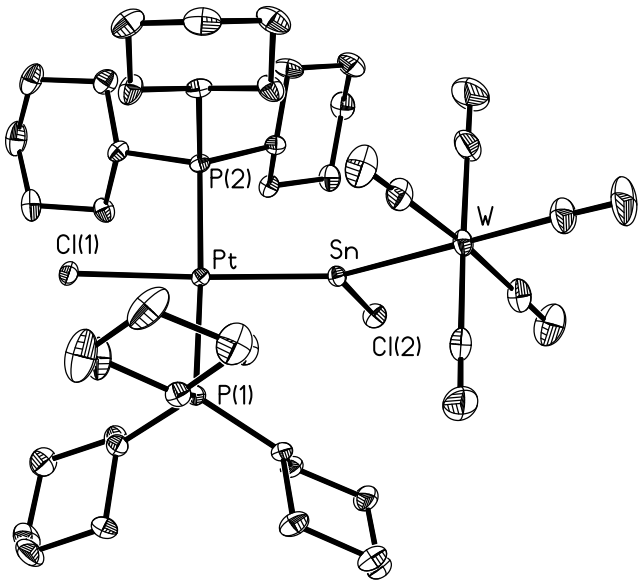

Figure 3.6. Molecular structure of $ClPt(PCy_3)_2Sn(Cl){\bullet}W(CO)_5$ (**6**) with thermal ellipsoids presented at a 30 % probability level. All hydrogen atoms have been omitted for clarity. Selected bond lengths (Å) and angles (deg): Pt-Sn 2.5061(3), Sn-Cl(2) 2.4149(11), Pt-Cl(1) 2.4110(11), Sn-W 2.7309(3); Cl(1)-Pt-Sn 172.63(3), Pt-Sn-Cl(2) 107.89(3), Pt-Sn-W 144.019(13).

To see if one species could be converted into the other, the product mixture was heated in C_6D_6 at 50 °C for 5 hours, however no change in the relative ratio of intensities of two signals in the resulting $^{31}P\{^1H\}$ NMR spectrum was found. At higher temperatures (> 80 °C) both species decompose to yield multiple new species (*ca.* 10) from which no clean product could be isolated.

3.3 Conclusions

The reactivity of the metal centered Lewis basic complexes $CpRh(PMe_2Ph)_2$ and $Pt(PCy_3)_2$ towards various electron deficient E(II) dihalide units (E = Ge, Sn and Pb) was explored. When strong Lewis acids were combined with the Rh complex, $CpRh(PMe_2Ph)_2$, the formation of Cp-activated products and Rh-H bonds occurred in place of direct Rh-E bond formation. In the case of $Pt(PCy_3)_2$, the formal oxidative addition of Ge-Cl and Sn-Cl bonds transpired to give the products $ClPt(PCy_3)_2E(Cl)\bullet W(CO)_5$ (E = Ge and Sn). Attempts to form the corresponding group 14 hydrides via H^- addition to E-Cl residues were unsuccessful, and in each case hydride addition to the Rh complexes **1-3** afforded free $CpRh(PMe_2Ph)_2$. Future work will involve tailoring the nature of the metal centered Lewis bases and Lewis acidic partner to obtain viable EH_2 precursor complexes for mixed element deposition processes.

3.4 Experimental Details

3.4.1 Materials and Instrumentation. All reactions were performed using standard Schlenk line techniques under an atmosphere of nitrogen or in an inert atmosphere glovebox (Innovative Technology, Inc.). Solvents were dried using a Grubbs-type solvent purification system[26] manufactured by Innovative Technology, Inc., degassed (freeze−pump−thaw method), and stored under an atmosphere of nitrogen prior to use. $Li[BH_4]$, $K[HB^sBu_3]$ (1.0 M solution in THF), and $PbCl_2$ were purchased from Aldrich and used as received. $(THF)_2SnCl_2\bullet W(CO)_5$,[27] $THF\bullet GeCl_2\bullet W(CO)_5$,[16] $CpRh(PMe_2Ph)_2$,[12] $BAr^F{}_3$ (Ar^F = 3,5-$(F_3C)_2C_6H_3$),[28] and $(Cy_3P)_2Pt$[22] were prepared

according to literature procedures. ^{1}H, ^{11}B, $^{13}C\{^{1}H\}$, $^{31}P\{^{1}H\}$, ^{19}F, ^{119}Sn and ^{195}Pt NMR spectra were recorded on a Varian iNova-400 spectrometer and referenced externally to $SiMe_4$ (^{1}H and $^{13}C\{^{1}H\}$), 85 % H_3PO_4 ($^{31}P\{^{1}H\}$), $F_3B{\bullet}OEt_2$ (^{11}B), $CFCl_3$ (^{19}F), $SnMe_4$ (^{119}Sn), and $Na_2[PtCl_6]$ in D_2O (^{195}Pt) respectively. Elemental analyses were performed by the Analytical and Instrumentation Laboratory at the University of Alberta. Infrared spectra were recorded on a Nicolet IR100 FTIR spectrometer as Nujol mulls between NaCl plates. Melting points were measured in sealed glass capillaries under nitrogen using a MelTemp melting point apparatus and are uncorrected.

3.4.2 X-ray Crystallography. Crystals of suitable quality for X-ray diffraction studies were removed from a vial in a glovebox and immediately covered with a thin layer of hydrocarbon oil (Paratone-N). A suitable crystal was selected, mounted on a glass fiber, and quickly placed in a low temperature stream of nitrogen on an X-ray diffractometer.[29] All data were collected at the University of Alberta using a Bruker APEX II CCD detector/D8 diffractometer using Mo Kα, $[(CO)_5W{\bullet}GeCl_2(\eta^5\text{-}C_5H_4)]RhH(PMe_2Ph)_2$ (**1**), $CpRh(PMe_2Ph)_2{\bullet}PbCl_2$ (**3**), $ClPt(PCy_3)_2GeCl{\bullet}W(CO)_5$ (**5**), $ClPt(PCy_3)_2SnCl{\bullet}W(CO)_5$ (**6**)) or Cu Kα ($CpRh(PMe_2Ph)_2{\bullet}SnCl_2{\bullet}W(CO)_5$ (**2**), $[\eta^5\text{-}C_5H_4BAr^F{}_3]RhH(PMe_2Ph)_2$ (**4**)) radiation with the crystals cooled to −100 °C. The data were corrected for absorption through Gaussian integration from the indexing of the crystal faces.[30] Structures were solved using intrinsic phasing SHELXT[31] ($CpRh(PMe_2Ph)_2{\bullet}PbCl_2$ (**3**), $[\eta^5\text{-}C_5H_4BAr^F{}_3]RhH(PMe_2Ph)_2$ (**4**), $ClPt(PCy_3)_2GeCl{\bullet}W(CO)_5$ (**5**), and $ClPt(PCy_3)_2SnCl{\bullet}W(CO)_5$ (**6**)), or Patterson

search/ structure expansion facilities within the DIRDIF-2008 program suite[32] ([(CO)$_5$W•GeCl$_2$(η^5-C$_5$H$_4$)]RhH(PMe$_2$Ph)$_2$ (**1**), (CpRh(PMe$_2$Ph)$_2$•SnCl$_2$•W(CO)$_5$ (**2**)), structure refinement was accomplished using either SHELXL-97 or SHELXL-2013.[31] All carbon-bound hydrogen atoms were assigned positions on the basis of the sp^2 or sp^3 hybridization geometries of their attached carbon atoms, and were given thermal parameters 20 % greater than those of their parent atoms. For compounds **1**, and **4**, all hydrogen atoms attached to heteroatoms (Rh) were located from difference Fourier maps, and their coordinates and isotropic displacement parameters were allowed to refine freely.

3.4.3 Synthetic procedures

Synthesis of [(CO)$_5$W•GeCl$_2$(η^{5}C$_5$H$_4$)]RhH(PMe$_2$Ph)$_2$ (1). A 3 mL toluene solution of CpRh(PMe$_2$Ph)$_2$ (33 mg, 0.074 mmol) was added dropwise to a 3 mL toluene solution of (THF)•GeCl$_2$•W(CO)$_5$ (40 mg, 0.074 mmol), and the mixture was stirred for 12 hrs. The resulting dark yellow precipitate was separated from the mother liquor, washed with 5 mL of hexanes and dried under vacuum. Compound **1** was obtained in pure form by crystallization from hexanes/CH$_2$Cl$_2$ at -35 °C. Yield: 30 mg (45 %). ^{1}H NMR (500 MHz, CD$_2$Cl$_2$): δ = 7.42-7.48 (m, 2H, Ar*H*), 7.34-7.42 (br, 4H, Ar*H*), 7.18-7.27 (m, 4H, Ar*H*), 5.75 (s, 2H, Cp), 5.40 (s, 2H, Cp), 1.65 (vt, $N = |^2J_{\text{H-P}} + {}^4J_{\text{H-P}}|$ = 8.4 Hz, 6H, C*H*$_3$), 1.54 (vt, $N = |^2J_{\text{H-P}} + {}^4J_{\text{H-P}}|$ = 8.4 Hz, 6H, C*H*$_3$), -11.98 (dt, $^2J_{\text{H-P}}$ = 29.9 Hz, $^1J_{\text{H-Rh}}$ = 19.9 Hz, 1H, Rh-*H*). ^{13}C{^{1}H} NMR (125 MHz, CD$_2$Cl$_2$): δ = 202.6 (s, *C*O$_{ax}$), 199.1 (s, *C*O$_{\text{eq}}$, satellite: $^1J_{\text{C-W}}$ = 124 Hz), 135.0 (vt, $N = |^1J_{\text{C-P}} + {}^3J_{\text{C-P}}|$ = 53.6 Hz, Ar*C*), 130.8 (s, Ar*C*), 130.2 (s, Ar*C*), 128.8 (s, Ar*C*), 94.4 (s, Cp), 90.1 (s,

Cp), 22.1 (vt, N = 34.1 Hz, CH$_3$), 21.0 (vt, N = 37.9 Hz, CH$_3$). ^{31}P{^{1}H} NMR (161 MHz, CD_2Cl_2): δ = 14.6 (d, $^1J_{P\text{-}Rh}$ = 139 Hz). ^{1}H NMR (500 MHz, $CDCl_3$): δ = 7.41-7.49 (m, 2H, ArH), 7.33-7.41 (m, 4H, ArH), 7.14-7.28 (m, 4H, ArH), 5.66 (s, 2H, Cp), 5.43 (s, 2H, Cp), 1.65 (vt, N = $|^2J_{H\text{-}P} + {}^4J_{H\text{-}P}|$ = 10 Hz, 6H, CH_3), 1.56 (vt, N = $|^2J_{H\text{-}P} + {}^4J_{H\text{-}P}|$ = 10 Hz, 6H, CH_3), -11.92 (dt, Rh-H, $^2J_{H\text{-}P}$ = 29.9 Hz, $^1J_{H\text{-}Rh}$ = 19.9 Hz, 1H, Rh-H). ^{31}P{^{1}H} NMR (161 MHz, $CDCl_3$): δ = 14.1 (d, $^1J_{P\text{-}Rh}$ = 139.1 Hz). IR (Nujol, cm^{-1}): 1901 (br, υ_{CO}), 1970 (s, υ_{CO}), 2059 (s, υ_{CO}). Anal. Calcd. for $C_{26}H_{27}Cl_2GeO_5P_2RhW$: C, 34.25; H, 2.98. Found: C, 34.25; H, 3.14. Mp (°C): 132-135 (decomposes).

Synthesis of CpRh(PMe$_2$Ph)$_2$•SnCl$_2$•W(CO)$_5$ (2). A 3 mL toluene solution of CpRh(PMe$_2$Ph)$_2$ (18 mg, 0.041 mmol) was added dropwise to a 3 mL toluene solution of (THF)$_2$SnCl$_2$•W(CO)$_5$ (36 mg, 0.045 mmol), and the mixture was stirred for 12 hrs. The resulting orange yellow precipitate was separated from the mother liquor, washed with 5 mL of hexanes and dried under vacuum. Yield: 38 mg (94 %). Crystals suitable for X-ray crystallography were grown from CH_2Cl_2/hexanes at -35 °C. ^{1}H NMR (500 MHz, $CDCl_3$): δ = 7.44-7.50 (m, 2H, ArH), 7.36-7.44 (m, 4H, ArH), 7.14-7.22 (m, 4H, ArH), 5.25 (s, 5H, Cp), 2.08 (vt, N = 10 Hz, 6H, CH_3), 1.92 (vt, N = 10 Hz, 6H, CH_3). ^{13}C{^{1}H} NMR (125 MHz, $CDCl_3$): δ = 203.0 (s, CO_{ax}), 200.7 (s, CO_{eq}), 139.6 (vt, N = 48.6 Hz, ArC), 130.7 (s, ArC), 129.5 (s, ArC), 129.1 (s, ArC), 95.1 (s, Cp), 22.9 (vt, N = 35.9 Hz, CH$_3$), 15.6 (vt, N = 35.8 Hz, CH$_3$). ^{31}P{^{1}H} NMR (201 MHz, $CDCl_3$): δ = 4.6 (d, $^1J_{Rh\text{-}P}$ = 153 Hz, satellites: $^3J_{P\text{-}W}$ = 77 Hz). IR (Nujol, cm^{-1}): 1892 (br, υ_{CO}), 1965 (s, υ_{CO}), 2054 (s, υ_{CO}). Anal. Calcd. for

$C_{26}H_{27}Cl_2O_5P_2RhSnW$: C, 32.60; H, 2.84. Found: C, 32.42; H, 2.92. Mp (°C): 150-153 (decomposes).

Synthesis of $CpRh(PMe_2Ph)_2 \bullet PbCl_2$ (3). A 3 mL toluene solution of $CpRh(PMe_2Ph)_2$ (68 mg, 0.15 mmol) was added dropwise to a 3 mL toluene suspension of $PbCl_2$ (51 mg, 0.18 mmol), and the mixture was stirred for 15 hrs. The solvent was removed under vacuum and the remaining red powder was washed twice with 5 mL portions of hexanes and dried. The red solid was then dissolved in 10 mL of CH_2Cl_2 and the resulting solution was filtered. The solvent was removed from the filtrate and the product was dried under vacuum. Yield: 65 mg (60 %). Crystals suitable for X-ray crystallography were grown from hexanes/THF at -35 °C. ^{1}H NMR (500 MHz, CD_2Cl_2): δ = 7.41-7.58 (m, 6H, Ar*H*), 7.22-7.38 (m, 4H, Ar*H*), 5.11 (s, 5H, Cp), 1.62 (br, 6H, CH_3), 1.42 (br, 6H, C*H*$_3$). ^{13}C{^{1}H} NMR (125 MHz, CD_2Cl_2): δ = 136.7 (vt, *N* = 46.9 Hz, Ar*C*), 130.6 (s, Ar*C*), 129.9 (s, Ar*C*), 129.3 (s, Ar*C*), 94.0 (s, Cp), 22.1 (vt, *N* = 33.7 Hz, *C*H$_3$), 15.4 (vt, *N* = 33.4 Hz, *C*H$_3$). ^{31}P{^{1}H} NMR (201 MHz, CD_2Cl_2): δ = 8.2 (d, $^1J_{Rh\text{-}P}$ = 170 Hz). Anal. Calcd. for $C_{21}H_{27}Cl_2P_2PbRh$: C, 34.92; H, 3.77. Found: C, 35.07; H, 3.76. Mp (°C): 185-188 (decomposes).

Synthesis of $[\eta^5\text{-}C_5H_4BAr^F{}_3]RhH(PMe_2Ph)_2$ (4). A 3 mL toluene solution of $CpRh(PMe_2Ph)_2$ (83 mg, 0.19 mmol) was added dropwise to a 3 mL toluene solution of $BAr^F{}_3$ (136 mg, 0.19 mmol) and the mixture was stirred for 12 hrs to give a red solution. The solvent was removed from the mixture under vacuum to afford a deep yellow-orange oil. The oil was re-dissolved in 3 mL of Et_2O and the solvent was

removed to yield an orange powder. This product was then washed with a mixture of Et_2O/hexanes (1 mL + 3 mL) to give **4** as a white powder. Yield: 100 mg (48 %). Crystals suitable for X-ray were grown from hexanes/Et_2O at -35 °C C. ^{1}H NMR (500 MHz, C_6D_6): δ = 8.27 (s, 6H, *o*-$C_6H_3(CF_3)_2$), 7.80 (s, 3H, *p*-$C_6H_3(CF_3)_2$), 6.89-6.92 (m, 6H, Ar*H*), 6.55-6.75 (m, 4H, Ar*H*), 4.70 (s, 2H, Cp), 4.30 (s, 2H, Cp), 0.67 (vt, *N* = 10 Hz, 6H, C*H*$_3$), 0.58 (vt, *N* = 10 Hz, 6H, C*H*$_3$), -11.58 (dt, $^2J_{H\text{-}P}$ = 31.6 Hz, $^1J_{H\text{-}Rh}$ = 21.6 Hz, 1H, Rh-*H*). $^{13}C\{^1H\}$ NMR (125 MHz, C_6D_6): δ = 162.0 (q, $^1J_{B\text{-}C}$ = 51.2 Hz, *ipso*-$C_6H_3(CF_3)_2$), 135.8 (vt, *N* = 50.6 Hz, Ar*C*), 135.2 (s, *o*-$C_6H_3(CF_3)_2$), 130.7 (s, Ar*C*), 130.0 (br, Ar*C*), 129.9 (q, $^2J_{C\text{-}F}$ = 31.4 Hz, *m*-$C_6H_3(CF_3)_2$), 128.6 (s, Ar*C*), 125.8 (q, $^1J_{C\text{-}F}$ = 272.4 Hz, C*F*$_3$), 118.6 (s, *p*-$C_6H_3(CF_3)_2$), 92.8 (s, Cp), 89.2 (s, Cp), 21.6 (vt, *N* = 33.0 Hz, *C*H$_3$), 20.5 (vt, *N* = 37.0 Hz, *C*H$_3$). $^{31}P\{^1H\}$ NMR (161 MHz, C_6D_6): δ = 13.6 (d, $^1J_{P\text{-}Rh}$ = 133.3 Hz). $^{11}B\{^1H\}$ NMR (128 MHz, C_6D_6): δ = -10.1 (s, -*B*Ar$^F_3$). $^{19}F\{^1H\}$ NMR (376 MHz, C_6D_6): δ = -62.0 (s, C*F*$_3$). Anal. Calcd. for $C_{45}H_{36}BF_{18}P_2Rh$: C, 49.39; H, 3.32. C, 49.31; H, 3.62. Mp (°C): 152-155.

Reaction of [(CO)$_5$W•GeCl$_2$(η^5-C$_5$H$_4$)]RhH(PMe$_2$Ph)$_2$ (1) with K[HB^{s}Bu$_3$]. To a 5 mL toluene solution of **1** (110 mg, 0.12 mmol) was added K[HB^{s}Bu$_3$] (254 μL, 1.0 M solution in THF, 0.25 mmol), and the mixture was stirred for 12 hrs. The mother liquor was separated from the black precipitate by filtration and the solvent was removed from the filtrate to yield an orange oil containing a mixture of CpRh(PMe$_2$Ph)$_2$ and ^{s}Bu$_3$B (as determined by ^{1}H, ^{11}B and $^{31}P\{^1H\}$ NMR spectroscopy in C_6D_6).[33]

Reaction of $CpRh(PMe_2Ph)_2 \bullet SnCl_2 \bullet W(CO)_5$ (2) with $K[HB^sBu_3]$. To a 5 mL toluene solution of **2** (96 mg, 0.10 mmol), was added $K[HB^sBu_3]$ (210 μL, 1.0 M solution in THF, 0.21 mmol), and the mixture was stirred for 12 hrs. The mother liquor was separated from the black precipitate by filtration and the solvent was removed from the filtrate to yield an orange oil containing a mixture of $CpRh(PMe_2Ph)_2$ and $^sBu_3B$.

Reaction of $CpRh(PMe_2Ph)_2 \bullet PbCl_2$ (3) with $K[HB^sBu_3]$. To a 5 mL toluene solution of **3** (56 mg, 0.077 mmol) was added $K[HB^sBu_3]$ (178 μL, 1.0 M solution in THF, 0.18 mmol), and the mixture was stirred for 12 hrs. The mother liquor was separated from the grey precipitate by filtration and the solvent was removed from the filtrate to yield an orange oil consisting of a mixture of $CpRh(PMe_2Ph)_2$ and $^sBu_3B$.

Reaction of $CpRh(PMe_2Ph)_2 \bullet PbCl_2$ (3) with $THF \bullet GeCl_2 \bullet W(CO)_5$. A 3 mL toluene solution of $THF \bullet GeCl_2 \bullet W(CO)_5$ (25 mg, 0.043 mmol) was added dropwise to a 3 mL toluene suspension of $CpRh(PMe_2Ph)_2 \bullet PbCl_2$ (31 mg, 0.043 mmol) and the mixture was stirred for 12 hrs. The solvent was removed under vacuum from the black suspension to give a black powder. The only soluble product identified by ^1H and $^{31}P\{^1H\}$ NMR was $[\eta^5\text{-}C_5H_4GeCl_2 \bullet W(CO)_5]RhH(PMe_2Ph)_2$ (**1**).

Reaction of $CpRh(PMe_2Ph)_2 \bullet PbCl_2$ (3) with $BAr^F{}_3$. A 3 mL toluene solution of $BAr^F{}_3$ (40 mg, 0.062 mmol) was added dropwise to a 3 mL toluene suspension of $CpRh(PMe_2Ph)_2 \bullet PbCl_2$ (45 mg, 0.062 mmol) and the mixture was stirred for 12 hrs.

The solvent was removed under vacuum from the black suspension to obtain a black powder. The only NMR identified product was [η^5-$C_5H_4BAr^F{}_3$]RhH(PMe_2Ph)$_2$ (**4**).

Synthesis of ClPt(PCy$_3$)$_2$GeCl•W(CO)$_5$ (5). A solution of Pt(PCy$_3$)$_2$ (180 mg, 0.24 mmol) in 3 mL of toluene was added dropwise to a 3 mL toluene solution of THF•GeCl$_2$•W(CO)$_5$ (130 mg, 0.24 mmol). The reaction mixture was stirred for 24 hrs and the solvent was removed under vacuum. Then 5 mL of hexanes was added to the oily product followed by stirring for one hour. The precipitate was separated from the mother liquor and dried under vacuum to give a yellow powder. Yield: 210 mg (72%). Crystals suitable for X-ray were obtained from a concentrated hexanes solution at -35 °C. ^{1}H NMR (500 MHz, C_6D_6): δ = 2.40-2.62 (br, 6H, Cy), 2.10-2.30 (br, 12H, Cy), 1.14-1.90 (m, 48H, Cy). ^{13}C{^{1}H} NMR (125 MHz, C_6D_6): δ = 200.9 (s, *C*O$_{ax}$), 198.8 (s, *C*O$_{eq}$), 35.6 (br, C^1, Cy), 31.9 (s, C^{3,5}, Cy), 30.7 (s, C^{3,5}, Cy), 27.9 (br s, C^{2,6}, Cy), 27.5 (br s, C^{2,6}, Cy), 26.7 (s, C^4, Cy). ^{31}P{^{1}H} NMR (201 MHz, C_6D_6): δ = 16.9 (s, satellites: $^1J_{P\text{-}Pt}$ = 2412 Hz). ^{195}Pt{^{1}H} NMR (85.5 MHz, C_6D_6): δ = -3645 (t, $^1J_{P\text{-}pt}$ = 2447 Hz). IR (Nujol, cm^{-1}): 1932 (br, υ_{CO}), 1984 (s, υ_{CO}), 2065 (s, υ_{CO}). Anal. Calcd. for: $C_{41}H_{66}Cl_2GeO_5P_2PtW$: C, 40.25; H, 5.44. Found: C, 41.05; H, 5.51. Mp (°C): 120-123 (decomposes).

Reaction of ClPt(PCy$_3$)$_2$GeCl•W(CO)$_5$ (5) with K[HB^{s}Bu$_3$]. To a 5 mL THF solution of **5** (20 mg, 0.016 mmol), was added K[HB^{s}Bu$_3$] (34 μL, 1.0 M solution in THF, 0.034 mmol), and the mixture was stirred for 12 hrs. The solvent was removed

from the mixture to yield a dark orange oil containing a mixture of PCy_3 and $^sBu_3B$ as soluble products.[33]

Synthesis of $ClPt(PCy_3)_2SnCl{\bullet}W(CO)_5$ (6). A 3 mL toluene solution of $Pt(PCy_3)_2$ (180 mg, 0.24 mmol) was added dropwise to a 3 mL toluene solution of $(THF)_2SnCl_2{\bullet}W(CO)_5$ (130 mg, 0.24 mmol). The mixture was stirred for 24 hrs and the volatiles were removed under vacuum. 5 mL of hexanes was then added to the oily product followed by stirring for one hour. The precipitate was separated from the mother liquor and dried under vacuum to give a red powder. A few crystals suitable for X-ray crystallography were grown from the mixture in hexanes at -35 °C. The crystallographic data identified one of the products as $ClPt(PCy_3)_2SnCl{\bullet}W(CO)_5$ (**6**), whereas the $^{31}P\{^1H\}$ and $^{195}Pt\{^1H\}$ NMR spectroscopy of the product indicated the presence of two products with the following NMR data: $^{31}P\{^1H\}$ NMR (201 MHz, C_6D_6): δ = 26.1 (s, satellites: $^1J_{P\text{-}Pt}$ = 2392 Hz), 47.4 (s, satellites: $^1J_{P\text{-}Pt}$ = 3063 Hz). $^{195}Pt\{^1H\}$ NMR (85.5 MHz, C_6D_6): δ = -3725 (t, $^1J_{P\text{-}pt}$ = 2395 Hz), -4543 (t, $^1J_{P\text{-}pt}$ = 3056 Hz).

3.5 Crystallographic Data

Table 3.1: Crystallographic data for **1** and **2**.

Compound	**1**	**2**•0.25 CH_2Cl_2
Formula	$C_{26}H_{27}Cl_2GeO_5P_2RhW$	$C_{26.25}H_{27.5}Cl_{2.5}O_5P_2RhSnW$
Formula weight	911.66	979.00
Crystal system	monoclinic	monoclinic
Space group	$P2_1/n$	$P2_1/n$
a (Å)	8.9888 (3)	15.3972 (2)
b (Å)	24.3719 (7)	9.0453 (1)
c (Å)	14.4140 (4)	23.3877 (3)
α (deg)	90	90
β (deg)	104.3064 (3)	90.5374 (12)
γ (deg)	90	90
V(Å^3)	3059.81 (16)	3257.12 (7)
Z	4	4
ρ (g/cm^3)	1.979	1.996
abs coeff (mm^{-1})	5.572	19.58
T (K)	173(1)	173(1)
$2\theta_{max}$ (°)	56.65	145.17
total data	28051	21691
unique data(R_{int})	7477 (0.0162)	6344
Obs data [I>2($\sigma(I)$]	7036	5092
Params	351	347
R_1 [I>2$\sigma(I)$]^a	0.016	0.0345
wR_2 [all data]^a	0.0379	0.0868
max/min $\Delta\rho$ (e$^-$ Å^{-3})	1.032/-0.480	1.130/-1.373

^{a} $R_1 = \sum||F_o| - |F_c||/\sum|F_o|$; $wR_2 = [\sum w(F_o^2 - F_c^2)^2/\sum w(F_o^4)]^{1/2}$

Table 3.2: Crystallographic data for **3** and **4**.

Compound	**3**	**4**
Formula	$C_{21}H_{27}Cl_2P_2PbRh$	$C_{48}H_{43}BF_{18}P_2Rh$
Formula weight	722.36	1137.48
Crystal system	monoclinic	triclinic
Space group	$P2_1/n$	$P\bar{1}$ *(No. 2)*
a (Å)	17.346 (5)	12.2135 (3)
b (Å)	15.351 (4)	12.5991 (3)
c (Å)	18.164 (5)	17.0103 (4)
α (deg)	90	80.6961 (10)
β (deg)	95.470 (3)	81.3382 (8)
γ (deg)	90	75.2500 (8)
V(Å^3)	4814 (2)	2481.49 (10)
Z	8	2
ρ (g/cm^3)	1.993	1.522
abs coeff (mm^{-1})	8.030	4.305
T (K)	173(1)	173(1)
$2\theta_{max}$ (°)	55.52	144.46
total data	41795	17405
unique data(R_{int})	11064 (0.0573)	9416 (0.0129)
Obs data [I>2($\sigma(I)$)]	8280	9241
Params	495	716
R_1 [I>2$\sigma(I)$]^a	0.0364	0.0319
wR_2 [all data]^a	0.0816	0.0860
max/min $\Delta\rho$ (e$^-$ Å^{-3})	1.992/-1.824	1.112/-0.806

^{a} $R_1 = \sum||F_o| - |F_c||/\sum|F_o|$; $wR_2 = [\sum w(F_o^2 - F_c^2)^2/\sum w(F_o^4)]^{1/2}$

Table 3.3: Crystallographic data for **5** and **6**.

Compound	**5**•0.5n-hexane	**6**•*n*-hexane
Formula	$C_{44}H_{73}Cl_2GeO_5P_2PtW$	$C_{47}H_{80}Cl_2O_5P_2PtSnW$
Formula weight	1266.39	1355.58
Crystal system	triclinic	orthorhombic
Space group	$P\bar{1}$ *(No. 2)*	$P2_12_12_1$ *(No. 19)*
a (Å)	10.172 (2)	14.8910 (4)
b (Å)	12.807 (3)	16.3240 (4)
c (Å)	20.478 (4)	22.1599 (6)
α (deg)	105.848 (2)	90
β (deg)	103.959 (2)	90
γ (deg)	93.004 (3)	90
V(Å^3)	2470.6 (8)	5386.6 (2)
Z	2	4
ρ (g/cm^3)	1.702	1.672
abs coeff (mm^{-1})	5.964	5.379
T (K)	173(1)	173(1)
$2\theta_{max}$ (°)	55.18	54.98
total data	22384	47820
unique data(R_{int})	11338 (0.0148)	12339 (0.0289)
Obs data [I>2($\sigma(I)$)]	9930	11780
Params	534	512
R_1 [I>2$\sigma(I)$]^a	0.0212	0.0176
wR_2 [all data]^a	0.0603	0.0404
max/min $\Delta\rho$ (e$^-$ Å^{-3})	1.248/-1.042	0.737/-0.32

^{a} $R_1 = \sum||F_o| - |F_c||/\sum|F_o|$; $wR_2 = [\sum w(F_o^2 - F_c^2)^2/\sum w(F_o^4)]^{1/2}$

3.6 References

1. (*a*) Braunschweig, H.; Dewhurst, R. D.; Hammond, K.; Mies, J.; Radacki, K.; Vargas, A. *Science* **2012**, *336,* 1420; (*b*) Wang, Y.; Xie, Y.; Wei, P.; King, R. B.; Schaefer III, H. F.; Schleyer, P. v. R.; Robinson, G. H. *Science* **2008**, *321*, 1069; (*c*) Sidiropoulos, A.; Jones, C.; Stasch, A.; Klein S.; Frenking, G.; *Angew. Chem. Int. Ed.* **2009**, *48*, 9701; (*d*) Jones, C.; Sidiropoulos, A.; Holzmann, N.; Frenking, G.; Stasch, A. *Chem. Commun.* **2012**, *48*, 9855.
2. For recent highlights from this active research field, see: (*a*) Wang, Y.; Chen, M.; Xie, Y.; Wei, P.; Schaefer III, H. F.; Schleyer, P. v. R.; Robinson, G. H. *Nature Chem.* **2015**, *7*, 509; (*b*) Ahmad, S. U.; Szilvási, T.; Irran E.; Inoue, S. *J. Am. Chem. Soc.* **2015**, *137*, 5828; (*c*) Swarnakar, A. K.; Hering-Junghans, C.; Nagata, K.; Ferguson, M. J.; McDonald, R.; Tokitoh, N.; Rivard, E. *Angew. Chem. Int. Ed.* **2015**, *54*, 10666; (*d*) Braunschweig, H.; Dellermann, T.; Ewing, W. C.; Kramer, T.; Schneider C.; Ulrich, S. *Angew. Chem. Int. Ed.* **2015**, *54*, 10271; (*e*) Filippou, A. C.; Baars, B.; Chernov, O.; Lebedev, Y. N.; Schnakenburg, G. *Angew. Chem. Int. Ed.* **2014**, *53*, 565; (*f*) Dahcheh, F.; Martin, D.; Stephan, D. W.; Bertrand, G. *Angew. Chem. Int. Ed.* **2014**, *53*, 13159; (*g*) Jana, A.; Huch, V; Scheschkewitz, D. *Angew. Chem. Int. Ed.* **2013**, *52*, 12179; (*h*) Ghadwal, R. S.; Roesky, H. W.; Pröpper, K.; Dittrich, B.; Klein, S.; Frenking, G. *Angew. Chem. Int. Ed.* **2011**, *50*, 5374.
3. For selected examples, see: (*a*) Thimer, K. C.; Al-Rafia, S. M. I.; Ferguson, M. J.; McDonald, R.; Rivard, E. *Chem. Commun.* **2009**, 7119; (*b*) Al-Rafia, S. M. I.; Malcolm, A. C.; Liew, S. K.; Ferguson, M. J.; Rivard, E. *J. Am. Chem. Soc.* **2011**,

133, 777; (*c*) Al-Rafia, S. M. I.; Malcolm, A. C.; McDonald, R.; Ferguson, M. J.; Rivard, E. *Chem. Commun*. **2012**, *48*, 1308; (*d*) Al-Rafia, S. M. I.; Shynkaruk, O.; McDonald, S. M.; Liew, S. K.; Ferguson, M. J.; McDonald, R.; Herber, R. H.; Rivard, E. *Inorg. Chem.* **2013**, *52*, 5581; (*e*) Rivard, E. *Dalton. Trans.* **2014**, *43*, 8577.

4. (*a*) Al-Rafia, S. M. I.; Malcolm, A. C.; Liew, S. K.; Ferguson, M. J.; McDonald, R.; Rivard, E. *Chem. Commun*. **2011**, *47*, 6987; (*b*) Swarnakar, A. K.; McDonald, S. M.; Deutsch, K. C.; Choi, P.; Ferguson, M. J.; McDonald, R.; Rivard, E. *Inorg. Chem*. **2014**, *53*, 8662. For important early work, see: (*c*) Kuhn, N.; Bohnen, H.; Kreutzberg, J.; Bläser, D.; Boese, R. *J. Chem. Soc., Chem. Commun.* **1993**, 1136.
5. (*a*) Rivard, E. *Chem. Soc. Rev.* **2016**, *45*, 989; (*b*) Jasinski, J. M.; Gates, S. M. *Acc. Chem. Res.* **1991**, *24*, 9; (*c*) Weerts, W. L. M.; de Croon, M. H. J. M.; Marin, G. B. *J. Electrochem. Soc.* **1998**, *145*, 1318; (*d*) Dzarnoski, J.; O'Neal, H. E.; Ring, M. A. *J. Am. Chem. Soc.* **1981**, *103*, 5740 and references therein.
6. (a) Purkait, T. K.; Swarnakar, A. K.; De Los Reyes, G. B.; Hegmann, F. A.; Rivard, E.; Veinot, J. G. C. *Nanoscale* **2015**, *7*, 2241; (*b*) Millo, O.; Balberg, I., Azulay, D.; Purkait, T. K.; Swarnakar, A. K.; Rivard, E.; Veinot, J. G. C. *J. Phys. Chem. Lett.* **2015**, *6*, 3396.
7. Bauer, J.; Braunschweig, H.; Dewhurst, R. D. *Chem. Rev.* **2012**, *112*, 4329.
8. Nowell, I. N.; Russell, D. R. *J. Chem. Soc., Chem. Commun*. **1967**, *817*.
9. (*a*) Einstein, F. W. B.; Pomeroy, R. K.; Rushman, P.; Willis, A. C. *Organometallics* **1985**, *4*, 250; (*b*) Usón, R.; Forniés, J.; Espinet, P.; Fortuño, C.; Tomas, M.; Welch, A. J. *J. Chem. Soc., Dalton Trans.* **1988**, 3005.

10. (*a*) Braunschweig, H.; Gruß, K.; Radacki, K. *Angew. Chem. Int. Ed*. **2007**, *46*, 7782; (*b*) Bauer, J.; Braunschweig, H.; Brenner, P.; Kraft, K.; Radacki, K.; Schwab, K. *Chem. Eur. J.* **2010**, *16*, 11985; (*c*) Bauer, J.; Braunschweig, H.; Damme, A.; Gruß, K.; Radacki, K. *Chem. Commun.* **2011**, *47*, 12783; (*d*) Burlitch, J. M.; Leonowicz, M. E.; Petersen, R. B.; Hughes, R. E. *Inorg. Chem*. **1979**, *18*, 1097.

11. (*a*) Chan, D. M. T.; Marder, T. B. *Angew. Chem. Int. Ed. Engl.* **1988**, *27*, 442; (*b*) Béni, Z.; Ros, R.; Tassan, A.; Scopelliti, R.; Roulet, R. *Dalton Trans.* **2005**, 315; (*c*) Rutsch, P.; Huttner, G. Z. *Naturforsch.* **2002**, *57b*, 25; (*d*) Hupp, F.; Ma, M.; Kroll, F.; Jimenez-Halla, J. O. C.; Dewhurst, R. D.; Radacki, K.; Stasch, A.; Jones, C.; Braunschweig, H. *Chem. Eur. J.* **2014**, *20*, 16888.

12. Mayer, J. M.; Calabrese, J. C. *Organometallics* **1984**, *3*, 1292.

13. (*a*) Zadesenets, A.; Filatov, E.; Plyusnin, P.; Baidina, I.; Dalezky, V.; Korenev, S.; Bogomyakov, A. *Polyhedron* **2011**, *30*, 1305; (*b*) Shubin, Y.; Plyusnin, P.; Sharafutdinov, M. *Nanotechnology* **2012**, *23*, 405302.

14. Wakatsuki, Y.; Yamazaki, H. *J. Organometal. Chem.* **1974**, *64,* 393.

15. Simons, R. S.; Pu, L.; Olmstead, M. M.; Power, P. P. *Organometallics* **1997**, *16*, 1920.

16. Al-Rafia, S. M. I.; Momeni, M. R.; Ferguson, M. J.; McDonald, R.; Brown, A.; Rivard, E. *Organometallics* **2013**, *32*, 6658.

17. Choukroun, R.; Iraqi, A.; Gervais, D.; Daran, J. C.; Jeannin, Y. *Organometallics* **1987**, *6*, 1197.

18. Bott, S. G.; Machell, J. C.; Mingos, D. M. P.; Watson, M. J. *J. Chem. Soc., Dalton Trans.* **1991**, 859.

19. Gessner, V. H.; Dilsky, S.; Strohmann, C. *Chem. Commun*. **2010**, *46*, 4719.

20. For studies using the $[HB^{s}Bu_3]^-$ anion as a hydride source, see: (*a*) Richards, A. F.; Phillips, A. D.; Olmstead, M. M.; Power, P. P. *J. Am. Chem. Soc.* **2003**, *125*, 3204; (*b*) Lummis, P. A.; Momeni, M. R.; Lui, M. W.; McDonald, R.; Ferguson, M. J.; Miskolzie, M.; Brown, A.; Rivard, E. *Angew. Chem. Int. Ed.* **2014**, *53*, 9347.

21. Duchateau, R.; Lancaster, S. J.; Thornton-Pett, M.; Bochmann, M. *Organometallics* **1997**, *16*, 4995.

22. Otsuka, S.; Yoshida, T.; Matsumoto, M.; Nakatsu, K. *J. Am. Chem. Soc.* **1976**, *98*, 5850.

23. (*a*) Charmant, J. P. H.; Fan, C.; Norman, N. C.; Pringle, P. G. *Dalton Trans.* **2007**, 114; (*b*) Braunschweig, H.; Brenner, P.; Müller, A.; Radacki, K.; Rais, D.; Uttinger, K. *Chem. Eur. J.* **2007**, *13*, 7171; (*c*) Braunschweig, H.; Radacki, K.; Uttinger, K. *Inorg. Chem.* **2007**, *46*, 8796.

24. Braunschweig, H.; Gruss, K.; Radacki, K. *Inorg. Chem.* **2008**, *47*, 8595.

25. Braunschweig, H.; Brenner, P.; Cogswell, P.; Kraft, K.; Schwab, K. *Chem. Commun.* **2010**, *46*, 7894.

26. Pangborn, A. B.; Giardello, M. A.; Grubbs, R. H.; Rosen, R. K.; Timmers, F. J. *Organometallics* **1996**, *15*, 1518.

27. Balch, A. L.; Oram, D. E. *Organometallics* **1988**, *7*, 155.

28. Kolychev, E. L.; Bannenberg, T.; Freytag, M.; Daniliuc, C. G.; Jones, P. G.; Tamm, M. *Chem. Eur. J.* **2012**, *18*, 16938.

29. Hope, H. *Prog. Inorg. Chem.* **1994**, *41*, 1.

30. Blessing, R. H. *Acta Crystallogr.* **1995**, *A51*, 33.

31. Sheldrick, G. M. *Acta Crystallogr*. **2008**, *A64*, 112.

32. Beurskens, P. T.; Beurskens, G.; de Gelder, R.; Smits, J. M. M.; Garcia-Garcia, S.; Gould, R. O. *DIRDIF-2008*; Crystallography Laboratory, Radboud University: Nijmegen, The Netherlands **2008**.

33. Zaidlewicz, M.; Krzeminski, M. *Sci. Synth.* **2004**, *6*, 1097.

Chapter 4: Stabilization of Inorganic Acetylene, HBNH, Using Flanking Coordinative Interactions and Attempts to Isolate a Molecular BN Complex

4.1 Introduction

Iminoboranes (RB≡NR) are isoelectronic to alkynes, however they exhibit greatly enhanced reactivity due to the higher polarity of B-N bonds,[1] and thus self-oligomerize when smaller R groups are present.[2] In seminal studies, Paetzold and co-workers used steric protection to obtain iminoboranes (*e.g.* ^{t}BuB≡N^{t}Bu) as stable entities, and demonstrated initial coordination chemistry.[2b] Recent breakthroughs by the laboratories of Bertrand, Braunschweig and Stephan have demonstrated that both *N*-heterocyclic carbene (NHC) and cyclic(alkyl)amino carbene (CAAC) donors can bind functionalized iminoboranes such as $ClBNSiMe_3$ and ^{t}BuBN^{t}Bu as 1:1 adducts LB•RB=NR′ (LB = Lewis base).[3] Despite these excellent studies, the parent iminoborane, HBNH, remained only identifiable in cryogenic matrices (40 K) or as a fleeting species in the gas phase.[4,5] Furthermore HBNH is likely a key intermediate in the laser-induced preparation of nanodimensional boron nitride (BN) from $H_3N•BH_3$ dehydrogenation;[6] boron nitride is of great value to the materials community due to its insulating properties and ability to withstand harsh external conditions.[7]

In this chapter a donor-acceptor approach[8] is presented which led to the isolation of the first stable molecular adduct containing HBNH. Specifically, this parent iminoborane was sandwiched between Lewis basic (LB) and Lewis acidic

(LA) units to yield a stable complex of the form LB•HB=NH•LA, which could also be viewed as a formal Frustrated Lewis Pair (FLP)[9] interacting with HBNH. By judicious modification of the capping LB and LA groups it is expected that a solution-phase route to boron nitride could be possible via mild dehydrogenation of LB•HB=NH•LA,[10] followed by BN extrusion (Scheme 4.1); typically BN is prepared at temperatures exceeding 900 °C.[6] Herein a general method is introduced to form B-N (and possibly other element-nitrogen) multiple bonds by the energetically favored loss of N_2 from inorganic hydrido-azide precursors.[11] Key intermediates *en route* to a LB•HB=NH•LA complex were isolated and structurally characterized, and the mechanism of iminoborane adduct formation was probed by isotope labeling studies. In addition the reactivity of such species was studied in detail and attempts were made to convert the HBNH adduct into LB•B≡N•LA complexes. Moreover, the reactivity of a donor-stabilized azidohydride boronium cation $[BH(N_3)]^+$ was also discussed in this chapter.[12]

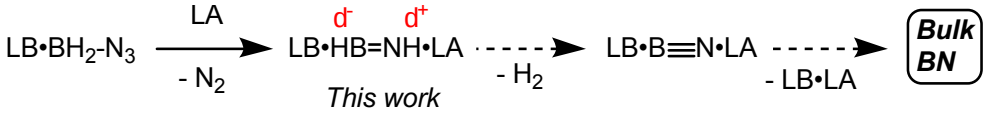

Scheme 4.1. Potential route to bulk boron nitride via an HBNH adduct; LA = Lewis acid, LB = Lewis base.

4.2 Results and discussions

The N_2 elimination process central to the current study was discovered in an attempt to form the electrophilic azidoborane adduct IPr•B(OTf)$_2$N$_3$ from the addition of two equivalents of MeOTf[13] to the known azidoborane,[14] IPr•BH$_2$N$_3$ (**1**) (IPr = [(HCNDipp)$_2$C:], Dipp = 2,6-^{i}Pr$_2$C$_6$H$_3$; OTf$^-$ = OSO$_2$CF$_3$). It was hoped that reduction of IPr•B(OTf)$_2$N$_3$ would afford an unstable B(I) species that would yield oligomeric adducts of [IPr•(BN)]$_x$ after loss of dinitrogen (Scheme 4.2).[12]

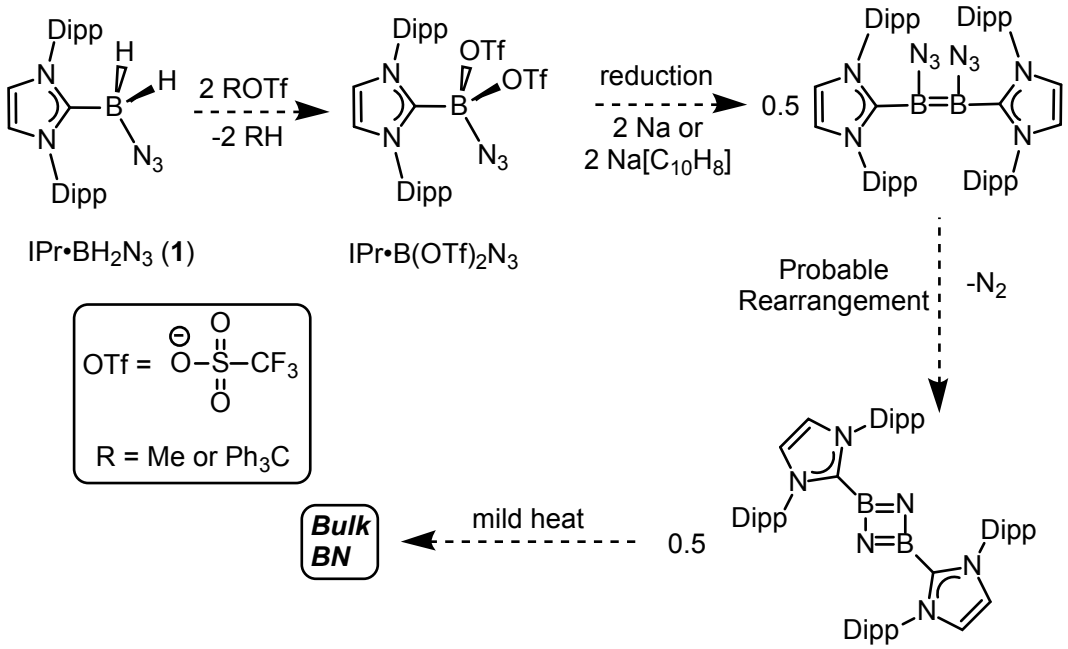

Scheme 4.2. A possible reaction pathway for the synthesis of a molecular BN precursor.

However when IPr•BH$_2$N$_3$ (**1**) was reacted with of MeOTf, gas evolution was noted and a new product was formed that contained a nitrogen-bound methyl group. This product proved to be thermally unstable in solution at room temperature, yet at -35 °C colorless crystals suitable for X-ray crystallography were obtained, revealing the

generation of the formal boraiminium adduct [IPr•HB=NH(Me)]OTf (**2**) (Scheme 4.3; Figure 4.1).

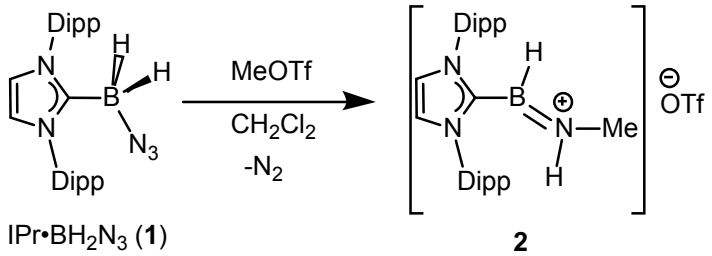

Scheme 4.3. Synthesis of **2** starting from **1** and MeOTf.

Compound **2** adopts a *trans* HBNH configuration in the solid state with a B−N distance of 1.361(5) Å, a value that is slightly elongated with respect to the B=N double bond lengths found in the abovementioned CAAC and NHC iminoborane adducts LB•RBNR′ [1.300(3) to 1.340(5) Å] (LB = Lewis base).[3] The C_{IPr}-B interaction in **2** [1.571(7) Å *avg.*] is nearly the same value within experimental error (3σ) as the related coordinative bond in CAAC•BrB=$NSiMe_3$ [1.606(4) Å],[3b] indicating that a similar C-B bonding environment is likely present in both species. Compound **2** was also characterized by different NMR techniques. The $^1H\{^{11}B\}$ NMR spectrum of compound **2** shows characteristic broad signals at 4.02 and 3.88 ppm for the N-*H* and B-*H* protons. Furthermore, the N-bound methyl group appears as a doublet ($^3J_{HH}$ = 4.8 Hz) at 1.98 ppm in the proton NMR spectrum of compound **2**. The ^{19}F NMR spectrum of **2** displays a sharp resonance at -77.7 ppm representing the OTf counter anion.

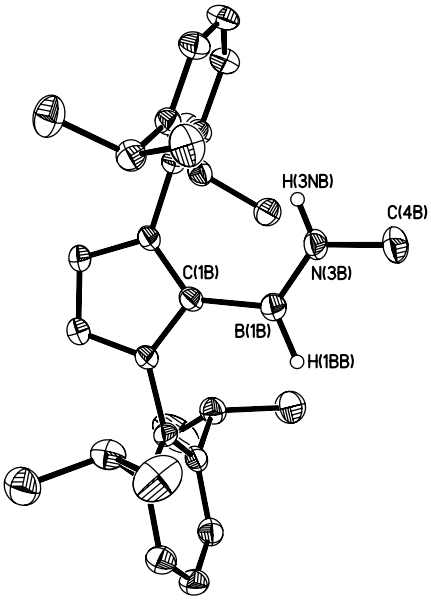

Figure 4.1. Molecular structure of [IPr•BH=NH(Me)]OTf (**2**) with thermal ellipsoids presented at a 30 % probability level. All carbon-bound hydrogen atoms and OTf^- counterion have been omitted for clarity. Selected bond lengths (Å) and angles (deg) with parameters associated with a second molecule in the asymmetric unit listed in square brackets: C(1B)−B(1B) 1.574(5) [1.568(5)], B(1B)−N(3B) 1.366(5) [1.361(5)], N(3B)−C(4B) 1.478(5) [1.460(5)]; C(1B)−B(1B)−N(3B) 121.3(4) [122.1(4)].

Compound **2** can be viewed as an NHC adduct of methylated HBNH, and accordingly it can be assumed that the N_2 elimination/1,2-H migration protocol in Scheme 4.3 could be extended to include other Lewis acidic entities.[15] Inspired by the prior success using $W(CO)_5$ as a Lewis acid,[8c,d,h] IPr•BH_2N_3 (**1**) was combined with THF•$W(CO)_5$, however no reaction occurred. Fortunately, the hindered fluoroarylborane $BAr^F{}_3$ (Ar^F = 3,5-$C_6H_3(CF_3)_2$)[16] binds to the azide moiety in **1** to yield IPr•BH_2N_3•$BAr^F{}_3$ (**3**) as a colorless solid (Scheme 4.4, Figure 4.2).

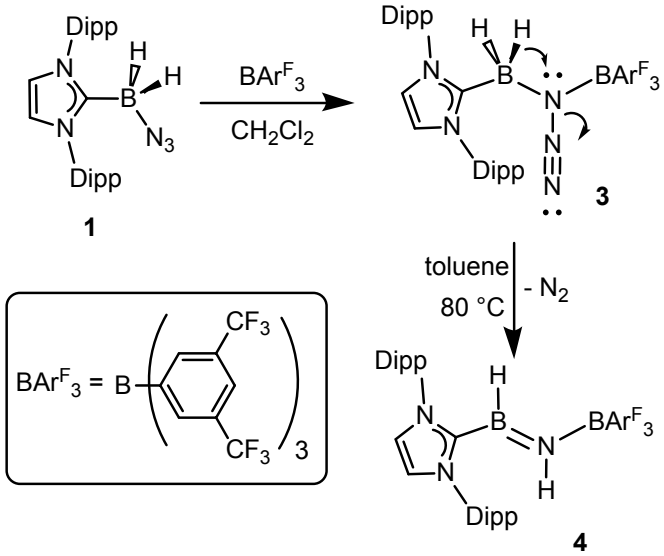

Scheme 4.4. Preparation of the azidoborane **3** and its conversion into the iminoborane complex **4**.

The most notable structural feature of IPr•BH_2N_3•$BAr^F{}_3$ (**3**) is the substantial shortening of the terminal N(4)−N(5) bond length [1.134(2) Å] in relation to the internal N(3)−N(4) linkage [1.253(2) Å], consistent with the accumulation of triple bond character. Interestingly, the bond lengths and the overall geometry of the $H_2B{-}N_3$ unit in **3** remain unperturbed in relation to those found in the precursor IPr•BH_2N_3 (**1**).[14] In addition to the B−H stretching mode at 2467 cm^{-1}, a diagnostic azide IR $\upsilon(N_3)$ band at 2134 cm^{-1} was noted for **3**, which matches well with the related stretches at 2189 and 2175 cm^{-1} found in the bis-silylated azide $[(Me_3Si)_2NNN]B(C_6F_5)_4$.[17]

IPr•BH_2N_3•$BAr^F{}_3$ (**3**) slowly decomposes at room temperature, both in solution (within 24 hrs) and in the solid state (4 days). As a result, the thermolysis of **3** was explored in more detail. The clean conversion of IPr•BH_2N_3•$BAr^F{}_3$ (**3**) to a new carbene-containing product was accomplished by heating a solution of **3** in toluene to

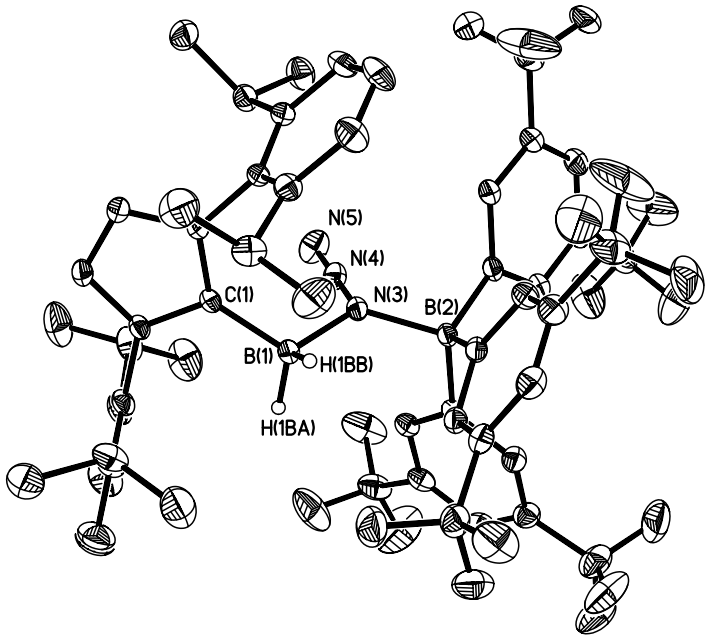

Figure 4.2. Molecular structure of IPr•BH_2N_3•$BAr^F{}_3$ (**3**) with thermal ellipsoids presented at a 30 % probability level; all carbon-bound hydrogen atoms have been omitted for clarity. Selected bond lengths (Å) and angles (deg): C(1)−B(1) 1.610(2), B(1)−N(3) 1.599(2), N(3)−N(4) 1.253(2), N(4)−N(5) 1.134(2), N(3)−B(2) 1.656(2); N(5)−N(4)−N(3) 177.68(18).

80 °C for 12 hrs.[18] The resulting highly lipophilic colorless solid afforded an IR spectrum devoid of an azide band, suggesting that N_2 loss occurred. Furthermore weak υ(N−H) and υ(B−H) vibrations emerged at 3370 and 2511 cm^{-1}, respectively, while the corresponding N−H and B−H resonances were located at 5.44 and 4.00 ppm in the $^1H\{^{11}B\}$ NMR spectrum of the product with an integration ratio of 1:1. The N−H group yields a doublet resonance due to $^3J_{HH}$ coupling with an adjacent B−H group, supporting the formation of an iminoborane HBNH array. X-ray crystallography conclusively identified the product as the donor-acceptor iminoborane complex IPr•HB=NH•$BAr^F{}_3$ (**4**) (Scheme 4.4, Figure 4.3). The central iminoborane B−N distance in **4** is 1.364(2) Å and is in line with the presence of a

double bond (Σr_{cov}(B=N) = 1.38 Å).[19] The capping IPr and $BAr^F{}_3$ units in **4** form a steric sheath about the central HB=NH unit and help enforce a *trans* core geometry [C(1)−B(1)−N(3)−B(2) torsion angle = 179.26(12)°] which minimizes IPr•••$BAr^F{}_3$ intramolecular repulsions. The C_{IPr}−B distance in **4** is 1.596(2) Å and is shorter in comparison to the dative C−B interaction in Im^iPr_2•^{t}BuB=N^{t}Bu [1.648(2) Å; Im^iPr_2 = $(HCN^iPr)_2C$:],[3c] illustrating the less hindered nature of the HBNH unit in **4**. The terminal *N*−*B*$Ar^F{}_3$ bond in **4** is 1.5708(18) Å and lies in the range of B−N single bonds noted in IPr•$BH_2NH_2BH_3$ [1.540(3)-1.605(2) Å];[20] of note, the capping *N*−*B*$Ar^F{}_3$ interaction in IPr•BH_2N_3•$BAr^F{}_3$ (**3**) is 1.599(2) Å.

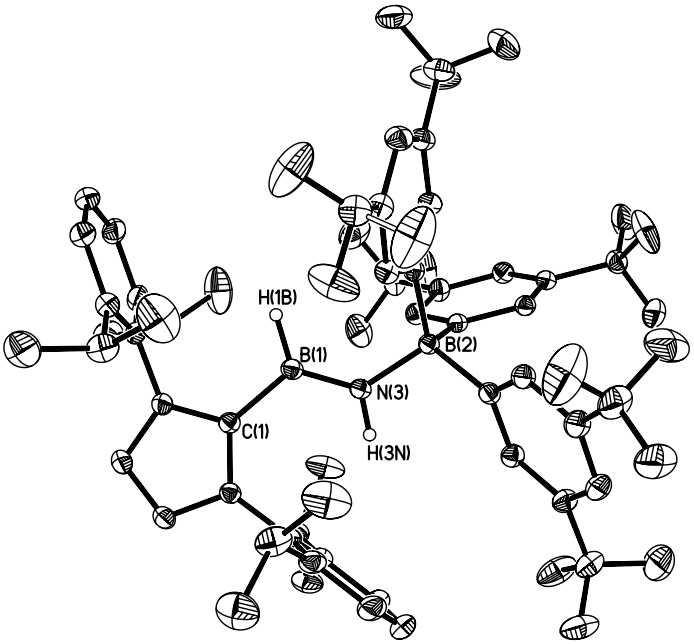

Figure 4.3. Molecular structure of IPr•HB=NH•$BAr^F{}_3$ (**4**) with thermal ellipsoids presented at a 30 % probability level. All carbon-bound hydrogen atoms have been omitted for clarity. Selected bond lengths (Å) and angles (deg): C(1)−B(1) 1.596(2), B(1)−N(3) 1.364(2), N(3)−B(2) 1.5708(18); C(1)−B(1)−N(3) 123.45(13), B(1)−N(3)−B(2) 130.72(12), N(3)−B(1)−H(1B) 122.3(10), B(1)−N(3)−H(3N) 117.3(12).

One could also depict the bonding in **4** as the zwitterion NHC(+)-HB=NH-B(-)$Ar^F{}_3$; in this case polar two center, two electron C_{NHC}-B and N-B_{ArF3} bonds are still present. As outlined in Scheme 4.4, the formation of **4** is postulated to occur via N_2 loss from **3** followed by a 1,2-hydride shift from boron to nitrogen (*vide infra*). A related process has been observed by Paetzold[1a] who prepared iminoboranes via alkyl-group migration (R_2N-B(R′)-N → R_2N-B≡N-R′) involving a transient boranitrene.[21] Cummins and Fox also observed nitrogen extrusion from the azido-borate salt $^nBu_4N[(N_3)B(C_6F_5)_3]$ in the presence of (THF)U[N(^{t}Bu)Ar]$_3$ (Ar = 3,5-$Me_2C_6H_3$) to yield the uranium(V) nitride $^nBu_4N[(F_5C_6)_3B{\bullet}N{=}U\{N(^tBu)Ar\}]_3$.[22]

To gain insight into the mechanism by which IPr•HB=NH•$BAr^F{}_3$ (**4**) is formed, the deuterium labeled analogue IPr•BD_2N_3•$BAr^F{}_3$ (**3-d**) was synthesized from the reaction of IPr•BD_2N_3 (**1-d**) with $BAr^F{}_3$ (Scheme 4.5). Subsequent thermolysis of **3-d** at 80 °C yielded the isotopomer IPr•DB=ND•$BAr^F{}_3$ (**4-d**) as confirmed by the broad resonances at 5.44 and 4.00 ppm for the N-*D* and B-*D* unit in the $^2H\{^1H\}$ NMR spectrum. Furthermore N-D and B-D IR stretches of **4-d** appear at 2495 and 1900 cm^{-1}.

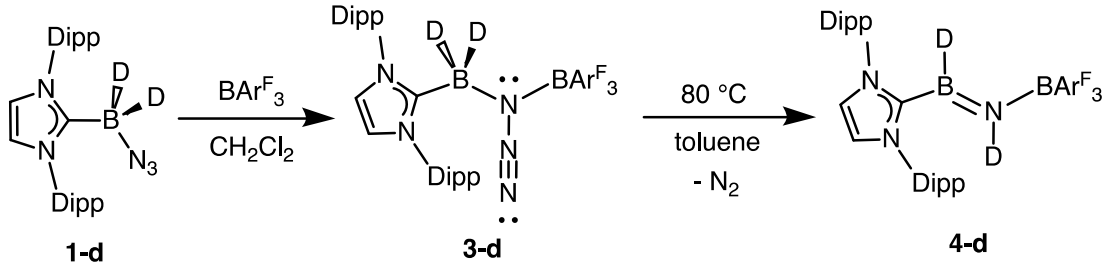

Scheme 4.5. Synthesis of the the deuterium isotopomer IPr•DB=ND•$BAr^F{}_3$ (**4-d**).

The kinetic isotope effect on the rate of the conversion from **3** to **4** (compound **3-d** to **4-d**) was studied. Compounds **3** and **3-d** were separately heated in J. Young NMR tubes in C_6D_6 at 75 °C; the initial concentration of **3** and **3-d** was 8.23×10^{-3} $mol\cdot L^{-1}$. As shown in Figure 4.4, A and A′ represent the integral of the characteristic backbone IPr C-*H* ^{1}H resonances for **3** and **3-d**. The reactions were found to be 1st order and the calculated rate constant (k) was 0.42 s^{-1} in both cases, thus giving a k_H/k_D = 1. Therefore the thermolysis of the deutero analogue **3-d** did not yield any discernable H/D kinetic isotope effect, suggesting that N_2 loss, and formation of a transient nitrene, is the rate determining step.

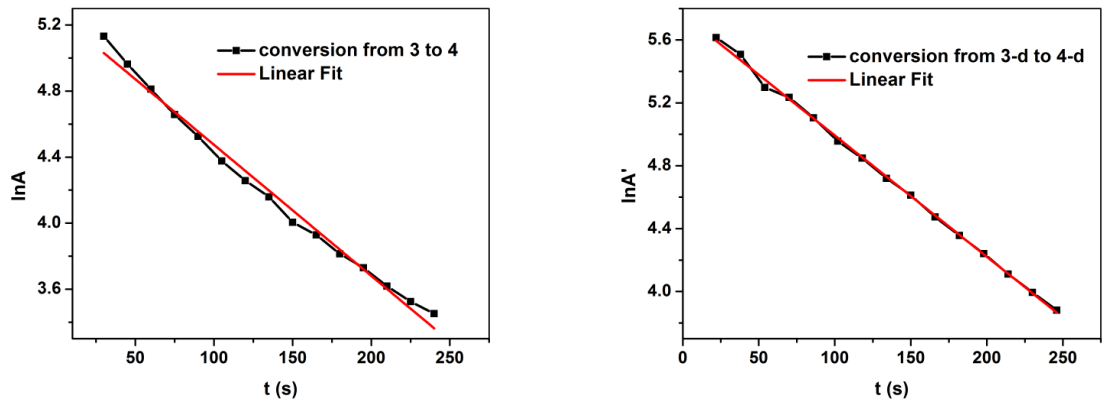

Figure 4.4. Kinetic isotope effect (KIE) studies of **3** and **3-d**.

In order to facilitate the recording of an ^{15}N NMR spectrum, the ^{15}N-labeled adduct IPr•HB=^{15}NH•BAr$^F_3$ was prepared as a 1:1 mixture with unlabeled **4** (Scheme 4.6). Interestingly the ^{15}N−H group in IPr•HB=^{15}NH•BAr$^F_3$ yielded a doublet of doublet resonance by ^{1}H NMR spectroscopy (Figure 4.5) with a $^1J_{H\text{-}15N}$ value of 69.6 Hz; for comparison, the $-NH_2$ group in 4-nitroaniline yields a $^1J_{H\text{-}15N}$ value of 86.3 Hz.[23] An ^{15}N NMR resonance for **4-N15** was located at 155.4 ppm, and is positioned

downfield in relation to the ^{15}N NMR resonance in borazine $[HBNH]_3$ (δ = −278 ppm).[24]

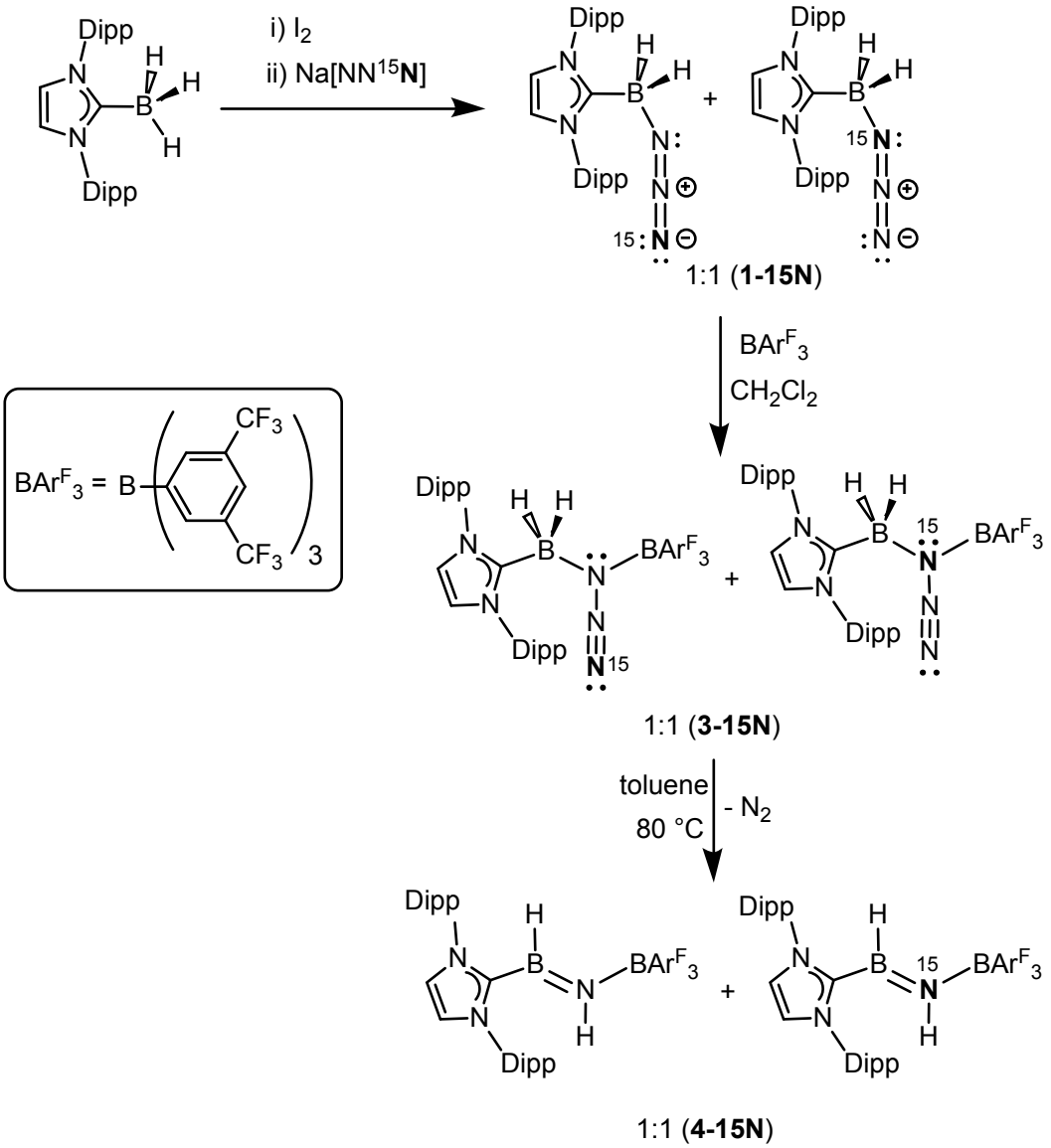

Scheme 4.6. Synthesis of the ^{15}N-labeled iminoborane adduct IPr•HB=^{15}**N**H•BAr$^F{}_3$ (**4-N15**).

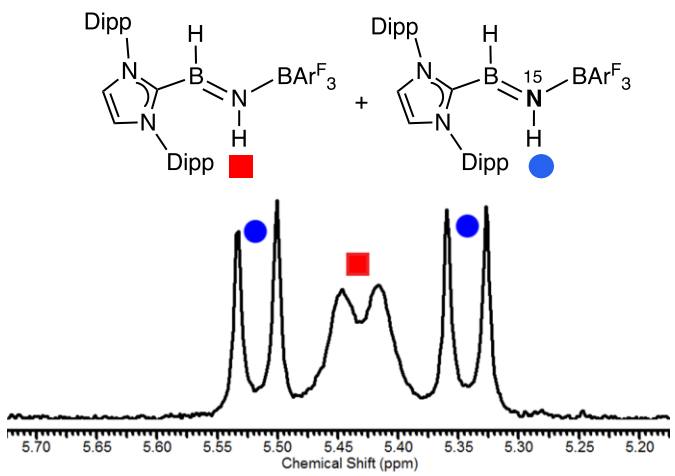

Figure 4.5. ^{1}H{^{11}B} NMR N−*H* resonances from a 1:1 mixture (**4-N15**) of IPr•HB=^{15}NH•BAr$^F_3$ and **4**.

In order to better understand the bonding and reactivity trends observed, computations were carried out at the pbe0/cc-pVDZ level. Natural bond orbital (NBO) analysis of IPr•BH$_2$N$_3$ (**1**) revealed a high negative partial charge of −0.54 on the internal (boron bound) N$_{azide}$ atom, thus explaining the electrophilic attack at this site by MeOTf and BAr$^F_3$ (Figure 4.6). Within IPr•BH$_2$N$_3$•BAr$^F_3$ (**3**) the borane-bound nitrogen [N(3) in Figure 4.2] has significant lone pair character, in line with the mesoionic form drawn in Scheme 4.4. The computed energies for the conversion of **3** into IPr•HB=NH•BAr$^F_3$ (**4**) are −64.5 kcal/mol ($\Delta_r H°$(298 K)) and −75.6 kcal/mol ($\Delta_r G°$(298 K)), while the estimated activation barrier for N$_2$ loss from **3** is 31.3 kcal/mol.[25] NBO analysis gives rise to a total charge of the central HB=NH fragment in **4** of −0.13. The B−N linkage in **4** can be formulated as a double bond, with significant polarization of the σ and π components towards N (78 % for each) (Figure 4.7). Moreover, the Wiberg bond index (WBI) for this linkage (1.32) supports the presence of multiple-bond character; accordingly, the Kohn-Sham orbitals reveal

a LUMO of B−N π*-character, while contributions to the BN double bond appear in the HOMO-7 (Figure 4.8).

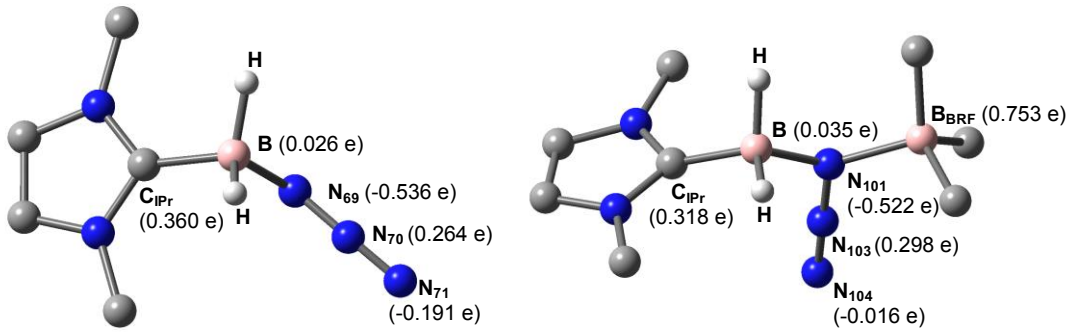

Figure 4.6. Left: Ball-and-stick representation of the optimized structure of **1** (the majority of the Dipp and Ar^F-groups are omitted for clarity) with atomic charges. Right: Ball-and-stick representation of the optimized structure of **3** (the majority of the Dipp and Ar^F-groups are omitted for clarity) with atomic charges.

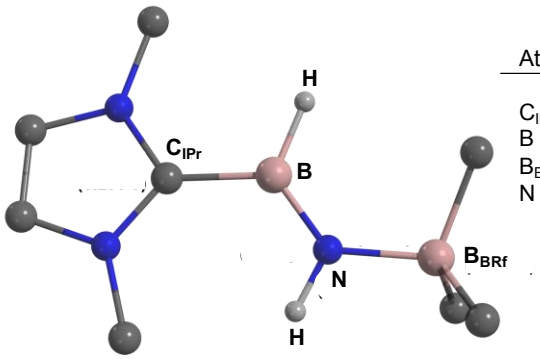

Atom	Charge	Bond	WBI	BD_{theo}	BD_{exp}
C_{IPr}	0.253 e	C_{IPr}-B	0.88	1.585	1.596
B	0.517 e				
B_{BRf}	0.721 e	B-N	1.32	1.374	1.364
N	-1.020 e				
		N-B_{BRf}	0.75	1.575	1.571

Figure 4.7. Left: Ball-and-stick representation of the optimized structure of **4** (the majority of the Dipp and Ar^F-groups are omitted for clarity). Right: Atomic charges of the atoms and *WBI*, $BD_{theor.}$, and BD_{exp} of the respective bonds (BD = bond distance).

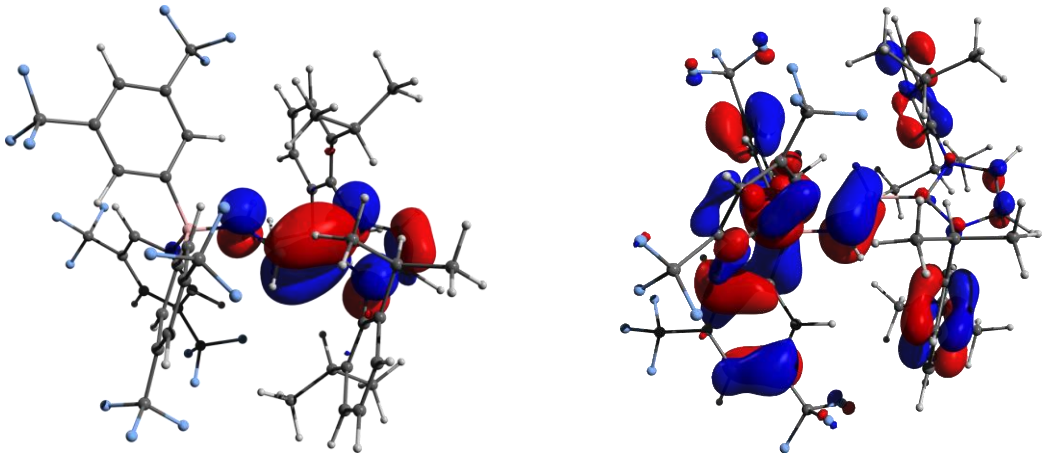

Figure 4.8. Depiction of selected Kohn-Sham orbitals of IPr•HB=NH•BAr$^F{}_3$ (**4**) LUMO (left) and HOMO-7 (right).

Given the presence of hydridic (B−H) and acidic (N−H) residues within the parent iminoborane adduct IPr•HB=NH•BAr$^F{}_3$ (**4**), the dehydrogenation[10] of this species was attempted to yield the first molecular adduct of boron nitride IPr•B≡N•BAr$^F{}_3$. However, when compound **4** was treated with 2 mol% of the active amine-borane dehydrogenation catalyst $[(COD)RhCl]_2$ (COD = 1,5-cyclooctadiene) at room temperature, and later at 90 °C, only the starting material could be recovered. Increasing the catalyst loading to 20 mol%, and prolonged heating to 140 °C (for 96 hrs) led to decomposition of **4** into an unidentifiable mixture of products. The lower reactivity of **4** in relation to other unsaturated B-N systems can be traced to the high degree of steric protection about the HB=NH unit due to the bulky flanking IPr and BAr$^F{}_3$ groups; in fact **4** can be handled in air (but decomposes in water) and remains unchanged in the presence of ^{n}BuLi, $K[N(SiMe_3)_2]$, $Ph_3C[B(C_6F_5)_4]$, MeOTf and even elemental I_2.

With the goal of promoting increased reactivity within a core HB=NH moiety, a HB=NH complex was synthesized with a less sterically encumbered carbene donor. Accordingly, the less hindered NHC, $ImMe_2{}^iPr_2$ [$ImMe_2{}^iPr_2$ = $(MeCN^iPr)_2C$:] was prepared and explored as a Lewis base for HB=NH adduct formation.[26] The required azidoborane for this synthesis, $ImMe_2{}^iPr_2{\bullet}BH_2N_3$ (**6**), was prepared from $ImMe_2{}^iPr_2{\bullet}BH_3$[27] in two high yielding steps as illustrated in Scheme 4.7.

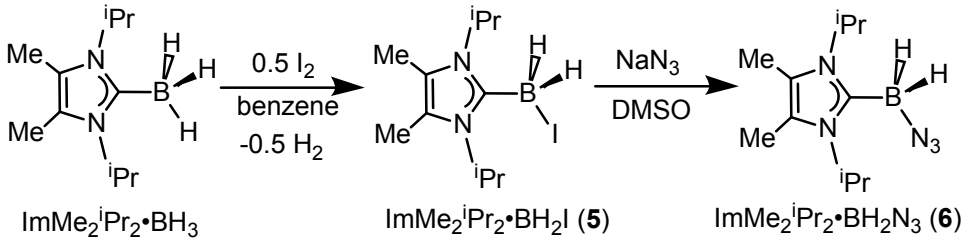

Scheme 4.7. Synthesis azidoborane adduct $ImMe_2{}^iPr_2{\bullet}BH_2N_3$ (**6**).

$ImMe_2{}^iPr_2{\bullet}BH_2N_3$ (**6**) was then combined with a stoichiometric amount of the fluoroarylborane, $BAr^F{}_3$, followed by heating to 80 °C for 12 hrs in toluene to afford the target iminoborane adduct $ImMe_2{}^iPr_2{\bullet}HB{=}NH{\bullet}BAr^F{}_3$ (**7**) as a colorless solid in a 64 % yield (Mp = 142-146 °C). Based on prior studies this reaction is believed to proceed via initial N_2 elimination and trapping of the resulting nitrene adduct, $ImMe_2{}^iPr_2{\bullet}H_2B\text{-}N{\bullet}BAr^F{}_3$ by a 1,2-hydride migration from B to N (Scheme 4.8). As expected, the $^1H\{^{11}B\}$ NMR spectrum of $ImMe_2{}^iPr_2{\bullet}HB{=}NH{\bullet}BAr^F{}_3$ (**7**) gave discernable N-H and B-H resonances at 5.42 and 4.62 ppm, respectively (in C_6D_6), which are similar to the corresponding resonances found in $IPr{\bullet}HB{=}NH{\bullet}BAr^F{}_3$ (**4**). X-ray crystallography later conclusively identified the presence of an HB=NH moiety in **7** (Figure 4.9). The core iminoborane unit in **7** adopts a *trans* arrangement [C-B-N-B dihedral angle = 178.1(2)°] thereby minimizing intramolecular repulsion between

the $ImMe_2{}^iPr_2$ and $BAr^F{}_3$ groups. The central B=N and $C_{(NHC)}$-B bond distances in **7** are 1.369(3) Å and 1.596(4) Å, which are the same within experimental error as in IPr•HB=NH•$BAr^F{}_3$ (**4**). A slightly elongated B-N distance was reported in the iminoborane $(HC{\equiv}C)_2B\text{-}N{}^iPr_2$ (1.385(3) Å).[28]

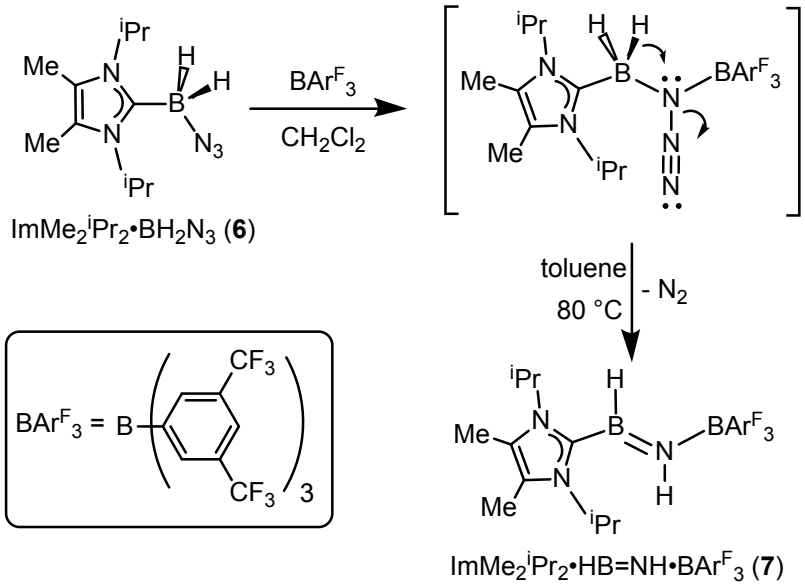

Scheme 4.8. Synthesis of $ImMe_2{}^iPr_2$•HB=NH•$BAr^F{}_3$ (**7**) starting from the azidoborane adduct $ImMe_2{}^iPr_2$•BH_2N_3 (**6**).

$ImMe_2{}^iPr_2$•HB=NH•$BAr^F{}_3$ (**7**) was examined by computational methods (M062X functional with 6-31G(d,p)) and an overall charge of -0.13 e was found for the central HB=NH moiety. As anticipated, the B=N linkage (Wiberg bond index, WBI = 1.33) has considerable polarization of the σ- and π-components towards N (ca. 80 % located on N), according to NBO analysis (Figure 4.10). The LUMO shows B-N π* and B-C π-character, while contributions to the B-N π-manifold appear in HOMO-2 and HOMO-6 (Figure 4.11). The computed HOMO-LUMO gap is 173 kcal mol^{-1} and is in agreement with the observed inertness of **7** (*vide infra*).

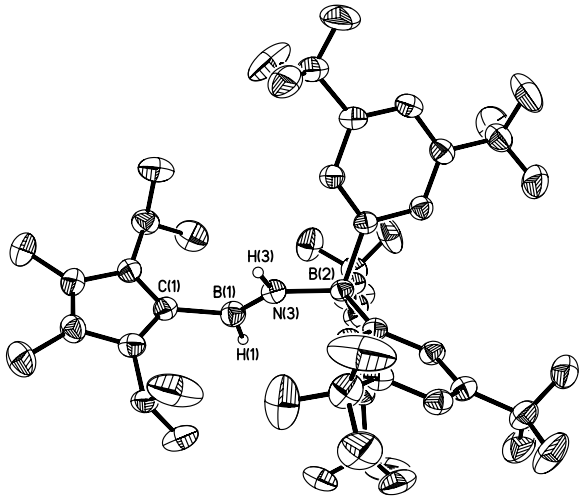

Figure 4.9. Molecular structure of $ImMe_2{}^iPr_2$•HB=NH•$BAr^F{}_3$ (**7**) with thermal ellipsoids presented at a 30 % probability level. All carbon-bound hydrogen atoms have been omitted for clarity. Selected bond lengths (Å) and angles (deg): C(1)−B(1) 1.596(2), B(1)−N(3) 1.369(3), N(3)−B(2) 1.572(2); C(1)−B(1)−N(3) 121.8(2), B(1)−N(3)−B(2) 130.5(2), N(3)−B(1)−H(1B) 125.2(16), B(1)−N(3)−H(3N) 115.8(19).

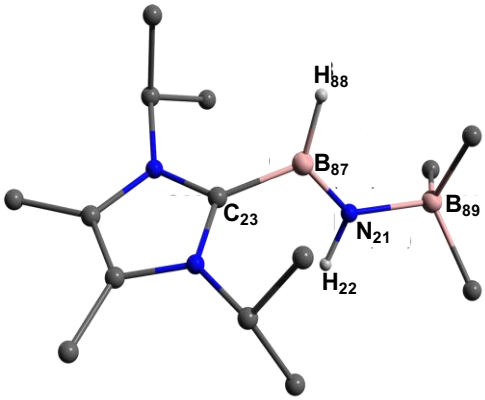

Atom	Charge	Bond	WBI	BD_{theo}	BD_{exp}
C_{23}	0.245 e	C_{23}-B_{87}	0.85	1.606	1.596
B_{87}	0.506 e				
B_{89}	0.594 e	B_{87}-N_{21}	1.33	1.372	1.370
N_{21}	-1.021 e				
H_{88}	-0.026 e				
H_{22}	0.409 e				

Figure 4.10. Left: Ball-and-stick representation of the optimized structure of **7** (the majority of the Ar^F-groups are omitted for clarity). Right: Atomic charges of the atoms and *WBI*, $BD_{theor.}$, and BD_{exp} of the respective bonds (BD = bond distance).

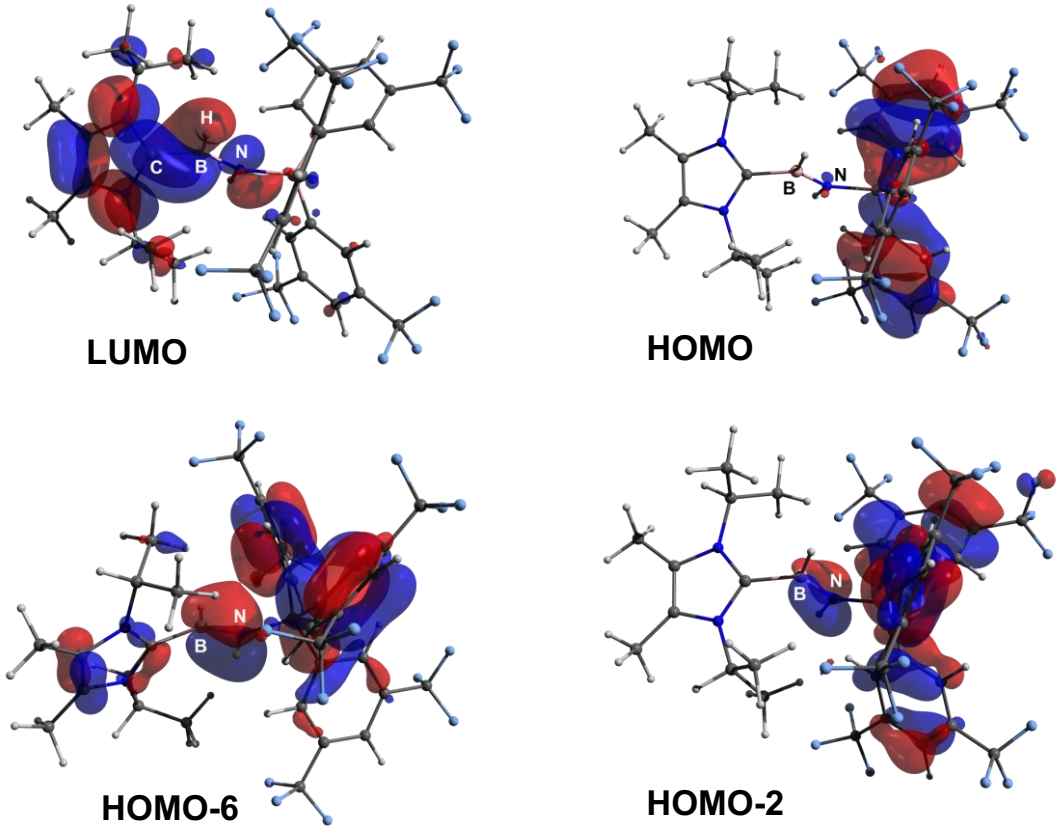

Figure 4.11. POV-ray depiction of selected Kohn-Sham orbitals of **7**.

With the less hindered HBNH complex **7** in hand, attempts were made to promote its dehydrogenation to afford the BN adduct $ImMe_2{}^iPr_2$•B≡N•$BAr^F{}_3$. When $ImMe_2{}^iPr_2$•HB=NH•$BAr^F{}_3$ (**7**) was treated with the well-known dehydrogenation pre-catalyst $[Rh(COD)Cl]_2$ (2-5 mol%) in toluene, no reaction occurred at room temperature. When the same dehydrogenation reaction was attempted at 90 °C for 7 days, only partial decomposition of **7** (<10 %; $[ImMe_2{}^iPr_2\text{-}H]^+$ salt) was noted. Moreover, compound **7** was also combined with the potential dehydrogenation catalyst $CpFe(CO)_2OTf$ and the FLP, $^tBu_3P$ and $BAr^F{}_3$, (both known to promote H_2

loss from amine-boranes) however in each case no reaction with **7** transpired. Likewise attempted H_2 release from **7** by photolysis (300 W Hg lamp in Et_2O) gave no reaction.

Undaunted by the lack of thermally- or catalytically-instigated H_2 release from **7**, it was then verified if the core HBNH unit underwent chemical transformations one would expect for a polarized B=N linkage.[29] When $ImMe_2{}^iPr_2$•HB=NH•$BAr^F{}_3$ (**7**) was combined with one equivalent of HCl in Et_2O, the resulting ^{11}B NMR spectrum was consistent with the presence of two four-coordinate boron centers (δ = -3.7 and -9.5 ppm, in C_6D_6). X-ray crystallography confirmed the successful addition of HCl across the B=N bond to form $ImMe_2{}^iPr_2$•H(Cl)B-NH_2•$BAr^F{}_3$ (**8**) as a racemic mixture due to the presence of a chiral boron atom (Figure 4.12; eqn. 4.1). The addition of chloride to the boron center in **8** illustrates the Lewis acidic nature of the boron atom in coordinated HB=NH in **7**. The central B-N bond distance in **8** is 1.585(4) Å and is comparable to the B-N bond lengths found in structurally related amine-boranes, such as IPr•$BH_2NH_2BH_3$.[30] The $C_{(NHC)}$-B bond distance in **8** is 1.616(5) Å which, somewhat to our surprise, is similar in length as the corresponding $C_{(NHC)}$-B bond distance of 1.596(4) Å in **7**, despite the change in hybridization at boron to sp^3 in **8**; however, the capping N-*B*$Ar^F{}_3$ interaction in **8** (1.632(4) Å) is longer than in the HBNH adduct **7** (1.572(2) Å). Addition of HCl also leads to a substantial canting of the relative arrangement of the capping NHC and borane groups (*vs.* in **7**), as evidenced by the C-B-N-B dihedral angle of 65.3(3)°.

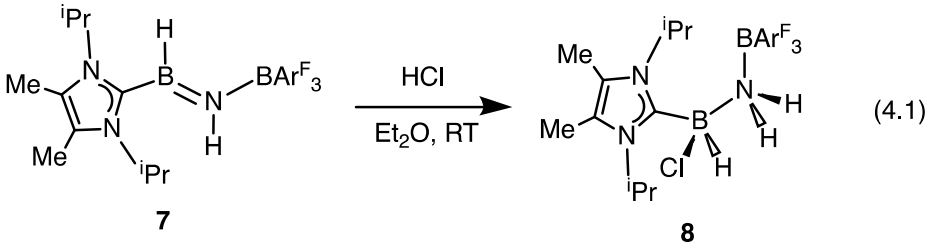

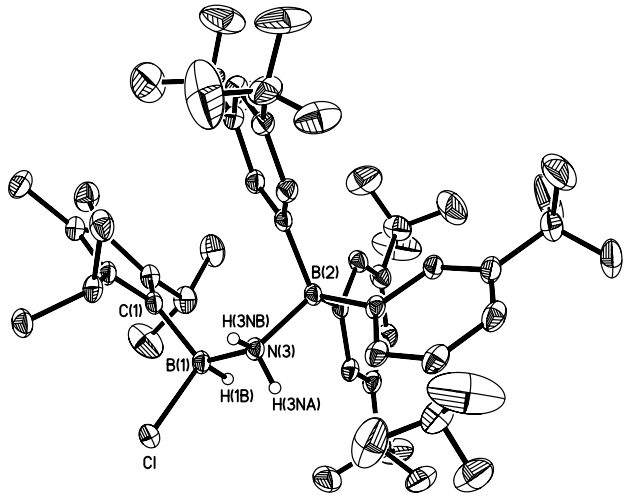

Figure 4.12. Molecular structure of $ImMe_2{}^iPr_2$•H(Cl)B-NH_2•$BAr^F{}_3$ (**8**) with thermal ellipsoids presented at a 30 % probability level. All carbon-bound hydrogen atoms have been omitted for clarity. Selected bond lengths (Å) and angles (deg): C(1)−B(1) 1.616(5), B(1)−N(3) 1.585(4), N(3)−B(2) 1.632(4), B(1)-Cl 1.906(4); C(1)−B(1)−N(3) 115.7(3), B(1)−N(3)−B(2) 124.4(2), N(3)−B(1)−Cl 107.2(2), B(1)−N(3)−H(3NA) 105(2).

While the polarized B=N linkage in $ImMe_2{}^iPr_2$•HB=NH•$BAr^F{}_3$ (**7**) did not exhibit FLP type reactivity with H_2, CO or CO_2,[31] effective transfer hydrogenation[32] occurred between the amine-borane Me_2NH•BH_3 and **7** (eqn. 4.2). The resulting hydrogenated product $ImMe_2{}^iPr_2$•H_2B-NH_2•$BAr^F{}_3$ (**9**) formed after 12 hrs at room temperature; the expected dehydrogenated by-products $[Me_2N\text{-}BH_2]_2$ and Me_2NH-BH_2-NMe_2-BH_3 were also detected by NMR spectroscopy. To probe the mechanism of this transformation in more detail, compound **7** was combined with Me_2ND•BH_3; the resulting product $ImMe_2{}^iPr_2$•H_2B-N(H)D•$BAr^F{}_3$ (**9-d**) suggested direct H/D atom

transfer from B to B and N to N.[32a] The molecular structure of **9** (Figure 4.13) has similar overall structural features as the HCl addition product $ImMe_2{}^iPr_2$•H(Cl)B-NH_2•$BAr^F{}_3$ (**9**) with an elongated C_{NHC}-B distance of 1.627(3) Å in accordance with the decreased electrophilicity of the –BH_2-NH_2-$BAr^F{}_3$ unit in **9**.

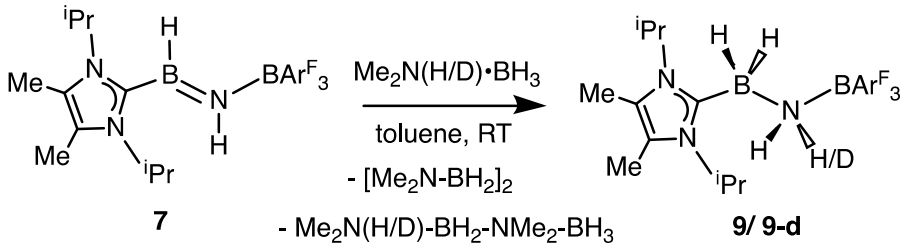

(4.2)

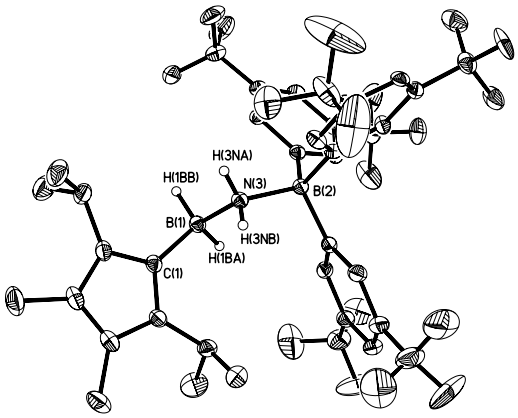

Figure 4.13. Molecular structure of $ImMe_2{}^iPr_2$•H_2B-NH_2•$BAr^F{}_3$ (**9**) with thermal ellipsoids presented at a 30 % probability level. All carbon-bound hydrogen atoms have been omitted for clarity. Selected bond lengths (Å) and angles (deg): C(1)−B(1) 1.627(3), B(1)−N(3) 1.613(3), N(3)−B(2) 1.622(2); C(1)−B(1)−N(3) 110.23(15), B(1)−N(3)−B(2) 120.11(14), N(3)−B(1)−H(1BB) 109.0(12), B(1)−N(3)−H(3NA) 106.8(15).

Despite the presence of both hydridic and acidic H atoms in $ImMe_2{}^iPr_2$•H_2B-NH_2•$BAr^F{}_3$ (**9**), efforts to induce dehydrogenation (and reform the HBNH adduct **7**) by heating up to 100 °C in the presence of known dehydrogenation pre-catalysts $[Rh(COD)Cl]_2$ or $CpFe(CO)_2OTf$ did not afford a discernable reaction. Furthermore,

9 remained unreactive towards the possible H_2 acceptors, PhN=NPh and the FLP ($^tBu_3P/BAr^F{}_3$), and did not yield **7** upon attempted photolysis (300 W Hg lamp). Accordingly, the calculated NPA charges for **9** show less hydridic character for the B-*H* array (−0.009 and −0.020 e) compared to the reactive amine-borane $MeNH_2{\bullet}BH_3$ (B-*H* charges of -0.030 to -0.034 e), thus partially explaining the higher reactivity for the latter species (Figure 4.14). The computed positive charges for N-bound hydrogen atoms in **9** (0.429 and 0.437 e) are similar to those in $MeNH_2{\bullet}BH_3$.

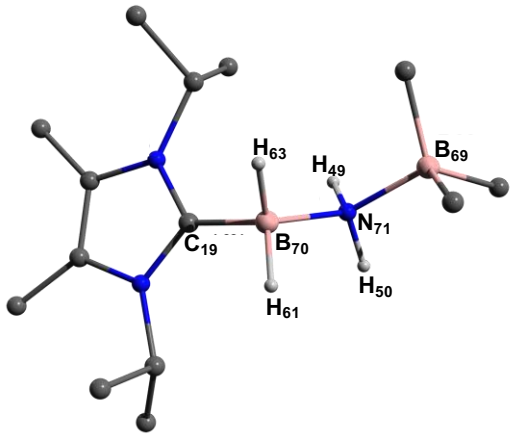

Atom	Charge
C_{19}	0.306 e
B_{70}	-0.002 e
B_{69}	0.629 e
N_{71}	-0.986 e
H_{50}	0.437 e
H_{49}	0.428 e
H_{61}	-0.020 e
H_{63}	-0.009 e

Bond	WBI	BD_{theo}	BD_{exp}
C_{19}-B_{70}	0.86	1.631	1.628
B_{70}-N_{71}	0.69	1.605	1.613

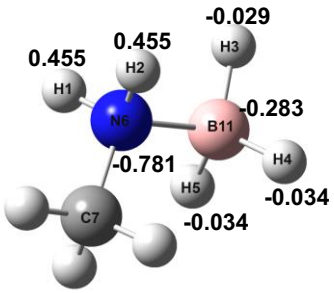

Figure 4.14. Left: Ball-and-stick representation of the optimized structure of **9** (the majority of the Ar^F-groups are omitted for clarity) Right-top: Atomic charges of the atoms and *WBI*, $BD_{theor.}$, and BD_{exp} of the respective bonds (BD = bond distance). Right-bottom: Ball-and-stick representation of optimized structure of **$MeNH_2{\bullet}BH_3$** with the atomic charges.

In order to directly probe the Lewis acidity of the HBNH unit in **7**,[33] an additional equivalent of the carbene donor $ImMe_2{}^iPr_2$ was combined with $ImMe_2{}^iPr_2{\bullet}HB{=}NH{\bullet}BAr^F{}_3$ (**7**). While the expected bis adduct $(ImMe_2{}^iPr_2)_2HBNH{\bullet}BAr^F{}_3$ (**10**) could be isolated in the solid state as a yellow solid (88 % yield) and characterized by X-ray crystallography (Figure 4.15, *vide infra*), the

NMR spectra of this product in solution exhibited dynamic behavior, consistent with partial dissociation of one NHC ligand. Addition of the Lewis acid acceptor BH_3 (delivered in the form of $Me_2S{\bullet}BH_3$) led to the quantitative removal of one equiv. of $ImMe_2{}^iPr_2$ from **10** to reform **7** (eqn. 4.3).

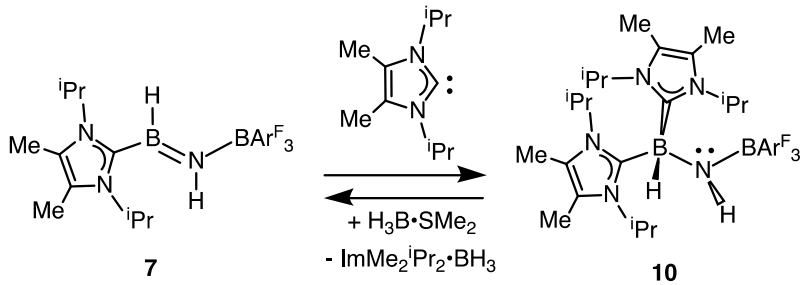

(4.3)

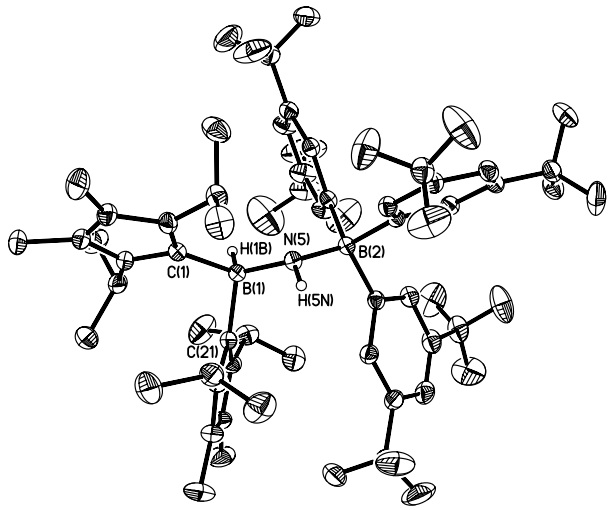

Figure 4.15. Molecular structure of $[ImMe_2{}^iPr_2]_2{\bullet}HB\text{-}NH{\bullet}BAr^F{}_3$ (**10**) with thermal ellipsoids presented at a 30 % probability level. All carbon-bound hydrogen atoms have been omitted for clarity. Selected bond lengths (Å) and angles (deg): C(1)−B(1) 1.684(3), C(21)−B(1) 1.660(2), B(1)−N(5) 1.512(2), N(5)−B(2) 1.539(2); C(1)−B(1)−N(5) 117.28(14), B(1)−N(5)−B(2) 125.03(14), N(5)−B(1)−C(21) 112.26(14), N(5)−B(1)−H(1B) 113.4(11), B(1)−N(5)−H(5N) 112.5(14).

Consistent with weaker overall C_{NHC}-B interactions in **10** relative to the HBNH adduct **7**, elongated distances of 1.684(3) and 1.660(2) Å were found in **10** (by *ca.* 0.06-0.08 Å). For comparison, the C-B distances in Bertrand's mixed

NHC/CAAC complex [CAAC•B(L)H(OTf)]BPh_4 [CAAC = cyclic alkyl(amino) carbene; L = benzimidiazolylidene] were slightly shorter (1.645(2) and 1.627(2) Å).[34] Coordination of two NHCs at boron in **10** resulted in substantial lengthening of the core B-N distance from a value of 1.369(3) in **7** to 1.512(2) Å, suggesting a lack of a B-N π-bond interaction in **10**. Computational studies on **10** support this postulate with a computed B-N Wiberg bond index (WBI) of 0.85 (vs. 1.33 in **7**). Moreover, interaction of the Lewis base $ImMe_2{}^iPr_2$ with the LUMO in **7** populates an orbital with B-N π*-character.

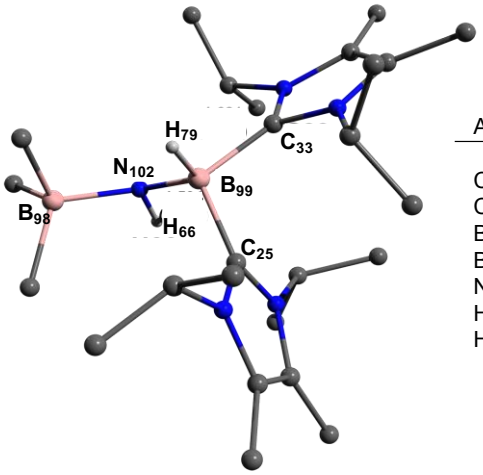

Atom	Charge	Bond	WBI	BD_{theo}	BD_{exp}
C_{33}	0.321 e	C_{33}-B_{99}	0.82	1.681	1.684
C_{25}	0.302 e				
B_{99}	0.239 e	C_{25}-B_{99}	0.80	-	-
B_{98}	0.602 e				
N_{102}	-1.138 e	B_{99}-N_{102}	0.85	1.504	1.513
H_{79}	-0.003 e				
H_{66}	0.369 e	N_{102}-B_{98}	0.77	1.547	1.539

Figure 4.16. Left: Ball-and-stick representation of the optimized structure of **9** (the majority of the Ar^F-groups are omitted for clarity) Right: Atomic charges of the atoms and *WBI*, $BD_{theor.}$, and BD_{exp} of the respective bonds (BD = bond distance).

As described in the beginning part of this chapter, N_2 loss/1,2-hydride migration in IPr•BH_2N_3 could also be instigated with the methylating agent MeOTf (Scheme 4.3), eventually leading to the formation of [IPr•HB=N(Me)H]OTf (**2**). It was desired to expand the range of known electrophiles that could trigger this potentially general transformation. However with the Ph_3COTf and R_3SiOTf (R = Me

and Ph), divergent reactivity was uncovered (Scheme 4.9). Specifically, when IPr•BH_2N_3 (**1**) or the less hindered analogue $ImMe_2{}^iPr_2$•BH_2N_3 (**6**) was combined with Ph_3COTf in CH_2Cl_2, hydride abstraction occurred to yield triphenylmethane (Ph_3CH) and the new azido(hydrido)borane adducts IPr•BH(OTf)N_3 (**11**) and $ImMe_2{}^iPr_2$•BH(OTf)N_3 (**12**) in isolated yields of 95 and 66 %, respectively (see Figures 4.17 and 4.18 for the corresponding X-ray structures). The ^{19}F NMR spectra of **11** and **12** show the retention of strong B-OTf contacts in solution (*e.g.* δ = -76.9 ppm for **11** in C_6D_6), while intense azide IR stretches were present at 2117 and 2116 cm^{-1} for compounds **11** and **12**, respectively; these values compare well with the $\upsilon(N_3)$ of 2117 cm^{-1} reported for Cummins' azido borate salt [$^nBu_4N$][$(N_3)B(C_6F_5)_3$].[22] Thus by simply replacing MeOTf with Ph_3COTf, H/OTf exchange chemistry can transpire in place of N_2 loss.

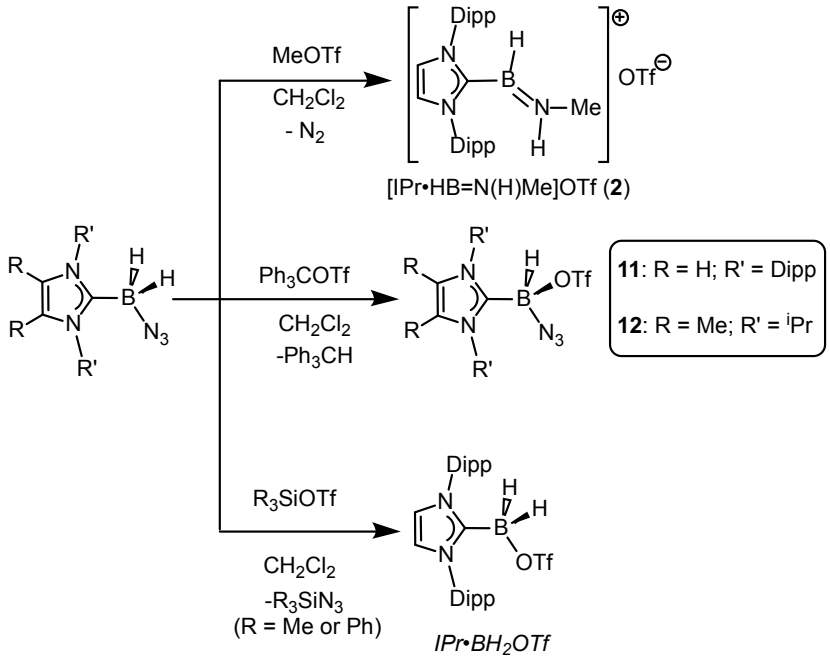

Scheme 4.9. Divergent reactivity of NHC•BH_2N_3 adducts with MeOTf, R″$_3$SiOTf (R″ = Me or Ph), and Ph_3COTf.

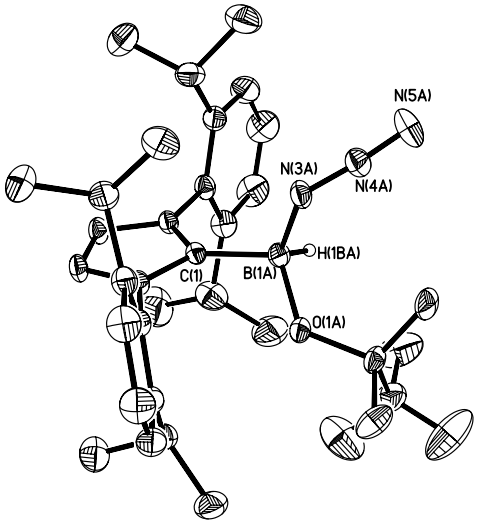

Figure 4.17. Molecular structure of IPr•BHN_3(OTf) (**11**) with thermal ellipsoids presented at a 30 % probability level. All carbon-bound hydrogen atoms have been omitted for clarity. Selected bond lengths (Å) and angles (deg) with parameters associated with a second molecule in the asymmetric unit listed in square brackets: C(1)-B(1A) 1.590(11) [1.652(10)], B(1A)-N(3A) 1.542(8) [1.482(12)], N(3A)-N(4A) 1.223(7) [1.211(8)], N(4A)−N(5A) 1.168(9) [1.145(11)], B(1A)-O(1A) 1.552(11) [1.562(11)]; N(3A)-N(4A)-N(5A) 175.0(11) [178.2(11)].

Yet another reaction pathway occurred when IPr•BH_2N_3 was combined with the silyltriflates Me_3SiOTf and Ph_3SiOTf (Scheme 4.9). In each case, complete OTf/azide exchange transpired to form the corresponding silylazides (Me_3SiN_3 and Ph_3SiN_3; identified by NMR spectroscopy) and the known borane adduct IPr•BH_2OTf.[14] It appears that N_3/OTf exchange is driven by the relatively strong Si-N bonds (*ca.* 355 kJ/mol)[35] in relation to the C-N linkages (*ca.* 305 kJ/mol), thus azide abstraction by Ph_3C^+ sources is not as favorable. To recap, NHC•BH_2N_3 shows three distinct possible reactivity pathways in the presence of electrophiles: a) HBNH formation via N_2 loss/1,2-H shift; b) hydride abstraction; c) azide abstraction.

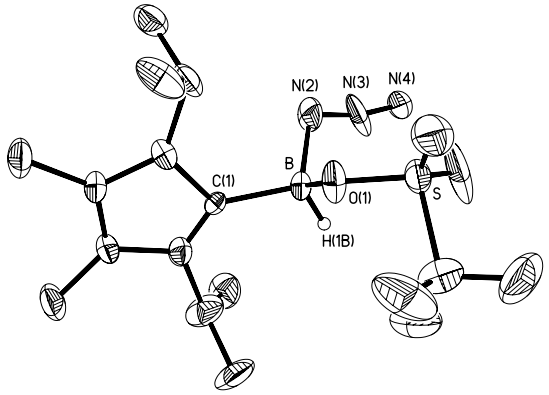

Figure 4.18. Molecular structure of $ImMe_2{}^iPr_2{\bullet}BHN_3(OTf)$ (**12**) with thermal ellipsoids presented at a 30 % probability level. All carbon-bound hydrogen atoms have been omitted for clarity. Selected bond lengths (Å) and angles (deg): C(1)−B 1.636(9), B−N(2) 1.519(19), B−O(1) 1.609(16), N(2)−N(3) 1.261(19), N(3)−N(4) 1.157(15); C(1)−B−N(2) 110.9(11), B−N(2)−N(3) 112.5(14), N(2)−N(3)−N(4) 169(3).

The accidentally uncovered high yield syntheses of the $NHC{\bullet}BH(OTf)N_3$ adducts **11** and **12** (Scheme 4.9) opened another possible path to boron nitride (BN). Motivated by the balanced equation ($NHC{\bullet}BH(OTf)N_3 \rightarrow BN + N_2 + [NHC\text{-}H]OTf$) the reactivity of both **11** and **12** was investigated in more detail. Initially, the direct thermolysis of **11** and **12** in solution was explored at temperatures approaching 100 °C (*Caution!*) but these adducts proved to be stable under these conditions. Treatment of **12** with potassium as reducing agent (in order to promote the possible reaction: **12** + K → ½ H_2 + N_2 + KOTf + BN + NHC) produced the free carbene $ImMe_2{}^iPr_2$ as the only soluble product by NMR spectroscopy. Whereas the reaction of **12** with KC_8 produced three different carbene containing products: free carbene $ImMe_2{}^iPr_2$, $ImMe_2{}^iPr_2{\bullet}BH_2N_3$ and $ImMe_2{}^iPr_2{\bullet}BH_3$.[36] Analysis of the insoluble fractions from both of the reactions by IR identified the presence of $K[N_3]$ and K[OTf], indicating that B-N(azide) bond scission transpired in place of H_2 loss and

boron nitride formation; in support of this reaction path, no IR bands for bulk BN could be found in the product mixtures (Figures 4.19 and 4.20).

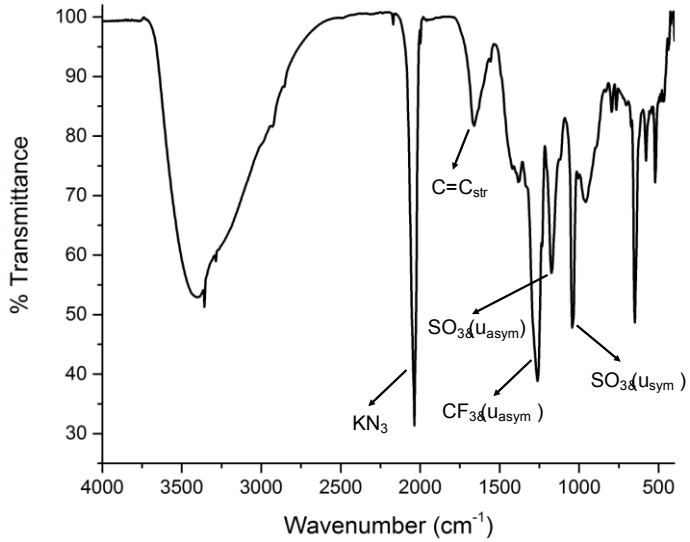

Figure 4.19. IR spectrum of the insoluble part from the reduction of $ImMe_2{}^iPr_2$•BH(OTf)N_3 (**12**) with K.

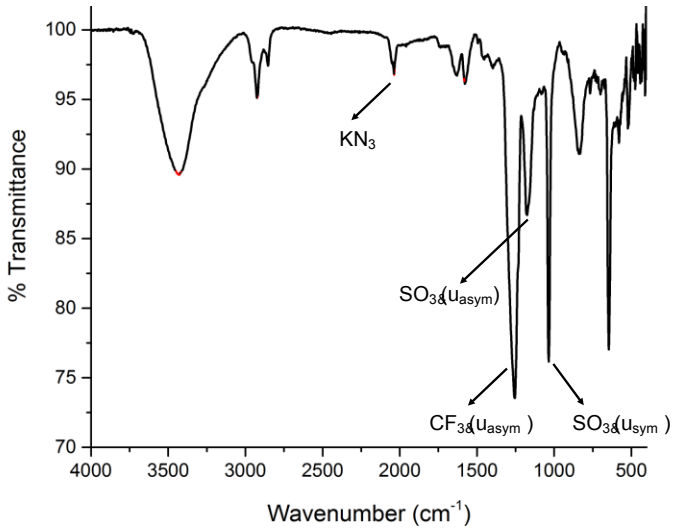

Figure 4.20. IR spectrum of the insoluble part from the reduction of $ImMe_2{}^iPr_2$•BH(OTf)N_3 (**12**) with KC_8.

Furthermore, the LUMO computed for the model species $ImMe_2$•B(H)N_3(OTf) ($ImMe_2$ = $(HCNMe)_2C$:) revealed B-N σ*-character, thus explaining the preferential B-N bond scission noted upon reduction (Figure 4.21).

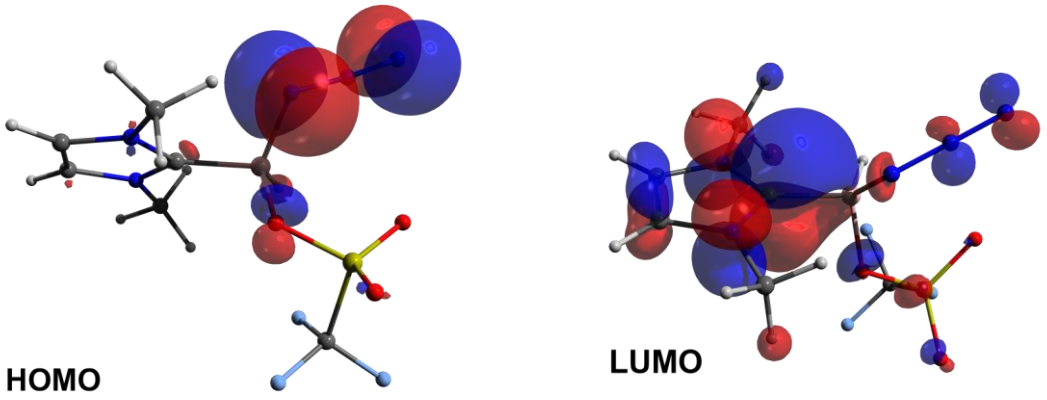

Figure 4.21. Selected molecular orbitals of $ImMe_2$•BHN_3(OTf) calculated at the M062X/6-31g(d,p) level of density functional theory.

In order to induce 1,2-H transfer in the NHC•BHN_3(OTf) species **11** and **12** the donor $ImMe_2{}^iPr_2$ was added to form the respective bis(carbene) boronium salts [IPr($ImMe_2{}^iPr_2$)•BH(N_3)]OTf (**13**) and [($ImMe_2{}^iPr_2$)$_2$•BH(N_3)]OTf (**14**) (eqn. 4.4).

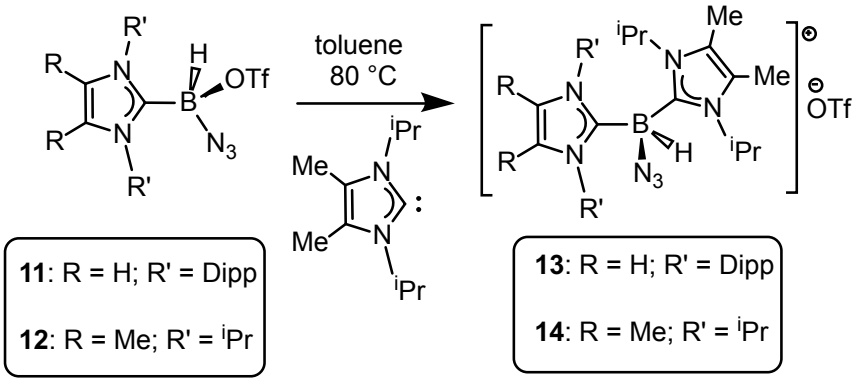

The spectral parameters of these salts were consistent with free OTf^- counteranions (*e.g.* ^{19}F resonance at -78.1 ppm for **14** in $CDCl_3$) and the retention of boron-bound azide and hydride substituents (*e.g.* IR stretches at *ca.* 2107 and 2400

cm^{-1} for **13**). Structural confirmation of the proposed bonding environment was provided by an X-ray structure of the tetraarylfluoroborate salt $[(ImMe_2{}^iPr_2)_2{\bullet}BH(N_3)]BAr^F{}_4$ (**15**) (eqn. 4.5; Figure 4.22).

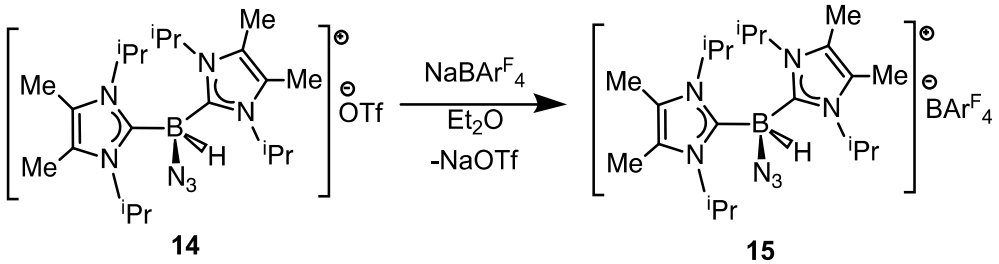

(4.5)

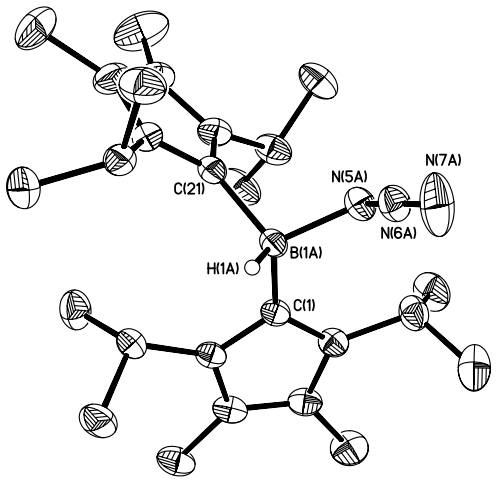

Figure 4.22. Molecular structure of $[(ImMe_2{}^iPr_2)_2{\bullet}BHN_3][B\{C_6H_3(m\text{-}CF_3)_2\}_4]$ (**15**) with thermal ellipsoids presented at a 30 % probability level. All carbon-bound hydrogen atoms and $BAr^F{}_4$ anion have been omitted for clarity. Selected bond lengths (Å) and angles (deg.) with parameters associated with a second molecule in the asymmetric unit listed in square brackets: C(1)-B(1A) 1.642(9) [1.71(3)], C(21)-B(1A) 1.650(9) [1.59(3)], B(1A)-N(5A) 1.553(7) [1.514(13)], N(5A)-N(6A) 1.202(6) [1.206(11)], N(6A)-N(7A) 1.147(10) [1.159(14)]; N(5A)-N(6A)-N(7A) 173.7(6) [158(2)].

With the goal of taking advantage of possibly higher nucleophilic character of the azide group in **15** in relation to the mono-carbene congener **12**, compound **15** was combined with one equivalent of $BAr^F{}_3$. In place of observing Lewis acid-assisted N_2 elimination/H-migration to give the "trapped" BNH adduct

[(ImMe$_2$^{i}Pr$_2$)$_2$•B=NH•BAr$^F{}_3$]OTf, no reaction transpired. Likewise no conversion of **15** was noted upon heating this species with BAr$^F{}_3$ at 90-100 °C or under UV irradiation.

Computational investigations (M062X/6-31g(d,p) level) were conducted on the model species [(ImMe$_2$)$_2$BH(N$_3$)]$^+$ and the charge of the boron-bound hydrogen atom was noted to be slightly acidic character (NPA = +0.010) (Figure 4.23). An attempt was made to promote BN formation from **14** by treatment with sodium metal in Et$_2$O; however this reaction yielded free ImMe$_2$^{i}Pr$_2$ with no sign of bulk BN formation by IR spectroscopy.

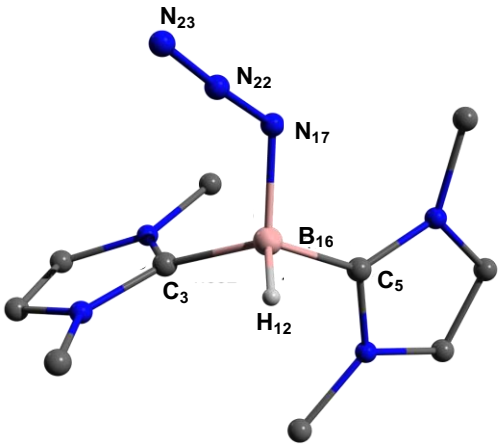

Atom	Charges
C_3	0.282 e
C_5	0.298 e
H_{12}	0.001 e
B_{16}	0.171 e
N_{17}	-0.583 e
N_{22}	0.251 e
N_{23}	-0.061 e

Figure 4.23. Left: Ball-and-stick representation of the optimized structure of model compound **[(ImMe$_2$)$_2$•B(H)N$_3$]$^+$**; Right: Atomic charges of the atoms calculated at the M062X/6-31g(d,p) level.

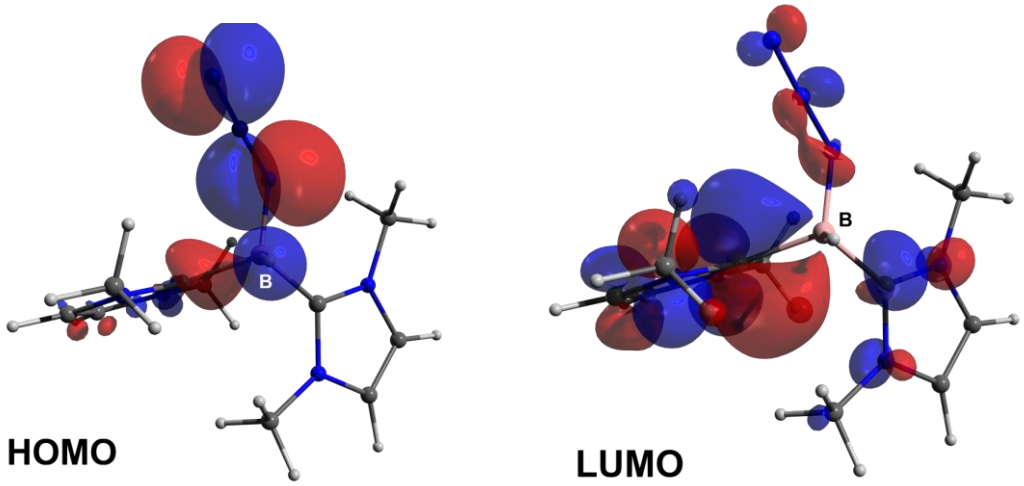

Figure 4.24. Selected molecular orbitals of $[(ImMe_2)_2{\bullet}B(H)N_3]^+$ calculated at the M062X/6-31g(d,p) level.

4.3 Conclusions

A novel Lewis acid-induced N_2 elimination/hydride-shift process was developed to yield the first stable adducts of the parent iminoborane HBNH starting from a readily available carbene-azidoborane adduct. However the use of bulky substituents restricted access to the HBNH array by potential reagents/catalysts. As a result, a more reactive HBNH complex with less sterically hindered *N*-heterocyclic carbene was introduced and the reactivity of this species was investigated in detail. In addition the reactivity of the donor-stabilized azidohydride boronium cation $[BH(N_3)]^+$ was also explored. While investigations aimed at forming bulk boron nitride (BN) from these species under mild conditions were not directly successful, it is hoped that this work inspires others to seek low temperature (< 200 °C) routes to this important inorganic wide band gap material. By suitable modification of the capping stabilizing groups, related B-N sources could be potentially used as building blocks for the rational construction of boron nitride materials and π-extended structures.[37]

4.4 Experimental Details

4.4.1 Materials and Instrumentation. All reactions were performed using standard Schlenk line techniques under an atmosphere of nitrogen or in an inert atmosphere glovebox (Innovative Technology, Inc.). Solvents were dried using a Grubbs-type solvent Purification system[38] manufactured by Innovative Technology, Inc., degassed (freeze−pump−thaw method), and stored under an atmosphere of nitrogen prior to use. $H_3B{\bullet}SMe_2$ (2.0 M in THF), $D_3B{\bullet}THF$ (1.0 M solution in THF), NaN_3, I_2, MeOTf, and $NaBD_4$, Na, K, HCl (2.0 M in Et_2O [diluted to 0.2 M in Et_2O]), $Me_2NH{\bullet}BH_3$, Me_3SiOTf, $^tBu_3P$, and PhN=NPh were purchased from Aldrich and Na[NN^{15}**N**] was purchased from Cambridge Isotope Laboratory (CIL) and each of these reagents were used as received. $NaBAr^F{}_4$ (Ar^F = 3,5-$(F_3C)_2C_6H_3$) was purchased from Matrix Chemicals and dried under vacuum at 110 °C for 48 hrs. IPr,[39] IPr•BH_2N_3 (**1**),[14] B(3,5-$(F_3C)_2C_6H_3)_3$ ($BAr^F{}_3$),[16] IPr•$SnCl_4$,[40] $ImMe_2{}^iPr_2$,[26] $ImMe_2{}^iPr_2{\bullet}BH_3$,[27] $Me_2ND{\bullet}BH_3$,[41] Ph_3COTf,[42] Ph_3SiOTf,[43] and KC_8[44] were prepared according to literature procedures; IPr = [$(HCNDipp)_2C$:]; Dipp = 2,6-$^iPr_2C_6H_3$ and $ImMe_2{}^iPr_2$ = $(MeCN^iPr)_2C$:. ^1H, $^2H\{^1H\}$, ^{11}B, $^{13}C\{^1H\}$, ^{19}F and $^{15}N\{^1H\}$ NMR spectra were recorded on a Varian iNova-400 spectrometer and referenced externally to $SiMe_4$ (^1H and $^{13}C\{^1H\}$), $Si(CD_3)_4$ ($^2H\{^1H\}$), $F_3B{\bullet}OEt_2$ (^{11}B), and 90% CH_3NO_2 ($^{15}N\{^1H\}$), $CFCl_3$ (^{19}F) respectively. Elemental analyses were performed by the Analytical and Instrumentation Laboratory at the University of Alberta. Infrared spectra were recorded on a Nicolet IR100 FTIR spectrometer as Nujol mulls between KBr plates. Melting points were measured in sealed glass capillaries under nitrogen using a MelTemp melting point apparatus and are uncorrected. Mass spectra were

obtained on Agilient Technology 6220 TOF (for ESI) and Kratos MS50G (for EI) spectrometers.

4.4.2 X-ray Crystallography. Crystals of appropriate quality for X-ray diffraction studies were removed from either a Schlenk tube under a stream of nitrogen, or from a vial (glove box) and immediately covered with a thin layer of hydrocarbon oil (Paratone-N). A suitable crystal was then selected, attached to a glass fiber, and quickly placed in a low-temperature stream of nitrogen.[45] All data were collected using a Bruker APEX II CCD detector/D8 diffractometer using Mo Kα or Cu Kα radiation, with the crystal cooled to -100 °C. The data were corrected for absorption[46] through Gaussian integration from indexing of the crystal faces. Structures were solved using intrinsic phasing SHELXT.[47] Structure refinement was accomplished using either SHELXL-97 or SHELXL-2013.[48] Hydrogen atoms were assigned positions based on the sp^2 or sp^3 hybridization geometries of their attached carbon atoms, and were given thermal parameters 20 % greater than those of their parent atoms.

4.4.3 Synthetic Procedures

Synthesis of [IPr•HB=NHMe]OTf (2). MeOTf (45 μL, 0.41 mmol) was added to a 10 mL CH_2Cl_2 solution of IPr•BH_2N_3 (**1**) (152 mg, 0.34 mmol). The mixture was stirred for 2 hrs and the volatiles were removed under vacuum. The product was washed with 10 mL of a toluene/hexanes mixture (ratio: 1:2) and dried under vacuum to yield **2** as a white powder (183 mg, 90 %). X-ray quality crystals were grown from

a hexanes/CH_2Cl_2 mixture at -35 °C. $^1H\{^{11}B\}$ NMR (400 MHz, C_6D_6): δ = 8.16 (s, 2H, N-C*H*), 7.33 (t, $^3J_{H-H}$ = 7.6 Hz, 2H, Ar*H*), 7.09 (d, $^3J_{H-H}$ = 7.9 Hz, 4H, Ar*H*), 4.02 (br, 1H, N*H*), 3.88 (br, 1H, B*H*), 2.34 (sept, $^3J_{H-H}$ = 6.8 Hz, 4H, C*H*(CH_3)$_2$), 1.98 (d, $^3J_{H-H}$ = 4.8 Hz, 3H, NH(C*H*$_3$)), 1.14 (d, $^3J_{H-H}$ = 6.8 Hz, 12H, CH(C*H*$_3$)$_2$), 0.99 (d, $^3J_{H-H}$ = 6.8 Hz, 12H, CH(C*H*$_3$)$_2$). $^{13}C\{^1H\}$ NMR (125 MHz, C_6D_6): δ = 145.1 (N-*C*H), 132.5 (Ar*C*), 131.1 (Ar*C*), 129.8 (Ar*C*), 125.3 (s, Ar*C*), 35.2 (N-*C*H$_3$), 29.1 (*C*H(CH_3)$_2$), 24.2 (CH(*C*H$_3$)$_2$), 23.7 (CH(*C*H$_3$)$_2$). $^{11}B\{^1H\}$ NMR (128 MHz, C_6D_6): δ = 28.6 (br, *B*H, $\omega_{1/2}$ = 527 Hz). ^{19}F NMR (376 MHz, C_6D_6): δ = -77.7 (s, C*F*$_3$). IR (Nujol, cm^{-1}): 3395 (m, υ_{NH}) and 2548 (m, υ_{BH}). Anal. Calcd. for $C_{29}H_{41}BF_3N_3O_3S$: C, 60.10; H, 7.13; N, 7.25; S, 5.53. Found: C, 60.13; H, 7.14; N, 7.74; S, 5.53.

Synthesis of IPr•BH_2N_3•BAr^F_3 (3). A solution of BAr^F_3 (220 mg, 0.34 mmol) in 5 mL of CH_2Cl_2 was added dropwise to a 3 mL CH_2Cl_2 solution of IPr•BH_2N_3 (**1**) (137 mg, 0.31 mmol). The mixture was stirred for 1 hr and the solvent was removed under vacuum to yield **3** as a white powder (324 mg, 96 %). X-ray quality crystals were grown from a hexanes/Et_2O mixture at -35 °C. $^1H\{^{11}B\}$ NMR (400 MHz, C_6D_6): δ = 7.85 (s, 6H, *o*-$C_6H_3(CF_3)_2$), 7.68 (s, 3H, *p*-$C_6H_3(CF_3)_2$), 7.26 (t, $^3J_{H-H}$ = 7.6 Hz, 2H, Ar*H* in Dipp), 7.03 (d, $^3J_{H-H}$ = 7.6 Hz, 4H, Ar*H* in Dipp), 6.19 (s, 2H, N-C*H*), 2.38 (br, 2H, B*H*), 2.19 (sept, $^3J_{H-H}$ = 5.6 Hz, 4H, C*H*(CH_3)$_2$), 1.07 (d, $^3J_{H-H}$ = 5.6 Hz, 12H, CH(C*H*$_3$)$_2$), 0.85 (d, $^3J_{H-H}$ = 5.6 Hz, 12H, CH(C*H*$_3$)$_2$). $^{13}C\{^1H\}$ NMR (125 MHz, C_6D_6): δ = 150.8 (br, *ipso*-$C_6H_3(CF_3)_2$), 144.9 (N-*C*H), 133.9 (*o*-$C_6H_3(CF_3)_2$), 132.1 (Ar*C*), 131.7 (Ar*C*), 130.8 (q, $^2J_{C-F}$ = 32.4 Hz, *m*-$C_6H_3(CF_3)_2$), 124.8 (Ar*C*), 124.3 (q, $^1J_{C-F}$ = 272.7 Hz, *C*F$_3$), 123.8 (Ar*C*), 121.1 (br, *p*-$C_6H_3(CF_3)_2$), 28.9 (*C*H(CH_3)$_2$), 25.2

($CH(CH_3)_2$), 22.3 ($CH(CH_3)_2$). $^{11}B\{^1H\}$ NMR (128 MHz, C_6D_6): δ = -15.6 (br, *B*H_2, $\omega_{1/2}$ = 368 Hz). ^{19}F NMR (376 MHz, C_6D_6): δ = -62.5 (s, C*F*$_3$). IR (Nujol, cm^{-1}): 2467 (br, υ_{BH}) and 2134 (m, υ_{N3}). Anal. Calcd. for $C_{51}H_{47}B_2F_{18}N_5$: C, 56.02; H, 4.33; N, 6.40. Found: C, 55.89; H, 4.51; N, 5.93.

Synthesis of IPr•HB=NH•BAr$^F_3$ (4). A solution of IPr•BH_2N_3•BAr$^F_3$ (**3**) (324 mg, 0.30 mmol) in 10 mL of toluene was heated to 80 °C for 12 hrs to give a clear colorless solution. The solvent was then removed under vacuum from the mixture to yield a colorless oil. A 5 mL portion of hexanes was then added to the oil and the mixture was stirred for another 30 minutes. The mother liquor was decanted from the resulting precipitate and the solid was dried under vacuum to afford **4** as a white powder (250 mg, 81 %). Crystals suitable for X-ray diffraction were grown from hexanes/CH_2Cl_2 at -35 °C. $^1H\{^{11}B\}$ NMR (400 MHz, C_6D_6): δ = 7.78 (s, 6H, *o*-$C_6H_3(CF_3)_2$), 7.64 (s, 3H, *p*-$C_6H_3(CF_3)_2$), 7.20 (t, $^3J_{H-H}$ = 7.6 Hz, 2H, Ar*H* in Dipp), 6.93 (d, $^3J_{H-H}$ = 7.9 Hz, 4H, Ar*H* in Dipp), 6.06 (s, 2H, N-C*H*-), 5.44 (d, $^3J_{H-H}$ = 11.6 Hz, 1H, N*H*), 4.00 (br, 1H, B*H*), 2.06 (sept, $^3J_{H-H}$ = 6.8 Hz, 4H, C*H*(CH_3)$_2$), 0.99 (d, $^3J_{H-H}$ = 6.8 Hz, 12H, CH(C*H*$_3$)$_2$), 0.85 (d, $^3J_{H-H}$ = 6.8 Hz, 12H, CH(C*H*$_3$)$_2$). $^{13}C\{^1H\}$ NMR (125 MHz, C_6D_6): δ = 160.0 (br, N-*C*-N), 152.3 (br, *ipso*-$C_6H_3(CF_3)_2$), 144.4 (br, N-*C*H), 133.6 (*o*-$C_6H_3(CF_3)_2$), 132.7 (Ar*C*), 131.1 (Ar*C*), 129.9 (q, $^2J_{C-F}$ = 31.5 Hz, *m*-$C_6H_3(CF_3)_2$), 125.2 (Ar*C*), 125.1 (Ar*C*), 124.9 (q, $^1J_{C-F}$ = 272.5 Hz, *C*F$_3$), 118.9 (*p*-$C_6H_3(CF_3)_2$), 29.2 (*C*H(CH_3)$_2$), 23.9 (CH(*C*H$_3$)$_2$), 23.3 (CH(*C*H$_3$)$_2$). $^{11}B\{^1H\}$ NMR (128 MHz, C_6D_6): δ = 28.5 (br, *B*H, $\omega_{1/2}$ = 178 Hz), -3.9 (s, *B*Ar$^F_3$). ^{19}F NMR (376 MHz, C_6D_6): δ = -62.1 (s, C*F*$_3$). IR (Nujol, cm^{-1}): 3370 (w, υ_{NH}) and 2511 (m, υ_{BH}).

Anal. Calcd. for $C_{51}H_{48}B_2F_{18}N_3$: C, 57.49; H, 4.45; N, 3.94. Found: C, 57.48; H, 4.58; N, 3.79. Mp (°C): 202-205 °C.

Synthesis of IPr•BH$_2$N$_3$* (1-N15). 5 mL of DMSO was added to a mixture of IPr•BH$_2$I (415 mg, 0.78 mmol) and Na[NN^{15}**N**] (62 mg, 0.94 mmol) and stirred for 24 hrs. 80 mL of ethyl acetate was then added to the mixture and the organic layer was washed with water (3 × 50 mL). The organic layer was dried over $MgSO_4$, filtered and the solvent was removed under vacuum to yield **1-N15** as a white powder (250 mg, 72 %). **1-N15** was used as is in subsequent syntheses (> 95 % pure by ^{1}H NMR spectroscopy). ^{1}H and ^{11}B NMR: similar to the values reported for IPr•BH$_2$N$_3$ (**1**).[14]

Synthesis of IPr•BH$_2$N$_3$*•BAr$^F_3$ (3-N15). Compound **3-N15** was synthesized from **1-N15** following the synthetic procedure for compound **3** (see above). A solution of BAr$^F_3$ (169 mg, 0.26 mmol) in 5 mL of CH_2Cl_2 was added dropwise to a 3 mL CH_2Cl_2 solution of **IPr•BH$_2$N$_3$*** (**1-N15**) (105 mg, 0.23 mmol). The mixture was stirred for 1 hr and the solvent was removed under vacuum to yield **3-N15** as a white powder (240 mg, 96 %). ^{1}H{^{11}B}, ^{11}B and ^{19}F NMR: similar to **3**. ^{15}N{^{1}H} NMR (40.5 MHz, C_6D_6): δ = 123.0 (s), 93.5 (s). IR (Nujol, cm^{-1}): 2463 (br, υ_{BH}) and 2129 (m, υ_{N3}).

Synthesis of IPr•HB=N*H•BAr$^F_3$ (4-N15). Compound **4-N15** was synthesized from **3-N15** following the synthetic procedure for compound **4** (see above). A solution of IPr•BH$_2$N$_3$*•BAr$^F_3$ (**3-N15**) (150 mg, 0.14 mmol) in 10 mL of toluene was heated to

80 °C for 12 hrs to get a clear colorless solution. The solvent was removed under vacuum from the mixture to yield a colorless oil. A 5 mL portion of hexanes was then added to the oil and the mixture was stirred for another 30 minutes. The mother liquor was decanted from the resulting precipitate and the solid was dried under vacuum to afford a 1:1 mixture of **4** and IPr•HB=^{15}**N**H•BAr$^{F}_{3}$ as a white powder (120 mg, 84 %). Data for IPr•HB=^{15}**N**H•BAr$^{F}_{3}$: ^{1}H{^{11}B} NMR (400 MHz, C_6D_6): Same as **4** except it shows resonance for ^{15}N-H at δ = 5.44 (dd, $^{1}J_{H\text{-}15N}$ = 69.6 Hz, $^{3}J_{H\text{-}H}$ = 13.2 Hz, 1H, N15-*H*). ^{11}B and ^{9}F NMR: similar to **4**. ^{15}N{^{1}H} NMR (40.5 MHz, C_6D_6): δ = 155.4 (s). IR (Nujol, cm^{-1}): 3360 (w, $\upsilon_{NH\ and\ 15NH}$) and 2507 (m, υ_{BH}).

Synthesis of IPr•BD$_3$. To a solution of IPr (507 mg, 1.3 mmol) in 10 mL of hexanes was added 1.5 mL of THF•BD$_3$ (1.0 M solution in THF). The mixture was stirred for 24 hrs and the solvent was removed under vacuum to yield IPr•BD$_3$ as a white powder (500 mg, 95 %). ^{1}H{^{11}B} NMR: similar to IPr•BH$_3$ with the absence of a B-H resonance.[49] ^{11}B NMR (128 Mz, C_6D_6): δ = -35.8 (s). ^{2}H{^{1}H} NMR (61.4 MHz, C_6H_6): δ = 1.33 (br).

Alternate synthesis of IPr•BD$_3$. 20 mL of diethyl ether was added to a mixture of IPr•SnCl$_4$ (502 mg, 0.77 mmol) and NaBD$_4$ (131 mg, 3.2 mmol). The mixture was stirred for 5 hrs and the filtrate was separated from the black precipitate. The solvent was removed from the filtrate under vacuum to yield IPr•BD$_3$ as a spectroscopically pure white solid (250 mg, 81 %).

Synthesis of IPr•BD_2I. A 10 mL benzene solution containing I_2 (143 mg, 0.56 mmol) was added dropwise to a 10 mL benzene solution of IPr•BD_3 (450 mg, 1.1 mmol), and the mixture was stirred for 4 hrs. The volatiles were removed from the mixture under vacuum to yield IPr•BD_2I as a yellow powder (580 mg, 98 %). $^1H\{^{11}B\}$ NMR: similar to IPr•BH_2I with the absence of a B-H resonance.[14] ^{11}B NMR (128 Mz, C_6D_6): δ = -32.8 (br, $\omega_{1/2}$ = 319 Hz). $^2H\{^1H\}$ NMR (61.4 MHz, C_6H_6): δ = 2.49 (br).

IPr•BD_2N_3 (1-d). 5 mL of DMSO was added to a mixture of IPr•BD_2I (540 mg, 1.00 mmol) and NaN_3 (80 mg, 1.2 mmol) and stirred for 24 hrs. 100 mL of ethyl acetate was added to the mixture and the organic layer was washed with water (3 × 70 mL). The organic layer was dried over $MgSO_4$, filtered and the solvent was removed under vacuum to yield **1-d** as a white solid (310 mg, 70 %). **1-d** was used as is in subsequent syntheses (*ca.* 95 % pure by ^1H NMR spectroscopy). $^1H\{^{11}B\}$ NMR: similar to IPr•BH_2N_3 (**1**) with the absence of a B-H resonance.[14] ^{11}B NMR (128 Mz, $CDCl_3$): δ = 17.4 (s). $^2H\{^1H\}$ NMR (61.4 MHz, $CHCl_3$): δ = 2.29 (br).

Synthesis of IPr•BD_2N_3•BAr^F_3 (3-d). Compound **3-d** was synthesized from **1-d** following the synthetic procedure for compound **3** (see above). A solution of BAr^F_3 (127 mg, 0.20 mmol) in 5 mL of CH_2Cl_2 was added dropwise to a 3 mL CH_2Cl_2 solution of IPr•BD_2N_3 (**1-d**) (80 mg, 0.17 mmol). The mixture was stirred for 1 hr and the solvent was removed under vacuum to yield **3-d** as a white powder (170 mg, 92 %). $^1H\{^{11}B\}$: similar to **3** with the absence of a B-H resonance. ^{11}B NMR: similar to

3. $^{2}H\{^{1}H\}$ NMR (61.4 MHz, C_6H_6): δ = 2.35 (br). IR (Nujol, cm^{-1}): 2138 (m, υ_{N3}) and 1856 (m, υ_{BD}).

Synthesis of IPr•DB=ND•BAr$^{F}_{3}$ (4-d). Compound **4-d** was synthesized following the synthetic procedure for compound **4** (see above). A solution of IPr•BD_2N_3•BAr$^{F}_{3}$ (**3-d**) (80 mg, 0.073 mmol) in 5 mL of toluene was heated to 80 °C for 12 hrs to give a colorless solution. The volatiles were removed under vacuum to yield a colorless oil. A 3 mL portion of hexanes was then added to the oil and the mixture was stirred for another 30 minutes. The mother liquor was decanted from the resulting precipitate and the solid was dried under vacuum to afford **4-d** as a white powder (50 mg, 70 %). $^{1}H\{^{11}B\}$ NMR: similar to **4** with the absence of B-H and N-H resonances. ^{11}B NMR: similar to **4**. $^{2}H\{^{1}H\}$ NMR (61.4 MHz, C_6H_6): δ = 5.44 (br, N-D), 4.00 (br, B-D). IR (Nujol, cm^{-1}): 2495 (w, υ_{ND}) and 1900 (m, υ_{BD}).

ImMe$_2$^{i}Pr$_2$•BH$_2$I (5). A solution of I_2 (718 mg, 2.83 mmol) in 10 mL of benzene was added dropwise to a 15 mL benzene solution of ImMe$_2$^{i}Pr$_2$•BH_3 (1.09 g, 5.61 mmol), and the mixture was stirred for 2 hrs. The volatiles were removed from the mixture under vacuum to yield ImMe$_2$^{i}Pr$_2$•BH$_2$I as a yellow powder (1.61 g, 90 %). $^{1}H\{^{11}B\}$ NMR (400 MHz, C_6D_6): δ = 5.43 (br, 2H, C*H*$(CH_3)_2$), 3.27 (br, 2H, B*H*), 1.45 (s, 6H, Im-C*H*$_3$), 1.10 (d, $^{3}J_{HH}$ = 6.4 Hz, 12H, CH(C*H*$_3$)$_2$). $^{13}C\{^{1}H\}$ NMR (125 MHz, C_6D_6): δ = 124.8 (N-*C*-CH_3), 50.5 (*C*H$(CH_3)_2$), 20.8 (CH(*C*H$_3$)$_2$), 9.7 (Im-*C*H$_3$). ^{11}B NMR (128 MHz, C_6D_6): δ = -30.1 (br). Anal. Calcd. for $C_{11}H_{22}BIN_2$: C, 41.28; H, 6.93; N, 8.75. Found: C, 41.30; H, 6.89; N, 8.49. Mp (°C): 185-190.

$ImMe_2{}^iPr_2{\bullet}BH_2N_3$ (6). 5 mL of DMSO was added to a mixture of $ImMe_2{}^iPr_2{\bullet}BH_2I$ (**5**) (2.05 g, 6.41 mmol) and NaN_3 (500 mg, 7.69 mmol) followed by stirring for 24 hrs. 100 mL of ethyl acetate was then added to the mixture and the organic layer was washed with water (3 × 70 mL). The organic layer was dried over $MgSO_4$, filtered and the solvent was removed under vacuum to yield **6** as a white solid (1.02 g, 68 %). The product was further purified by crystallization from Et_2O/hexanes at -35 °C. $^1H\{^{11}B\}$ NMR (400 MHz, C_6D_6): δ = 5.34 (br, 2H, C*H*$(CH_3)_2$), 3.47 (br, 2H, B*H*), 1.46 (s, 6H, Im-C*H*$_3$), 1.09 (d, $^3J_{HH}$ = 7.2 Hz, 12H, CH(C*H*$_3$)$_2$). $^{13}C\{^1H\}$ NMR (125 MHz, C_6D_6): δ = 162.7 (br, N-*C*-N), 124.5 (N-*C*-CH_3), 50.4 (*C*H$(CH_3)_2$), 21.4 (CH(*C*H$_3$)$_2$), 9.7 (Im-*C*H$_3$). ^{11}B NMR (160 MHz, C_6D_6): δ = -16.9 (t, $^1J_{BH}$ = 98.0 Hz). IR (Nujol, cm^{-1}): 2324 (w, υ_{BH}), 2118 (m, υ_{N3}), 2085 (s, υ_{N3}). HR-MS (EI) $(C_{11}H_{22}BN_5)^+$: m/z: Calcd: 235.1968; Found: 235.1967 (Δ ppm = 0.7). Anal. calcd. for $C_{11}H_{22}BN_5$: C, 56.19; H, 9.43; N, 29.78. Found: C, 56.63; H, 9.54; N, 29.25. Mp (°C): 90-94.

$ImMe_2{}^iPr_2{\bullet}HB{=}NH{\bullet}BAr^F{}_3$ (7). A solution of $BAr^F{}_3$ (440 mg, 0.68 mmol) in 5 mL CH_2Cl_2 was added dropwise to a 3 mL CH_2Cl_2 solution of $ImMe_2{}^iPr_2{\bullet}BH_2N_3$ (**6**) (159 mg, 0.68 mmol). The mixture was stirred for 1 hr and the volatiles were removed under vacuum. The product was then dissolved in 10 mL of toluene and heated to 80 °C for 12 hrs to give a colorless solution. The solvent was removed under vacuum to yield a colorless oil. A 3 mL portion of Et_2O was then added to the oil and the resulting mixture was layered with 3 mL of hexanes to precipitate out a white solid.

The mother liquor was decanted from the resulting precipitate and the solid was dried under vacuum to afford **7** as a white powder (374 mg, 64 %). Crystals suitable for X-ray diffraction were grown from hexanes/CH_2Cl_2 at -35 °C. $^1H\{^{11}B\}$ NMR (400 MHz, C_6D_6): δ = 8.19 (s, 6H, *o*-$C_6H_3(CF_3)_2$), 7.79 (s, 3H, *p*-$C_6H_3(CF_3)_2$), 5.42 (d, $^3J_{HH}$ = 10.0 Hz, 1H, N*H*), 4.62 (br, 1H, B*H*), 3.75 (sept, $^3J_{HH}$ = 6.9 Hz, 2H, C*H*$(CH_3)_2$), 1.12 (s, 6H, Im-CH_3), 0.79 (d, $^3J_{HH}$ = 6.8 Hz, 12H, CH(CH_3)$_2$). $^{13}C\{^1H\}$ NMR (125 MHz, C_6D_6): δ = 159.8 (br, N-*C*-N), 133.9 (*o*-$C_6H_3(CF_3)_2$), 130.4 (q, $^2J_{CF}$ = 31.8 Hz, *m*-$C_6H_3(CF_3)_2$), 125.6 (N-*C*-CH_3), 125.1 (q, $^1J_{CF}$ = 272.6 Hz, *C*F_3), 119.2 (*p*-$C_6H_3(CF_3)_2$), 51.6 (*C*H$(CH_3)_2$), 21.5 (CH(*C*H_3)$_2$), 8.6 (Im-*C*H_3). $^{11}B\{^1H\}$ NMR (128 MHz, C_6D_6): δ = 32.6 (br, *B*H), -3.9 (s, *B*$Ar^F{}_3$). ^{19}F NMR (376 MHz, C_6D_6): δ = -62.3 (s, C*F*$_3$). IR (Nujol, cm^{-1}): 3367 (w, υ_{NH}), 2489 (w, υ_{BH}). Anal. Calcd. for $C_{35}H_{31}B_2F_{18}N_3$: C, 49.04; H, 3.65; N, 4.90. Found: C, 48.63; H, 4.03; N, 4.45. Mp (°C): 142-146.

ImMe$_2$^{i}Pr$_2$•H(Cl)B-NH$_2$•BAr$^F{}_3$ (8). To a 5 mL Et_2O solution of ImMe$_2$^{i}Pr$_2$•HB=NH•BAr$^F{}_3$ (**7**) (205 mg, 0.24 mmol) was added HCl (1.6 mL, 0.2 M solution in Et_2O, 0.3 mmol) and the mixture was stirred for 2 hrs. The solvent was removed from the mixture under vacuum to yield a white powder. The product (**8**) was further purified by crystallization from Et_2O/ hexanes at -35 °C (128 mg, 60 %). $^1H\{^{11}B\}$ NMR (500 MHz, C_6D_6): δ = 7.83 (s, 6H, *o*-$C_6H_3(CF_3)_2$), 7.66 (s, 3H, *p*-$C_6H_3(CF_3)_2$), 4.53 (br, 2H, C*H*$(CH_3)_2$), 3.75 (br, 1H, B*H*), 3.61 (d, $^3J_{HH}$ = 13.0 Hz, 1H, N*H*), 3.40 (br, 1H, N*H*), 1.36 (s, 6H, Im-CH_3), 0.69 (br, 12H, CH(CH_3)$_2$). $^{13}C\{^1H\}$ NMR (125 MHz, C_6D_6): δ = 154.1 (br, N-*C*-N), 133.4 (*o*-$C_6H_3(CF_3)_2$), 130.9

(q, $^2J_{CF}$ = 32.1 Hz, *m*-$C_6H_3(CF_3)_2$), 124.5 (q, $^1J_{CF}$ = 272.9 Hz, CF_3), 120.4 (*p*-$C_6H_3(CF_3)_2$), 51.3 ($CH(CH_3)_2$), 20.5 ($CH(CH_3)_2$), 9.6 (Im-CH_3). $^{11}B\{^1H\}$ NMR (128 MHz, C_6D_6): δ = -3.7 (s, $BAr^F{}_3$), -9.5 (br, *B*HCl). ^{19}F NMR (376 MHz, C_6D_6): δ = -62.6 (s, CF_3). Anal. Calcd. for $C_{35}H_{32}B_2ClF_{18}N_3$: C, 47.04; H, 3.61; N, 4.70. Found: C, 47.03; H, 3.69; N, 4.68. Mp (°C): 117-121.

$ImMe_2{}^iPr_2$•H_2B-NH_2•$BAr^F{}_3$ (9). To a 5 mL Et_2O solution of $ImMe_2{}^iPr_2$•HB=NH•$BAr^F{}_3$ (**7**) (131 mg, 0.15 mmol) was added Me_2NH•BH_3 (9 mg, 0.2 mmol) and the mixture was stirred for 12 hrs. The solvent was removed from the mixture under vacuum and the remaining residue washed three times with hexanes (3 × 5 mL). The product was then dried under vacuum to yield **9** as a white solid. Crystals suitable for X-ray diffraction were grown from hexanes/CH_2Cl_2 at -35 °C (110 mg, 85 %). $^1H\{^{11}B\}$ NMR (400 MHz, C_6D_6): δ = 7.98 (s, 6H, *o*-$C_6H_3(CF_3)_2$), 7.72 (s, 3H, *p*-$C_6H_3(CF_3)_2$), 4.41 (br, 2H, $CH(CH_3)_2$), 2.43 (br, 2H, N*H*), 2.29 (br, 2H, B*H*), 1.34 (s, 6H, Im-CH_3), 0.73 (d, $^3J_{HH}$ = 6.8 Hz, 12H, $CH(CH_3)_2$). $^{13}C\{^1H\}$ NMR (125 MHz, C_6D_6): δ = 160.5 (br, N-*C*-N), 155.4 (br, *ipso*-$C_6H_3(CF_3)_2$), 133.6 (*o*-$C_6H_3(CF_3)_2$), 130.7 (q, $^2J_{CF}$ = 32.1 Hz, *m*-$C_6H_3(CF_3)_2$), 125.4 (N-*C*-CH_3), 124.4 (q, $^1J_{CF}$ = 272.2 Hz, CF_3), 120.0 (*p*-$C_6H_3(CF_3)_2$), 50.7 ($CH(CH_3)_2$), 20.7 ($CH(CH_3)_2$), 9.5 (Im-CH_3). $^{11}B\{^1H\}$ NMR (128 MHz, C_6D_6): δ = -3.9 (s, $BAr^F{}_3$), -21.6 (br, BH_2). ^{19}F NMR (376 MHz, C_6D_6): δ = -62.5 (s, CF_3). Anal. Calcd. for $C_{35}H_{33}B_2F_{18}N_3$: C, 48.92; H, 3.87; N, 4.89. Found: C, 48.24; H, 3.83; N, 4.89. Mp (°C): 175-179.

To identify the amine-borane by-product a similar reaction was performed by combining $ImMe_2{}^iPr_2$•HB=NH•$BAr^F{}_3$ (**7**) (52 mg, 0.06 mmol) and Me_2NH•BH_3 (4

mg, 0.06 mmol) in 5 mL of C_6D_6. The identified dimethyl amine-borane by-products by ^{11}B NMR spectroscopy were $[Me_2N\text{-}BH_2]_2$ (84 %)[50] and $Me_2NH\text{-}BH_2\text{-}NMe_2\text{-}BH_3$ (14 %).[50]

$ImMe_2{}^iPr_2$•H_2B-N(D)H•$BAr^F{}_3$ (9-d). To a 5 mL Et_2O solution of $ImMe_2{}^iPr_2$•HB=NH•$BAr^F{}_3$ (**7**) (191 mg, 0.2 mmol) was added Me_2ND•BH_3 (13 mg, 0.2 mmol) and the mixture was stirred for 12 hrs. The solvent was removed from the mixture under vacuum and the remaining residue was washed three times with hexanes (3 × 5 mL). The product was then dried under vacuum to yield **9-d** as a white solid (120 mg, 70 %). $^1H\{^{11}B\}$ NMR: similar to **9** except the signal at 2.43 (br) ppm, which integrates as one N-*H* proton. ^{11}B NMR: similar to **9**. $^2H\{^1H\}$ NMR (61.4 MHz, C_6H_6): δ = 2.36 (br, ND).

$[ImMe_2{}^iPr_2]_2$•HB-NH•$BAr^F{}_3$ (10). A solution of $ImMe_2{}^iPr_2$ (28 mg, 0.16 mmol) in 5 mL of Et_2O was added dropwise to a 5 mL Et_2O solution of $ImMe_2{}^iPr_2$•HB=NH•$BAr^F{}_3$ (**7**) (130 mg, 0.15 mmol). The mixture was stirred for 12 hrs and the solvent was removed under vacuum to yield **10** as a light yellow powder (155 mg, 88 %). Crystals suitable for X-ray diffraction were grown from hexanes/CH_2Cl_2 at -35 °C. $^1H\{^{11}B\}$ NMR (400 MHz, C_6D_6): δ = 8.17 (br, 6H, *o*-$C_6H_3(CF_3)_2$), 7.77 (br, 3H, *p*-$C_6H_3(CF_3)_2$), 5.52 (br, 2H, N*H*), 3.80 (br, 2H, C*H*$(CH_3)_2$), 0.60-1.70 (br, 36H, Im-CH_3 and CH(CH_3)$_2$). $^{13}C\{^1H\}$ NMR spectrum was not obtained due to the low solubility and dynamic behavior in solution. $^{11}B\{^1H\}$ NMR (128 MHz, C_6D_6): δ = -3.6 (s, *B*$Ar^F{}_3$), -14.3 (br, *B*H). $^{19}F\{^1H\}$ NMR (376

MHz, C_6D_6): δ = -62.3 to -62.0 (m, C*F*$_3$). Anal. Calcd. for $C_{46}H_{51}B_2F_{18}N_5$: C, 53.25; H, 4.95; N, 6.75. Found: C, 52.84; H, 4.88; N, 6.41. Mp (°C): 147-151.

Reaction of [ImMe$_2$^{i}Pr$_2$]$_2$•HB-NH•BAr^F$_3$ (10) with Me$_2$S•BH$_3$. To a solution of [ImMe$_2$^{i}Pr$_2$]$_2$•HB-NH•BAr^F$_3$ (**10**) (76 mg, 0.07 mmol) in 10 mL of Et_2O was added 37 μL of Me_2S•BH_3 (2.0 M solution in THF). The mixture was stirred for 12 hrs and the solvent was removed under vacuum to yield a white powder. ^{1}H{^{11}B} and ^{11}B NMR confirmed the presence of ImMe$_2$^{i}Pr$_2$•BH$_3$[27] and ImMe$_2$^{i}Pr$_2$•HB=NH•BAr^F$_3$ (**7**).

IPr•BH(OTf)N$_3$ (11). A 5 mL CH_2Cl_2 solution of Ph_3COTf (224 mg, 0.56 mmol) was added dropwise to a 10 mL CH_2Cl_2 solution of IPr•BH_2N_3 (**1**) (253 mg, 0.56 mmol), and the mixture was stirred for 1 hrs. The volatiles were removed from the mixture under vacuum and the product was washed with hexanes (3 × 5 mL). The residue was then dried under vacuum to give **11** as yellow solid (323 mg, 95 %). Crystals suitable for X-ray diffraction were grown from fluorobenzene/hexanes at -35 °C. ^{1}H{^{11}B} (400 MHz, C_6D_6): δ = 7.22 (t, $^3J_{HH}$ = 8.0 Hz, 2H, Ar*H*), 7.05-7.07 (m, 4H, Ar*H*), 6.29 (s, 2H, N-C*H*), 3.94 (br, 1H, B*H*), 2.53 (sept, $^3J_{HH}$ = 7.0 Hz, 2H, C*H*(CH$_3$)$_2$), 2.48 (sept, $^3J_{HH}$ = 7.0 Hz, 2H, C*H*(CH$_3$)$_2$), 1.38 (d, $^3J_{HH}$ = 10.0 Hz, 6H, CH(C*H*$_3$)$_2$), 1.36 (d, $^3J_{HH}$ = 10.0 Hz, 6H, CH(C*H*$_3$)$_2$), 0.95 (d, $^3J_{HH}$ = 7.0 Hz, 12H, CH(C*H*$_3$)$_2$). ^{13}C{^{1}H} NMR (125 MHz, C_6D_6): δ = 145.1 (N-*C*H), 145.0 (N-*C*H), 132.7 (Ar*C*), 131.4 (Ar*C*), 124.6 (Ar*C*), 124.5 (Ar*C*), 124.1 (Ar*C*), 119.6 (q, $^1J_{C\text{-}F}$ = 318.9 Hz, *C*F$_3$), 29.4 (*C*H(CH$_3$)$_2$), 29.3 (*C*H(CH$_3$)$_2$), 25.6 (CH(*C*H$_3$)$_2$), 25.4 (CH(*C*H$_3$)$_2$), 22.5 (CH(*C*H$_3$)$_2$), 22.4 (CH(*C*H$_3$)$_2$). ^{11}B NMR (128 MHz, C_6D_6): δ = -

2.0 (br). ^{19}F NMR (376 MHz, C_6D_6): δ = -76.9 (s, C*F*$_3$). IR (Nujol, cm^{-1}): 2462 (m, υ_{BH}), 2201 (w, υ_{N3}), 2117 (s, υ_{N3}). Anal. Calcd. for $C_{28}H_{37}BF_3N_5O_3S$: C, 56.86; H, 6.31; N, 11.84; S, 5.42. Found: C, 56.37; H, 6.22; N, 10.82; S, 5.06. Mp (°C): >195.

ImMe$_2$^{i}Pr$_2$•BH(OTf)N$_3$ (12). A 5 mL CH_2Cl_2 solution of Ph_3COTf (369 mg, 0.94 mmol) was added dropwise to a 10 mL CH_2Cl_2 solution of ImMe$_2$^{i}Pr$_2$•BH$_2$N$_3$ (**6**) (220 mg, 0.94 mmol), and the mixture was stirred for 1 hr. The volatiles were removed from the mixture under vacuum and the product was washed with hexanes (3 × 5 mL). The residue was then dried under vacuum to afford **12** as white powder (237 mg, 66 %). Crystals suitable for X-ray diffraction were grown from hexanes/CH_2Cl_2 at -35 °C. ^{1}H{^{11}B} NMR (400 MHz, C_6D_6): δ = 5.12 (br, 2H, C*H*(CH$_3$)$_2$), 4.56 (br, 1H, B*H*), 1.31 (s, 6H, Im-C*H*$_3$), 1.00 (br, 12H, CH(C*H*$_3$)$_2$). ^{13}C{^{1}H} NMR (125 MHz, C_6D_6): δ = 125.9 (N-*C*-CH$_3$), 50.9 (*C*H(CH$_3$)$_2$), 21.1 (CH(*C*H$_3$)$_2$), 9.6 (Im-*C*H$_3$), *C*F$_3$ and ^{Im}*C*-B resonances could not be located. ^{11}B NMR (128 MHz, C_6D_6): δ = -1.6 (br). ^{19}F NMR (376 MHz, C_6D_6): δ = -76.3 (s, OTf). IR (Nujol, cm^{-1}): 2478 (m, υ_{BH}), 2116 (s, υ_{N3}). Anal. Calcd. for $C_{12}H_{21}BF_3N_5O_3S$: C, 37.61; H, 5.52; N, 18.28; S, 8.37. Found: C, 37.01; H, 5.45; N, 15.91; S, 8.88. Mp (°C): 74-77. Despite repeated attempts, analyses for N content were always low.

Reaction of IPr•BH$_2$N$_3$ (1) with R$_3$SiOTf (R = Me or Ph). A 5 mL of CH_2Cl_2 solution of Ph_3SiOTf (33 mg, 0.08 mmol) or Me_3SiOTf (22 μL, 0.12 mmol) was dropwise added to a 5 mL CH_2Cl_2 solution of IPr•BH$_2$N$_3$ (**1**) (35 mg, 0.08 mmol) or (54 mg, 0.12 mmol) and stirred for 12 hrs. The volatiles were removed under vacuum

to yield a white solid. Upon washing with hexanes (3 × 5 mL) and dried under vacuum afforded IPr•BH_2OTf as a white powder (27 mg, 61 %) or (60 mg, 90 %). The $^1H\{^{11}B\}$, ^{11}B and ^{19}F NMR in spectra in $CDCl_3$ confirmed the product as IPr•BH_2OTf.[14] Also $^{13}C\{^1H\}$ NMR analysis of the hexanes soluble fraction (with Ph_3SiOTf as a reagent) confirmed the presence of Ph_3SiN_3.[51]

[IPr(ImMe$_2$^{i}Pr$_2$)•BH(N$_3$)](OTf) (13). A solution of ImMe$_2$^{i}Pr$_2$ (57 mg, 0.32 mmol) and IPr•BH(OTf)N_3 (**11**) (186 mg, 0.31 mmol) in 10 mL of toluene was heated at 80 °C for 12 hrs to give a white slurry. The resulting precipitate was separated from the mother liquor and dried under vacuum to give **13** as a white powder. The product was further purified by washing with 10 mL of fluorobenzene (168 mg, 68 %). $^1H\{^{11}B\}$ (400 MHz, $CDCl_3$): δ = 7.56 (t, $^3J_{HH}$ = 8.0 Hz, 2H, Ar*H*), 7.45 (s, 2H, N-C*H*), 7.38 (d, 2H, $^3J_{HH}$ = 7.6 Hz, Ar*H*), 7.28 (d, 2H, $^3J_{HH}$ = 7.2 Hz, Ar*H*), 4.49 (sept, $^3J_{HH}$ = 7.2 Hz, 1H, C*H*(CH_3)$_2$), 4.23 (sept, $^3J_{HH}$ = 6.8 Hz, 1H, C*H*(CH_3)$_2$), 3.69 (br, 1H, B*H*), 2.40-2.55 (m, 4H, C*H*(CH_3)$_2$), 2.28 (s, 3H, Im-C*H*$_3$), 2.13 (s, 3H, Im-C*H*$_3$), 1.47 (d, $^3J_{HH}$ = 7.2 Hz, 3H, CH(C*H*$_3$)$_2$), 1.40 (d, $^3J_{HH}$ = 7.0 Hz, 6H, CH(C*H*$_3$)$_2$), 1.37 (d, $^3J_{HH}$ = 7.0 Hz, 3H, CH(C*H*$_3$)$_2$), 1.18-1.24 (m, 9H, CH(C*H*$_3$)$_2$), 1.09 (d, $^3J_{HH}$ = 7.0 Hz, 12H, CH(C*H*$_3$)$_2$), 0.81 (d, $^3J_{HH}$ = 7.2 Hz, 3H, CH(C*H*$_3$)$_2$). $^{13}C\{^1H\}$ NMR (125 MHz, $CDCl_3$): δ = 145.1 (N-*C*H), 145.0 (br, C_{NHC}-B), 133.2 (Ar*C*), 131.9 (Ar*C*), 127.6 (Ar*C*), 127.4 (Ar*C*), 127.1 (Ar*C*), 125.0 (N-*C*-CH_3, 124.6 (N-*C*-CH_3), 121.1 (q, $^1J_{C\text{-}F}$ = 321.3 Hz, *C*F_3), 52.3 (*C*H(CH_3)$_2$), 51.6 (*C*H(CH_3)$_2$), 29.3 (*C*H(CH_3)$_2^{IPr}$), 29.1 (*C*H(CH_3)$_2^{IPr}$), 26.5 (CH(*C*H$_3$)$_2^{IPr}$), 25.9 (CH(*C*H$_3$)$_2^{IPr}$), 23.3 (*C*H(CH_3)$_2$), 22.9 (*C*H(CH_3)$_2^{IPr}$), 22.0 (*C*H(CH_3)$_2^{IPr}$), 20.1 (*C*H(CH_3)$_2$), 11.1 (Im-*C*H$_3$), 10.9 (Im-*C*H$_3$).

$^{11}B\{^1H\}$ NMR (128 MHz, $CDCl_3$): δ = -14.3 (br, *B*H). ^{19}F NMR (376 MHz, $CDCl_3$): δ = -78.1 (s, C*F*$_3$). IR (Nujol, cm^{-1}): 2400 (w, υ_{BH}), 2186 (w, υ_{N3}), 2107 (s, υ_{N3}). HR-MS (ESI) $(C_{37}H_{57}BN_7)^+$: m/z: Calcd: 622.4763; Found: 622.4756 (Δ ppm = 1.2). Anal. Calcd. for $C_{39}H_{57}BF_3N_7O_3S$: C, 60.69; H, 7.44; N, 12.70; S, 4.15. Found: C, 59.50; H, 7.01; N, 11.33; S, 4.10. Mp (°C): >195. Despite repeated attempts, analyses for C and N content were always low.

[(ImMe$_2$^{i}Pr$_2$)$_2$•BH(N$_3$)](OTf) (14). A solution of ImMe$_2$^{i}Pr$_2$ (85 mg, 0.47 mmol) and ImMe$_2$^{i}Pr$_2$•BH(OTf)N$_3$ (**12**) (179 mg, 0.47 mmol) in 10 mL of toluene was heated at 80 °C for 12 hrs. The solvent was removed under from mixture vacuum and the residue was washed with Et_2O (3 × 5 mL). The product was then dried under vacuum to yield a white solid (195 g, 74 %). $^1H\{^{11}B\}$ NMR (500 MHz, $CDCl_3$): δ = 5.05 (br, 4H, C*H*$(CH_3)_2$), 3.92 (s, 1H, B*H*), 2.34 (s, 12H, Im-C*H*$_3$), 1.45 (d, $^3J_{HH}$ = 7.0 Hz, 12H, CH(C*H*$_3$)$_2$), 1.43 (d, $^3J_{HH}$ = 7.2 Hz, 12H, CH(C*H*$_3$)$_2$). $^{13}C\{^1H\}$ NMR (125 MHz, $CDCl_3$): δ = 127.6 (N-*C*-CH$_3$), 50.8 (*C*H(CH$_3$)$_2$), 21.5 (CH(*C*H$_3$)$_2$), 21.3 (CH(*C*H$_3$)$_2$), 10.9 (Im-*C*H$_3$), CF$_3$ group was not located. ^{11}B NMR (128 MHz, $CDCl_3$): δ = -14.5 (d, $^1J_{B\text{-}H}$ = 94.5 Hz). ^{19}F NMR (376 MHz, $CDCl_3$): δ = -78.1 (s, OTf). IR (Nujol, cm^{-1}): 2379 (m, υ_{BH}), 2105 (s, υ_{N3}). HR-MS (ESI) $(C_{22}H_{41}BN_7)^+$: m/z: Calcd: 414.3511; Found: 414.3514 (Δ ppm = 0.8). Anal. Calcd. for $C_{23}H_{41}BF_7N_7O_3S$: C, 49.03; H, 7.33; N, 17.40, S, 5.69. Found: C, 49.02; H, 7.20; N, 16.42; S, 5.78. Mp (°C): 97-101. Despite repeated attempts, analyses for N content were always low.

[(ImMe$_2$^{i}Pr$_2$)$_2$•BH(N$_3$)]BAr^F$_4$ (15). [(ImMe$_2$^{i}Pr$_2$)$_2$•BH(N$_3$)](OTf) (**14**) (87 mg, 0.15 mmol) and NaBAr^F$_4$ (137 mg, 0.15 mmol) were combined in 10 mL of Et$_2$O. The mixture was stirred for 2 hrs and filtered. The volatiles were removed from the filtrate under vacuum to yield a white solid as **15** (173 mg, 87 %). Crystals suitable for X-ray diffraction were grown from hexanes/CH$_2$Cl$_2$ at -35 °C (110 mg, 85 %). ^{1}H{^{11}B} NMR (500 MHz, CDCl$_3$): δ = 7.68 (s, 8H, *o*-C$_6$*H*$_3$(CF$_3$)$_2$), 7.52 (s, 4H, *p*-C$_6$*H*$_3$(CF$_3$)$_2$), 5.04 (br, 4H, C*H*(CH$_3$)$_2$), 3.90 (s, 1H, B*H*), 2.22 (s, 12H, Im-C*H*$_3$), 1.37 (d, $^3J_{HH}$ = 7.0 Hz, 12H, CH(C*H*$_3$)$_2$), 1.36 (d, $^3J_{HH}$ = 7.5 Hz, 12H, CH(C*H*$_3$)$_2$). ^{13}C{^{1}H} NMR (125 MHz, CDCl$_3$): δ = 161.8 (q, $^1J_{BC}$ = 49.8 Hz, B-*C*$_6$H$_3$(CF$_3$)$_2$), 134.9 (*o*-*C*$_6$H$_3$(CF$_3$)$_2$), 129.0 (q, $^2J_{CF}$ = 32.2 Hz, *m*-*C*$_6$H$_3$(CF$_3$)$_2$), 127.4 (N-*C*-CH$_3$), 124.7 (q, $^1J_{CF}$ = 272.5 Hz, *C*F$_3$), 117.6 (*p*-*C*$_6$H$_3$(CF$_3$)$_2$), 50.7 (*C*H(CH$_3$)$_2$), 21.2 (CH(*C*H$_3$)$_2$), 21.1 (CH(*C*H$_3$)$_2$), 10.6 (Im-*C*H$_3$). ^{11}B NMR (128 MHz, CDCl$_3$): δ = -6.6 (s, *B*Ar^F$_4$), -14.6 (d, $^1J_{BH}$ = 92.9 Hz). ^{19}F NMR (376 MHz, CDCl$_3$): δ = -62.4 (s, C*F*$_3$). IR (Nujol, cm^{-1}): 2384 (m, υ_{BH}), 2193 (w, υ_{N3}), 2110 (s, υ_{N3}). HR-MS (ESI) (C$_{22}$H$_{41}$BN$_7$)$^+$: m/z: Calcd: 414.3511; Found: 414.3507 (Δ ppm = 0.9). Anal. Calcd. for C$_{54}$H$_{53}$B$_2$F$_{24}$N$_7$: C, 50.76; H, 4.18; N, 7.67. Found: C, 50.95; H, 4.19; N, 6.67. Mp (°C): 130-134. Despite repeated attempts, analyses for N content were always low.

Reduction of ImMe$_2$^{i}Pr$_2$•BH(N$_3$)OTf (12) with K. ImMe$_2$^{i}Pr$_2$•BH(N$_3$)OTf (**12**) (450 mg, 1.1 mmol) was combined with K (215 mg, 5.3 mmol) in 20 mL of toluene and the mixture was stirred for 24 hrs. The solution was separated from the precipitate by filtration. The volatiles were removed under vacuum from the filtrate to afford a white solid. The ^{1}H NMR spectrum of the resulting toluene soluble solid revealed the

presence of free $ImMe_2{}^iPr_2$ (>90 %) with some other minor unidentified products. The IR spectrum of the insoluble fraction was consistent with the formation of K[OTf] and $K[N_3]$ (Figure 4.19).

Reduction of $ImMe_2{}^iPr_2$•BH(N_3)OTf (12) with KC_8. $ImMe_2{}^iPr_2$•BH(N_3)OTf (**12**) (131 mg, 0.34 mmol) was combined with KC_8 (92 mg, 0.68 mmol) in 10 mL of toluene. The mixture was stirred for 24 hrs and filtered. All the volatiles were removed under vacuum from the filtrate to give a white solid. The ^1H and ^{11}B NMR spectra of the resulting solid indicated the formation of $ImMe_2{}^iPr_2$ (44 %), $ImMe_2{}^iPr_2$•BH_2N_3 (20 %), $ImMe_2{}^iPr_2$•BH_3 (13 %) with some other minor unidentified products (*ca.* 23 %). The IR spectrum of the insoluble part showed the formation of K[OTf] and $K[N_3]$ (Figure 4.20).

4.5 Crystallographic Data

Table 4.1: Crystallographic data for **2** and **3**.

Compound	**2**	**3**
Formula	$C_{29}H_{41}BF_3N_3O_3S$	$C_{51}H_{47}B_2F_{18}N_5$
Formula weight	579.52	1093.55
Crystal system	monoclinic	monoclinic
Space group	$P2_1/n$ (No. 14)	$P2_1/c$
a (Å)	9.1416(2)	21.9870(5)
b (Å)	19.2202(4)	11.9409(3)
c (Å)	36.1690(8)	20.9899(4)
α (deg)	90	90
β (deg)	90.1284(16)	105.4316(10)
γ (deg)	90	90
V(Å^3)	6355.0(2)	5312.1(2)
Z	8	4
ρ (g/cm^3)	1.211	1.367
abs coeff (mm^{-1})	1.331	1.094
T (K)	173(1)	173(1)
$2\theta_{max}$ (°)	139.00	148.37
total data	42037	37286
unique data(R_{int})	11914 (0.1034)	10752(0.0338)
Obs data [I>2($\sigma(I)$]	8692	9432
Params	741	693
R_1 [$I>2\sigma(I)$]^a	0.0613	0.0542
wR_2 [all data]^a	0.1755	0.1496
max/min $\Delta\rho$ (e$^-$ Å^{-3})	0.562/-0.543	0.592/-0.411

^{a} $R_1 = \sum||F_o| - |F_c||/\sum|F_o|$; $wR_2 = [\sum w(F_o^2 - F_c^2)^2/\sum w(F_o^4)]^{1/2}$

Table 4.2: Crystallographic data for **4** and **7**.

Compound	**4**	**7**•0.5 toluene
Formula	$C_{51}H_{47}B_2F_{18}N_3$	$C_{38.50}H_{35}B_2F_{18}N_3$
Formula weight	1065.53	903.31
Crystal system	triclinic	monoclinic
Space group	$P\bar{1}$ *(No. 2)*	$P2_1/n$ (No. 14)
a (Å)	12.3716(4)	12.2423(2)
b (Å)	12.5289(4)	22.6420(4)
c (Å)	18.9781(6)	14.6138(2)
α (deg)	83.5864(4)	90
β (deg)	86.5835(3)	92.7542(11)
γ (deg)	63.4884(3)	90
V(Å^3)	2615.69(14)	4046.12 (11)
Z	2	4
ρ (g/cm^3)	1.353	1.483
abs coeff (mm^{-1})	0.123	1.290
T (K)	173(1)	173(1)
$2\theta_{max}$ (°)	56.57	148.69
total data	24418	28779
unique data(R_{int})	12615(0.0122)	8210(0.0306)
Obs data [I>2($\sigma(I)$)]	10273	6089
Params	710	653
R_1 [I>2$\sigma(I)$][a]	0.0512	0.0633
wR_2 [all data][a]	0.1590	0.1957
max/min $\Delta\rho$ (e$^-$ Å^{-3})	0.494/-0.379	0.355/-0.369

[a] $R_1 = \sum||F_o| - |F_c||/\sum|F_o|$; $wR_2 = [\sum w(F_o^2 - F_c^2)^2/\sum w(F_o^4)]^{1/2}$

Table 4.3: Crystallographic data for **8** and **9**.

Compound	**8**	**9**•0.375 CH_2Cl_2
Formula	$C_{35}H_{32}B_2ClF_{18}N_3$	$C_{35.38}H_{33.75}B_2Cl_{0.75}F_{18}N_3$
Formula weight	893.70	891.11
Crystal system	monoclinic	monoclinic
Space group	$P2_1/n$ (No. 14)	$I2/a$ (No. 15)
a (Å)	11.3790 (6)	25.1883(19)
b (Å)	22.2822 (12)	12.1920(9)
c (Å)	16.4411(9)	26.4276(18)
α (deg)	90	90
β (deg)	107.567(4)	98.253(3)
γ (deg)	90	90
V(Å^3)	3974.2(4)	8031.8(10)
Z	4	8
ρ (g/cm^3)	1.494	1.474
abs coeff (mm^{-1})	1.910	1.738
T (K)	173(1)	173(1)
$2\theta_{max}$ (°)	148.41	148.06
total data	27726	28202
unique data(R_{int})	8048(0.0333)	7870(0.0197)
Obs data [I>2($\sigma(I)$)]	6920	7250
Params	546	670
R_1 [I>2$\sigma(I)$]^a	0.0762	0.0608
wR_2 [all data]^a	0.2120	0.1632
max/min $\Delta\rho$ (e$^-$ Å^{-3})	0.858/-0.570	0.780/-0.682

^{a} $R_1 = \sum||F_o| - |F_c||/\sum|F_o|$; $wR_2 = [\sum w(F_o^2 - F_c^2)^2/\sum w(F_o^4)]^{1/2}$

Table 4.4: Crystallographic data for **10** and **11**.

Compound	**10**	**11**•*0.5* PhF
Formula	$C_{46}H_{51}B_2F_{18}N_5$	$C_{31}H_{39.50}BF_{3.50}N_5O_3S$
Formula weight	1037.53	639.54
Crystal system	monoclinic	triclinic
Space group	*C*2/*a* (No. 15)	$P\bar{1}$ (No. 2)
a (Å)	12.9360 (4)	9.3972(2)
b (Å)	18.7832 (6)	12.2337 (3)
c (Å)	41.0326 (12)	16.8072 (4)
α (deg)	90	73.1735 (10)
β (deg)	94.5442 (15)	77.1382 (11)
γ (deg)	90	68.1258 (10)
V(Å^3)	9938.7 (5)	1701.94 (7)
Z	8	2
ρ (g/cm^3)	1.387	1.248
abs coeff (mm^{-1})	1.133	1.333
T (K)	173(1)	173(1)
$2\theta_{max}$ (°)	144.77	144.69
total data	34208	11942
unique data(R_{int})	9814(0.0327)	6460(0.0136)
Obs data [I>2($\sigma(I)$)]	8438	5942
Params	741	523
R_1 [$I>2\sigma(I)$][a]	0.0543	0.0434
wR_2 [all data][a]	0.1447	0.1255
max/min $\Delta\rho$ (e$^-$ Å^{-3})	0.509/-10.422	0.276/-0.264

[a] $R_1 = \sum||F_o| - |F_c||/\sum|F_o|$; $wR_2 = [\sum w(F_o^2 - F_c^2)^2/\sum w(F_o^4)]^{1/2}$

Table 4.5: Crystallographic data for **12** and **15**.

Compound	**12**	**15**
Formula	$C_{12}H_{21}BF_3N_5O_3S$	$C_{54}H_{53}B_2F_{24}N_7$
Formula weight	383.21	1277.65
Crystal system	orthorhombic	monoclinic
Space group	$Cmc2_1$ (No. 36)	$P2_12_12_1$ (No. 19)
a (Å)	13.5787 (3)	12.6084 (3)
b (Å)	12.2769 (2)	19.7795 (6)
c (Å)	11.1774 (2)	24.1204 (6)
α (deg)	90	90
β (deg)	90	90
γ (deg)	90	90
V(Å^3)	1863.32 (6)	6015.3 (3)
Z	4	4
ρ (g/cm^3)	1.366	1.411
abs coeff (mm^{-1})	2.013	1.206
T (K)	173(1)	173(1)
$2\theta_{max}$ (°)	140.55	144.70
total data	5885	42409
unique data(R_{int})	1850 (0.0452)	11860(0.0192)
Obs data [I>2($\sigma(I)$)]	1733	11579
Params	201	812
R_1 [I>2$\sigma(I)$]^a	0.0684	0.0480
wR_2 [all data]^a	0.1940	0.1337
max/min $\Delta\rho$ (e$^-$ Å^{-3})	0.536/-0.385	0.480/-0.351

^{a} $R_1 = \sum||F_o| - |F_c||/\sum|F_o|$; $wR_2 = [\sum w(F_o^2 - F_c^2)^2/\sum w(F_o^4)]^{1/2}$

4.6 References

1. (*a*) Paetzold, P. *Adv. Inorg. Chem.* **1987**, *31*, 123; (*b*) Nöth, H. *Angew. Chem. Int. Ed. Engl.* **1988**, *27*, 1603; (*c*) Paetzold, P. *Pure Appl. Chem.* **1991**, *63*, 345; (*d*) Fischer, R. C.; Power, P. P. *Chem. Rev.* **2010**, *110*, 3877; For related M-B≡NR chemistry, see: (*e*) Braunschweig, H.; Dewhurst, R. D.; Schneider, A. *Chem. Rev.* **2010**, *110*, 3924; **(*f*)** Paetzold, P.; Plotho, C. V. *Chem. Ber.* **1982**, *115*, 2819.
2. (*a*) Paetzold, P.; Richter, A.; Thijssen, T.; Wurtenberg, S. *Chem. Ber.* **1979**, *112*, 3811; (*b*) Balak, E.; Herberich, G. E.; Manners, I.; Mayer, H.; Paetzold, P. *Angew. Chem. Int. Ed. Engl.* **1988**, *27*, 958.
3. (*a*) Dahcheh, F.; Martin, D.; Stephan, D. W.; Bertrand, G. *Angew. Chem. Int. Ed.* **2014**, *53*, 13159; (*b*) Dahcheh, F.; Stephan, D. W.; Bertrand, G. *Chem. Eur. J.* **2015**, *21*, 199; (*c*) Braunschweig, H.; Ewing, W. C.; Geetharani, K.; Schaefer, M. *Angew. Chem. Int. Ed.* **2015**, *54*, 1662.
4. (*a*) Lory, E. R.; Porter, R. F. *J. Am. Chem. Soc.* **1973**, *95*, 1766; (*b*) Kawashima, Y.; Kawaguchi, K.; Hirota. E. *J. Chem. Phys*. **1987**, *87*, 6331; (*c*) Thompson, C. A.; Andrews, L. *J. Am. Chem. Soc.* **1995**, *117*, 10125; (*d*) Zhang, F.; Maksyutenko, P.; Kaiser, R. I.; Mebel, A. M.; Gregusova, A.; Perera, S. A.; Bartlett, R. J. *J. Phys. Chem. A* **2010**, *114*, 12148.
5. For selected computational studies on HBNH, see: (*a*) Baird, N. C.; Datta, R. K. *Inorg. Chem.* **1972**, *11*, 17; (*b*) Matus, M. H.; Grant, D. J.; Nguyen, M. T.; Dixon, D. A. *J. Phys. Chem. C* **2009**, *113*, 16553; (*c*) Sundaram, R.; Scheiner, S.; Roy, A. K.; Kar, T. *J. Phys. Chem. C* **2015**, *119*, 3253.

6. Liu, H.; Jin, P.; Xue, Y.-M.; Dong, C.; Li, X.; Tang, C.-C.; Du, X.-W. *Angew. Chem. Int. Ed.* **2015**, *54*, 7051.

7. (*a*) Paine, R. T.; Narula, C. K. *Chem. Rev.* **1990**, *90*, 73; (*b*) Geim, A. K.; Grigorieva, I. V. *Nature* **2013**, *499*, 419; c) Liu, L.; Park, J.; Siegel, D. A.;. McCarty, K. F.; Clark, K. W.; Deng, W.; Basile, L.; Idrobo, J. C.; Li, A. P.; Gu, G.; *Science* **2014**, *343*, 16.

8. (*a*) Vogel, U.; Timonshkin, A. Y.; Scheer, M. *Angew. Chem. Int. Ed.* **2001**, *40*, 4409; (*b*) Rupar, P. A.; Jennings, M. C.; Ragogna, P. J.; Baines, K. M. *Organometallics* **2007**, *26*, 4109; (*c*) Al-Rafia, S. M. I.; Malcolm, A. C.; Liew, S. K.; Ferguson, M. J.; Rivard, E. *J. Am. Chem. Soc*. **2011**, *133*, 777; (*d*) Al-Rafia, S. M. I.; Malcolm, A. C.; McDonald, R.; Ferguson, M. J.; Rivard, E. *Angew. Chem. Int. Ed.* **2011**, *50*, 8354; (*e*) Yamaguchi, T.; Sekiguchi, A.; Driess, M. *J. Am. Chem. Soc.* **2010**, *132*, 14061; (*f*) Ghadwal, R. S.; Roesky, H. W. *Acc. Chem. Res.* **2013**, *46*, 444; (*g*) Filippou, A. C.; Baars, B.; Chernov, O.; Lebedev, Y. N.; Schnakenburg, G. *Angew. Chem. Int. Ed.* **2014**, *53*, 565; (*h*) Rivard, E. *Dalton Trans.* **2014**, *43*, 8577.

9. Stephan, D. W. *Acc. Chem. Res.* **2015**, *48*, 306.

10. (*a*) Hamilton, C. W.; Baker, R. T.; Staubitz, A.; Manners, I. *Chem. Soc. Rev.* **2009**, *38*, 279; (*b*) Leitao, E. M.; Titel, J.; Manners, I. *Nature Chem.* **2013**, *5*, 817; (*c*) Krieg, M.; Reicherter, F.; Haiss, P.; Ströbele, M.; Eichele, K.; Treanor, M.-J.; Schaub, R.; Bettinger, H. F. *Angew. Chem. Int. Ed.* **2015**, *54*, 8284.

11. For related rearrangements involving organic azides, see: (*a*) Rokade, B. V.; Prabhu, J. R. *J. Org. Chem.* **2012**, *77*, 5364; (*b*) Albertin, G.; Antoniutti, S.; Baldan, D.; Castro, J.; García-Fontán, S. *Inorg. Chem.* **2008**, *47*, 742.

12. For recent computational study on LB•BN•LA species, see: Momeni, M. R.; Shulman, L.; Rivard, E.; Brown, A. *Phys. Chem. Chem. Phys.* **2015**, *17*, 16525.

13. A related H/OTf exchange process is known within zinc(II) hydride chemistry: Lummis, P. A.; Momeni, M. R.; Lui, M. W.; McDonald, R.; Ferguson, M. J.; Miskolzie, M.; Brown, A.; Rivard, E. *Angew. Chem. Int. Ed.* **2014**, *53*, 9347.

14. Solovyev, A.; Chu, Q.; Geib, S. J.; Fensterbank, L.; Malacria, M.; Lacôte, E.; Curran, D. P. *J. Am. Chem. Soc.* **2010**, *132*, 15072.

15. (*a*) Al-Rafia, S. M. I.; McDonald, R.; Ferguson, M. J.; Rivard, E. *Chem. Eur. J.* **2012**, *18*, 13810; (*b*) Stubbs, N. E.; Jurca, T.; Leitao, E. M.; Woodall, C. H.; Manners, I. *Chem. Commun.* **2013**, *49*, 9098.

16. Kolychev, E. L.; Bannenberg, T.; Freytag, M.; Daniliuc, C. G.; Jones, P. G.; Tamm, M. *Chem. Eur. J.* **2012**, *18*, 16938.

17. Schulz, A.; Villinger, A. *Chem. Eur. J.* **2010**, *16*, 7276.

18. Photolysis of **3** (Hg lamp, 200 W) for 3 hrs in toluene or CH_2Cl_2 gave the new product, **4**, along with unknown by-products.

19. Pyykkö, P.; Atsumi, M. *Chem. Eur. J.* **2009**, *15*, 12770.

20. Malcolm, A. C.; Sabourin, K. J.; McDonald, R.; Ferguson, M. J.; Rivard, E. *Inorg. Chem.* **2012**, *51*, 12905.

21. For a related study on boranitrenes, see: Filthaus, M.; Schwertmann, L.; Neuhaus, P.; Seidel, R. W.; Oppel, I.; Bettinger, H. F. *Organometallics* **2012**, *31*, 3894.

22. Fox, A. R.; Cummins, C. C. *J. Am. Chem. Soc.* **2009**, *131*, 5716.

23. Axenrod, T.; Pregosin, P. S.; Wieder, M. J.; Becker, E. D.; Bradley, R. B.; Milne, G. W. A. *J. Am. Chem. Soc.* **1971**, *93*, 6536.

24. Wrackmeyer, B.; Tok, O. L. *Z. Naturforsch. B* **2007**, *62b*, 220.

25. To estimate the activation barrier, the N3-N4 bond length in **3** was scanned. The extrusion of N_2 is accompanied by a 1,2-H-shift and formation of **4**.

26. Kuhn, N.; Kratz, T. *Synthesis* **1993**, 561.

27. Kuhn, N.; Henkel, G.; Kratz, T.; Kreutzberg, J.; Boese, R.; Maulitz, A. M. *Chem. Ber.* **1993**, *126*, 2041.

28. Ge, F.; Kehr, G.; Daniliuc, C. G.; Mück-Lichtenfeld, C.; Erker, G.; *Organometallics* **2015**, *34*, 4205.

29. (*a*) Laubengayer, A. W.; Beachley Jr., O. T.; Porter, R. F. *Inorg. Chem.* **1965**, *4*, 578; (*b*) Beachley Jr., O. T.; Washburn, B. *Inorg. Chem*. **1975**, *14*, 120.

30. Malcolm, A. C.; Sabourin, K. J.; McDonald, R.; Ferguson, M. J.; Rivard, E. *Inorg. Chem.* **2012**, *51*, 12905.

31. (*a*) Sumerin, V.; Schulz, F.; Atsumi, M.; Wang, C.; Nieger, M.; Leskelä, M.; Repo, T.; Pyykkö, P.; Rieger, B. *J. Am. Chem. Soc.* **2008**, *130*, 14117; (*b*) Legare, M.-A.; Courtemanche, M. –A.; Rochette, E.; Fontaine, F.-G. *Science* **2015**, *349*, 513; (*c*) Wang, T.; Kehr, G.; Liu, L.; Grimme, S.; Daniliuc, C. G.; Erker, G. *J. Am. Chem. Soc*. **2016**, *138*, 4302; (*d*) Mo, Z.; Rit, A.; Campos, J.; Kolychev, E. L.; Aldridge, S. *J. Am. Chem. Soc.* **2016**, *138*, 3306; (*e*) Stephan, D. W. *Acc. Chem. Res.* **2015**, *48*, 306.

32. For related examples of transfer hydrogenation between amine-boranes and unsaturated B-N compounds, see: (*a*) Robertson, A. P. M.; Leitao, E. M.; Manners, I. *J. Am. Chem. Soc.* **2011**, *133*, 19322; (*b*) Lui, M. W.; Paisley, N. R.; McDonald, R.; Ferguson, M. J.; Rivard, E. *Chem. Eur. J.* **2016**, *22*, 2134; (*c*) Leitao, E. M.; Stubbs, N. E.; Robertson, A. P. M.; Helten, H.; Cox, R. J.; Lloyd-Jones, G. C.; Manners, I. *J. Am. Chem. Soc*. **2012**, *134*, 16805.

33. We also explored the possible Lewis basic nature of **7**. When **7** was combined with CuI and $BAr^F{}_3$, no reaction was found; treatment of **7** with $Me_2S{\bullet}BH_3$ (as a source of BH_3) gave a complicated product mixture.

34. Ruiz, D. A.; Melaimi, M.; Bertrand, G. *Chem. Commun*. **2014**, *50*, 7837.

35. (*a*) Benson, S. W. *J. Chem. Educ.* **1965,** *42*, 502; (*b*) Walsh, R. *Acc. Chem. Res*. **1981**, *14*, 246.

36. For the synthesis of BN by treating $[XBNH]_3$ (X = Cl or Br) with molten alkali metals, see: (*a*) Hamilton, E. J. M.; Dolan, S. E.; Mann, C. M.; Colijn, H. O.; McDonald, C. E.; Shore, S. G. *Science* **1993**, *260*, 659; (*b*) Hamilton, E. J. M.; Dolan, S. E.; Mann, C. M.; Colijn, H. O.; Shore, S. G. *Chem. Mater.* **1995**, *7*, 111.

37. (*a*) Dewar, M. J. S.; Kubba, V. P.; Pettit, R. *J. Chem. Soc.* **1958**, 3073; (*b*) Emslie, D. J. H.; Piers, W. E.; Parvez, M. *Angew. Chem. Int. Ed.* **2003**, *42*, 1252; (*c*) Campbell, P. G.; Marwitz, A. J. V.; Liu, S.-Y. *Angew. Chem. Int. Ed.* **2012**, *51*, 6074; (*d*) Edel, K.; Brough, S. A.; Lamm, A. N.; Liu, S.-Y.; Bettinger, H. F. *Angew. Chem. Int. Ed.* **2015**, *54*, 7819.

38. Pangborn, A. B.; Giardello, M. A.; Grubbs, R. H.; Rosen, R. K.; Timmers, F. J. *Organometallics.* **1996**, *15*, 1518.

39. Jafarpour, L.; Stevens, E. D.; Nolan, S. P. *J. Organomet. Chem*. **2000**, *606*, 49.

40. Al-Rafia, S. M. I.; Lummis, P. A.; Swarnakar, A. K.; Deutsch, K. C.; Ferguson, M. J.; McDonald, R.; Rivard, E. *Aust. J. Chem.* **2013**, *66*, 1235.

41. Sloan, M. E.; Staubitz, A.; Clark, T. J.; Russell, C. A.; Lloyd-Jones, G. C.; Manners, I. *J. Am. Chem. Soc.* **2010**, *132*, 3831.

42. Straus, D. A.; Zhang, C.; Tilley, T. D. *J. Organomet. Chem*. **1989**, *369*, C13.

43. Asadi, A.; Avent, A. G.; Hill, M. S.; Hitchcock, P. B.; Meehan, M. M.; Smith, J. D. *Organometallics* **2002**, *21*, 2183.

44. Savoia, D.; Trombini, C.; Umani-Ronchi, A. *J. Org. Chem.* **1978**, *43*, 2907.

45. Hope, H. *Prog. Inorg. Chem.* **1994**, *41*, 1.

46. Blessing, R. H. *Acta Crystallogr.* **1995**, *A51*, 33.

47. Sheldrick, G. M. *Acta Crystallogr*. **2008**, *A64*, 112.

48. Beurskens, P. T.; Beurskens, G.; de Gelder, R.; Smits, J. M. M.; Garcia-Garcia, S.; Gould, R. O. DIRDIF-2008; Crystallography Laboratory, Radboud University: Nijmegen, The Netherlands, **2008**.

49. Wang, Y.; Quillian, B.; Wei, P.; Wannere, C. S.; Xie, Y.; King, R. B.; Schaefer, H. F.; Schleyer, P. v: R.; Robinson, G. H. *J. Am Chem. Soc*. **2007**, *129*, 12412.

50. (*a*) Jaska, C. A.; Temple, K.; Lough, A. J.; Manners, I. *J. Am. Chem. Soc.* **2003**, *125*, 9424; (*b*) Robertson, A. P. M.; Leitao, E. M.; Manners, I. *J. Am. Chem. Soc.* **2011**, *133*, 19322; (*c*) Nöth, H.; Thomas, S. *Eur. J. Inorg. Chem*. **1999**, 1373.

51. Kuhn, A.; Sander, W. *Organometallics* **1998**, *17*, 4776.

Chapter 5: Azido- and Amido-substituted Gallium Hydrides Supported by *N*-Heterocyclic Carbenes

5.1 Introduction

It is now well accepted that the coordination of main group element centers by carbon-based donors, such as *N*-heterocyclic carbenes (NHCs),[1] cyclic(alkyl)aminocarbenes (CAACs),[2] and *N*-heterocyclic olefins (NHOs)[3] can provide access to many species that are unstable or unattainable under conventional synthetic conditions. Drawing focus to the group 13 (triel) elements, the recent isolation of homodiatomic B_2 molecular adducts[4] can be viewed as a particularly salient example of the stabilization brought forth by the abovementioned carbon-based donors.

As described in the previous chapter, a complex containing the elusive inorganic acetylene HBNH placed between a sterically encumbered NHC donor and a large triarylfluoroborane acceptor was synthesized.[5] The resulting complex IPr•HB=NH•$BAr^F{}_3$ [IPr = $[(HCNDipp)_2C:]$; Dipp = 2,6-$^iPr_2C_6H_3$); Ar^F = 3,5-$(F_3C)_2C_6H_3$)] was synthesized via Lewis acid-assisted N_2 elimination from the non-explosive azidoborane complex IPr•BH_2N_3[6] followed by hydride migration from B to N. Motivated by this result, parallel chemistry[7] was explored with gallium. The iminogallane HGa=NH could be a possible building block for the future low temperature deposition of bulk gallium nitride (GaN), a highly valued material for its luminescent and semi-conducting properties.[8,9] Preliminary investigations involving

the preparation of NHC-supported azido- and amido-gallium hydrides and behavior upon heating are reported herein.

5.2 Results and Discussions

The attempted synthesis of an HGa=NH complex required the discovery of a suitable route to an azidogallane adduct NHC•GaH_2N_3. It was hoped that one analogue, IMes•GaH_2N_3, could be synthesized from known IMes•GaH_2X (IMes = [{HCN(Mes)}$_2$C:]; Mes = 2,4,6-$Me_3C_6H_2$; X = Cl, Br or I) complexes[10] by reaction with common azide sources such as Me_3SiN_3 or NaN_3. However previous reports associated with the synthesis of the necessary starting material IMes•GaH_3 involved the reaction of the *N*-heterocyclic carbene IMes with thermally unstable Li[GaH_4].[11] To make an eventual route to IMes•GaH_2N_3 more convenient, a modified synthesis of IMes•GaH_3 using K[HB^sBu_3] as a hydride source was developed. Specifically, IMes•$GaCl_3$[12] was combined with three equivalents of K[HB^sBu_3] in THF at room temperature to give IMes•GaH_3 in a 75 % isolated yield via Cl/H exchange (eqn. 5.1).

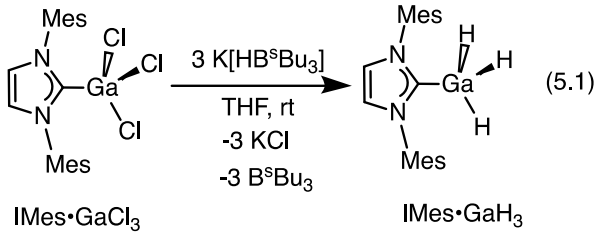

(5.1)

Later, IMes•GaH_3 was treated with 0.5 equivalents of IMes•GaI_3, according to literature procedures,[10c,12] to afford IMes•GaH_2I. In order to synthesize the desired azido-gallane adduct IMes•GaH_2N_3, IMes•GaH_2I was reacted with either Me_3SiN_3 or NaN_3 in THF; however no reaction transpired. A successful synthesis of

IMes•GaH_2N_3 (**1**) was accomplished by combining IMes•GaH_2I with the lipophilic azide salt [$^nBu_4N$]N_3 in THF (eqn. 5.2). The ^{1}H NMR spectrum of the resulting product (**1**) afforded a broad resonance at 4.52 ppm, due to the retention of two gallium-bound hydrides. Moreover a diagnostic azide $\upsilon(N_3)$ band for compound **1** was detected at 2084 cm^{-1}, which matched well with the related asymmetric azide stretch at 2104 cm^{-1} found in Me_3N•$GaCl_2N_3$.[9b] The composition of **1** was substantiated by X-ray crystallography (Figure 5.1) and revealed the presence of a tetrahedral geometry about the Ga center. The $C_{(NHC)}$-Ga bond distance in **1** is 2.041(4) Å and is similar to values found within known NHC-gallane complexes.[10,12] The Ga-N bond length in **1** is 1.953(4) Å and comparable to the Ga-N bond distances in Christe's pentaazido gallate salt $[PPh_4]_2[Ga(N_3)_5]$ [1.937(2)-2.049(2) Å].[13]

After the successful isolation of IMes•GaH_2N_3 (**1**), the Lewis acid-triggered N_2 elimination/hydride migration from Ga to N was attempted to form IMes•HGa=NH•BAr^F_3 (Ar^F = 3,5-$(F_3C)_2C_6H_3$); a similar transformation was previously used to yield an HB=NH complex.[5] Accordingly, IMes•GaH_2N_3 (**1**) was combined with a stoichiometric amount of BAr^F_3 followed by the heating of the reaction mixture to 80 °C in toluene. The ^{1}H NMR spectrum of the resulting white solid indicated the formation of multiple carbene-containing products, however conclusive evidence for the formation of an HGa=NH complex was not found. Instead, a salt consisting of the known $[HBAr^F_3]^-$ anion[14] was identified (Scheme 5.1) as one of the products in the mixture by ^{1}H and ^{11}B NMR spectroscopy. Attempts to isolate pure products by fractional crystallization were unsuccessful.

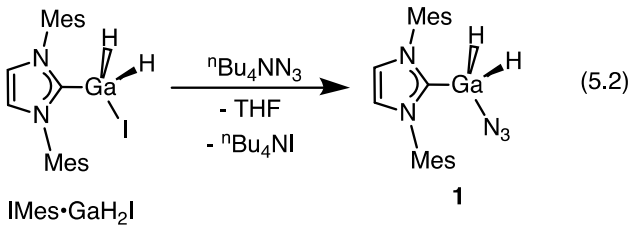

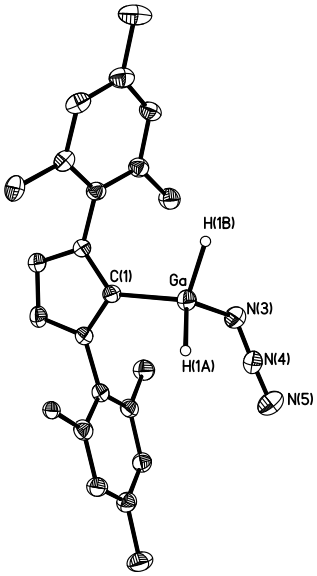

Figure 5.1. Molecular structure of IMes•GaH_2N_3 (**1**) with thermal ellipsoids presented at a 30 % probability level. All carbon bound hydrogen atoms have been omitted for clarity. Selected bond lengths (Å) and angles (deg): Ga-C(1) 2.041(4), Ga-N(3) 1.953(4), Ga-H(1A) 1.52(5), Ga-H(1B) 1.52(5), N(3)-N(4) 1.199(6), N(4)-N(5) 1.146(6); N(3)-Ga-C(1) 101.41(18), N(3)-N(4)-N(5) 174.6(6).

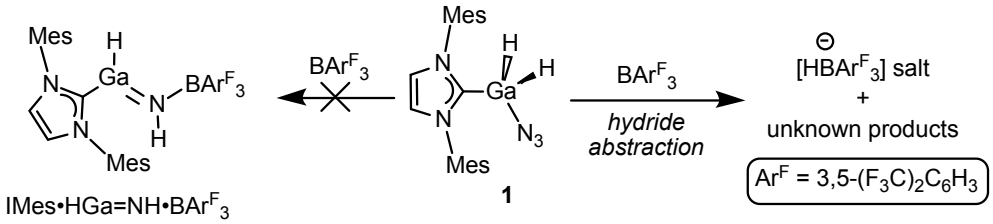

Scheme 5.1. Reaction of IMes•GaH_2N_3 (**1**) with $BAr^F{}_3$.

It was also shown in the previous chapter that N_2 loss/1,2-hydride migration in IPr•BH_2N_3 could also be instigated by addition of the strong electrophile MeOTf

(OTf = OSO_2CF_3), leading to the formation of the *N*-methylated adduct [IPr•HB=NHMe]OTf.[5a] However when IMes•GaH_2N_3 (**1**) was treated with one equivalent of MeOTf in CH_2Cl_2, multiple products were found according to ^1H and ^{19}F NMR spectroscopy. Increasing the stoichiometry of MeOTf to four molar equivalents resulted in clean formation of the new hydrido/triflate adduct IMes•GaH$(OTf)_2$ (**2**) (Scheme 5.2) in 80 % yield as a colorless moisture-sensitive solid.

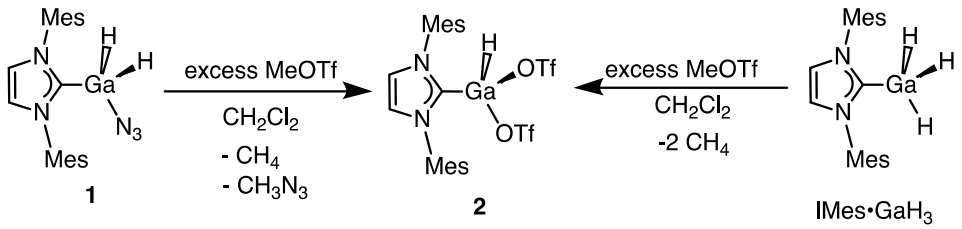

Scheme 5.2. Syntheses of IMes•GaH$(OTf)_2$ (**2**).

Compound **2** was identified by a combination of X-ray crystallography (Figure 5.2) and NMR spectroscopy. Due to the possible explosive nature of the likely by-product, MeN_3 (**Caution!**),[15] this reaction was not repeated again. However, the outcome of the reaction was further confirmed by an independent synthesis of **2** via the reaction of IMes•GaH_3 with excess MeOTf (Scheme 5.2). The ^{19}F NMR spectrum of IMes•GaH$(OTf)_2$ (**2**) showed a sharp resonance at -77.4 ppm that was assigned to the covalently bound OTf groups. As displayed in Figure 5.2, the refined structure of **2** afforded the expected coordination of two OTf⁻ substituents at gallium with corresponding Ga-O bond lengths of 1.9023(15) and 1.9186(16) Å. These bonds are significantly elongated relative the those [1.8021(1) Å] found in the four-

coordinate bis(hydroxy) gallium complex $LGa(OH)_2$ (L = $HC[C(Me)NDipp]_2$; Dipp = 2,6-$^iPr_2C_6H_3$),[16] suggesting that the Ga-OTf interactions in **2** are weak in nature.

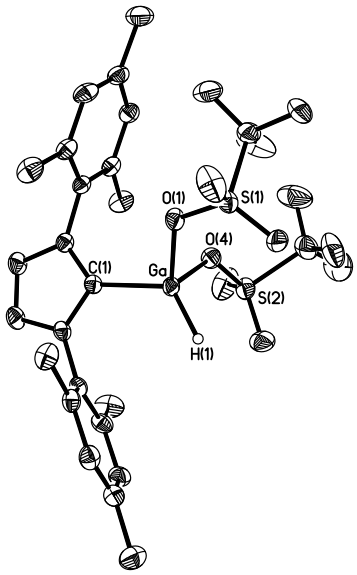

Figure 5.2. Molecular structure of IMes•$GaH(OTf)_2$ (**2**) with thermal ellipsoids presented at a 30 % probability level. All carbon bound hydrogen atoms have been omitted for clarity. Selected bond lengths (Å) and angles (deg): Ga-C(1) 1.9855(19), Ga-O(1) 1.9023(15), Ga-O(4) 1.9186(16), Ga-H(1) 1.45(3); O(1)-Ga-C(1) 104.12(7), C(1)-Ga-H(1) 123.2(11).

The above results indicate that in the presence of a Lewis acid ($BAr^F{}_3$) or electrophile MeOTf, IMes•GaH_2N_3 (**1**) undergoes preferential azide or hydride abstraction processes in place of N_2 loss/hydride migration. The differing reactivity of the azido-gallane IMes•GaH_2N_3 (**1**) compared with IPr•BH_2N_3 is likely a consequence of the increased polarity and reactivity of Ga-N and Ga-H bonds due to the lower electronegativity of Ga in relation to B. Thus it appears that an alternate route to a molecular complex of HGa=NH has to be devised.

In keeping with the theme of eventually generating molecular precursors to bulk gallium nitride, the gallium-silylamide complexes IMes•$GaH_2N(SiMe_3)_2$ (**3**) and

IPr•$GaCl_2N(SiMe_3)_2$ (**4**) were synthesized. The amido-gallane complex IMes•$GaH_2N(SiMe_3)_2$ (**3**) was prepared in a 93 % yield as a white solid from the reaction of IMes•GaH_2Cl[12] with a stoichiometric amount of $Li[N(SiMe_3)_2]$ (eqn. 5.3).

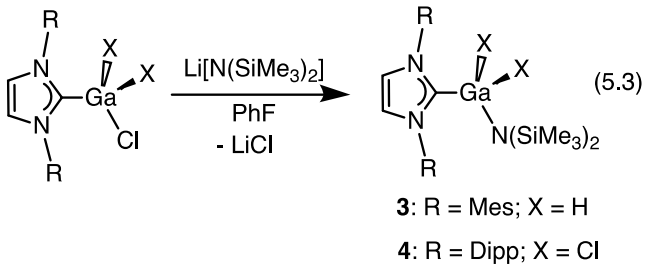

The ^1H NMR spectrum of **3** afforded a sharp up-field positioned resonance at 0.23 ppm due to the capping $–N(SiMe_3)_2$ group, while expected resonances for the gallium hydrides (4.51 ppm) and IMes ligand were also detected. The crystallographically determined structure of **3** is shown in Figure 5.3; despite the presence of co-crystallized IMes•GaH(Cl)-$N(SiMe_3)_2$ as part of the crystalline lattice, bulk samples of **3** afforded both satisfactory elemental analyses and clean NMR spectra. Perhaps the most salient structural feature of **3** is the substantially longer $C_{(NHC)}$-Ga length [2.0743(15) Å] in relation to that found in the bis(triflato) gallane IMes•$GaH(OTf)_2$ (**2**) [1.9855(19) Å]; this is likely a consequence of the less Lewis acidic $GaH_2N(SiMe_3)_2$ unit in **3** in relation to the $GaH(OTf)_2$ moiety in **2**. The nitrogen atom within the silylamido group in **3** [N(3); Figure 5.3] is slightly pyramidalized as revealed by an angle sum (Σ°N) value of 353.41(12)°. Due to the presence of the bulky $SiMe_3$ groups at nitrogen, the Ga-N bond distance in **3** [1.9226(13) Å] is longer compared to the *Ga-N*Me_2 bond length [1.816(2) Å] reported in {[(cyclopentyl)N-$C_6H_4]_2O$}$GaNMe_2$.[17]

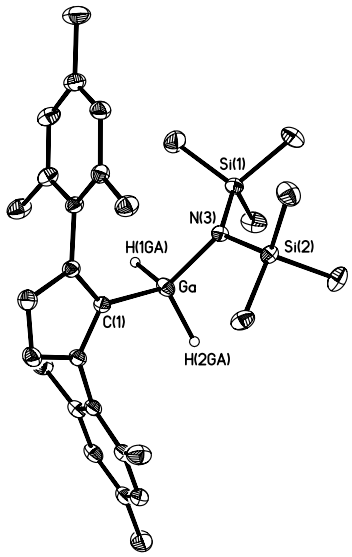

Figure 5.3. Molecular structure of IMes•$GaH_2N(SiMe_3)_2$ (**3**) with thermal ellipsoids presented at a 30 % probability level. All carbon bound hydrogen atoms have been omitted for clarity; **3** co-crystallizes with *ca.* 15% of the mixed hydrido/chloride adduct IMes•GaH(Cl)-$N(SiMe_3)_2$. Selected bond lengths (Å) and angles (deg) for **3**: Ga-C(1) 2.0743(15), Ga-H(1Ga) 1.503(18), Ga-H(2Ga) 1.512(19), Ga-N(3) 1.9226(13); N(3)-Ga-C(1) 112.30(6), Si(1)-N(3)-Si(2) 123.25(8), Ga-N(3)-Si(1) 112.09(7), Ga-N(3)-Si(2) 118.07(7).

A halogenated analogue of **3**, IPr•$GaCl_2N(SiMe_3)_2$ (**4**) was also readily prepared from the known adduct IPr•$GaCl_3$[12*b*] and one equivalent of Li[$N(SiMe_3)_2$] (eqn. 5.3). The molecular structure of IPr•$GaCl_2N(SiMe_3)_2$ (**4**) is shown in Figure 5.4 and displays similar overall structural features as the hydrido congener **3**.

After the successful preparation of IMes•$GaH_2N(SiMe_3)_2$ (**3**) and IPr•$GaCl_2N(SiMe_3)_2$ (**4**), the possible synthesis of extended GaN structures was attempted[9] via thermolysis. Surprisingly, both of these species were found to be quite thermally stable and do not show any signs of $HSiMe_3$, $ClSiMe_3$ or $HN(SiMe_3)_2$ loss upon heating to 100 °C in toluene. Compound **3** was also stable upon microwave irradiation for 1.5 h at 130 °C in toluene, while under the same microwave

conditions, compound **4** underwent partial decomposition to an $[IPrH]^+$ salt (20 %) and a new unidentified carbene-containing product (24 %).

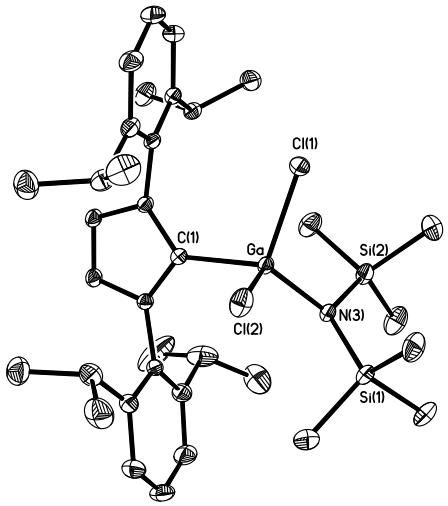

Figure 5.4. Molecular structure of IPr•$GaCl_2N(SiMe_2)_2$ (**4**) with thermal ellipsoids presented at a 30 % probability level. All hydrogen atoms have been omitted for clarity. Selected bond lengths (Å) and angles (deg): Ga-C(1) 2.0570(15), Ga-N(3) 1.8932(13), Ga-Cl(1) 2.2054(4), Ga-Cl(2) 2.2047(5); N(3)-Ga-C(1) 119.05(6), Cl(1)-Ga-Cl(2) 103.54(2), Si(2)-N(3)-Si(1) 121.46(8).

In order to encourage possible intermolecular Ga-N bond forming processes I hoped to replace the chloride substituents in IPr•$GaCl_2N(SiMe_3)_2$ (**4**) with more labile OTf^- groups (to form IPr•$Ga(OTf)_2N(SiMe_3)_2$). Towards this goal, IPr•$GaCl_2N(SiMe_3)_2$ (**4**) was combined with two equivalents of Ag[OTf] in CH_2Cl_2, however under these conditions the exchange of only one chloride transpired to form IPr•$GaCl(OTf)N(SiMe_3)_2$ (**5**) (eqn. 5.4).

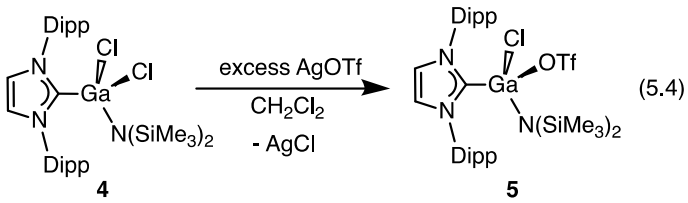

(5.4)

Compound **5** was obtained as a racemic mixture due to the presence of a chiral gallium center (Figure 5.5). A sharp signal at -76.2 ppm in the ^{19}F NMR spectrum of **5** indicated that the OTf group remained covalently bound to gallium in solution. Despite replacing one of the chlorine atom with a OTf group, compound **5** was also thermally stable to 100 °C in toluene for prolonged periods of time (12 hrs). However, compound **5** underwent a complete decomposition to several unidentified products upon microwave irradiation for 1.5 h at 130 °C in fluorobenzene.

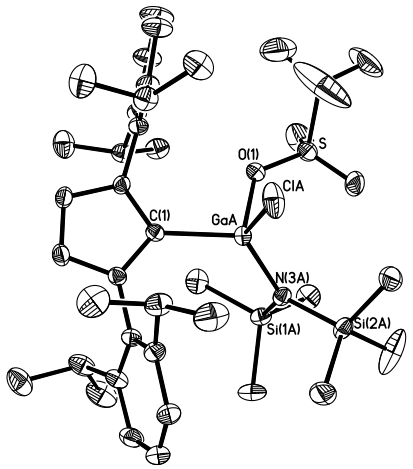

Figure 5.5. Molecular structure of IPr•GaCl(OTf)N($SiMe_2$)$_2$ (**5**) with thermal ellipsoids presented at a 30 % probability level. All hydrogen atoms have been omitted for clarity. Selected bond lengths (Å) and angles (deg) with parameters associated with a second molecule in the asymmetric unit listed in square brackets: Ga(A)-C(1) 2.042(3) [2.167(6)], Ga(A)-N(3A) 1.846(3) [1.840(9)], Ga(A)-Cl(A) 2.1668(11) [2.171(10)], Ga(A)-O(1) 1.969(2) [1.982(5)]; N(3A)-Ga(A)-C(1) 124.52(14) [129.1(11)], Cl(A)-Ga(A)-O(1) 102.10(9) [112.5(15)].

5.3 Conclusions

The successful isolation of *N*-heterocyclic carbene complexes of azido- and amido-gallanes has been described. These species represent members of a general compound class that could be eventually used to generate bulk gallium nitride under mild conditions (after suitable ligand modification). The reported gallium hydrides also

have similar structural features as the recently reported active ketone hydrosilylation/borylation catalyst IPr•Zn(H)OTf•THF[18a] and thus future work would involve exploring the catalytic activity[18] of these main group, NHC-supported, gallium hydrides in more detail.

5.4 Experimental Details

5.4.1 Materials and Instrumentation. All reactions were performed using standard Schlenk techniques under an atmosphere of nitrogen or in an inert atmosphere glovebox (Innovative Technology, Inc.).[19] Solvents were dried using a Grubbs-type solvent purification system manufactured by Innovative Technology, Inc., degassed (freeze−pump−thaw method), and stored under an atmosphere of nitrogen prior to use. $K[HB^sBu_3]$ (1.0 M solution in THF), $GaCl_3$, $Li[N(SiMe_3)_2]$, and $[^nBu_4N]N_3$ were purchased from Aldrich and used as received. NHC•GaX_3 (NHC = IMes or IPr; X = Cl or I),[12b,20] IMes•GaH_2X (X = Cl or I)[10a,10c] and BAr^F_3 (Ar^F = 3,5-$(F_3C)_2C_6H_3$)[21] were prepared according to literature procedures. ^1H, ^{11}B, $^{13}C\{^1H\}$, ^{19}F, NMR spectra were recorded on a Varian iNova-400 spectrometer and referenced externally to $SiMe_4$ (^1H and $^{13}C\{^1H\}$), $F_3B•OEt_2$ (^{11}B), and $CFCl_3$ (^{19}F) respectively. Elemental analyses were performed by the Analytical and Instrumentation Laboratory at the University of Alberta. Melting points were measured in sealed glass capillaries under nitrogen using a MelTemp apparatus and are uncorrected.

5.4.2 X-ray Crystallography. Crystals of suitable quality for X-ray diffraction studies were removed from a vial in a glovebox and immediately covered with a thin

layer of hydrocarbon oil (Paratone-N). A suitable crystal was selected, mounted on a glass fiber, and quickly placed in a low temperature stream of nitrogen on an X-ray diffractometer.[22] All data were collected at the University of Alberta using a Bruker APEX II CCD detector/D8 diffractometer using Cu Kα radiation with the crystals cooled to −100 °C. The data were corrected for absorption through Gaussian integration from the indexing of the crystal faces.[23] Structures were solved using the direct methods program SHELXS-97[24] (IPr•GaCl(OTf)N($SiMe_3$)$_2$ (**5**)) or intrinsic phasing SHELXT[24] (IMes•GaH_2N_3 (**1**), IMes•GaH(OTf)$_2$ (**2**), IMes•$GaH_2N(SiMe_3)_2$ (**3**), IPr•$GaCl_2N(SiMe_3)_2$ (**4**)). Structure refinement was accomplished using either SHELXL-97 or SHELXL-2013.[24] All carbon-bound hydrogen atoms were assigned positions on the basis of the sp^2 or sp^3 hybridization geometries of their attached carbon atoms, and were given thermal parameters 20 % greater than those of their parent atoms.

5.4.3 Synthetic procedures

Synthesis of IMes•GaH_3. To a 40 mL THF solution of IMes•$GaCl_3$ (1.67 g, 3.48 mmol) was added dropwise K[HB^sBu_3] (11 mL, 1.0 M solution in THF, 11 mmol) and the mixture was stirred for 24 hrs. The mother liquor was separated from the white precipitate by filtration and the solvent was removed under vacuum from the filtrate. The resulting product was washed three times with hexanes (3 × 10 mL) and dried under vacuum to yield IMes•GaH_3 as a white powder (980 mg, 75 %). The ^1H and $^{13}C\{^1H\}$ NMR spectra matched those found in the literature.[10a]

Synthesis of IMes•GaH_2N_3 (1). To a 3 mL THF solution of IMes•GaH_2I (154 mg, 0.31 mmol), was added dropwise a 3 mL THF solution of [^{n}Bu$_4$N]N_3 (77 mg, 0.28 mmol) and the reaction mixture was stirred for 3 hrs. The solvent was removed from the mixture under vacuum and the resulting white solid was re-dissolved in 20 mL of toluene. The solution was filtered and the solvent was removed from the filtrate under vacuum to yield IMes•GaH_2N_3 (**1**) (80 mg, 62 %) as a white solid. Crystals suitable for X-ray diffraction were grown from a toluene/hexanes mixture at -35 °C). ^{1}H NMR (400 MHz, C_6D_6): δ = 6.74 (s, 4H, Ar*H*), 5.96 (s, 2H, Ar*H*), 4.52 (br, 2H, Ga*H*), 2.07 (s, 6H, C*H*$_3$), 1.98 (s, 12H, C*H*$_3$). ^{13}C{^{1}H} NMR (125 MHz, C_6D_6): δ = 171.7 (s, N-*C*-N), 140.1 (s, Ar*C*), 134.9 (s, Ar*C*), 134.2 (s, Ar*C*), 129.6 (s, Ar*C*), 123.0 (s, N-*C*H), 21.1 (s, *C*H$_3$), 17.4 (s, *C*H$_3$). IR (Nujol, cm^{-1}): 2084 (s, υ_{N3}), 1890 (m, $^{asym}\upsilon_{Ga-H}$), 1843 (m, $^{sym}\upsilon_{Ga-H}$). Anal. Calcd. for $C_{21}H_{26}GaN_5$: C, 60.31; H, 6.21; N, 16.75. Found: C, 60.13; H, 6.22; N, 16.55. Mp (°C): 183-186.

Independent Synthesis of IMes•GaH(OTf)$_2$ (2). To a 5 mL CH_2Cl_2 solution of IMes•GaH_3 (96 mg, 0.25 mmol) was added MeOTf (114 μL, 1.04 mmol) and the mixture was stirred for 12 hrs. All the volatiles were removed under vacuum and the resulting white solid was washed with 5 mL of hexanes. The product was dried under vacuum to yield **2** as a white powder (140 mg, 83 %). ^{1}H NMR (400 MHz, C_6D_6): δ = 6.72 (s, 4H, Ar*H*), 5.89 (s, 2H, N-C*H*), 5.10 (br, 1H, Ga*H*), 2.02 (s, 6H, C*H*$_3$), 1.94 (s, 12H, C*H*$_3$). ^{13}C{^{1}H} NMR (125 MHz, C_6D_6): δ = 158.0 (s, N-*C*-N), 141.8 (s, Ar*C*), 134.7 (s, Ar*C*), 131.7 (s, Ar*C*), 130.1 (s, Ar*C*), 125.1 (s, N-*C*H), 119.9 (q, $^1J_{CF}$ = 318 Hz, *C*F$_3$), 21.0 (s, *C*H$_3$), 17.1 (s, *C*H$_3$). ^{19}F NMR (376 MHz, C_6D_6): δ = -77.4. IR

(Nujol, cm^{-1}): 2062 (m, υ_{Ga-H}). Anal. Calcd. for $C_{23}H_{25}F_6GaN_2O_6S_2$: C, 41.03; H, 3.74; N, 4.16; S, 9.52. Found: C, 40.23; H, 3.67; N, 4.01; S, 9.52. Mp (°C): 180-185.

Synthesis of IMes•$GaH_2N(SiMe_3)_2$ (3). To a 5 mL fluorobenzene solution of IMes•GaH_2Cl (159 mg, 0.39 mmol) was added a 5 mL fluorobenzene solution of $Li[N(SiMe_3)_2]$ (65 mg, 0.39 mmol) and the mixture was stirred for 12 hrs. The volatiles were then removed under vacuum and the resulting white solid was re-dissolved in 20 mL of Et_2O and filtered. The solvent was removed under vacuum from the filtrate to yield **3** as a white powder (190 mg, 93 %). Crystals suitable for X-ray diffraction were grown from toluene/hexanes at -35 °C. ^1H NMR (400 MHz, C_6D_6): δ = 6.77 (s, 4H, Ar*H*), 5.96 (s, 2H, N-C*H*), 4.51 (br, 2H, Ga*H*), 2.10 (s, 6H, CH_3), 2.07 (s, 12H, CH_3), 0.23 (s, 18H, Si(CH_3)$_3$). $^{13}C\{^1H\}$ NMR (125 MHz, C_6D_6): δ = 176.8 (s, N-*C*-N), 139.6 (s, Ar*C*), 135.1 (s, Ar*C*), 129.8 (s, Ar*C*), 128.6 (s, Ar*C*), 122.9 (s, N-*C*H), 21.0 (s, *C*H_3), 18.3 (s, *C*H_3), 5.5 (s, Si(*C*H_3)$_3$). IR (Nujol, cm^{-1}): 1833 (s, $^{asym}\upsilon_{Ga-H}$), 1805 (s, $^{sym}\upsilon_{Ga-H}$). Anal. Calcd. for $C_{27}H_{44}GaN_3Si_2$: C, 60.44; H, 8.27; N, 7.83. Found: C, 60.29; H, 7.96; N, 7.42. Mp (°C): 150-155.

Synthesis of IPr•$GaCl_2N(SiMe_3)_2$ (4). A 5 mL fluorobenzene solution of $Li[N(SiMe_3)_2]$ (29 mg, 0.17 mmol) was dropwise added to a 10 mL fluorobenzene solution of IPr•$GaCl_3$ (105 mg, 0.19 mmol). The resulting white slurry was stirred for 12 hrs and all the volatiles were removed under vacuum. The remaining white powder was dissolved in 20 mL of Et_2O and filtered. The solvent was removed under vacuum from the filtrate to yield **4** as a white solid (95 mg, 74 %). Crystals suitable

for X-ray diffraction were grown from Et_2O/hexanes at -35 °C. ^{1}H NMR (400 MHz, C_6D_6): δ = 7.24 (t, $^3J_{H-H}$ = 8.0 Hz, 2H, Ar*H*), 7.13 (d, $^3J_{H-H}$ = 7.5 Hz, 4H, Ar*H*), 6.40 (s, 2H, N-C*H*-), 2.92 (sept, $^3J_{H-H}$ = 6.5 Hz, 4H, C*H*(CH_3)$_2$), 1.48 (d, $^3J_{H-H}$ = 7.0 Hz, 12H, CH(C*H*$_3$)$_2$), 0.91 (d, $^3J_{H-H}$ = 7.0 Hz, 12H, CH(C*H*$_3$)$_2$), 0.30 (s, 18H, Si(C*H*$_3$)$_3$). ^{13}C{^{1}H} NMR (125 MHz, C_6D_6): δ = 167.0 (s, N-*C*-N), 145.9 (s, N-*C*H), 134.9 (s, Ar*C*), 131.5 (s, Ar*C*), 126.0 (s, Ar*C*), 124.7 (s, Ar*C*), 29.1 (s, *C*H(CH_3)$_2$), 26.4 (s, CH(*C*H$_3$)$_2$), 23.1 (s, CH(*C*H$_3$)$_2$), 6.5 (s, Si(C*H*$_3$)$_3$). Anal. Calcd. for $C_{33}H_{54}Cl_2GaN_3Si_2$: C, 57.48; H, 7.89; N, 6.09. Found: C, 57.96; H, 7.88; N, 5.78. Mp (°C): 165-170.

Synthesis of IPr•GaCl(OTf)N(SiMe$_3$)$_2$ (5). A solution of IPr•$GaCl_2N(SiMe_3)_2$ (**4**) (150 mg, 0.22 mmol) in 10 mL of CH_2Cl_2 was added to a 5 mL CH_2Cl_2 solution of AgOTf (123 mg, 0.47 mmol) and the mixture was stirred for 2 hrs. The resulting slurry was filtered and the volatiles were removed from the filtrate to yield **5** as an off-white powder (130 mg, 74 %). Crystals suitable for X-ray diffraction were grown from fluorobenzene/hexanes at -35 °C. ^{1}H NMR (400 MHz, $CDCl_3$): δ = 7.54 (t, $^3J_{H-H}$ = 7.7 Hz, 2H, Ar*H*), 7.39-7.35 (m, 4H, Ar*H*), 7.20 (s, 2H, N-C*H*-), 2.82 (sept, $^3J_{H-H}$ = 6.5 Hz, 2H, C*H*(CH_3)$_2$), 2.73 (sept, $^3J_{H-H}$ = 6.5 Hz, 2H, C*H*(CH_3)$_2$), 1.46 (d, $^3J_{H-H}$ = 6.5 Hz, 6H, CH(C*H*$_3$)$_2$), 1.42 (d, $^3J_{H-H}$ = 6.5 Hz, 6H, CH(C*H*$_3$)$_2$), 1.08 (d, $^3J_{H-H}$ = 7.5 Hz, 6H, CH(C*H*$_3$)$_2$), 1.07 (d, $^3J_{H-H}$ = 7.5 Hz, 6H, CH(C*H*$_3$)$_2$), 0.07 (br, 9H, Si(C*H*$_3$)$_3$), -0.15 (br, 9H, Si(C*H*$_3$)$_3$). ^{13}C{^{1}H} NMR (125 MHz, $CDCl_3$): δ = 163.2 (s, N-*C*-N), 145.5 (s, N-*C*H), 145.3 (s, N-*C*H), 133.9 (s, Ar*C*), 131.8 (s, Ar*C*), 127.0 (s, Ar*C*), 125.2 (s, Ar*C*), 125.0 (s, Ar*C*), 118.7 (q, $^1J_{CF}$ = 319.6 Hz, *C*F$_3$), 29.1 (s, *C*H(CH_3)$_2$),

29.0 (s, *C*H(CH_3)$_2$), 27.0 (s, CH(*C*H_3)$_2$), 26.8 (s, CH(*C*H_3)$_2$), 22.7 (s, CH(*C*H_3)$_2$), 22.5 (s, CH(*C*H_3)$_2$), 5.8 (br, Si(*C*H_3)$_3$), 5.4 (br, Si(*C*H_3)$_3$). ^{19}F NMR (376 MHz, $CDCl_3$): δ = -76.2 (s, C*F*$_3$). Anal. Calcd. for $C_{34}H_{54}ClF_3GaN_3O_3SSi_2$: C, 50.84; H, 6.78; N, 5.23. Found: C, 50.17; H, 6.56; N, 5.07. Mp (°C): 177-182.

Reaction of 1 with MeOTf. To a 10 mL CH_2Cl_2 solution of IMes•GaH_2N_3 (**1**) (156 mg, 0.37 mmol) was added MeOTf (163 μL, 1.48 mmol) and the mixture was stirred for 12 hrs. All the volatiles were removed under vacuum and the resulting white solid was washed with 10 mL of hexanes. The product was dried under vacuum to yield **2** as a white powder (202 mg, 80 %). Crystals suitable for X-ray diffraction were grown from CH_2Cl_2/hexanes at -35 °C. ^{1}H, ^{13}C{^{1}H} and ^{19}F NMR spectra: same as compound **2** (see above).

Reaction of 1 with BAr^F$_3$. A solution of BAr^F$_3$ (171 mg, 0.26 mmol) in 10 mL of CH_2Cl_2 was added dropwise to a 5 mL CH_2Cl_2 solution of IMes•GaH_2N_3 (**1**) (110 mg, 0.26 mmol). The mixture was stirred for 2 hrs and the volatiles were removed under vacuum. The product was then dissolved in 10 mL of toluene and heated to 80 °C for 12 hrs to give a colorless solution. All the volatiles were removed under vacuum and the remaining solid was washed with 10 mL of hexanes and dried. The resulting white solid represented the formation of several products. Attempts to fully characterize the products were unsuccessful, however a salt consisting of the [HBAr^F$_3$]$^-$ anion was identified as one of the products by ^{1}H and ^{11}B NMR spectroscopy.[14]

5.5 Crystallographic Data

Table 5.1: Crystallographic data for **1** and **2**.

Compound	**1**•0.5 toluene	**2**
Formula	$C_{24.5}H_{30}GaN_5$	$C_{23}H_{25}F_6GaN_2O_6S_2$
Formula weight	464.25	673.29
Crystal system	monoclinic	monoclinic
Space group	$P2_1/c$	$P2_1/c$
a (Å)	18.7477(5)	12.2187(10)
b (Å)	8.4344(2)	15.2841(13)
c (Å)	15.3559(4)	15.7675(13)
α (deg)	90	90
β (deg)	95.0657(17)	102.522(4)
γ (deg)	90	90
V(Å^3)	2418.68(11)	2874.6(4)
Z	4	4
ρ (g/cm^3)	1.275	1.556
abs coeff (mm^{-1})	1.700	3.391
T (K)	173(1)	173(1)
$2\theta_{max}$ (°)	139.98	145.34
total data	15845	19732
unique data (R_{int})	4451(0.0706)	5488(0.0240)
Obs data [I>2($\sigma(I)$]	3400	5048
Params	308	371
R_1 [I>2$\sigma(I)$]^a	0.0668	0.0330
wR_2 [all data]^a	0.1905	0.0988
max/min $\Delta\rho$ (e$^-$ Å^{-3})	1.249/-0.629	0.355/-0.468

^{a} $R_1 = \sum||F_o| - |F_c||/\sum|F_o|$; $wR_2 = [\sum w(F_o^2 - F_c^2)^2/\sum w(F_o^4)]^{1/2}$

Table 5.2: Crystallographic data for **3** and **4**.

Compound	IMes•$GaH_{1.85}Cl_{0.15}N(SiMe_3)_2$	**4**•1.75 Et_2O
Formula	$C_{27}H_{43.85}Cl_{0.15}GaN_3Si_2$	$C_{40}H_{71.5}Cl_2GaN_3O_{1.75}Si_2$
Formula weight	541.72	819.30
Crystal system	triclinic	monoclinic
Space group	$P\bar{1}$	$P2_1/c$
a (Å)	9.3467(2)	12.2392(2)
b (Å)	9.9910(2)	36.3301(7)
c (Å)	18.9915(4)	11.9340(2)
α (deg)	81.5099(8)	90
β (deg)	79.0123(7)	117.5323(6)
γ (deg)	62.4631(8)	90
V(Å^3)	1540.13(6)	4705.51(14)
Z	2	4
ρ (g/cm^3)	1.168	1.156
abs coeff (mm^{-1})	2.213	2.576
T (K)	173(1)	173(1)
$2\theta_{max}$ (°)	147.80	148.22
total data	11040	33450
unique data (R_{int})	5997(0.0124)	9547(0.0171)
Obs data [I>2($\sigma(I)$)]	5883	9244
Params	321	421
R_1 [I>2$\sigma(I)$]^a	0.0296	0.0324
wR_2 [all data]^a	0.0828	0.0807
max/min $\Delta\rho$ (e$^-$ Å^{-3})	0.305/-0.255	0.312/-0.229

^{a} $R_1 = \sum||F_o| - |F_c||/\sum|F_o|$; $wR_2 = [\sum w(F_o^2 - F_c^2)^2/\sum w(F_o^4)]^{1/2}$

Table 5.3: Crystallographic data for **5**.

Compound	**5**
Formula	$C_{34}H_{54}ClF_3GaN_3O_3SSi_2$
Formula weight	803.21
Crystal system	monclinic
Space group	$P2_1/c$
a (Å)	11.1905(2)
b (Å)	22.5860(4)
c (Å)	16.2428(3)
α (deg)	90
β (deg)	91.6950(12)
γ (deg)	90
V(Å^3)	4103.55(13)
Z	4
ρ (g/cm^3)	1.300
abs coeff (mm^{-1})	2.959
T (K)	173(1)
$2\theta_{max}$ (°)	148.15
total data	26507
unique data (R_{int})	8220(0.0581)
Obs data [I>2($\sigma(I)$)]	6507
Params	475
R_1 [I>2$\sigma(I)$][a]	0.0552
wR_2 [all data][a]	0.1572
max/min $\Delta\rho$ (e$^-$ Å^{-3})	0.597/-0.549

[a] $R_1 = \sum||F_o| - |F_c||/\sum|F_o|$; $wR_2 = [\sum w(F_o^2 - F_c^2)^2/\sum w(F_o^4)]^{1/2}$

5.6 References

1. (a) Jones, C. *Chem. Commun.* **2001**, 2293; (*b*) Kuhn, N.; Al-Sheikh, A. *Coord. Chem. Rev.* **2005**, *249*, 829; (*c*) Wang, Y.; Robinson, G. H. *Dalton Trans.* **2012**, *41*, 337; (*d*) Ghadwal, R. S.; Azhakar, R.; Roesky, H. W. *Acc. Chem. Res.* **2013**, *46*, 444; (*e*) Murphy, L. K.; Robertson, K. N.; Masuda, J. D.; Clyburne, J. A. C. in *N-Heterocyclic Carbenes*, S. P. Nolan (ed.), Wiley-VCH, Weinheim, **2014**, pp-427-497; (*f*) Rivard, E. *Dalton Trans.* **2014**, *43*, 8577; (*g*) Prabusankar, G.; Sathyanarayana, A.; Suresh, P.; Babu, C. N.; Srinivas, K.; Metla, B. P. R. *Coord. Chem. Rev.* **2014**, *269*, 96; (*h*) Präsang, C.; Scheschkewitz, D. *Chem. Soc. Rev.* **2016**, *45,* 900; (*i*) Würtemberger-Pietsch, S.; Radius, U.; Marder, T. B. *Dalton Trans.* **2016**, *45*, 5880.
2. (*a*) Martin, D.; Melaimi, M.; Soleilhavoup, M.; Bertrand, G. *Organometallics* **2011**, *30*, 5304; (*b*) Mondal, K. C.; Roy, S.; Roesky, H. W. *Chem. Soc. Rev.* **2016**, *45*, 1080; (*c*) Soleilhavoup, M.; Bertrand, G. *Acc. Chem. Res.* **2015**, *48*, 256.
3. (*a*) Kuhn, N.; Bohnen, H.; Kreutzberg, J.; Bläser, D.; Boese, R. *J. Chem. Soc., Chem. Commun.* **1993**, 1136; (*b*) Al-Rafia, S. M. I.; Malcolm, A. C.; Liew, S. K.; Ferguson, M. J.; McDonald, R.; Rivard, E. *Chem. Commun.* **2011**, *47*, 6987; (*c*) Y. Wang, Y.; Abraham, M. Y.; Gilliard Jr., R. J.; Sexton, D. R.; Wei, P.; Robinson, G. H. *Organometallics* **2013**, *32*, 6639; (*d*) Ghadwal, R. S. *Dalton Trans.* **2016**, *45*, 16081; (*e*) Powers, K.; Hering-Junghans, C.; McDonald, R.; Ferguson, M. J.; Rivard, E. *Polyhedron* **2016**, *108*, 8; (*f*) Huang, J. -S.; Lee, W. -H.; Shen, C. -T.; Lin, Y. -F.; Liu, Y. -H.; Peng, S. -M.; Chiu, C. -W. *Inorg. Chem.* **2016**, *55*, 12427.

4. (*a*) Braunschweig, H.; Dewhurst, R. D.; Hammond, K.; Mies, J.; Radacki, K.; Vargas, A. *Science* **2012**, *336*, 1420; (*b*) Böhnke, J.; Braunschweig, H.; Ewing, W. C.; Hörl, C.; Kramer, T.; Krummenacher, I.; Mies, J.; Vargas, A. *Angew. Chem. Int. Ed.* **2014**, *53*, 9082.
5. (*a*) Swarnakar, A. K.; Hering-Junghans, C.; Nagata, K.; Ferguson, M. J.; McDonald, R.; Tokitoh, N.; Rivard, E. *Angew. Chem. Int. Ed.* **2015**, *54*, 10666; (*b*) Swarnakar, A. K.; Hering-Junghans, C.; Ferguson, M. J.; McDonald, R.; Rivard, E. *Chem. Sci*. **2017**, *8,* 2337.
6. Solovyev, A.; Chu, Q.; Geib, S. J.; Fensterbank, L.; Malacria, M.; Lacôte, E.; Curran, D. P. *J. Am. Chem. Soc.* **2010**, *132*, 15072.
7. For related donor-acceptor chemistry in the main group, see: (*a*) Marks, T. J. *J. Am. Chem. Soc.* **1971**, *93*, 7090; (*b*) Vogel, U.; Timoshkin, A. Y.; Scheer, M. *Angew. Chem. Int. Ed.* **2001**, *40*, 4409; (*c*) Al-Rafia, S. M. I.; Malcolm, A. C.; McDonald, R.; Ferguson, M. J.; Rivard, E. *Angew. Chem. Int. Ed.* **2011**, *50*, 8354; (*d*) Filippou, A. C.; Baars, B.; Chernov, O.; Lebedev, Y. N.; Schnakenburg, G. *Angew. Chem. Int. Ed.* **2014**, *53*, 565; (*e*) Dielmann, F.; Peresypkina, E. V.; Krämer, B.; Hastreiter, F.; Johnson, B. P.; Zabel, M.; Heindl, C.; Scheer, M. *Angew. Chem. Int. Ed.* **2016**, *55*, 14833; (*f*) Zhou, Y. –P.; Karni, M.; Yao, S.; Apeloig, Y.; Driess, M. *Angew. Chem. Int. Ed.* **2016**, *55*, 15096.
8. (*a*) Amano, H.; Sawaki, N.; Akasaki, I.; Toyoda, Y. *Appl. Phys. Lett.* **1986**, *48*, 353; (*b*) Nakamura, S.; Harada, Y.; Seno, M. *Appl. Phys. Lett.* **1991**, *58*, 2021; (*c*) Morkoc, H.; Mohammad, S. N. *Science* **1995**, *267*, 51.

9. (*a*) Neumayer, D. A.; Cowley, A. H.; Decken, A.; Jones, R. A.; Lakhotia, V.; Ekerdt, J. G. *J. Am. Chem. Soc.* **1995**, *117*, 5893; (*b*) Kouvetakis, J.; McMurran, J.; Matsunaga, P.; O'Keeffe, M.; Hubbard, J. L. *Inorg. Chem.* **1997**, *36*, 1792; (*c*) Dingman, S. D.; Rath, N. P.; Buhro, W. E. *Dalton Trans.* **2003**, 3675; (*d*) Beachley Jr., O. T.; Pazik, J. C.; Noble, M. J. *Organometallics* **1998**, *17*, 2121.
10. Cole, M. L.; Furfari, S. K.; Kloth, M. *J. Organomet. Chem.* **2009**, *694*, 2934; (*b*) Abernethy, C. D.; Cole, M. L.; Jones, C. *Organometallics* **2000**, *19*, 4852; (*c*) Baker, R. J.; Jones, C. *Appl. Organomet. Chem.* **2003**, *17*, 807; (*d*) Francis, M.D.; Hibbs, D. E.; Hursthouse, M. B.; Jones, C.; Smithies, N. A. *J. Chem. Soc., Dalton Trans*. **1998**, 3249.
11. Shirk, A. E.; Shriver, D. F.; Dilts, J. A.; Nutt, R. W. *Inorg. Synth.* **1977**, *17*, 45.
12. (*a*) Ball, G. E.; Cole, M. L.; McKay, A. I. *Dalton Trans.* **2012**, *41*, 946; (*b*) Marion, N.; Escudero-Adán, E. C.; Benet-Buchholz, J.; Stevens, E. D.; Fensterbank, L.; Malacria, M.; Nolan, S. P. *Organometallics* **2007**, *26*, 3256.
13. Haiges, R.; Boatz, J. A.; Williams, J. M.; Christe, K. O. *Angew. Chem. Int. Ed.* **2011**, *50*, 8828.
14. (*a*) Herrington, T. J.; Thom, A. J. W.; White, A. J. P.; Ashley, A. E. *Dalton Trans.* **2012**, *41*, 9019; (*b*) Blagg, R. J.; Lawrence, E. J.; Resner, K.; Oganesyan, V. S.; Herrington, T. J.; Ashley, A. E.; Wildgoose, G. G. *Dalton Trans*. **2016**, *45*, 6023.
15. (*a*) Burns, M. E.; Smith Jr, R. H. *Chem. Eng. News* **1984**, *62*, 2; (*b*) Hassner, A.; Stern, M.; Gottlieb, H. E.; Frolow, F. *J. Org. Chem.* **1990**, *55*, 2304.
16. Jancik, V.; Pineda, L. W.; Stückl, A. C.; Roesky, H. W.; Herbst-Irmer, R. *Organometallics* **2005**, *24*, 1511.

17. Hild, F.; Dagorne, S. *Organometallics* **2012**, *31*, 1189.

18. For related work on using main group species as hydrosilylation/borylation catalysts, see: (*a*) Lummis, P. A.; Momeni, M. R.; Lui, M. W.; McDonald, R.; Ferguson, M. J.; Misklozie, M.; Brown, A.; Rivard, E. *Angew. Chem. Int. Ed.* **2014**, *53*, 9347; (*b*) Revunova, K.; Nikonov, G. I. *Dalton Trans.* **2015**, *44*, 840; (*c*) Chong, C. C.; Kinjo, R. *ACS Catal.* **2015**, *5*, 3238; (*d*) Wiegand, A.-K.; Rit, A. Okuda, J. *Coord. Chem. Rev.* **2016**, *314*, 71; (*e*) Roy, M. M. D.; Ferguson, M. J.; McDonald, R.; Rivard, E. *Chem. Eur. J.* **2016**, *22*, 18236; (*f*) Hadlington, T. J.; Hermann, M.; Frenking, G.; Jones, C. *J. Am. Chem. Soc.* **2014**, *136*, 3028; (*g*) Bismuto, A.; Thomas, S. P.; Cowley, M. J. *Angew. Chem. Int. Ed.* **2016**, *55*, 15356. Initial studies show that **2** is a competent catalyst for the hydrosilylation of benzophenone at room temperature.

19. Pangborn, A. B.; Giardello, M. A.; Grubbs, R. H.; Rosen, R. K.; Timmers, F. J. *Organometallics* **1996**, *15*, 1518.

20. Tang, S.; Monot, J.; El-Hellani, A.; Michelet, B.; Guillot, R.; Bour, C.; Gandon, V. *Chem. Eur. J.* **2012**, *18*, 10239.

21. Kolychev, E. L.; Bannenberg, T.; Freytag, M.; Daniliuc, C. G.; Jones, P. G.; Tamm, M. *Chem. Eur. J.* **2012**, *18*, 16938.

22. Hope, H. *Prog. Inorg. Chem.* **1994**, *41*, 1.

23. Blessing, R. H. *Acta Crystallogr. Sect. A* **1995**, *51*, 33.

24. Sheldrick, G. M. *Acta Crystallogr. Sect. A* **2007**, *64*, 112.

Chapter 6: Isolable Oxoborane (RBO) Complexes and their Role in Mediating C-F Bond Activation

6.1 Introduction

Monomeric oxoboranes (RBO) represent the fundamental building block of synthetically useful boroxines $(RBO)_3$,[1] and due to their unsaturated nature and reactive polar B=O bonds, oxoboranes have only been identified in low temperature matrices or in the gas phase at high temperatures.[2] However encouraging work by Pachaly and West revealed the intermediacy of the bulky oxoborane, (2,4,6-$(H_3C)_3C_6H_2$)BO by trapping experiments.[3,4] This study was complimented by impressive recent work by Braunschweig *et al.* who used metal complexation to stabilize B≡O as a monodentate ligand within the first isolable species featuring B-O triple bonding.[5] Such breakthroughs challenge conventional bonding models and provide chemists with new reactive entities[6] for use as reagents for advanced material design,[7] and for non-metal mediated small molecule activation/catalysis.[8] In this chapter a general donor-acceptor protocol[9] is applied to isolate adducts of ClB=O. It was also found that intermediary oxoboronium cations activate C-F bonds within fluoroalkanes in a synthetically productive manner.

6.2 Results and Discussions

In order to gain access to a target chloroboroxane, ClB=O complex, the requisite adduct IPr•BCl_2OSiMe_3 (**1**)[10] was prepared (eqn. 6.1) by coordinating *in situ* generated $Cl_2BOSiMe_3$ (made from BCl_3 and $NaOSiMe_3$) with the hindered carbene donor IPr [IPr = $(HCNDipp)_2C$:; Dipp = 2,6-$^iPr_2C_6H_3$]. X-ray crystallography confirmed the formation of IPr•BCl_2OSiMe_3 (**1**) which exhibits tetrahedral coordination at boron (Figure 6.1) and a B-O bond length [1.393(2) Å] that is comparable in length to known B-O single bonds.[4e]

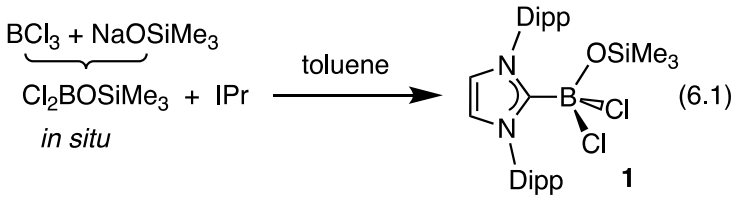

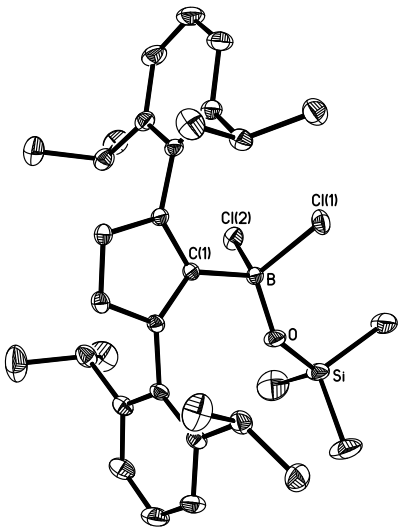

Figure 6.1. Molecular structure of IPr•BCl_2OSiMe_3 (**1**) with thermal ellipsoids presented at a 30 % probability level. All hydrogen atoms have been omitted for clarity. Selected bond lengths (Å) and angles (deg): C(1)-B 1.638(2), B-O 1.393(2), B-Cl(1) 1.904(2), B-Cl(2) 1.903(2); C(1)-B-O 111.72(13), Cl(1)-B-Cl(2) 105.80(9).

Compound **1** was then heated to 100 °C in toluene for 12 hrs in an attempt to release Me_3SiCl and form transient ClB=O, however no reaction transpired. Treatment of **1** with the Lewis acid BAr^{F}_3[11,12] (Ar^F = 3,5-$(F_3C)_2C_6H_3$) followed by heating to 80 °C for 12 hrs afforded partial conversion of **1** (20 % by NMR) into the novel oxoborane donor-acceptor complex IPr•ClB=O•BAr^{F}_3 (**2**; Scheme 6.1) which was later identified by X-ray crystallography (Figure 6.2). Prolonged heating of an equimolar mixture of **1** and BAr^{F}_3 in toluene for 60 hrs at 80 °C yielded IPr•BF_3[13] as the identified carbene-containing product; this observation indicates that activation of the C(sp^3)-F bonds in Ar^F transpired, with strong B-F bond formation as the likely driving force (*vide infra*).

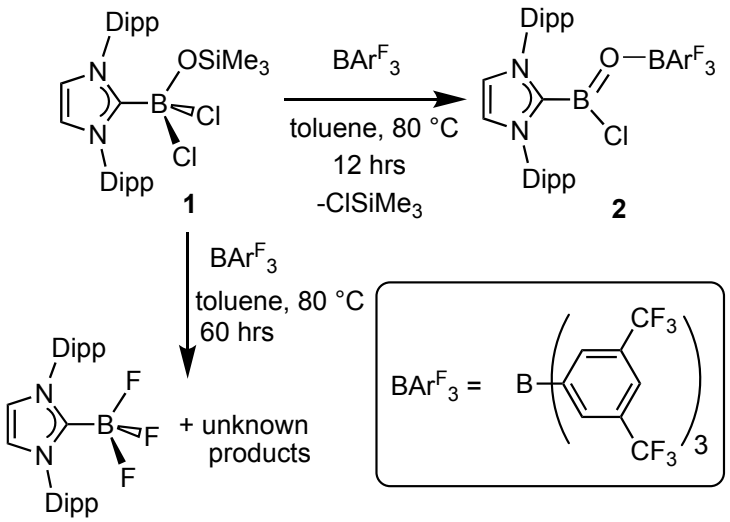

Scheme 6.1. Reaction of **1** with BAr^{F}_3 leading to the formation of IPr•B(Cl)O•BAr^{F}_3 (**2**) and eventual C-F bond activation.

In order to mitigate degradative C-F activation, BAr^{F}_3 was replaced with $B(C_6F_5)_3$ as this borane contains less reactive C(sp^2)-F bonds.[14] Stirring a toluene solution of IPr•BCl_2OSiMe_3 (**1**) and $B(C_6F_5)_3$ at 105 °C for 24 hrs results in the

formation of IPr•B(Cl)O•B(C_6F_5)$_3$ (**3**) as colorless crystals in an isolated yield of 88 %; thus C-F bond activation was effectively suppressed (eqn. 6.2).

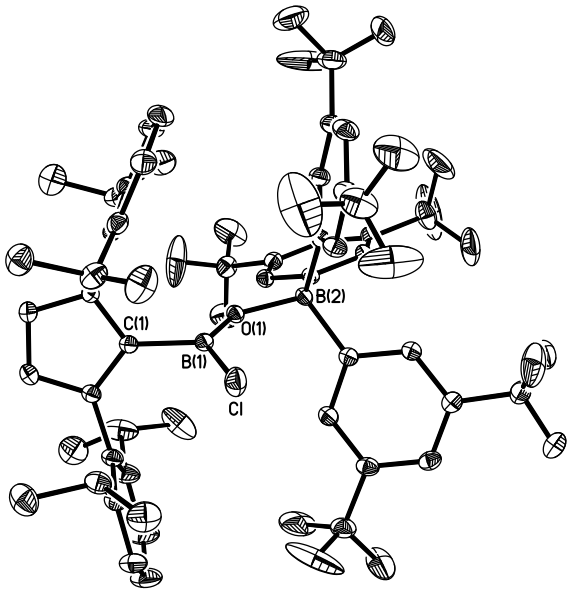

Figure 6.2. Molecular structure of IPr•B(Cl)O•BAr$^F_3$ (**2**) with thermal ellipsoids presented at a 30 % probability level. All hydrogen atoms have been omitted for clarity. Selected bond lengths (Å) and angles (deg): C(1)-B(1) 1.601(3), B(1)-O(1) 1.288(3), B(1)-Cl 1.771(2), B(2)-O(1) 1.549(2); C(1)-B(1)-O(1) 119.55(18), B(1)-O(1)-B(2) 133.00(16), Cl-B(1)-O(1) 126.85(16), C(1)-B(1)-Cl 113.59(14).

Two singlet resonances were found at 26.1 and -2.7 ppm in the ^{11}B NMR spectrum of **3**, in line with the presence of 3- and 4-coordinate environments, respectively. A trigonal planar geometry exists about the oxoborane boron atom in **3** (B(1); Figure 6.3) with a bond angle sum of 359.97(19)°. Most striking was the very short B-O length in **3** [1.296(3)] Å, consistent with B=O π-bond character. A similar B-O bond distance [1.304(2) Å] was found in Cowley's nacnac complex HC{C(CH_3)N(C_6F_5)}$_2$BO•$AlCl_3$,[4c] however the B-O linkage in **3** is substantial longer than the B-O triple bond length of 1.210(3) Å found in Braunschweig's *trans*-PhS(Cy_3P)$_2$PtBO.[5] After $ClSiMe_3$ elimination, the remaining B-Cl bond in **3** is much

shorter than in the precursor IPr•BCl_2OSiMe_3 (**1**) (1.773(3) Å in **3** vs 1.904(2) Å in **1**). A diagnostic ν(BO) IR band is present at 1646 cm^{-1} in **3** which is comparable to the ν(BO) vibration noted in Kinjo's 1,2,3,4-triazaborole-based oxoborane, {CH(^{t}Bu)N(H)N(Ph)N(Dipp)}BO•$AlCl_3$ (1636 cm^{-1}).[4f]

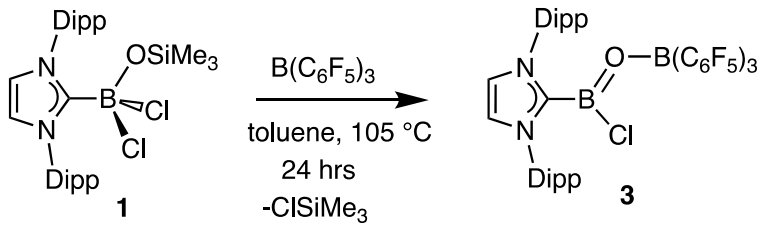

(6.2)

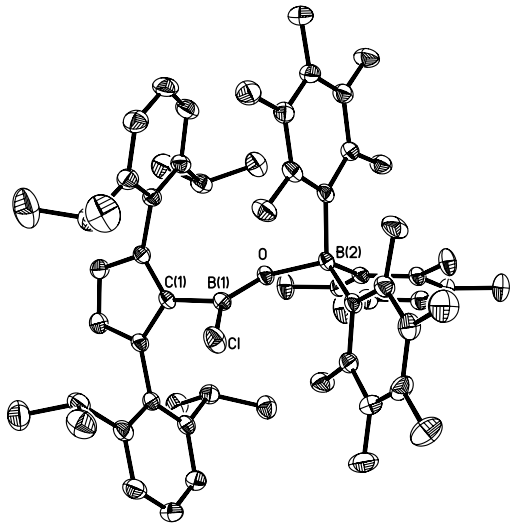

Figure 6.3. Molecular structure of IPr•B(Cl)O•$B(C_6F_5)_3$ (**3**) with thermal ellipsoids presented at a 30 % probability level. All hydrogen atoms have been omitted for clarity. Selected bond lengths (Å) and angles (deg): C(1)-B(1) 1.601(4), B(1)-O(1) 1.296(3), B(1)-Cl(1) 1.773(3), B(2)-O(1) 1.518(3); C(1)-B(1)-O(1) 117.3(2), B(1)-O(1)-B(2) 142.1(2), Cl-B(1)-O(1) 127.7(2), C(1)-B(1)-Cl 114.97(19).

Compounds **1** and **3** were investigated by DFT methods, and as anticipated, NBO analysis afforded a Wiberg Bond Index (WBI) for the central B-O linkage in **3** of 1.123, indicative of double bond character (Figure 6.5). Substantial polarization of the σ and π components of this B-O multiple bond toward O was also found (ca. 83 % of

overall B-O bonding density located at oxygen). Natural Population Analysis (NPA) revealed a higher positive charge, and possible electrophilic character, at the central Cl*B*O unit in **3** (0.887 e) in relation to the boron center in IPr•BCl_2OSiMe_3 (**1**) (0.621 e) (Figures 6.4 and 6.5). The LUMO of **3** has distinct B=O π*-character whereas the B=O π interaction in ClB=O complex is energetically low lying (HOMO-12) (Figure 6.6) .

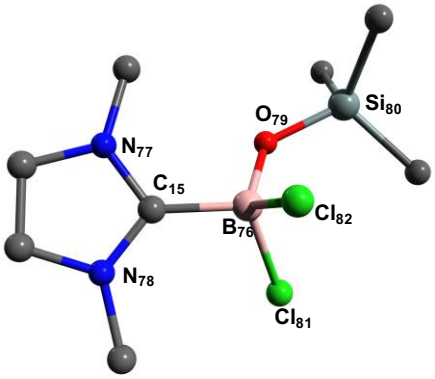

Atom	Charge
C_{15}	0.26169 e
B_{76}	0.62067 e
N_{77}	-0.36590 e
N_{78}	-0.36538 e
O_{79}	-1.12793 e
Si_{80}	2.09948 e
Cl_{81}	-0.2970 e
Cl_{82}	-0.32162 e

Bond	WBI	BD_{theo}	BD_{exp}
C_{15}-B_{76}	0.7609	1.648	1.638(2)
B_{76}-O_{79}	0.7770	1.392	1.393(2)
B_{76}-Cl_{81}	0.9114	1.885	1.903(2)
B_{76}-Cl_{82}	0.8480	1.923	1.904(2)
O_{79}-Si_{80}	0.5310	1.671	1.6441(13)

Figure 6.4. Left: Ball-and-stick representation of the optimized structure of **1** (the majority of the Dipp group and all hydrogen atoms have been omitted for clarity). Right: Atomic charges of the atoms and *WBI*, $BD_{theor.}$, and BD_{exp} of the respective bonds (BD = bond distance).

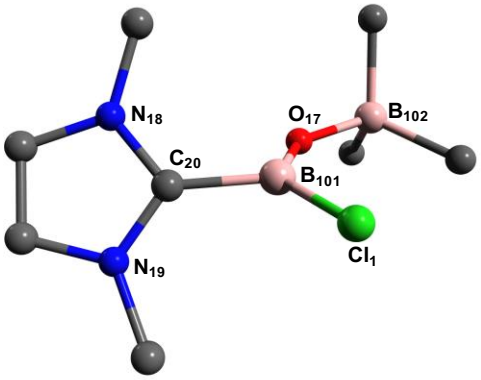

Atom	Charge
C_{20}	0.21223 e
B_{101}	0.86678 e
N_{18}	-0.34523 e
N_{19}	-0.35050 e
O_{17}	-0.84727 e
B_{102}	0.69222 e
Cl_1	-0.19937 e

Bond	WBI	BD_{theo}	BD_{exp}
C_{20}-B_{101}	0.7942	1.601	1.601(4)
B_{101}-O_{17}	1.1217	1.292	1.296(3)
B_{101}-Cl_1	1.0776	1.784	1.773(3)
O_{17}-B_{102}	0.6101	1.503	1.518(3)

Figure 6.5. Left: Ball-and-stick representation of the optimized structure of **3** (the majority of the Dipp and $B(C_6F_5)_3$-groups, as well as all hydrogen atoms have been omitted for clarity). Right: Atomic charges of the atoms and *WBI*, $BD_{theor.}$, and BD_{exp} of the respective bonds (BD = bond distance).

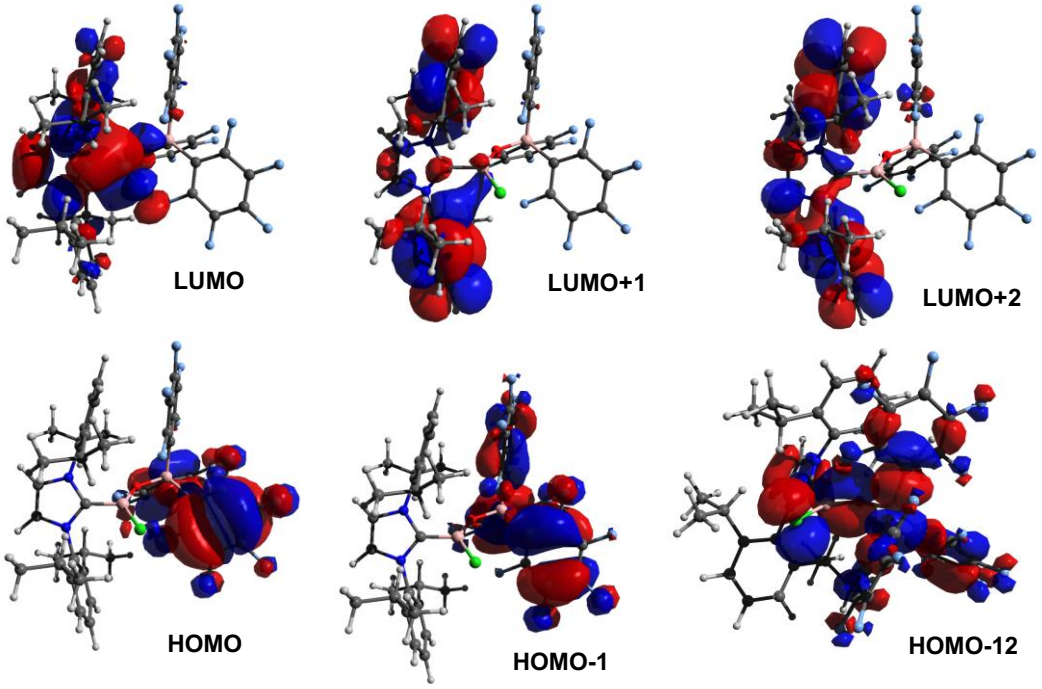

Figure 6.6. Depiction of selected Kohn-Sham orbitals of IPr•BClO•B$(C_6F_5)_3$ (**3**).

Motivated by the presence of a potentially functionalizable B-Cl bond in **3**, attempts were made to synthesize the donor-acceptor complexes of parent oxoborane, HBO or RBO (R = Me or Ph). When IPr•B(Cl)O•B$(C_6F_5)_3$ (**3**) was combined with the hydride source K-selectride (K[HB^{s}Bu$_3$]), no reaction occurred at room temperature or at 80 °C in toluene. However reaction of **3** with MeLi (or PhLi) in Et_2O led to formation of IPr-backbone deptonated[16] product [$(Et_2O)_2$Li][IPr•B(Cl)O•B$(C_6F_5)_3$] (**4•(**$OEt_2)_2$) (eqn. 6.3) in high yields. This product was crystallographically identified as its mixed THF/Et_2O solvate [(THF)(Et_2O)Li]IPr•B(Cl)O•B$(C_6F_5)_3$ (**4**•(THF)(OEt_2)) (Figure 6.7).

Given the possibility for further abstraction of a chloride from the ClB=O unit in **3** (to possibility yield [IPr•B≡O]$^+$), IPr•ClB=O•B$(C_6F_5)_3$ (**3**) was heated to 140 °C

in xylenes for 3 days; this resulted in the complete conversion of **3** into $[IPrH]ClB(C_6F_5)_3$. One possible reaction path is chloride abstraction/transfer by $B(C_6F_5)_3$ to yield a highly reactive oxoboryne adduct $[IPr{\bullet}B{\equiv}O]ClB(C_6F_5)_3$. This transient source of electrophilic $[B{\equiv}O]^+$ could then react with accesible Si-OH groups on the surface of the glass to liberating H^+ (that is trapped as $IPrH^+$).

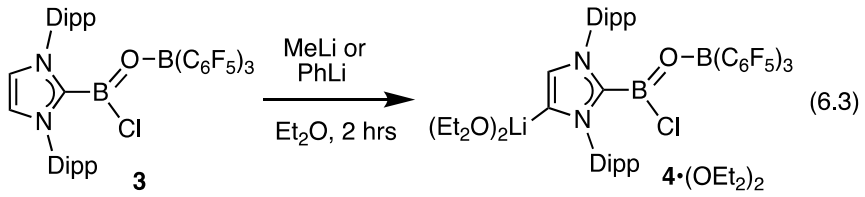

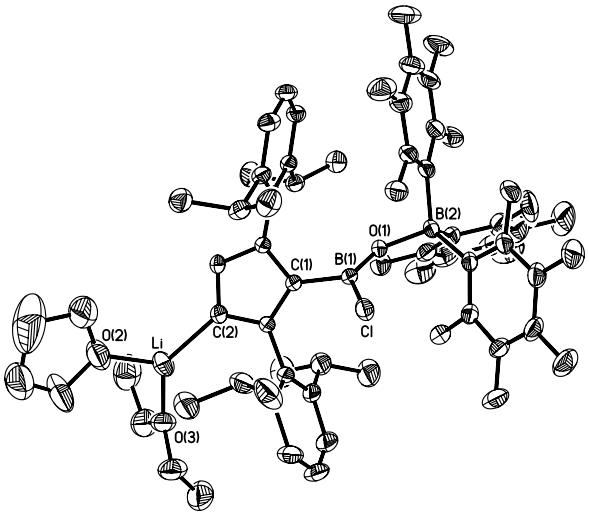

Figure 6.7. Molecular structure of $(THF)(Et_2O)Li[IPr{\bullet}B(Cl)O{\bullet}B(C_6F_5)_3]$ (**4**•$(THF)(OEt_2)$) with thermal ellipsoids presented at a 30 % probability level. All hydrogen atoms have been omitted for clarity. Selected bond lengths (Å) and angles (deg): C(1)-B(1) 1.582(3), B(1)-O(1) 1.297(3), B(1)-Cl(1) 1.790(3), B(2)-O(1) 1.501(3), Li-C(2) 2.082(6); C(1)-B(1)-O(1) 120.0(2), B(1)-O(1)-B(2) 141.88(19), Cl-B(1)-O(1) 126.09(18), C(1)-B(1)-Cl 113.81(17).

An attempt was also made to form $[BO]^+$ oxoborylium adducts, $IPr{\bullet}BO{\bullet}B(C_6F_5)_3]A^-$ (A^- = weakly coordinating anion), by treating **3** with either $NaBAr^F{}_4$ (Ar = 3,5-$(F_3C)_2C_6H_3$) or AgOTf (OTf = OSO_2CF_3). However in each case

no reaction occurred, a likely consequence of the short and strong B-Cl bond in **3** (*vide supra*).

During investigations geared towards understanding how the ClBO adduct **3** is formed from IPr•$Cl_2BOSiMe_3$ (**1**), a salt containing a possible boronium cation intermediate $[IPr•BCl(OSiMe_3)]^+$ was formed (eqn. 6.4). Specifically $AlCl_3$ was combined with **1** in toluene to afford a quantitative yield of $[IPr•BCl(OSiMe_3)]AlCl_4$ (**5**). X-ray crystallography (Figure 6.8) showed the presence of a rigorously three-coordinate and planar boron center in **5**, with B-O and B-Cl distances [1.310(4) Å and 1.758(3) Å, respectively] that match well those noted within the ClB=O unit of **3**.

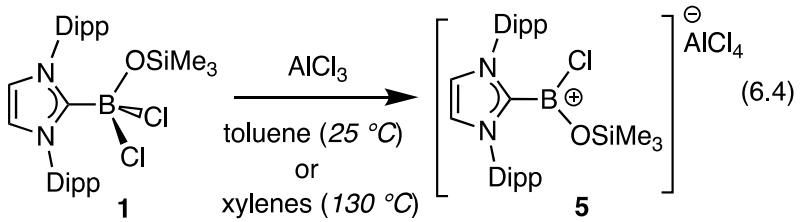

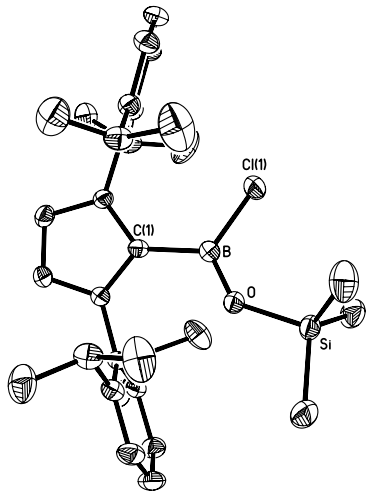

Figure 6.8. Molecular structure of $[IPr•BCl(OSiMe_3)]AlCl_4$ (**5**) with thermal ellipsoids presented at a 30 % probability level. All hydrogen atoms and $AlCl_4$ anion have been omitted for clarity. Selected bond lengths (Å) and angles (deg): C(1)-B 1.578(4), B-O 1.310(4), B-Cl(1) 1.758(3), O-Si 1.7023(19); C(1)-B-O 119.3(2), C(1)-B-Cl(1) 119.1(2), Cl(1)-B-O 121.7(2).

NBO analysis of the $[IPr{\bullet}BCl(OSiMe_3)]^+$ cation in **5** afforded a WBI of 1.049 for the B-O bond, pointing towards partial double bond character; the computed NPA charge for the boron center in **5** (0.863 e) is also similar to that found within the ClB=O array in **3** (Figure 6.9). Thus possible parallel C-F activation chemistry could be instigated by the electrophilic boron center in **5**.

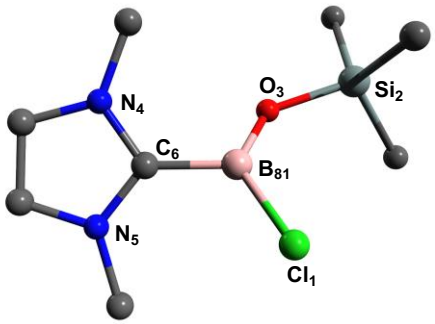

Atom	Charge	Bond	WBI	BD_{theo}	BD_{exp}
C_6	0.16841 e	C_6-B_{81}	0.8261	1.591	1.578(4)
B_{81}	0.86317 e				
N_4	-0.33419 e	B_{81}-O_3	1.0494	1.315	1.310(4)
N_5	-0.33310 e				
O_3	-1.02892 e	B_{81}-Cl_1	1.1300	1.772	1.758(3)
Cl_1	-0.16289 e				
Si_2	2.06232 e	O_3-Si_2	0.4424	1.732	1.7023(19)

Figure 6.9. Left: Ball-and-stick representation of the optimized structure of **5** (the majority of the Dipp and all hydrogen atoms have been omitted for clarity). Right: Atomic charges of the atoms and *WBI*, $BD_{theor.}$, and BD_{exp} of the respective bonds (BD = bond distance).

$[IPr{\bullet}BCl(OSiMe_3)]AlCl_4$ (**5**) is thermally stable with no sign of decomposition or $ClSiMe_3$ release found after heating in xylenes at 130 °C for 18 hrs. However compound **5** was found to be an effective reagent for the C-F activation and functionalization (halogenation) of 1-fluoroadamantane, AdF (eqn. 6.5). When **5** was reacted with 3 equivalents of Ad-F at 80 °C in toluene for 16 hrs, the formation of 1-chloroadamantane (Ad-Cl) occurred (75 % isolated yield), along with the spectroscopic identification of $IPr{\bullet}BF_3$ (60 %), an $[IPrH]^+$ salt (32 %) and a minor unknown carbene-containing species (<8 %) as co-products. As before, strong B-F bond formation is likely driving this process. Attempts to induce $C(sp^2)$-F activation by heating **5** in fluorobenzene at 80 °C gave no reaction. To best of my knowledge

this is the first example of selective C-F activation by a cationic borinium species. Along these lines, Stephan and co-workers reported that organofluorophosphonium salt ($[(F_5C_6)_3PF]B(C_6F_5)_4$) is an active catalyst for the hydrodefluorination of fluoroalkanes.[14] These transformations are buoyed by other examples of selective C-F activation by electron deficient main group element centers.[16]

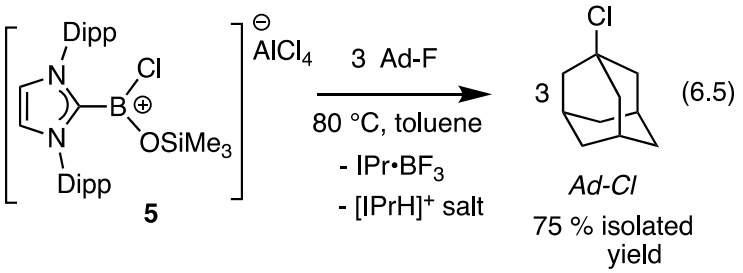

(6.5)

6.3 Conclusions

The first coordination complex of chlorooxoborane, ClB=O was synthesized. These ClB=O adducts could be a viable sources of the electrophilic oxoborylium cation $[B{\equiv}O]^+$, an inorganic analogue of CO. Moreover initial studies show that the electron deficient oxoborinum cations $[IPr{\bullet}BCl(OSiMe_3)]AlCl_4$ (**5**) can successfully activate/functionalize alkane C-F bonds.

6.4 Experimental Details

6.4.1 Materials and Instrumentation. All reactions were performed using standard Schlenk line techniques under an atmosphere of nitrogen or in an inert atmosphere glovebox (Innovative Technology, Inc.). Solvents were dried using a Grubbs-type solvent purification system[17] manufactured by Innovative Technology, Inc., degassed (freeze-pump-thaw method), and stored under an atmosphere of nitrogen prior to use.

BCl_3 (1.0 M in heptane), K-Selectride (K[$^sBu_3BH$], 1.0 M in THF), MeLi (1.6 M in Et_2O), PhLi (1.8 M in Bu_2O), $AlCl_3$, AgOTf (OTf = OSO_2CF_3) were purchased from Sigma-Aldrich and were used as received. 1-Fluoroadamantane and $NaOSiMe_3$ (1.0 M in CH_2Cl_2) and were purchased from TCI and Acros Chemicals, respectively, and used as received. $NaBAr^F_4$ (Ar^F = 3,5-$(F_3C)_2C_6H_3$) was purchased from Matrix Chemicals and dried under vacuum at 110 °C for 48 hrs prior to use. IPr,[18] BAr^F_3,[11] $B(C_6F_5)_3$,[19] were prepared according to literature procedures. ^1H, ^{11}B, $^{13}C\{^1H\}$, ^{29}Si NMR and $^{19}F\{^1H\}$ NMR spectra were recorded on a Varian iNova 400 spectrometer and referenced externally to $SiMe_4$ (^1H, $^{13}C\{^1H\}$ and ^{29}Si), $F_3B{\bullet}OEt_2$ (^{11}B) and $CFCl_3$ (^{19}F), respectively. Elemental analyses were performed by the Analytical and Instrumentation Laboratory at the University of Alberta. Infrared spectra were recorded on a Nicolet IR100 FTIR spectrometer as Nujol mulls between NaCl plates. Melting points were measured in sealed glass capillaries under nitrogen using a MelTemp apparatus and are uncorrected.

6.4.2 X-ray Crystallography. Crystals of suitable quality for X-ray diffraction studies were removed from a vial in a glovebox and immediately covered with a thin layer of hydrocarbon oil (Paratone-N). A suitable crystal was selected, mounted on a glass fiber, and quickly placed in a low-temperature stream of nitrogen on an X-ray diffractometer.[20] All data were collected at the University of Alberta using a Bruker APEX II CCD detector/D8 diffractometer or using Cu or Mo Kα radiation with the crystals cooled to −100 °C. The data were corrected for absorption through Gaussian integration from the indexing of the crystal faces.[21] Structures were solved using

direct method *SHELXD* or intrinsic phasing *SHELXT*.[22] Structure refinement was accomplished using *SHELXL-2014*.[23] All carbon-bound hydrogen atoms were assigned positions on the basis of the sp^2 or sp^3 hybridization geometries of their attached carbon atoms, and were given thermal parameters 20 % greater than those of their parent atoms.

6.4.3 Synthetic Procedures

Synthesis of IPr•BCl_2OSiMe_3 (1).

To a 300 mL toluene solution of BCl_3 (2.0 mL, 1.0 M in heptane, 2.0 mmol) was added $NaOSiMe_3$ (2.0 mL, 1.0 M in CH_2Cl_2, 2.0 mmol) dropwise and the mixture was stirred for 30 minutes at room temperature. A 100 mL toluene solution of IPr (777 mg, 2.0 mmol) was then added dropwise and the resulting cloudy mixture was stirred for another 12 hrs. The mixture was then filtered though Celite and the solvent was removed from the filtrate to yield **1** as a white solid as **1** (750 mg, 68 %). Crystals suitable for X-ray diffraction were grown from toluene/hexanes at -35 °C. ^{1}H NMR (400 MHz, C_6D_6): δ = 7.21 (t, $^3J_{H-H}$ = 7.6 Hz, 2H, Ar*H*), 7.08 (d, $^3J_{H-H}$ = 7.6 Hz, 4H, Ar*H*), 6.29 (s, 2H, N-C*H*-), 2.86 (sept, $^3J_{H-H}$ = 6.8 Hz, 4H, C*H*(CH_3)$_2$), 1.44 (d, $^3J_{H-H}$ = 6.8 Hz, 12H, CH(C*H*$_3$)$_2$), 0.99 (d, $^3J_{H-H}$ = 6.8 Hz, 12H, CH(C*H*$_3$)$_2$), 0.13 (s, 9H, Si(C*H*$_3$)$_3$). ^{13}C{^{1}H} NMR (125 MHz, C_6D_6): δ = 145.5 (N-*C*H), 135.3 (Ar*C*), 130.6 (Ar*C*), 124.1 (Ar*C*), 123.8 (Ar*C*), 29.4 (*C*H(CH_3)$_2$), 25.7 (CH(*C*H$_3$)$_2$), 23.0 (CH(*C*H$_3$)$_2$), 2.6 (Si(*C*H$_3$)$_3$). ^{11}B{^{1}H} NMR (128 MHz, C_6D_6): δ = 1.7 (s). ^{29}Si NMR (79 MHz, C_6D_6): δ = 8.4 (s). Anal. Calcd. for $C_{30}H_{45}BCl_2N_2OSi$: C, 64.40; H, 8.11; N, 5.01. Found: C, 64.64; H, 8.19; N, 4.97. Mp (°C): >190.

Synthesis of IPr•B(Cl)O•B(C_6F_5)$_3$ (3).

A 4 mL toluene solution of B(C_6F_5)$_3$ (390 mg, 0.76 mmol) was added to a 4 mL toluene solution of IPr•BCl_2OSiMe_3 (**1**) (426 mg, 0.76 mmol) in a Teflon-capped Schlenk flask. The mixture was stirred for 25 hrs at 105 °C to yield a colorless solution. The volatiles were removed then from the mixture under reduced pressure. The resulting oil was washed with 5 mL of hexanes and dried under vacuum to yield **3** as a white powder (645 mg, 88 %). Crystals suitable for X-ray diffraction were grown from Et_2O/hexanes at -35 °C. ^{1}H NMR (400 MHz, C_6D_6): δ = 7.15 (t, $^3J_{H-H}$ = 7.6 Hz, 2H, Ar*H*), 6.91 (d, $^3J_{H-H}$ = 8.0 Hz, 4H, Ar*H*), 6.18 (s, 2H, N-C*H*-), 2.42 (sept, $^3J_{H-H}$ = 7.0 Hz, 4H, C*H*(CH_3)$_2$), 1.17 (d, $^3J_{H-H}$ = 6.5 Hz, 12H, CH(C*H*$_3$)$_2$), 0.80 (d, $^3J_{H-H}$ = 6.5 Hz, 12H, CH(C*H*$_3$)$_2$). ^{13}C{^{1}H} NMR (125 MHz, C_6D_6): δ = 148.5 (d, $^1J_{C-F}$ = 240.8 Hz, *o*-*C*$_6$F$_5$), 144.9 (N-*C*H), 139.8 (d, $^1J_{C-F}$ = 247.2 Hz, *p*-*C*$_6$F$_5$), 137.2 (dm, $^1J_{C-F}$ = 246.5 Hz, *m*-*C*$_6$F$_5$), 132.2 (Ar*C*), 131.4 (Ar*C*), 29.3 (*C*H(CH_3)$_2$), 25.8 (CH(*C*H$_3$)$_2$), 21.8 (CH(*C*H$_3$)$_2$). ^{11}B{^{1}H} NMR (128 MHz, C_6D_6): δ = 26.1 (br, *B*O), -2.7 (s, *B*(C_6F_5)$_3$). ^{19}F NMR (376 MHz, C_6D_6): δ = -131.3 (d, $^3J_{F-F}$ = 20.1 Hz, 6F, *o*-*C*$_6$F$_5$), 160.4 (t, $^3J_{F-F}$ = 18.6 Hz, 3F, *p*-*C*$_6$F$_5$), 165.6 (t, $^3J_{F-F}$ = 18.7 Hz, 6F, *m*-*C*$_6$F$_5$). IR (Nujol, cm^{-1}): 1646 (s, $\upsilon_{B=O}$). Anal. Calcd. for $C_{45}H_{36}B_2ClF_{15}N_2O$: C, 56.14; H, 3.77; N, 2.91. Found: C, 56.07; H, 3.80; N, 2.84. Mp (°C): >190.

Thermolysis of IPr•B(Cl)O•B(C_6F_5)$_3$ (3) and formation of [IPrH][ClB(C_6F_5)$_3$]

A solution of IPr•B(Cl)O•B(C_6F_5)$_3$ (**3**) (170 mg, 0.17 mmol) in 10 mL of xylenes was stirred at 140 °C in a Teflon-capped Schlenk flask for 3 days. The volatiles were removed from the mixture under vacuum and the resulting product was washed with

5 mL of hexanes and dried to yield [IPrH][ClB(C_6F_5)$_3$] as a light yellow powder (135 mg, 84 %). Crystals suitable for X-ray diffraction were grown from Et_2O/hexanes at -35 °C. ^{1}H NMR (400 MHz, C_6D_6): δ = 7.77 (s, 1H, N-C*H*-N), 7.21 (t, $^3J_{H-H}$ = 7.6 Hz, 2H, Ar*H*), 6.94 (d, $^3J_{H-H}$ = 7.6 Hz, 4H, Ar*H*), 6.65 (s, 2H, N-C*H*-), 2.02 (sept, $^3J_{H-H}$ = 6.8 Hz, 4H, C*H*(CH_3)$_2$), 0.99 (d, $^3J_{H-H}$ = 6.8 Hz, 12H, CH(C*H*$_3$)$_2$), 0.94 (d, $^3J_{H-H}$ = 6.8 Hz, 12H, CH(C*H*$_3$)$_2$). ^{13}C{^{1}H} NMR (125 MHz, C_6D_6): δ = 148.8 (d, $^1J_{C-F}$ = 242.8 Hz, *o*-*C*$_6$F$_5$), 144.7 (N-*C*H), 139.4 (d, $^1J_{C-F}$ = 253.9 Hz, *p*-*C*$_6$F$_5$), 137.8 (N-*C*H-N), 137.4 (d, $^1J_{C-F}$ = 259.4 Hz, *m*-*C*$_6$F$_5$), 132.7 (Ar*C*), 129.5 (Ar*C*), 125.2 (Ar*C*), 124.9 (Ar*C*), 29.2 (*C*H(CH_3)$_2$), 23.7 (CH(*C*H$_3$)$_2$), 23.6 (CH(*C*H$_3$)$_2$). ^{11}B{^{1}H} NMR (128 MHz, C_6D_6): δ = -6.5 (s, Cl*B*(C_6F_5)$_3$). ^{19}F NMR (376 MHz, C_6D_6): δ = -131.8 (d, $^3J_{F-F}$ = 18 Hz, 6F, *o*-*C*$_6$F$_5$), 161.5 (t, $^3J_{F-F}$ = 20.6 Hz, 3F, *p*-*C*$_6$F$_5$), 166.3 (t, $^3J_{F-F}$ = 20.6 Hz, 6F, *m*-*C*$_6$F$_5$). Anal. Calcd. for $C_{45}H_{37}BClF_{15}N_2$: C, 57.68; H, 3.98; N, 2.99. Found: C, 57.61; H, 4.10; N, 2.91. Mp (°C): 165-170.

Reaction of IPr•B(Cl)O•B(C_6F_5)$_3$ (3) with MeLi.

To a solution of IPr•B(Cl)O•B(C_6F_5)$_3$ (**3**) (96.5 mg, 0.10 mmol) in 5 mL of Et_2O was added MeLi (1.6 M solution in Et_2O, 90 μL, 0.14 mmol) and the mixture was stirred for 3 hrs at room temperature. The volatiles were removed under reduced pressure and the resulting product was washed with 5 mL of hexanes. The remaining solid was dried under vacuum to yield **4**•(OEt_2)$_2$ as a white powder (93 mg, 83 %). Crystals suitable for X-ray diffraction were grown from fluorobenzene/hexanes at -35 °C. During crystallization in the glovebox, one of the Et_2O molecule was replaced by the residual THF in glovebox environment and the molecular structure of the resulting

compound was determined as [(THF)(Et_2O)Li]IPr•B(Cl)O•B(C_6F_5)$_3$ (**4**•(THF)(OEt_2)) by single crystal X-ray diffraction analysis. NMR data for **4**•(OEt_2)$_2$: ^{1}H NMR (400 MHz, C_6D_6): δ = 7.29 (t, $^3J_{H-H}$ = 7.6 Hz, 2H, Ar*H*), 7.11 (d, $^3J_{H-H}$ = 8.0 Hz, 2H, Ar*H*), 6.99 (d, $^3J_{H-H}$ = 8.0 Hz, 2H, Ar*H*), 6.43 (s, 1H, N-C*H*-), 2.85 (q, $^3J_{H-H}$ = 7.2 Hz, 8H, Et_2O), 2.74-2.84 (m, 4H, C*H*(CH_3)$_2$), 1.35 (d, $^3J_{H-H}$ = 6.8 Hz, 6H, CH(C*H*$_3$)$_2$), 1.31 (d, $^3J_{H-H}$ = 6.8 Hz, 6H, CH(C*H*$_3$)$_2$), 1.09 (d, $^3J_{H-H}$ = 6.8 Hz, 6H, CH(C*H*$_3$)$_2$), 0.98 (d, $^3J_{H-H}$ = 6.8 Hz, 6H, CH(C*H*$_3$)$_2$), 0.65 (t, $^3J_{H-H}$ = 7.2 Hz, 12H, Et_2O). ^{13}C{^{1}H} NMR (125 MHz, C_6D_6): δ = 148.6 (dm, $^1J_{C-F}$ = 234.0 Hz, *o*-*C*$_6$F$_5$), 145.4 (N-*C*H), 144.9 (N-*C*H), 139.6 (dm, $^1J_{C-F}$ = 246.5 Hz, *p*-*C*$_6$F$_5$), 139.6 (Ar*C*), 137.1 (dm, $^1J_{C-F}$ = 267.6 Hz, *m*-*C*$_6$F$_5$), 134.1 (Ar*C*), 133.4 (Ar*C*), 130.7 (Ar*C*), 129.5 (Ar*C*), 124.1 (Ar*C*), 123.8 (Ar*C*), 65.6 (coord. Et_2O), 29.1 (*C*H(CH_3)$_2$), 28.8 (*C*H(CH_3)$_2$), 26.2 (CH(*C*H$_3$)$_2$), 25.5 (CH(*C*H$_3$)$_2$), 22.6 (CH(*C*H$_3$)$_2$), 22.3 (CH(*C*H$_3$)$_2$), 14.1 (coord. Et_2O). ^{11}B{^{1}H} NMR (128 MHz, C_6D_6): δ = -3.2 (s, *B*(C_6F_5)$_3$). ^{19}F NMR (376 MHz, C_6D_6): δ = -131.5 (d, $^3J_{F-F}$ = 19.5 Hz, 6F, *o*-*C*$_6$F$_5$), 161.6 (t, $^3J_{F-F}$ = 20.3 Hz, 3F, *p*-*C*$_6$F$_5$), 166.2 (t, $^3J_{F-F}$ = 19.1 Hz, 6F, *m*-*C*$_6$F$_5$). ^{7}Li{^{1}H} NMR (155 MHz, C_6D_6): δ = 0.4 (s). Anal. Calcd. for $C_{53}H_{55}B_2ClF_{15}LiN_2O_3$: C, 56.99; H, 4.96; N, 2.51. Found: C, 56.49; H, 4.95; N, 2.44. Mp (°C): 135-140.

Reaction of IPr•B(Cl)O•B(C_6F_5)$_3$ (3) with PhLi: Alternate preparation of 4•(OEt_2)

To a solution of IPr•B(Cl)O•B(C_6F_5)$_3$ (**3**) (109 mg, 0.11 mmol) in 5 mL of Et_2O was added PhLi (1.8 M solution in Bu_2O, 75 μL, 0.13 mmol) and the mixture was stirred for 3 hrs at room temperature. The volatiles were removed under reduced pressure

and the resulting product was washed with 5 mL of hexanes. The remaining product was dried under vacuum to yield **4**•$(OEt_2)_2$ as a white powder (120 mg, 89 %); the spectroscopic data matched those listed above.

Synthesis of [IPr•B(Cl)OSiMe$_3$][AlCl$_4$] (5).

A solution of IPr•BCl_2OSiMe_3 (**1**) (201 mg, 0.36 mmol) in 4 mL of toluene was added to a suspension of $AlCl_3$ (48 mg, 0.36 mmol) in 4 mL of toluene and the mixture was stirred for 3 hrs at room temperature. The mother liquor was decanted from the resulting precipitate and the remaining solid dried under vacuum to yield **5** as a white solid (235 mg, 94 %). Crystals suitable for X-ray diffraction were grown from fluorobenzene/hexanes at -35 °C. ^{1}H NMR (400 MHz, $CDCl_3$): δ = 7.97 (s, 2H, N-C*H*-), 7.62 (t, $^3J_{H-H}$ = 8.0 Hz, 2H, Ar*H*), 7.38 (d, $^3J_{H-H}$ = 8.0 Hz, 4H, Ar*H*), 2.35 (sept, $^3J_{H-H}$ = 7.0 Hz, 4H, C*H*(CH_3)$_2$), 1.28 (d, $^3J_{H-H}$ = 6.5 Hz, 12H, CH(C*H*$_3$)$_2$), 1.20 (d, $^3J_{H-H}$ = 7.0 Hz, 12H, CH(C*H*$_3$)$_2$), -0.07 (s, 9H, Si(C*H*$_3$)$_3$). ^{13}C{^{1}H} NMR (125 MHz, $CDCl_3$): δ = 144.4 (N-*C*H), 132.4 (Ar*C*), 131.7 (Ar*C*), 129.7 (Ar*C*), 125.1 (Ar*C*), 29.3 (*C*H(CH_3)$_2$), 24.9 (CH(*C*H$_3$)$_2$), 23.7 (CH(*C*H$_3$)$_2$), 0.5 (Si(*C*H$_3$)$_3$). ^{11}B{^{1}H} NMR (128 MHz, $CDCl_3$): δ = 28.6 (s). Anal. Calcd. for $C_{30}H_{45}AlBCl_5N_2OSi$: C, 52.01; H, 6.55; N, 4.04. Found: C, 52.32; H, 6.64; N, 3.93. Mp (°C): 148-150.

Reaction of [IPr•B(Cl)OSiMe$_3$][AlCl$_4$] (4) with 1-fluoroadamantane (Ad-F).

[IPr•B(Cl)OSiMe$_3$][AlCl$_4$] (**4**) (177 mg, 0.26 mmol) and Ad-F (119 mg, 0.77 mmol) were combined in 10 mL of toluene within a Teflon-capped Schlenk flask stirred for 24 hrs at 100 °C. The volatiles were removed under vacuum to yield a viscous semi-

solid. 5 mL of hexanes was then added to the product mixture followed by stirring for 15 minutes. The soluble fraction was separated from the precipitate by filtration and the solvent was removed from the filtrate to yield 1-chloroadamantane (Ad-Cl) as spectroscopically pure solid (98 mg, 75 %).[24]

Furthermore, the insoluble fraction was also recovered and dried and characterized by multinuclear NMR spectroscopy. The $^{1}H\{^{11}B\}$, ^{19}F and ^{11}B NMR spectra of the resulting product revealed the formation of IPr•BF_3 (60 %),[13] an $[IPrH]^+$ salt (32 %) and a minor amount of an unknown IPr-containing species (>8 %).

Reaction of IPr•BCl_2OSiMe_3 (1) with BAr^F_3 and formation of IPr•B(Cl)O•BAr^F_3 (2)

A 5 mL toluene suspension of BAr^F_3 (378 mg, 0.58 mmol) was added to a 5 mL toluene solution of IPr•BCl_2OSiMe_3 (**1**) (325 mg, 0.58 mmol) in a Teflon-capped Schlenk flask. The mixture was stirred for 12 hrs at 80 °C to yield a colorless solution. The volatiles were removed from the mixture under reduced pressure. The resulting oil was washed with 5 mL of hexanes and dried under vacuum. A small batch of crystals suitable for X-ray diffraction were grown from Et_2O/hexanes at -35 °C which identified the product as IPr•B(Cl)O•BAr^F_3 (**2**). The NMR spectra of the product mixture suggested only 20-25 % conversion to product **2**. NMR data for compound **2**: ^{1}H NMR (400 MHz, C_6D_6): δ = 7.81 (s, 6H, *o*-$C_6H_3(CF_3)_2$), 7.67 (s, 3H, *p*-$C_6H_3(CF_3)_2$), 6.19 (s, 2H, N-C*H*-), 2.41 (sept, $^{3}J_{H-H}$ = 6.8 Hz, 4H, C*H*$(CH_3)_2$), 1.09 (d, $^{3}J_{H-H}$ = 6.4 Hz, 12H, CH(CH_3)$_2$), 0.83 (d, $^{3}J_{H-H}$ = 6.4 Hz, 12H, CH(CH_3)$_2$). The aromatic protons of Dipp overlapped with those from starting material. ^{11}B NMR

(128 MHz, C_6D_6): δ = 27.2 (br, *B*ClO). ^{19}F NMR (376 MHz, C_6D_6): δ = -62.2 (s, BAr^{F}_3).

Heating a mixture of **1** and BAr^{F}_3 at 80 °C in toluene for 60 hrs results in formation of IPr•BF_3 (24 %)[13] and another unidentified IPr-containing product (76 %).

6.5 Crystallographic Data

Table 6.1: Crystallographic data for **1** and **2**.

Compound	**1**	**2**•Et_2O
Formula	$C_{30}H_{45}BCl_2N_2OSi$	$C_{55}H_{55}B_2ClF_{18}N_2O_2$
Formula weight	559.48	1175.08
Crystal system	orthorhombic	monoclinic
Space group	*$P2_12_12_1$ (No. 19)*	*$P2/c$ (No. 13)*
a (Å)	13.5717 (2)	20.5429 (8)
b (Å)	14.3900 (2)	13.2877 (5)
c (Å)	16.5638 (3)	22.3054 (8)
α (deg)	90	90
β (deg)	90	111.6851 (15)
γ (deg)	90	90
V(Å^3)	3234.86(9)	5657.8 (4)
Z	4	4
ρ (g/cm^3)	1.149	1.380
abs coeff (mm^{-1})	2.333	1.500
T (K)	173(1)	173(1)
$2\theta_{max}$ (°)	147.98	148.46
total data	23154	39969
unique data(R_{int})	6562 (0.0205)	11237 (0.0237)
Obs data [I>2($\sigma(I)$]	6485	10483
Params	339	758
R_1 [I>2$\sigma(I)$]^a	0.0252	0.0625
wR_2 [all data]^a	0.0713	0.1739
max/min $\Delta\rho$ (e Å^{-3})	0.311/-0.271	0.994/-0.794

^{a} $R_1 = \sum||F_o| - |F_c||/\sum|F_o|$; $wR_2 = [\sum w(F_o^2 - F_c^2)^2/\sum w(F_o^4)]^{1/2}$

Table 6.2: Crystallographic data for **3** and **4**.

Compound	**3**•Et_2O	**4**•(Et_2O)(THF)
Formula	$C_{49}H_{46}B2ClF_{15}N_2O_2$	$C_{53}H_{53}B_2ClF_{15}N_2O_3$
Formula weight	1036.95	1114.98
Crystal system	monoclinic	monoclinic
Space group	*P*2$_1$/*c (No. 14)*	*P*2/*n (No. 14)*
a (Å)	14.3031 (19)	18.3193 (9)
b (Å)	15.706 (2)	15.4693 (8)
c (Å)	23.224 (3)	20.7292 (10)
α (deg)	90	90
β (deg)	107.7367 (15)	112.4560 (6)
γ (deg)	90	90
V(Å^3)	4969.1 (11)	5428.9 (5)
Z	4	4
ρ (g/cm^3)	1.386	1.364
abs coeff (mm^{-1})	0.174	0.165
T (K)	173(1)	173(1)
$2\theta_{max}$ (°)	51.58	52.78
total data	36599	41048
unique data(R_{int})	9498 (0.0670)	11111 (0.0261)
Obs data [I>2($\sigma(I)$)]	5853	8132
Params	595	712
R_1 [I>2$\sigma(I)$]^a	0.0506	0.0613
wR_2 [all data]^a	0.1516	0.2007
max/min $\Delta\rho$ (e Å^{-3})	0.397/-0.318	0.837/-0.530

^{a} $R_1 = \sum||F_o| - |F_c||/\sum|F_o|$; $wR_2 = [\sum w(F_o^2 - F_c^2)^2/\sum w(F_o^4)]^{1/2}$

Table 6.3: Crystallographic data for **5**.

Compound	**5**
Formula	$C_{30}H_{45}AlBCl5N_2OSi$
Formula weight	692.81
Crystal system	monoclinic
Space group	*P*2$_1$/*c (No. 14)*
a (Å)	9.8574 (5)
b (Å)	18.9588 (9)
c (Å)	20.6447 (10)
α (deg)	90
β (deg)	99.8346 (7)
γ (deg)	90
V(Å^3)	3801.5 (3)
Z	4
ρ (g/cm^3)	1.211
abs coeff (mm^{-1})	0.461
T (K)	173(1)
$2\theta_{max}$ (°)	52.86
total data	27816
unique data(R_{int})	7813 (0.0443)
Obs data [I>2($\sigma(I)$)]	5373
Params	373
R_1 [I>2$\sigma(I)$]^a	0.0570
wR_2 [all data]^a	0.1674
max/min $\Delta\rho$ (e Å^{-3})	0.619/-0.537

^{a} $R_1 = \sum||F_o| - |F_c||/\sum|F_o|$; $wR_2 = [\sum w(F_o^2 - F_c^2)^2/\sum w(F_o^4)]^{1/2}$

6.6 References

1. (*a*) Coté, A. P.; Benin, A. I.; Ockwig, N. W.; O'Keeffe, M.; Matzger, A. J.; Yaghi, O. M. *Science* **2005**, *310*, 1166; (*b*) El-Kaderi, H. M.; Hunt, J. R.; Mendoza-Cortes, J. L.; Cote, A. P.; Taylor, R. E.; O'Keeffe, M.; Yaghi, O. M. *Science* **2007**, *316*, 268; (*c*) De, P.; Gondi, S. R.; Roy, D.; Sumerlin, B. S. *Macromolecules* **2009**, *42*, 5614; (*d*) Perttu, E. K.; Arnold, M.; Iovine, P. M. *Tetrahedron Lett.* **2005**, *46*, 8753; (*e*) Hawkins, R. T.; Lennarz, W. J.; Snyder, H. R. *J. Am. Chem. Soc.* **1960**, *82*, 3053; (*f*) Li, Y.; Ding, J.; Day, M.; Tao, Y.; Lu, J.; D'iorio, M. *Chem. Mater.* **2003**, *15,* 4936.
2. (*a*) Kirk, R. W.; Timms, P. L. *Chem. Commun.* **1967**, 18; (*b*) Kroto, H. W. *Chem. Soc. Rev*. **1982**, *11*, 435; (*c*) Groteklaes, M.; Paetzold, P. *Chem. Ber.* **1988**, *121*, 809; (*d*) Burkholder T. R.; Andrews, L. *J. Chem. Phys*. **1991**, *95*, 8697; (*e*) Page, M. *J. Phys. Chem*. **1989**, *93*, 3639; (*f*) Paetzold, P.; Neyses, S.; Géret, L.; *Z. Anorg. Allg. Chem.* **1995**, *621*, 732; (*g*) Osiac, M.; Röpcke, J.; Davies, P. B. *Chem. Phys. Lett.* **2001**, *344*, 92; (*h*) Bettinger, H. *Organometallics* **2007**, *26*, 6263.
3. Pachaly, B.; West, R. *J. Am. Chem. Soc.* **1985**, *107*, 2987.
4. For related studies on isolating reactive LBO species (L = supporting ligand(s)), see: (*a*) Nöth, H. *Angew. Chem. Int. Ed. Engl.* **1988**, *27*, 1603; (*b*) Ito, M.; Tokitoh, N.; Okazaki, R. *Tet. Lett.* **1997**, *38*, 4451; (*c*) Vidovic, D.; Moore, J. A.; Jones, J. N.; Cowley, A. H. *J. Am. Chem. Soc*. **2005**, *127*, 4566; (*d*) Wang, Y.; Hu, H.; Zhang, J.; Cui, C. *Angew. Chem. Int. Ed*. **2011**, *50*, 2816; (*e*) Del Grosso, A.; Clark, E. R.; Montoute, N.; Ingleson, M. J. *Chem. Commun*. **2012**, *48*, 7589; (*f*) Loh, Y. K.; Chong, C. C.; Ganguly, R.; Li, Y.; Vidovic, D.; Kinjo, R. *Chem. Commun*. **2014**, *50*, 8561.

5. Braunschweig, H.; Radacki, K.; Schneider, A. *Science* **2010**, *328*, 345.

6. (*a*) Paetzold, P. *Adv. Inorg. Chem.* **1987**, *31*, 123; (*b*) Fischer, R. C.; Power, P. P. *Chem. Rev.* **2010**, *110*, 3877; (*c*) Wang, Y.; Robinson, G. H. *Dalton Trans*. **2012**, *41*, 337; (*d*) Mizuhata, Y.; Sasamori, T.; Tokitoh, N. *Chem. Rev.* **2009**, *109*, 3479; (*e*) Asay, M.; Jones, C.; Driess, M. *Chem. Rev.* **2011**, *111*, 354; (*f*) He, G.; Shynkaruk, O.; Lui, M. W.; Rivard, E. *Chem. Rev.* **2014**, *114*, 7815; (*g*) Brand, J.; Braunschweig, H.; Sen, S. S. *Acc. Chem. Res.* **2014**, *47*, 180; (*h*) Präsang. C.; Scheschkewitz, D. *Chem. Soc. Rev.* **2016**, *45*, 900.

7. (*a*) Parker, D. S. N.; Dangi, B. B.; Balucani, N.; Stranges, D.; Mebel, A. M.; Kaiser, R. I. *J. Org. Chem.* **2013**, *78*, 11896; (*b*) Liu, H.; Jin, P.; Xue, Y.-M.; Dong, C.; Li, X.; Tang, C.-C.; Du, X.-W. *Angew. Chem. Int. Ed.* **2015**, *54*, 7051; (*c*) Purkait; Swarnakar, A. K.; De Los Reyes, G. B.; Hegmann, F. A.; Rivard, E.; Veinot, J. G. C. *Nanoscale* **2015**, *7*, 2241; (*d*) Velian, A.; Cummins, C. C. *Science* **2015**, *348*, 1001.

8. (*a*) Power, P. P. *Nature* **2010**, *463*, 171; (*b*) Hadlington, T. J.; Hermann, M.; Frenking, G.; Jones, C. *J. Am. Chem. Soc.* **2014**, *136*, 3028.

9. (*a*) Rivard, E. *Chem. Soc. Rev.* **2016**, *45*, 989; FLP can also be viewed as donor-acceptor complexes: (*b*) Stephan, D. W.; Erker, G. *Angew. Chem. Int. Ed.* **2010**, *49*, 46.

10. The related dihalosilylether species $Br_2BOSiMe_3$ was prepared previously (see ref. 5).

11. Kolychev, E. L.; Bannenberg, T.; Freytag, M.; Daniliuc, C. G.; Jones, P. G.; Tamm, M. *Chem. Eur. J.* **2012**, *18*, 16938.

12. For the use of BAr^F_3 to intercept main group species, see: (*a*) Swarnakar, A. K.; Hering-Junghans, C.; Nagata, K.; Ferguson, M. J.; McDonald, R.; Tokitoh, N;

Rivard, E. *Angew. Chem. Int. Ed.* **2015**, *54*, 10666; (*b*) Swarnakar, A. K.; Hering-Junghans, C.; Ferguson, M. J.; McDonald, R.; Rivard, E. *Chem. Sci.* **2017**, *8*, 2337.

13. Brahmia, M. M.; Malacria, M.; Curran, D. P.; Fensterbank, L.; Lacôte, E. *Synlett.* **2013**, *24*, 1260.
14. Caputo, C. B.; Hounjet, L. J.; Dobrovetsky, R.; Stephan, D. W. *Science* **2013**, *341*, 1374.
15. Wang, Y.; Xie, Y.; Abraham, M. Y.; Wei, P.; Schaefer III, P. H. F.; Schleyer, P. v. R.; Robinson, G. H. *J. Am. Chem. Soc.* **2010**, *132*, 14370.
16. (*a*) Stahl, T.; Klare, H. F. T.; Oestreich, M. *ACS Catal*. **2013**, *3*, 1578; (*b*) Douvris, C.; Ozerov, O. V. *Science* **2008**, *321*, 1188; (*c*) Caputo, C. B.; Stephan, D. W. *Organometallics* **2012**, *31*, 27; (*d*) Alcarazo, M.; Gomez, C.; Holle, S.; Goddard, R. *Angew. Chem. Int. Ed.* **2010**, *49*, 5788; (*e*) Ahrens, M.; Scholz, G.; Braun, T.; Kemnitz, E. *Angew. Chem. Int. Ed*. **2013**, *52*, 5328.
17. Pangborn, A. B.; Giardello, M. A.; Grubbs, R. H.; Rosen, R. K.; Timmers, F. J. *Organometallics* **1996**, *15*, 1518.
18. Jafarpour, L.; Stevens, E. D.; Nolan, S. P. *J. Organomet. Chem*. **2000**, *606*, 49.
19. (*a*) Kuprat, M.; Lehmann, M.; Schulz, A.; Villinger, A. *Organometallics* **2010**, *29*, 1421; (*b*) Massey, A. G.; Park, A. J. *J. Organomet. Chem.* **1964**, *2*, 245.
20. Hope, H. *Prog. Inorg. Chem.* **1994**, *41*, 1.
21. Blessing, R. H. *Acta Crystallogr.* **1995**, *A51*, 33.
22. Sheldrick, G. M. *Acta Crystallogr*. **2008**, *A64*, 112.

23. Beurskens, P. T.; Beurskens, G.; de Gelder, R.; Smits, J. M. M.; Garcia-Garcia, S.; Gould, R. O. DIRDIF-2008; Crystallography Laboratory, Radboud University: Nijmegen, The Netherlands **2008**.

24. Candish, L.; Standley, E. A.; Gómez-Suμrez, A.; Mukherjee, S.; Glorius, F. *Chem. Eur. J.* **2016**, *22*, 9971.

7.1 Summary and Future Work

Chapter 2 described the use of a Wittig reagent as a donor to encapsulate the reactive targets, GeH_2 and SnH_2 within the donor-acceptor complexes Ph_3PCMe_2•GeH_2•BH_3 and Ph_3PCM_2•SnH_2•$W(CO)_5$, respectively. Parallel chemistry with commonly employed N- and P-based donors was unsuccessful due to their weaker electron donating ability compared to the carbon-based donors. This work can be considered as the most recent contribution of a Wittig reagent as a donor in main group element chemistry. In addition, the donor-acceptor GeH_2 complex (Ph_3PCMe_2•GeH_2•BH_3) was found to be a potential precursor for the one-pot synthesis of germanium nanoparticles (GeNPs). GeNPs with hydrophilic and hydrophobic surfaces were synthesized by thermal or microwave assisted decomposition of the bottleable GeH_2 precursor in presence of capping ligands, 3-dimethylamino-1-propyne and 1-dodecene, respectively. The 3-dimethylamino-1-propene capped-GeNPs show blue photoluminescent which may be due to the surface defects and are the subjects of future investigations.

The future work involves the synthesis of GeH_2 donor-acceptor complex with comparatively smaller Lewis base to improve the yield of GeNPs. The precursor complex, Ph_3PCMe_2•GeH_2•BH_3 contains 18.5 wt % of germanium; by replacing Ph_3PCMe_2 with $^iPr_3PCMe_2$ the percentage of germanium can be increased to 25.0 wt %. Moreover, use of $ImMe_2$ ($ImMe_2$ = $[H_2CNMe]_2C$:) as a Lewis base can enrich the Ge percentage upto 39 wt % in the corresponding donor-acceptor complex (Figure 7.1).

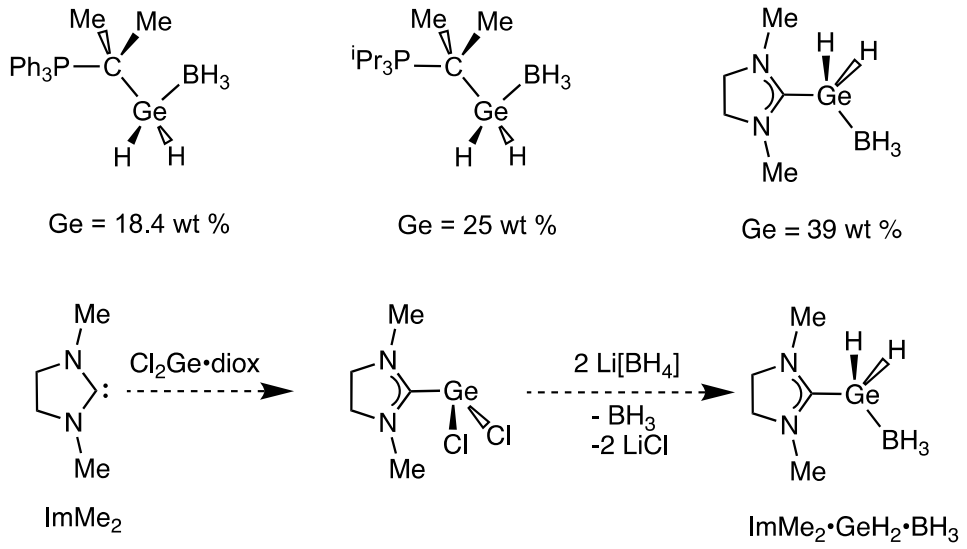

Figure 7.1. Top: Weight percentage of Ge in Ph_3PCMe_2•GeH_2•BH_3, $^iPr_3PCMe_2$•GeH_2•BH_3 and $ImMe_2$•GeH_2•BH_3. Bottom: Planned synthetic strategy for $ImMe_2$•GeH_2•BH_3

Chapter 3 described the reactivity of metal center Lewis basic complex $CpRh(PMe_2Ph)_2$ toward electron deficient "ECl_2•$W(CO)_5$" (E = Ge and Sn) and $PbCl_2$. The less Lewis acidic "$SnCl_2$•$W(CO)_5$" and $PbCl_2$ formed usual Lewis acid-base adducts with $CpRh(PMe_2Ph)_2$, whereas the more Lewis acidic "$GeCl_2$•$W(CO)_5$" gave the Cp-H activation product. In addition, the reactivity of "ECl_2•$W(CO)_5$" (E = Ge and Sn) toward $Pt(PCy_3)_2$ was explored which resulted in the oxidative addition of Ge-Cl and Sn-Cl bonds to give the products, $ClPt(PCy_3)_2E(Cl)$•$W(CO)_5$ (E = Ge and Sn). Attempts to form the corresponding group 14 hydrides via H^- addition to E-Cl residues were unsuccessful, and in each case hydride addition to the resulting complexes led to the generation of free metal Lewis base complexes or decomposition product mixture.

In the future the Cp group of $CpRh(PMe_2Ph)_2$ can be replaced with Cp* to prevent the Cp ring C-H activation during the reaction with "$GeCl_2$•$W(CO)_5$".

Reaction of $Cp^*Rh(PMe_2Ph)_2$ with $THF{\bullet}GeCl_2{\bullet}W(CO)_5$ could form the desired Lewis acid-base adduct, $Cp^*Rh(PMe_2Ph)_2{\bullet}GeCl_2{\bullet}W(CO)_5$. Futhermore, the stabilization of Ge-H bonds is less challenging compared to Sn-H and Pb-H;[1] therefore, stabilization of the GeH_2 unit could be possible within the donor-acceptor complex $Cp^*Rh(PMe_2Ph)_2{\bullet}GeH_2{\bullet}W(CO)_5$ (Scheme 7.1). An ultimate goal would be to generate mixed metal donor-acceptor complexes of EH_2 units (E = Ge, Sn and Pb) for the later preparation of binary E_xM_y (M = metal) bulk or nanomaterials.

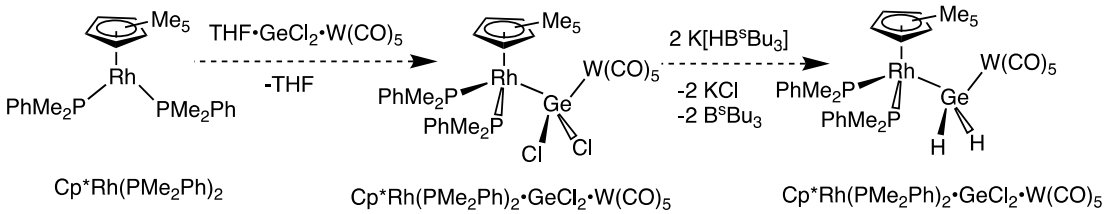

Scheme 7.1. Use of Cp* to prevent the C-H activation of Cp ring and stabilization of GeH_2 complex.

Chapter 4 involved the Lewis acid (LA) assisted elimination of N_2 followed by H^- migration from B to N of an carbene-azidoborane adduct $IPr{\bullet}BH_2N_3$ (IPr = $[(HCNDipp)_2C:]$, Dipp = 2,6-$^iPr_2C_6H_3$) to yield the first stable adduct of the parent iminoborane $IPr{\bullet}HB{=}NH{\bullet}BAr^F{}_3$ (Ar^F = 3,5-$C_6H_3(CF_3)_2$). However, the use of bulky substituents restricted the access to the HBNH array by potential reagents/catalysts. Therefore, a more reactive HBNH adduct with less sterically hindered *N*-heterocyclic carbene was prepared and the reactivity of this species was investigated in detailed. In addition, a donor-stabilized azidohydride boronium cation $[BH(N_3)]^+$ was also synthesized and its reactivity was explored. However, the detailed investigations aimed at forming bulk boron nitride (BN) from these species under mild conditions were not directly successful. Future work would involve the thermal decomposition

(*ca.* 200-400 °C) study of the HBNH complexes to form the bulk boron nitride (BN) materials.

The other possible way to synthesize molecular BN is presented in Scheme 7.2. If NHC•BI_3 is treated with $^nBu_4N[N_3B(C_6F_5)_3]$[2] it could form NHC•BI_2N_3•$B(C_6F_5)_3$; later, reaction with a suitable reducing agent may lead to the formation of molecular BN precursor NHC•BN•$B(C_6F_5)_3$ (Scheme 7.2).

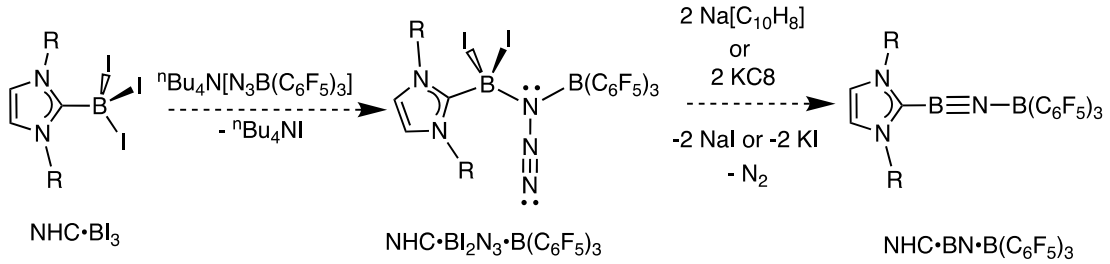

Scheme 7.2. Synthesis of molecular BN from NHC•BI_3.

Chapter 5 described the successful isolation of *N*-heterocyclic carbene complexes of azido- and amido-gallane. Moreover, a similar donor-acceptor stabilization approach via Lewis acid-assisted N_2 elimination was applied to isolate the HGa=NH complex from the azidogallane adduct IMes•GaH_2N_3 (IMes = $[(HCNMes)_2C:]$, Mes = 2,4,6-$Me_3C_6H_2$). However the high reactivity of Ga-H bonds did not permit the isolation of such species.

The amido-gallium hydride complexes (IMes•$GaH(OTf)_2$ and IMes•GaH_2N_3) have similar structural features as the recently reported active ketone hydrosilylation/borylation catalyst IPr•Zn(H)OTf•THF[3a] and thus future work would involve exploring the catalytic activity[3] of these main group, NHC-supported, gallium hydrides for hydrosilylation and hydroboration of ketone in more detail. Also, initial

studies show that IMes•GaH(OTf)$_2$ is a competent catalyst for the hydrosilylation of benzophenone at room temperature (eqn. 7.1).

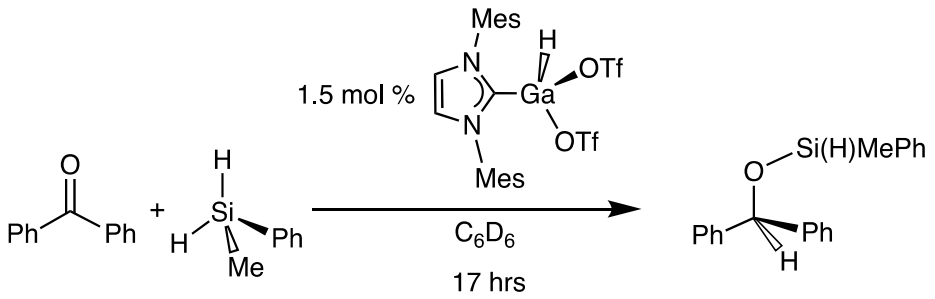

(7.1)

Chapter 6 involved the borane-based Lewis acid assisted elimination of $ClSiMe_3$ from IPr•BCl_2OSiMe_3 to form the donor-acceptor adduct of chlorooxoborane, IPr•BClO•$B(C_6F_5)_3$. Initial experiment showed that the loss of $[B{\equiv}O]^+$ occurred during the thermal decomposition of the chlorooxoborane complex IPr•BClO•$B(C_6F_5)_3$. One possible reaction path is chloride abstraction/transfer by $B(C_6F_5)_3$ to yield a highly reactive oxoborane adduct [IPr•B≡O]$ClB(C_6F_5)_3$. This transient source of electrophilic $[B{\equiv}O]^+$ could then react with accesible Si-OH groups on the surface of the glass to liberating H^+ (that is trapped as $IPrH^+$). Therefore, to prove this hypothesis, future work would involve the reaction of IPr•BClO•$B(C_6F_5)_3$ with Ph_3SiOH to trap $[B{\equiv}O]^+$ as boroxine $[Ph_3SiOBO]_3$ (Scheme 7.3).

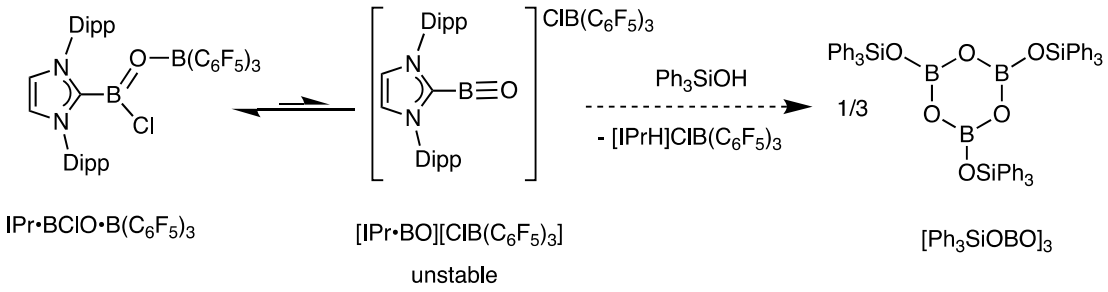

Scheme 7.3. Reaction of IPr•BClO•$B(C_6F_5)_3$ with Ph_3SiOH to trap $[B{\equiv}O]^+$ as boroxine.

In the future a similar strategy could be applied to isolate the elusive HBO donor-acceptor complex using known $Me_2S{\bullet}BH_2Cl$ as the borane precursor (Scheme 7.4).

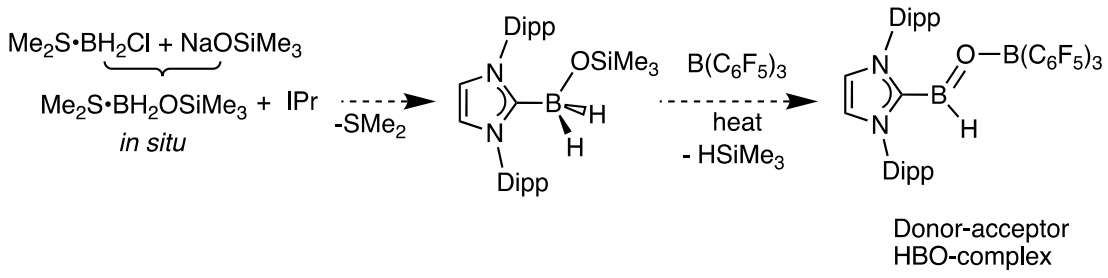

Scheme 7.4. Stabilization of donor-acceptor complex of HBO.

7.1 Reference

1. (*a*) Al-Rafia, S. M. I.; Malcolm, A. C.; Liew, S. K.; Ferguson, M. J.; Rivard, E. *J. Am. Chem. Soc.* **2011**, *133*, 777; (*b*) Swarnakar, A. K.; McDonald, S. M.; Deutsch, K. C.; Choi, P.; Ferguson, M. J.; McDonald, R.; Rivard, E. *Inorg. Chem*. **2014**, *53*, 8662.
2. Fox, A. R.; Cummins, C. C. *J. Am. Chem. Soc.* **2009**, *131*, 5716.
3. (*a*) Lummis, P. A.; Momeni, M. R.; Lui, M. W.; McDonald, R.; Ferguson, M. J.; Misklozie, M.; Brown, A.; Rivard, E. *Angew. Chem. Int. Ed.* **2014**, *53*, 9347; (*b*) Revunova, K.; Nikonov, G. I. *Dalton Trans.* **2015**, *44*, 840; (*c*) Chong, C. C.; Kinjo, R. *ACS Catal.* **2015**, *5*, 3238; (*d*) Wiegand, A.-K.; Rit, A. Okuda, J. *Coord. Chem. Rev.* **2016**, *314*, 71; (*e*) Roy, M. M. D.; Ferguson, M. J.; McDonald, R.; Rivard, E. *Chem. Eur. J.* **2016**, *22*, 18236; (*f*) Hadlington, T. J.; Hermann, M.; Frenking, G.; Jones, C. *J. Am. Chem. Soc.* **2014**, *136*, 3028; (*g*) Bismuto, A.; Thomas, S. P.; Cowley, M. J. *Angew. Chem. Int. Ed.* **2016**, *55*, 15356.

Complete Bibliography

Chapter 1

1. (*a*) Welch, G. C.; Juan, R. R. S.; Masuda, J. D.; Stephan, D. W. *Science* **2006**, *314*, 1124; (*b*) Welch, G. C.; Stephan, D. W. *J. Am. Chem. Soc*. **2007**, *129*, 1880; (*c*) McCahill, J. S. J.; Welch, G. C.; Stephan, D. W. *Angew. Chem. Int. Ed.* **2007**, *46*, 4968; (*d*) Chase, P. A.; Jurca, T.; Stephan, D. W. *Chem. Commun.* **2008**, 1701; (*e*) Hounjet, L. J.; Stephan, D. W. *Org. Process Res. Dev.* **2014**, *18*, 385.
2. (*a*) Manasevit, H. M. *Appl. Phys. Lett*. **1968**, *12*, 156; (*b*) Cowley, A. H.; Jones, R. A. *Polyhedron* **1994**, *13*, 1149; (*c*) Maury, F. *Adv. Mater*. **1991**, *3*, 542; (*d*) Thangaraju, B.; Kaliannan, P. *J. Phys. D: Appl. Phys.* **2000**, *33*, 1054; (*e*) Knapp, C. E.; Carmalt, C. J. *Chem. Soc. Rev.* **2016**, *45*, 1036; (*f*) Malik, M. D.; Afzaal, M.; O'Brien, P. *Chem. Rev*. **2010**, *110,* 4817; (*g*) Ekerdt, J. G.; Sun, Y. -M.; Szabo, A.; Szulczewski, G. J.; White, J. M. *Chem. Rev*. **1996**, *96*, 1499 and references therein.
3. (*a*) Power, P. P. *Chem. Rev.* **1999**, *99*, 3463; (*b*) Mizuhata, Y.; Sasamori, T.; Tokitoh, N. *Chem. Rev.* **2009**, *109*, 3479; (*c*) Power, P. P. *Nature* **2010**, *463*, 171; (*d*) Fischer, R. C.; Power, P. P. *Chem. Rev*. **2010**, *810*, 3877; (*e*) Rivard, E. *Chem. Soc. Rev.* **2016**, *45*, 989.
4. (*a*) Rivard, E.; Power, P. P. *Inorg. Chem.* **2007**, *46*, 10047; (*b*) Kays, D. L. *Chem. Soc. Rev.* **2016**, *45*, 1004.
5. (*a*) Stender, M.; Phillips, A. D.; Wright, R. J.; Power, P. P. *Angew. Chem. Int. Ed.* **2002**, *41*, 1785; (*b*) Phillips, A. D.; Wright, R. J.; Olmstead, M. M.; Power, P. P. *J. Am. Chem. Soc.* **2002**, *124*, 5930; (*c*) Pu, L.; Twamley, B.; Power, P. P. *J. Am. Chem. Soc.* **2000**, *122*, 3524.

6. Marks, T. J.; Newman, A. R. *J. Am. Chem. Soc*. **1973**, *95*, 769.

7. (*a*) Braunschweig, H.; Dewhurst, R. D.; Hammond, K.; Mies, J.; Radacki, K.; Vargas, A. *Science* **2012**, *336*, 11420; (*b*) Wang, Y.; Xie, Y.; Wei, P.; King, R. B.; Schaefer III, H. F.; Schleyer, P. v. R.; Robinson, G. H. *J. Am. Chem. Soc.* **2008**, *130*, 14970.

8. Gavrilova, A. L.; Bosnich, B. *Chem. Rev.* **2004**, *104*, 349.

9. (*a*) Wang, Y.; Robinson, G. H. *Inorg. Chem*. **2011**, *50*, 12326; (*b*) Rivard, E. *Dalton Trans.* **2014**, *43*, 8577; (*c*) Soleilhavoup, M.; Bertrand, G. *Acc. Chem. Res.* **2015**, *58*, 256.

10. (*a*) Beswick, M. A.; Palmer, J. S.; Wright, D. S. *Chem. Soc. Rev.* **1998**, *27*, 225; (*b*) Jutzi, P.; Burford, N. *Chem. Rev.* **1999**, *99*, 969.

11. (*a*) Almenningen, A.; Haaland, A.; Motzfeldt, T. *J. Organomet. Chem*. **1967**, *7*, 97; (*b*) Jutzi, P.; Kanne, D.; Kruger, C. *Angew. Chem. Int. Ed. Engl.* **1986**, *25*, 164; (*c*) Panatonni, C.; Bombieri, G.; Croatto, U. *Acta. Crystallogr*. **1966**, *21A*, 823; (*d*) Jutzi, P.; Kohl, F.; Hofman, P.; Kruger, C.; Tsay, Y. –H. *Chem. Ber.* **1980**, *113*, 757; (*e*) Cowley, A. H.; Jutzi, P.; Kohl, F. X.; Lasch, J. G.; Norman, N. C.; Schltiter. E. *Angew. Chem. Int. Ed. Engl.* **1984**, *23*, 616.

12. (*a*) Filippou, A. C.; Philippopoulos, A. I.; Portius, P.; Neumann, D. U. *Angew. Chem. Int. Ed*. **2000**, *39*, 2778; (*b*) Filippou, A. C.; Portius, P.; Philippopoulos, A. I. *Organometallics* **2002**, *21,* 653.

13. (*a*) Voigt, A.; Filipponi, S.; Macdonald, C. L. B.; Gorden, J. D.; Cowley, A. H. *Chem. Commun*. **2000**, 911; (*b*) Dohmeier, C.; Schnockel, H.; Robl, C.; Uwe, S.;

Ahlrichs, R. *Angew. Chem. Int. Ed. Engl.* **1993**, *32*, 1655; (*c*) Burns, C. T.; Shapiro, P. J.; Budzelaar, P. H. M.; Willett, R.; Vij, A. *Organometallics* **2000,** *19,* 3361.

14. (*a*) Jutzi, P.; Wippermann, T.; Kruger, C.; Kraus, H. –J. *Angew. Chem. Int. Ed. Engl.* **1983**, *22*, 250; (*b*) Wiacek, R. J.; Jones, J. N.; Macdonald, C. L. B.; Cowley, A. H. *Can. J. Chem*. **2002**, *80*, 1518.
15. (*a*) Schiemenz, B.; Power, P. P. *Organometallics* **1996**, *15*, 958; (*b*) Simons, R. S.; Haubrich, S. T.; Mork, B. V.; Niemeyer, M.; Power, P. P. *Main Group Chem.* **1998**, *2*, 275; (*c*) Du, C. -J. F.; Hart, H.; Ng, D. K. -K. *J. Org. Chem.* **1986**, *51*, 3162; (*d*) Saednya, A.; Hart, H. *Synthesis* **1996**, *12*, 1455.
16. Su, J.; Li, X.-W.; Crittendon, R. C.; Robinson, G. H. *J. Am. Chem. Soc.* **1997**, *119*, 5471.
17. (*a*) Bytheway, I.; Lin, Z. *J. Am. Chem. Soc.* **1998**, *120*, 12133; (*b*) Xie, Y.; Schaefer, H. F.; Robinson, G. H. *Chem. Phys. Lett.* **2000**, *317*, 174.
18. Takagi, N.; Schmidt, M. W.; Nagase, S. *Organometallics* **2001**, *20*, 1646.
19. (*a*) Hardman, N. J.; Wright, R. J.; Phillips, A. D.; Power, P. P. *Angew. Chem. Int. Ed.* **2002**, *41*, 2842; (*b*) Wright, R. J.; Phillips, A. D.; Hardman, N. J.; Power, P. P. *J. Am. Chem. Soc.* **2002**, *124*, 8538; (*c*) Wright, R. J.; Phillips, A. D.; Hino, S.; Power, P. P. *J. Am. Chem. Soc.* **2005**, *127*, 4794.
20. Okazaki, R.; Unno, M.; Inamoto, N. *Chem. Lett.* **1987**, 2293.
21. Tokitoh, N.; Sasamori, T.; Okazaki, R. *Chem. Lett.* **1998**, 725.
22. (*a*) Tokitoh, N.; Arai, Y.; Okazaki, R.; Nagase, S. *Science* **1997**, *277*, 78; (*b*) Sasamori, T.; Takeda, N.; Tokitoh, N. *Chem. Commun*. **2000**, 1353.
23. Tokitoh, N.; Matsumoto, T.; Okazaki, R. *Bull. Chem. Soc. Jpn*. **1999**, *72*, 1165.

24. Okazaki, R.; Tokitoh, N. *Acc. Chem. Res.* **2000**, *33*, 625.

25. Suzuki, H.; Tokitoh, N.; Okazaki, R. Nagase, S.; Goto, M. *J. Am. Chem. Soc.* **1994**, *116*, 11578.

26. (*a*) Tokitoh, N.; Matsumoto, T.; Manmaru, K.; Okazaki, R. *J. Am. Chem. Soc.* **1993**, *115*, 8855; (*b*) Matsumoto, T.; Tokitoh, N.; Okazaki, R. *Angew. Chem. Int. Ed. Engl.* **1994**, *33*, 2316; (*c*) Matsumoto, T.; Tokitoh, N.; Okazaki, R. *J. Am. Chem. Soc.* **1999**, *121*, 8811.

27. Saito, M.; Tokitoh, N.; Okazaki, R. *J. Am. Chem. Soc.* **1997**, *119*, 11124.

28. Li, L.; Fukawa, T.; Matsuo, T.; Hashizume, D.; Fueno, H.; Tanaka, K.; Tamao, K. *Nat. Chem.* **2012**, *4*, 361.

29. Allen, F. H. *Acta Crystallogr.* **2002***, B58*, 380.

30. Igau, A.; Grutzmacher, H.; Baceiredo, A.; Bertrand, G. *J. Am. Chem. Soc*. **1988**, *110*, 6463.

31. Arduengo, A. J.; Harlow, R. L.; Kline, M. A. *J. Am. Chem. Soc.* **1991**, *113*, 361.

32. (*a*) Wang, Y.; Robinson, G. H. *Chem. Commun.* **2009**, 5201; (*b*) Siemeling, U. *Aust. J. Chem.* **2011**, *64*, 1109; (*c*) Martin, D.; Soleilhavoup, M.; Bertrand, G. *Chem. Sci.* **2011**, *2*, 389; (*d*) Wang, Y.; Robinson, G. H. *Dalton Trans.* **2012**, *41*, 337; (*e*) Clyburne, J. A. C.; McMullen, N. *Coord. Chem. Rev.* **2000**, *210*, 73.

33. Wang, Y.; Quillian, B.; Wei, P.; Wannere, C. S.; Xie, Y.; King, R. B.; Schaefer III, H. F.; Schleyer, P. v. R.; Robinson, G. H. *J. Am. Chem. Soc.* **2007**, *129*, 12412.

34. (*a*) Wang, Y.; Xie, Y.; Wei, P.; King, R. B.; Schäfer III, H. F.; Schleyer, P. v. R.; Robinson, G. H. *Science* **2008**, *321*, 1069; (*b*) Sidiropoulos, A.; Jones, C.; Stasch, A.; Klein, S.; Frenking, G. *Angew. Chem. Int. Ed.* **2009**, *48*, 9701; (*c*) Jones, C.;

Sidiropoulos, A.; Holzmann, N.; Frenking, G.; Stasch, A. *Chem. Commun.* **2012**, *48*, 9855.

35. Lavallo, V.; Canac, Y.; Präsang, C.; Donnadieu, B.; Bertrand, G. *Angew. Chem. Int. Ed.* **2005**, *44*, 5705.
36. Back, O.; Henry-Ellinger, M.; Martin, C. D.; Martin, D.; Bertrand, G. *Angew. Chem. Int. Ed.* **2013**, *52*, 2939.
37. (*a*) Kinjo, R.; Donnadieu, B.; Ali Celik, M.; Frenking, G.; Bertrand, G. *Science* **2011**, *333*, 610; (*b*) Ruiz, D. A.; Melaimi, M.; Bertrand, G. *Chem. Commun*. **2014**, *50*, 7837.
38. Ruiz, D. A.; Ung, G.; Melaimi, M.; Bertrand, G. *Angew. Chem. Int. Ed.* **2013**, *52*, 7590.
39. (*a*) Back, O.; Donnadieu, B.; Parameswaran, P.; Frenking, G.; Bertrand, G. *Nat. Chem.* **2010**, *2*, 369; (*b*) Kretschmer, R.; Ruiz, D. A.; Moore, C. E.; Rheingold, A. L.; Bertrand, G. *Angew. Chem. Int. Ed.* **2014**, *53*, 8176; (*c*) Dorsey, C. L.; Mushinski, R. M.; Hudnall, T. W. *Chem. Eur. J.* **2014**, *20*, 8914; (*d*) Back, O.; Celik, M. A.; Frenking, G.; Melaimi, M.; Donnadieu, B.; Bertrand, G. *J. Am. Chem. Soc.* **2010**, *132*, 10262.
40. Kuhn, N.; Bohnen, H.; Kreutzberg, J.; Bläser, D.; Boese, R. *J. Chem. Soc., Chem. Commun.* **1993**, *14*, 1136.
41. (*a*) Al-Rafia, S. M. I.; Malcolm, A. C.; Liew, S. K.; Ferguson, M. J.; McDonald, R.; Rivard, E. *Chem. Commun*. **2011**, *47*, 6987; (*b*) Dumrath, A.; Wu, X. -F.; Neumann, H.; Spannenberg, A.; Jackstell, R.; Beller, M. *Angew. Chem. Int. Ed*. **2010**, *49*, 8988; (*c*) Wang, Y.; Abraham, M. Y.; Gilliard Jr., R. J.; Sexton, D. R.; Wei, P.;

Robinson, G. H. *Organometallics* **2013**, *32*, 6639; (*d*) Powers, K.; Hering-Junghans, C.; McDonald, R.; Ferguson, M. J.; Rivard. E. *Polyhedron* **2016**, *108*, 8.

42. (*a*) Al-Rafia, S. M. I.; Ferguson, M. J.; Rivard, E. *Inorg. Chem.* **2011**, *50*, 10543; (*b*) Al-Rafia, S. M. I.; Momeni, M. R.; McDonald, R.; Ferguson, M. J.; Brown, A.; Rivard, E. *Angew. Chem. Int. Ed*. **2013**, *52*, 6390; (*c*) Berger, C. J.; He, G.; Merten, C.; McDonald, R.; Ferguson, M. J.; Rivard, E. *Inorg. Chem.* **2014**, *53*, 1475.
43. (*a*) Lee, W. -H.; Lin, Y. -F.; Lee, G. -H.; Peng, S. -M.; Chiu. C. -W. *Dalton Trans.* **2016**, *45*, 5937; (*b*) Ghadwal, R. S.; Reichmann, S. O.; Engelhardt, F.; Andrada, D. M.; Frenking, G. *Chem. Commun*. **2013**, *49*, 9440; (*c*) Ghadwal, R. S.; Schurmann, C. J.; Andrada, D. M.; Frenking, G. *Dalton Trans*. **2015**, *44*, 14359; (*d*) Ghadwal, R. S.; Schürmann, C. J.; Engelhardt, F.; Steinmetzger, C. *Eur. J. Inorg. Chem.* **2014**, 4921; (*e*) El-Hellani, A.; Monot, J.; Guillot, R.; Bour, C.; Gandon, V. *Inorg. Chem.* **2013**, *52*, 506.
44. Wittig, G.; Schöllkopf, U. *Chem. Ber*. **1954**, *87*, 1318.
45. (*a*) Pörschke, K. -R.; Wilke, G.; Mynott, R. *Chem. Ber*. **1985**, *118*, 298; (*b*) Fortier, S.; Kaltsoyannis, N.; Wu, G.; Hayton, T. W. *J. Am. Chem. Soc.* **2011**, *133*, 14224.
46. (*a*) Bestmann, H. J.; Sühs, K.; Röder, T. *Angew. Chem. Int. Ed. Engl.* **1981**, *20*, 1038; (*b*) Bestmann, H. J.; Röder, T.; Sühs, K. *Chem. Ber.* **1988**, *121*, 1509; (*c*) Breitsameter, F.; Schrödel, H. -P.; Schmidpeter, A.; Nöth, H.; Rojas-Lima, S. *Z. Anorg. Allg. Chem.* **1999**, *625*, 1293.
47. Hawthorne, F. M. *J. Am. Chem. Soc*. **1958**, *80*, 3480.

48. Borisova, I. V.; Zemlyansky, N. N.; Belsky, V. K.; Kolosova, N. D.; Sobolev, A. N.; Luzikov, Y. N.; Ustynyuk, Y. A.; Beletskaya, I. P. *J. Chem. Soc., Chem. Commun.* **1982**, 1090.

49. (*a*) Swarnakar, A. K.; McDonald, S. M.; Deutsch, K. C.; Choi, P.; Ferguson, M. J.; McDonald, R.; Rivard, E. *Inorg. Chem*. **2014**, *53*, 8662; (*b*) Purkait, T. K.; Swarnakar, A. K.; De Los Reyes, G. B.; Hegmann, F. A.; Rivard, E.; Veinot, J. G. C. *Nanoscale* **2015**, *7*, 2241.

50. Nowell, I. N.; Russell, D. R. *J. Chem. Soc., Chem. Commun*. **1967**, *817.*

51. (*a*) Einstein, F. W. B.; Pomeroy, R. K.; Rushman, P.; Willis, A. C. *Organometallics* **1985**, *4*, 250; (*b*) Usón, R.; Forniés, J.; Espinet, P.; Fortuño, C.; Tomas, M.; Welch, A. J. *J. Chem. Soc., Dalton Trans.* **1988**, 3005.

52. Bauer, J.; Braunschweig, H.; Dewhurst, R. D. *Chem. Rev.* **2012**, *112*, 4329.

53. (*a*) Braunschweig, H.; Gruß, K.; Radacki, K. *Angew. Chem. Int. Ed.* **2007**, *46*, 7782; (*b*) Bauer, J.; Braunschweig, H.; Brenner, P.; Kraft, K.; Radacki, K.; Schwab, K. *Chem. Eur. J.* **2010**, *16*, 11985.

54. (*a*) Mayer, J. M.; Calabrese, J. C. *Organometallics* **1984**, *3*, 1292; (*b*) Burlitch, J. M.; Leonowicz, M. E.; Petersen, R. B.; Hughes, R. E. *Inorg. Chem.* **1979**, *18*, 1097; (*c*) Golden, J. T.; Peterson, T. H.; Holland, P. H.; Bergman, R. G.; Andersen, A. R. *J. Am. Chem. Soc.* **1998**, *120*, 223.

55. Steinke, T.; Fischer, R. A.; Winter, M; Cokoja, M.; Gemel, C. *Dalton Trans*. **2005**, 55; (*b*) Braunschweig, H.; Gruß, K.; Radacki, K. *Inorg. Chem*. **2008**, *47*, 8597; (*c*) Aldridge, S.; Kays, D. L.; Bunn, N. R.; Coombs, N. D. *Main Group Met. Chem*. **2005**, *28*, 201.

56. (*a*) Charmant, J. P. H.; Fan, C.; Norman, N. C.; Pringle, P. G. *Dalton Trans.* **2007**, 114; (*b*) Braunschweig, H.; Brenner, P.; Müller, A.; Radacki, K.; Rais, D.; Uttinger, K. *Chem. Eur. J.* **2007**, *13*, 7171; (*c*) Braunschweig, H.; Radacki, K.; Uttinger, K. *Inorg. Chem.* **2007**, *46*, 8796; (*d*) Braunschweig, H.; Gruss, K.; Radacki, K. *Inorg. Chem.* **2008**, *47*, 8595; (*e*) Braunschweig, H.; Brenner, P.; Cogswell, P.; Kraft, K.; Schwab, K. *Chem. Commun.* **2010**, *46*, 7894.

57. (*a*) Braunschweig, H.; Radacki, K.; Schneider, A. *Science* **2010**, *328*, 345; (*b*) Braunschweig, H.; Radacki, K.; Schneider, A. *Angew. Chem. Int. Ed.* **2010**, *49*, 5993; (*c*) Braunschweig, H.; Radacki, K.; Schneider, A. *Chem. Commun.* **2010**, 46, 6473.

58. (*a*) Chan, D. M. T.; Marder, T. B. *Angew. Chem. Int. Ed. Engl.* **1988**, *27*, 442; (*b*) Beńi, Z.; Ros, R.; Tassan, A.; Scopelliti, R.; Roulet, R. *Dalton Trans*. **2005**, 315.

59. (*a*) Hupp, F.; Ma, M.; Kroll, F.; Jiménez-Halla, J. O. C.; Dewhurst, R. D.; Radacki, K.; Stasch, A.; Jones, C.; Braunschweig, H. *Chem. Eur. J.* **2014**, *20*, 16888; (*b*) Braunschweig, H.; Damme, A.; Dewhurst, R. D.; Hupp, F.; Jiménez-Halla, J. O. C.; Radacki, K. *Chem. Commun.* **2012**, *48*, 10410.

60. Swarnakar, A. K.; Ferguson, M. J.; McDonald, R.; Rivard, E. *Dalton Trans*. **2016**, *45*, 6071.

61. (*a*) Vogel, U.; Timoshkin, A. Y.; Scheer, M. *Angew. Chem. Int. Ed.* **2001**, *40*, 4409; (*b*) Vogel, U.; Hoemensch, P.; Schwan, K. -Ch.; Timoshkin, A. Y.; Scheer, M. *Chem. Eur. J.* **2003**, *9*, 515; (*c*) Schwan, K. -Ch.; Timoshkin, A. Y.; Zabel, M.; Scheer, M. *Chem. Eur. J.* **2006**, *12*, 4900; (*d*) Bodensteiner, M.; Vogel, U.; Timoshkin, A. Y.; Scheer, M. *Angew. Chem. Int. Ed.* **2009**, *48*, 4629; (*e*)

Bodensteiner, M.; Timoshkin, A. Y.; Peresypkina, E. V.; Vogel, U.; Scheer, M. *Chem. –Eur. J.* **2013**, *19*, 957; (*f*) Marquardt, C.; Adolf, A.; Stauber, A.; Bodensteiner, M.; Virovets, A. V.; Timoshkin, A. Y.; Scheer, M. *Chem. –Eur. J.* **2013**, *19*, 11887; (*g*) Marquardt, C.; Thoms, C.; Stauber, A.; Balázs, G.; Bodensteiner, M.; Scheer, M. *Angew. Chem. Int. Ed*. **2014**, *53*, 3727; (*h*) Marquardt, C.; Jurca, T.; Schwan, K.-C.; Stauber, A.; Virovets, A. V.; Whittell, G. R.; Manners, I.; Scheer, M. *Angew. Chem. Int. Ed.* **2015**, *54*, 13782.

62. (*a*) Johnson, J. C.; Choi, H. J.; Knutsen, K. P.; Schaller, R. D.; Yang, P.; Saykally, R. J. *Nat. Mater.* **2002**, *1*, 106; (*b*) Chen, C. C.; Yeh, C. C.; *Adv. Mater.* **2000**, *12*, 738; (*c*) Kim, H. M.; Kim, D. S.; Park, Y. S.; Kim, D. Y.; Kang, T. W.; Chung, K. S. *Adv. Mater.* **2002**, *14*, 991; (*d*) Seryogin, G.; Shalish, I.; Moberlychan, W.; Narayanamurti, V. *Nanotechnology* **2005**, *16*, 2342.
63. Malcolm, A. C.; Sabourin, K. J.; McDonald, R.; Ferguson, M. J.; Rivard, E. *Inorg. Chem.* **2012**, *51*, 12905.
64. (*a*) Lory, E. R.; Porter, R. F. *J. Am. Chem. Soc.* **1973**, *95*, 1766; (*b*) Kawashima, Y.; Kawaguchi, K.; Hirota. E. *J. Chem. Phys*. **1987**, *87*, 6331; (*c*) Thompson, C. A.; Andrews, L. *J. Am. Chem. Soc.* **1995**, *117*, 10125; (*d*) Zhang, F.; Maksyutenko, P.; Kaiser, R. I.; Mebel, A. M.; Gregusova, A.; Perera, S. A.; Bartlett, R. J. *J. Phys. Chem. A* **2010**, *114*, 12148.
65. For selected computational studies on HBNH, see: (*a*) Baird, N. C.; Datta, R. K. *Inorg. Chem.* **1972**, *11*, 17; (*b*) Matus, M. H.; Grant, D. J.; Nguyen, M. T.; Dixon, D. A. *J. Phys. Chem. C* **2009**, *113*, 16553; (*c*) Sundaram, R.; Scheiner, S.; Roy, A. K.; Kar, T. *J. Phys. Chem. C* **2015**, *119*, 3253.

66. Liu, H.; Jin, P.; Xue, Y. -M.; Dong, C.; Li, X.; Tang, C. -C.; Du, X. -W. *Angew. Chem. Int. Ed.* **2015**, *54*, 7051.

67. (*a*) Piane, R. T.; Narula, C. K. *Chem. Rev.* **1990**, *90*, 73; (*b*) Geim, A. K.; Grigorieva, I. V. *Nature* **2013**, *499*, 419; (*c*) Liu, L.; Park, J.; Siegel, D. A.; McCarty, K. F.; Clark, K. W.; Deng, W.; Basile, L.; Idrobo, J. C.; Li, A. P.; Gu, G. *Science* **2014**, *343*, 16.

68. (*a*) Swarnakar, A. K.; Hering-Junghans, C.; Nagata, K.; Ferguson, M. J.; McDonald, R.; Tokitoh, N.; Rivard, E. *Angew. Chem. Int. Ed.* **2015**, *54*, 10666; (*b*) Swarnakar, A. K.; Hering-Junghans, C.; Ferguson, M. J.; McDonald, R.; Rivard, E. *Chem. Sci*. **2017**, *8,* 2337.

69. (*a*) Amano, H.; Sawaki, N.; Akasaki, I.; Toyoda, Y. *Appl. Phys. Lett.* **1986**, *48*, 353; (*b*) Nakamura, S.; Harada, Y.; Seno, M. *Appl. Phys. Lett.* **1991**, *58*, 2021; (*c*) Morkoc, H.; Mohammad, S. N. *Science* **1995**, *267*, 51.

70. Swarnakar, A. K.; Ferguson, M. J.; McDonald, R.; Rivard, E. *Dalton Trans*. **2017**, *46*, 1406.

71. (*a*) Jasinski, J. M.; Gates, S. M. *Acc. Chem. Res.* **1991**, *24*, 9; (*b*) Isobe, C.; Cho, H. -C., Sewell, J. E. *Surf. Sci*. **1993**, *295*, 117.

72. (*a*) Wang, X.; Andrews, L.; Kushto, G. P. *J. Phys. Chem. A* **2002**, *106*, 5809; (*b*) Smith, T. C.; Clouthier, D. J.; Sha, W. Adam, A. G. *J. Chem. Phys.* **2000**, *113*, 9567.

73. Thimer, K. C.; Al-Rafia, S. M. I.; Ferguson, M. J.; McDonald, R.; Rivard, E. *Chem. Commun.* **2009**, 7119.

74. Al-Rafia, S. M. I.; Malcolm, A. C.; Liew, S. K.; Ferguson, M. J.; Rivard, E. *J. Am. Chem. Soc.* **2011**, *133*, 777.

75. Al-Rafia, S. M. I.; Malcolm, A. C.; McDonald, R.; Ferguson, M. J.; Rivard, E. *Chem. Commun.* **2012**, *48*, 1308.

76. (*a*) Al-Rafia, S. M. I.; Momeni, M. R.; Ferguson, M. J.; McDonald, R.; Brown, A.; Rivard, E. *Organometallics* **2013**, *32*, 6658; (*b*) Al-Rafia, S. M. I.; Malcolm, A. C.; McDonald, R.; Ferguson, M. J.; Rivard, E. *Angew. Chem. Int. Ed.* **2011**, *50*, 8354.

77. Kamata, Y. *Mater. Today* **2008**, *11*, 30.

78. Maeda, Y. *Phys. Rev. B: Condens. Matter Mater. Phys.* **1995**, *51*, 1658.

79. (*a*) Pillarisetty, R. *Nature* **2011**, *479*, 324; (*b*) Hekmatshoar, B.; Shahrjerdi, D.; Hopstaken, M.; Fogel, K.; Sadana, D. K. *Appl. Phys. Lett*. **2012**, *101*, 032102; (*c*) Guter, W.; Schone, J.; Philipps, S. P.; Steiner, M.; Siefer, G.; Wekkeli, A.; Welser, E.; Oliva, E.; Bett, A. W.; Dimroth, F. *Appl. Phys. Lett*. **2009**, *94*, 223504; (*d*) Chakraborty, G.; Sengupta, A.; Requejo, F. G.; Sarkar, C. K. *J. Appl. Phys.* **2011**, *109*, 064504; (*e*) Assefa, S.; Xia, F. N. A.; Vlasov, Y. A. *Nature* **2010**, *464*, U80.

80. Lambert, T. N.; Andrews, N. L.; Gerung, H.; Boyle, T. J.; Oliver, J. M.; Wilson, B. S.; Han, S. M. *Small* **2007**, *3*, 691.

81. Vaughn II, D. D.; Schaak, R. E. *Chem. Soc. Rev.* **2013**, *42*, 2861.

82. (*a*) Kornowski, A.; Giersig, M.; Vogel, R.; Chemseddine, A.; Weller, H. *Adv. Mater.* **1993**, *5*, 634; (*b*) Chiu, H. W.; Chervin, C. N.; Kauzlarich, S. M. *Chem. Mater.* **2005**, *17*, 4858; (*c*) Lee, H.; Kim, M. G.; Choi, C. H.; Sun, Y. K.; Yoon, C. S.; Cho, J. *J. Phys. Chem. B* **2005**, *109*, 20719.

83. (*a*) Taylor, B. R.; Kauzlarich, S. M.; Lee, H. W. H.; Delgado, G. R. *Chem. Mater*. **1998**, *10*, 22; (*b*) Tanke, R. S.; Kauzlarich, S. M.; Patten, T. E.; Pettigrew, K. A.; Murphy, D. L.; Thompson, M. E.; Lee, H. W. H. *Chem. Mater*. **2003**, *15*, 1682.

84. (*a*) Wu, H. P.; Liu, J. F.; Wang, Y. W.; Zengand, Y. W.; Jiang, J. Z. *Mater. Lett*. **2006**, *60*, 986; (*b*) Fok, E.; Shih, M. L.; Meldrum, A.; Veinot, J. G. C.; *Chem. Commun*. **2004**, 386; (*c*) Lu, X. M.; Korgel, B. A.; Johnston, K. P. *Chem. Mater*. **2005**, *17*, 6479.

85. (*a*) Henderson, E. J.; Hessel, C. M.; Veinot, J. G. C. *J. Am. Chem. Soc.* **2008**, *130*, 3624; (*b*) Lee, D. C.; Pietryga, J. M.; Robel, I.; Werder, D. J.; Schaller, R. D.; Klimov, V. I. *J. Am. Chem. Soc*. **2009**, *131*, 3436.

Chapter 2

1. (*a*) Arduengo, A. J. III; Harlow, R. L.; Kline, M. *J. Am. Chem. Soc.* **1991,** *113*, 361; (*b*) Kuhn, N.; Kratz, T. *Synthesis* **1993**, 561; (*c*) Dröge, T.; Glorius, F. *Angew. Chem. Int. Ed.* **2010**, *49*, 6940; (*d*) Diéz-González, S.; Nolan, S. P. *Coord. Chem. Rev.* **2007**, *251*, 874; For related carbene-based donors, see: (*e*) Martin, D.; Melaimi, M.; Soleilhavoup, M.; Bertrand, G. *Organometallics* **2011**, *30*, 5304; (*f*) Crabtree, R. H. *Coord. Chem. Rev.* **2013**, *257*, 755.

2. (*a*) Braunschweig, H.; Dewhurst, R. D.; Hammond, K.; Mies, J.; Radacki, K.; Vargas, A. *Science* **2012**, *336*, 1420; (*b*) Wang, Y.; Xie, Y.; Wei, P.; King, R. B.; Schaefer, H. F. III; Schleyer, P. v. R.; Robinson, G. H. *Science* **2008**, *321*, 1069; (*c*) Sidiropoulos, A.; Jones, C.; Stasch, A.; Klein, S.; Frenking, G. *Angew. Chem. Int. Ed.* **2009**, *48*, 9701; (*d*) Jones, C., Sidiropoulos, A.; Holzmann, N.; Frenking, G.; Stasch, A. *Chem.*

Commun. **2012**, *48*, 9855; (*e*) Wang, Y.; Xie, Y.; Wei, P.; King, R. B.; Schaefer, H. F. III; Schleyer, P. v. R.; Robinson, G. H. *J. Am. Chem. Soc.* **2008**, *130*, 14970; (*f*) Abraham, M. Y.; Wang, Y.; Xie, Y.; Wei, P.; Schaefer, H. F. III; Schleyer, P. v. R.; Robinson, G. H. *Chem. Eur. J.* **2010**, *16*, 432.

3. For recent examples with IPr and related NHC donors, see: (*a*) Sindlinger, C. P.; Wesemann, L. *Chem. Sci.* **2014**, *5,* 2739; (*b*) Filippou, A.; Baars, B.; Chernov, O.; Lebedev, Y. N.; Schnakenburg, G. *Angew. Chem. Int. Ed.* **2014**, *53*, 565; (*c*) Wang, Y.; Xie, Y.; Wei, P.; Schaefer, H. F. III; Schleyer, P. v. R.; Robinson, G. H. *J. Am. Chem. Soc.* **2013**, *135*, 19139; (*d*) Xiong, Y.; Yao, S.; Inoue, S.; Epping, J. D.; Driess, M. *Angew. Chem., Int. Ed.* **2013**, *52*, 7147; (*e*) Mondal, K. C.; Samuel, P. P.; Tretiakov, M.; Sing, A. P.; Roesky, H. W.; Stückl, A. C.; Niepötter, B.; Carl, E.; Wolf, H.; Herbst-Irmer, R.; Stalke, D. *Inorg. Chem.* **2013**, *52*, 4736; (*f*) Al-Rafia, S. M. I.; Momeni, M. R.; McDonald, R.; Ferguson, M. J.; Brown, A.; Rivard, E. *Angew. Chem. Int. Ed.* **2013**, *52*, 6390; (*g*) Jana, A.; Huch, V.; Scheschkewitz, D. *Angew. Chem. Int. Ed.* **2013**, *52*, 12179.

4. (*a*) Thimer, K. C.; Al-Rafia, S. M. I.; Ferguson, M. J.; McDonald, R.; Rivard, E. *Chem. Commun.* **2009**, 7119; (*b*) Al-Rafia, S. M. I.; Malcolm, A. C.; Liew, S. K.; Ferguson, M. J.; Rivard, E. *J. Am. Chem. Soc.* **2011**, *133*, 777; (*c*) Al-Rafia, S. M. I.; Malcolm, A. C.; McDonald, R.; Ferguson, M. J.; Rivard, E. *Angew. Chem. Int. Ed.* **2011**, *50*, 8354; (*d*) Al-Rafia, S. M. I.; Malcolm, A. C.; McDonald, R.; Ferguson, M. J.; Rivard, E. *Chem. Commun.* **2012**, *48*, 1308; (*e*) Al-Rafia, S. M. I.; Shynkaruk, O.; McDonald, S. M.; Liew, S. K.; Ferguson, M. J.; McDonald, R.; Herber, R. H.; Rivard, E. *Inorg. Chem.* **2013**, *52*, 5581; (*f*) Al-Rafia, S. M.; Momeni, M. R.;

Ferguson, M. J.; McDonald, R.; Brown, A., Rivard, E. *Organometallics* **2013**, *32*, 6658; (*g*) For a recent review of this field, see: Rivard, E. *Dalton. Trans.* **2014**, *43*, 8577.

5. (*a*) Al-Rafia, S. M. I.; Malcolm, A. C.; Liew, S. K.; Ferguson, M. J.; McDonald, R.; Rivard, E. *Chem. Commun.* **2011**, *47*, 6987; For related studies involving NHOs, see: (*b*) Kuhn, N.; Bohnen, H.; Kreutzberg, J.; Bläser, D.; Boese, R. *J. Chem. Soc., Chem. Commun.* **1993**, 1136. (*c*) Fürstner, A.; Alcarazo, M.; Goddard, R.; Lehmann, C. W. *Angew. Chem. Int. Ed.* **2008**, *47*, 3210; (*d*) Dumrath, A.; Wu, X. -F.; Neumann, H.; Spannenberg, A.; Jackstell, R.; Beller, M. *Angew. Chem. Int. Ed.* **2010**, *49*, 8988; (*e*) Malcolm, A. C.; Sabourin, K. J.; McDonald, R.; Ferguson, M. J.; Rivard, E. *Inorg. Chem.* **2012**, *51*, 12905; (*f*) Wang, Y.; Abraham, M. Y; Gilliard, R. J. Jr.; Sexton, D. R.; Wei, P.; Robinson, G. H. *Organometallics* **2013**, *32*, 6639; (*g*) Berger, C. J.; He, G.; Merten, C.; McDonald, R.; Ferguson, M. J.; Rivard, E. *Inorg. Chem.* **2014**, *53*, 1475.
6. (*a*) Jasinski, J. M.; Gates, S. M. *Acc. Chem. Res.* 1991, *24*, 9; (*b*) Isobe, C.; Cho, H.-C.; Sewell, J. E. *Surf. Sci*. **1993**, *295*, 117.
7. Bestmann, H. J.; Kratzer, O. *Chem. Ber.* **1963**, *96*, 1899.
8. (*a*) Wittig, G.; Schöllkopf, U. *Chem. Ber.-Rec.* **1954**, *87*, 1318; (*b*) Beedham, I.; Micklefield, J. *Curr. Org. Syn.* **2005**, *2*, 231; (*c*) Xu, S.; He, Z. *RSC Adv.* **2013**, *3*, 16885.
9. For selected examples, see: (*a*) Pörschke, K. –R.; Wilke, G.; Mynott, R. *Chem. Ber*. **1985**, *118*, 298; (*b*) Fortier, S.; Kaltsoyannis, N.; Wu, G.; Hayton, T. W. *J. Am. Chem. Soc.* **2011**, *133*, 14224.

10. (*a*) Bestmann, H. J.; Sühs, K.; Röder, T. *Angew. Chem. Int. Ed. Engl.* **1981**, *20*, 1038; (*b*) Borisova, I. V.; Zemlyansky, N. N.; Belsky, V. K.; Kolosova, N. D.; Sobolev, A. N.; Luzikov, Y. N.; Ustynyuk, Y. A.; Beletskaya, I. P. *J. Chem. Soc., Chem. Commun.* **1982**, 1090; (*c*) Bestmann, H. J.; Röder, T.; Sühs, K. *Chem. Ber.* 1988, *121*, 1509. (*d*) Breitsameter, F.; Schrödel, H.-P.; Schmidpeter, A.; Nöth, H.; Rojas-Lima, S. *Z. Anorg. Allg. Chem.* **1999**, *625*, 1293.

11. (*a*) Prabusankar, G.; Sathyanarayana, A.; Suresh, P.; Babu, C. N.; Srinivas, K.; Metla, B. P. R. *Coord. Chem. Rev.* **2014**, *269*, 96; (*b*) Inoue, S.; Eisenhut, C. *J. Am. Chem. Soc.* **2013**, *135*, 18315; (*c*) Abraham, M. Y.; Wang, Y.; Xie, Y.; Wei, P.; Schaefer, H. F. III; Schleyer, P. v. R.; Robinson, G. H. *J. Am. Chem. Soc.* **2011**, *133*, 8874; (*d*) Al-Rafia, S. M. I.; McDonald, R.; Ferguson, M. J.; Rivard, E. *Chem. Eur. J.* **2012**, *18*, 13810; (*e*) Kinjo, R.; Donnadieu, B.; Celik, M. A.; Frenking, G.; Bertrand, G. *Science* **2011**, *333*, 610; (*f*) Bonyhady, S. J.; Collis, D.; Frenking, G.; Holzmann, N.; Jones, C.; Stasch, A. *Nat. Chem.* **2010**, *2*, 865.

12. (*a*) Chen, M.; Feng, Y.-G.; Wang, X.; Li, T.-C.; Zhang, J.-Y.; Qian, D.-J. *Langmuir* **2007**, *23,* 5296; (*b*) Nyamen, L. D.; Revaprasadu, N.; Pullabhotla, R. V. S. R.; Nejo, A. A.; Ndifon, P. T.; Malik, M. A.; O'Brien, P. *Polyhedron* **2013**, *56,* 62; (*c*) Hines, D. A.; Kamat, P. V. *ACS Appl. Mater. Interfaces* **2014**, *6*, 3041.

13. (*a*) King, R. B. *Inorg. Chem.* **1963**, *2*, 199; (*b*) Jutzi, P.; Hoffman, J.; Brauner, D. J.; Krüger, C. *Angew. Chem. Int. Ed. Engl.* **1973**, *12*, 1002; (*c*) du Mont, W.-W.; Neudert, B.; Rudolph, C.; Schumann, H. *Angew. Chem. Int. Ed. Engl.* **1976**, *15*, 308; (*d*) Ando, W.; Sekiguchi, A.; Hagiwara, K.; Sakakibara, A.; Yoshida, H. *Organometallics* **1988**, *7*, 558; (*e*) Pu, L.; Twamley, B.; Power, P. P. *Organometallics*

2000, *19*, 2874; (*f*) Hadlington, T. J.; Hermann, M.; Li, J.; Frenking, G.; Jones, C. *Angew. Chem. Int. Ed.* **2013,** *52*, 10199; (*g*) See also: Mizuhata, Y.; Sasamori, T.; Tokitoh, N. *Chem. Rev.* 2009, *109*, 3479.

14. For a prior report involving the preparation of $Cy_3P{\bullet}GeCl_2$, see: Doddi, A.; Gemel, C.; Winter, M.; Fischer, R. A.; Goedecke, C.; Rzepa, H. S.; Frenking, G. *Angew. Chem. Int. Ed.* **2013**, *52*, 450.
15. The identification of the $[HPCy_3]^+$ salt by-product formed in the reaction of Cy_3P with $Cl_2Ge{\bullet}$dioxane was accomplished by ^{31}P NMR spectroscopy (δ = 20.2 ppm) and the detection of a characteristic doublet ^1H NMR resonance for the P-H residue at 7.12 ($^1J_{PH}$ = 488 Hz) in C_6D_6; this latter resonance collapsed to a single resonance in the $^1H\{^{31}P\}$ spectrum. Phosphonium salts of $GeCl_3^-$ ($[HPR_3]GeCl_3$) have been reported in the literature: (*a*) du Mont, W.-W.; Rudolph, G. *Chem. Ber.* **1976**, *109*, 3419; (*b*) Dal Canto, R. A.; Roskamp, E. J. *J. Org. Chem.* **1992**, *57*, 406; (*c*) Davis, M. F.; Levason, W.; Reid, G.; Webster, M. *Dalton Trans.* **2008**, 2261.
16. (*a*) Kolodiazhnyi, O. I. *Tetrahedron* **1996**, *52*, 1855; (*b*) Cristau, H.-J. *Chem. Rev.* **1994**, *94*, 1299; (*c*) Bestmann, H. J.; Arenz, T. *Angew. Chem. Int. Ed. Engl.* **1986**, *25*, 559.
17. Rajendran, K. V.; Gilheany, D. G. *Chem. Commun*. **2012**, *48*, 817.
18. Papp, R.; Somoza Jr., F. B.; Sieler, J.; Blaurock, S.; Hey-Hawkins, E. *J. Organomet. Chem.* **1999**, *585*, 127.
19. For related studies involving hydride transfer to carbene donor sites (followed by ring-expansion), see: (*a*) Arrowsmith, M.; Hill, M. S.; Kociok-Köhn, MacDougall, D. J.; Mahon, M. F. *Angew. Chem. Int. Ed.* **2012**, *51*, 2098; (*b*) Schmidt, D.; Berthel, J.

H. J.; Pietsch, S.; Radius, U. *Angew. Chem. Int. Ed.* **2012**, *51*, 8881; (*c*) ref 11*d*. (*d*) Momeni, M. R.; Rivard, E.; Brown, A. *Organometallics* **2013**, *32*, 6201; (*e*) Iversen, K. J.; Wilson, D. J. D.; Dutton, J. L. *Organometallics* **2013**, *32*, 6209; (*f*) Fang, R.; Yang, L.; Wang, Q. *Organometallics* **2014**, *33*, 53.

20. Brown, H. C.; Krishnamurthy, S.; Hubbard, J. L.; Coleman, R. A. *J. Organometal. Chem.* **1979**, *166*, 281.
21. Balch, A. L.; Oram, D. E. *Organometallics* **1988**, *7*, 155.
22. For related low oxidation state Sn(II) hydrides compounds, see: (*a*) Eichler, B. E.; Power, P. P. *J. Am. Chem. Soc.* **2000**, *122*, 8785; (*b*) Ding, Y.; Hao, H.; Roesky, H. W.; Noltemeyer, M.; Schmidt, H. –G. *Organometallics* **2001**, *20*, 4806; (*c*) Rivard, E.; Fischer, R. C.; Wolf, R.; Peng, Y.; Merrill, W. A.; Schley, N. D.; Zhu, Z.; Pu, L.; Fettinger, J. C.; Teat, S. J.; Nowik, I.; Herber, R. H.; Takagi, N.; Nagase, S.; Power, P. P. *J. Am. Chem. Soc.* **2007**, *129*, 16197.
23. Gresback, R.; Holman, Z.; Kortshagen, U. *Appl. Phys. Lett.* **2007**, *91*, 093119.
24. Yuan, F. –W.; Tuan, H. –Y. *Chem. Mater.* **2014**, *26*, 2172.
25. Wilcoxon, J. P.; Provencio, P. P.; Samara, G. A. *Condens. Matter* **2001**, *64*, 035417.
26. Lambert, T. N.; Andrews, N. L.; Gerung, H.; Boyle, T. J.; Oliver, J. M.; Wilson, B. S.; Han, S. M. *Small* **2007**, *3*, 691.
27. Henderson, E. J.; Seino, M.; Puzzo, D. P.; Ozin, G. A. *ACS Nano* **2010**, *4*, 7683.
28. Vaughn II, D. D.; Schaak, R. E. *Chem. Soc. Rev.* **2013**, *42*, 2861.
29. Martienssen, W.; Warliomont, H. *Springer Handbook of Condensed Matter and Materials Data*; *Springer GmbH* **2005**.

30. Taylor, B. R.; Kauzlarich, S. M.; Lee, H. W. H.; Delgado, G. R. *Chem. Mater.* **1998**, *10*, 22.

31. Taylor, B. R.; Kauzlarich, S. M.; Delgado, G. R.; Lee, H. W. H. *Chem. Mater.* **1999**, *11*, 2493.

32. Ma, X.; Wu, F.; Kauzlarich, S. M. *J. Solid State Chem.* **2008**, *181*, 1628.

33. Lu, X.; Ziegler, K. J.; Ghezelbash, A.; Johnston, K. P.; Korgel, B. A. *Nano Lett.* **2004**, *4*, 969.

34. Fok, E.; Shih, M.; Meldrum, A.; Veinot, J. G. C. *Chem. Comm.* **2004**, 386.

35. Chiu, H. W.; Chervin, C. N.; Kauzlarich, S. M. *Chem. Mater.* **2005**, *17*, 4858.

36. Stoldt, C. R.; Haag, M. A.; Larsen, B. A. *Appl. Phys. Lett.* **2008**, *93*, 043125.

37. Kortshagen, U.; Anthony, R.; Gresback, R.; Holman, Z.; Ligman, R.; Liu, C.-Y.; Mangolini, L.; Campbell, S. A. *Pure Appl. Chem.* **2008**, *80*, 1901.

38. Gerung, H.; Bunge, S. D.; Boyle, T. J.; Brinker, C. J.; Han, S. M. *Chem. Commun.* **2005**, 1914.

39. Warner, J. H.; Tilley, R. D. *Nanotechnology* **2006**, *17*, 3745.

40. Prabakar, S.; Shiohara, A.; Hanada, S.; Fujioka, K.; Yamamoto, K.; Tilley, R. D. *Chem. Mater.* **2010**, *22*, 482.

41. Henderson, E. J.; Hessel, C. M.; Veinot, J. G. C. *J. Am. Chem. Soc.* **2008**, *130*, 3624.

42. Chou, N. H.; Oyler, K. D.; Motl, N. E.; Schaak, R. E. *Chem. Mater.* **2009**, *21*, 4105.

43. Muthuswamy, E.; Iskandar, A. S.; Amador, M. M.; Kauzlarich, S. M. *Chem. Mater.* **2013**, *25*, 1416.

44. Muthuswamy, E.; Zhao, J.; Tabatabaei, K.; Amador, M. M.; Holmes, M. A.; Osterloh, F. E.; Kauzlarich, S. M. *Chem. Mater.* **2014**, *26*, 2138.

45. Lu, X.; Korgel, B. A.; Johston, K. P. *Chem. Mater.* **2005**, *17*, 6479.

46. Buriak, J. M. *Chem. Rev*. **2002**, *102*, 1271.

47. Shirahata, N.; Hirakawa, D.; Masuda, Y.; Sakka, Y. *Langmuir* **2013**, *29*, 7401.

48. Lee, D. C.; Pietryga, J. M.; Robel, I.; Werder, D. J.; Schaller, R. D.; Klimov, V. I. *J. Am. Chem. Soc.* **2009**, *131*, 3436.

49. Wheeler, L. M.; Levij, L. M.; Kortshagen, U. R. *J. Phys. Chem. Lett.* **2013**, *4*, 3392.

50. Niquet, Y. M.; Allan, G.; Delerue, C.; Lannoo, M. *Appl. Phys. Lett.* **2000**, *77*, 1182.

51. Millo, O.; Balberg, I., Azulay, D.; Purkait, T. K.; Swarnakar, A. K.; Rivard, E.; Veinot, J. G. C. *J. Phys. Chem. Lett.* **2015**, *6*, 3396.

52. Pangborn, A. B.; Giardello, M. A.; Grubbs, R. H.; Rosen, R. K.; Timmers, F. J. *Organometallics* **199**6, *15*, 1518.

53. Hope, H. *Prog. Inorg. Chem.* **1994**, *41*, 1.

54. Blessing, R. H. *Acta Crystallogr.* **1995**, *A51*, 33.

55. Sheldrick, G. M. *Acta Crystallogr.* **2008**, *A64*, 112.

56. Beurskens, P. T.; Beurskens, G.; de Gelder, R.; Smits, J. M. M.; Garcia-Garcia, S.; Gould, R. O. *DIRDIF-2008*; Crystallography Laboratory, Radboud University: Nijmegen, The Netherlands **2008**.

57. Lesley, M. J. G.; Woodward, A.; Taylor, N. J.; Marder, T. B.; Cazenobe, I.; Ledoux, I.; Zyss, J.; Thornton, A.; Bruce, D. W.; Kakkar, A. K. *Chem. Mater.* **1998**, *10,* 1355.

58. Blumenthal, A.; Bissinger, P.; Schmidbaur, H. J. *J. Organomet. Chem.* **1993**, *462*, 107.

59. Williams, A. T. R.; Winfield, S. A.; Miller, J. N. *Analyst* **1983**, *108*, 1067.

60. Suzuki, K.; Kobayashi, A.; Kaneko, S.; Takehira, K.; Yoshihara, T.; Ishida, H.; Shiina, Y.; Oishi, S.; Tobita, S. *Phys. Chem. Chem. Phys.* **2009**, *11*, 9850.

Chapter 3

1. (*a*) Braunschweig, H.; Dewhurst, R. D.; Hammond, K.; Mies, J.; Radacki, K.; Vargas, A. *Science* **2012**, *336,* 1420; (*b*) Wang, Y.; Xie, Y.; Wei, P.; King, R. B.; Schaefer III, H. F.; Schleyer, P. v. R.; Robinson, G. H. *Science* **2008**, *321*, 1069; (*c*) Sidiropoulos, A.; Jones, C.; Stasch, A.; Klein S.; Frenking, G.; *Angew. Chem. Int. Ed.* **2009**, *48*, 9701; (*d*) Jones, C.; Sidiropoulos, A.; Holzmann, N.; Frenking, G.; Stasch, A. *Chem. Commun.* **2012**, *48*, 9855.
2. For recent highlights from this active research field, see: (*a*) Wang, Y.; Chen, M.; Xie, Y.; Wei, P.; Schaefer III, H. F.; Schleyer, P. v. R.; Robinson, G. H. *Nature Chem.* **2015**, *7*, 509; (*b*) Ahmad, S. U.; Szilvási, T.; Irran E.; Inoue, S. *J. Am. Chem. Soc.* **2015**, *137*, 5828; (*c*) Swarnakar, A. K.; Hering-Junghans, C.; Nagata, K.; Ferguson, M. J.; McDonald, R.; Tokitoh, N.; Rivard, E. *Angew. Chem. Int. Ed.* **2015**, *54*, 10666; (*d*) Braunschweig, H.; Dellermann, T.; Ewing, W. C.; Kramer, T.; Schneider C.; Ulrich, S. *Angew. Chem. Int. Ed.* **2015**, *54*, 10271; (*e*) Filippou, A. C.; Baars, B.; Chernov, O.; Lebedev, Y. N.; Schnakenburg, G. *Angew. Chem. Int. Ed.* **2014**, *53*, 565; (*f*) Dahcheh, F.; Martin, D.; Stephan, D. W.; Bertrand, G. *Angew. Chem. Int. Ed.* **2014**, *53*, 13159; (*g*) Jana, A.; Huch, V; Scheschkewitz, D. *Angew. Chem. Int. Ed.* **2013**, *52*, 12179; (*h*) Ghadwal, R. S.; Roesky, H. W.; Pröpper, K.; Dittrich, B.; Klein, S.; Frenking, G. *Angew. Chem. Int. Ed.* **2011**, *50*, 5374.

3. For selected examples, see: (*a*) Thimer, K. C.; Al-Rafia, S. M. I.; Ferguson, M. J.; McDonald, R.; Rivard, E. *Chem. Commun.* **2009**, 7119; (*b*) Al-Rafia, S. M. I.; Malcolm, A. C.; Liew, S. K.; Ferguson, M. J.; Rivard, E. *J. Am. Chem. Soc.* **2011**, *133*, 777; (*c*) Al-Rafia, S. M. I.; Malcolm, A. C.; McDonald, R.; Ferguson, M. J.; Rivard, E. *Chem. Commun*. **2012**, *48*, 1308; (*d*) Al-Rafia, S. M. I.; Shynkaruk, O.; McDonald, S. M.; Liew, S. K.; Ferguson, M. J.; McDonald, R.; Herber, R. H.; Rivard, E. *Inorg. Chem.* **2013**, *52*, 5581; (*e*) Rivard, E. *Dalton. Trans.* **2014**, *43*, 8577.

4. (*a*) Al-Rafia, S. M. I.; Malcolm, A. C.; Liew, S. K.; Ferguson, M. J.; McDonald, R.; Rivard, E. *Chem. Commun*. **2011**, *47*, 6987; (*b*) Swarnakar, A. K.; McDonald, S. M.; Deutsch, K. C.; Choi, P.; Ferguson, M. J.; McDonald, R.; Rivard, E. *Inorg. Chem*. **2014**, *53*, 8662. For important early work, see: (*c*) Kuhn, N.; Bohnen, H.; Kreutzberg, J.; Bläser, D.; Boese, R. *J. Chem. Soc., Chem. Commun.* **1993**, 1136.

5. (*a*) Rivard, E. *Chem. Soc. Rev.* **2016**, *45*, 989; (*b*) Jasinski, J. M.; Gates, S. M. *Acc. Chem. Res.* **1991**, *24*, 9; (*c*) Weerts, W. L. M.; de Croon, M. H. J. M.; Marin, G. B. *J. Electrochem. Soc.* **1998**, *145*, 1318; (*d*) Dzarnoski, J.; O'Neal, H. E.; Ring, M. A. *J. Am. Chem. Soc.* **1981**, *103*, 5740 and references therein.

6. (a) Purkait, T. K.; Swarnakar, A. K.; De Los Reyes, G. B.; Hegmann, F. A.; Rivard, E.; Veinot, J. G. C. *Nanoscale* **2015**, *7*, 2241; (*b*) Millo, O.; Balberg, I., Azulay, D.; Purkait, T. K.; Swarnakar, A. K.; Rivard, E.; Veinot, J. G. C. *J. Phys. Chem. Lett.* **2015**, *6*, 3396.

7. Bauer, J.; Braunschweig, H.; Dewhurst, R. D. *Chem. Rev.* **2012**, *112*, 4329.

8. Nowell, I. N.; Russell, D. R. *J. Chem. Soc., Chem. Commun*. **1967**, *817*.

9. (*a*) Einstein, F. W. B.; Pomeroy, R. K.; Rushman, P.; Willis, A. C. *Organometallics* **1985**, *4*, 250; (*b*) Usón, R.; Forniés, J.; Espinet, P.; Fortuño, C.; Tomas, M.; Welch, A. J. *J. Chem. Soc., Dalton Trans.* **1988**, 3005.

10. (*a*) Braunschweig, H.; Gruß, K.; Radacki, K. *Angew. Chem. Int. Ed*. **2007**, *46*, 7782; (*b*) Bauer, J.; Braunschweig, H.; Brenner, P.; Kraft, K.; Radacki, K.; Schwab, K. *Chem. Eur. J.* **2010**, *16*, 11985; (*c*) Bauer, J.; Braunschweig, H.; Damme, A.; Gruß, K.; Radacki, K. *Chem. Commun.* **2011**, *47*, 12783; (*d*) Burlitch, J. M.; Leonowicz, M. E.; Petersen, R. B.; Hughes, R. E. *Inorg. Chem*. **1979**, *18*, 1097.

11. (*a*) Chan, D. M. T.; Marder, T. B. *Angew. Chem. Int. Ed. Engl.* **1988**, *27*, 442; (*b*) Béni, Z.; Ros, R.; Tassan, A.; Scopelliti, R.; Roulet, R. *Dalton Trans.* **2005**, 315; (*c*) Rutsch, P.; Huttner, G. Z. *Naturforsch.* **2002**, *57b*, 25; (*d*) Hupp, F.; Ma, M.; Kroll, F.; Jimenez-Halla, J. O. C.; Dewhurst, R. D.; Radacki, K.; Stasch, A.; Jones, C.; Braunschweig, H. *Chem. Eur. J.* **2014**, *20*, 16888.

12. Mayer, J. M.; Calabrese, J. C. *Organometallics* **1984**, *3*, 1292.

13. (*a*) Zadesenets, A.; Filatov, E.; Plyusnin, P.; Baidina, I.; Dalezky, V.; Korenev, S.; Bogomyakov, A. *Polyhedron* **2011**, *30*, 1305; (*b*) Shubin, Y.; Plyusnin, P.; Sharafutdinov, M. *Nanotechnology* **2012**, *23*, 405302.

14. Wakatsuki, Y.; Yamazaki, H. *J. Organometal. Chem.* **1974**, *64,* 393.

15. Simons, R. S.; Pu, L.; Olmstead, M. M.; Power, P. P. *Organometallics* **1997**, *16*, 1920.

16. Al-Rafia, S. M. I.; Momeni, M. R.; Ferguson, M. J.; McDonald, R.; Brown, A.; Rivard, E. *Organometallics* **2013**, *32*, 6658.

17. Choukroun, R.; Iraqi, A.; Gervais, D.; Daran, J. C.; Jeannin, Y. *Organometallics* **1987**, *6*, 1197.

18. Bott, S. G.; Machell, J. C.; Mingos, D. M. P.; Watson, M. J. *J. Chem. Soc., Dalton Trans.* **1991**, 859.

19. Gessner, V. H.; Dilsky, S.; Strohmann, C. *Chem. Commun*. **2010**, *46*, 4719.

20. For studies using the $[HB^{s}Bu_3]^-$ anion as a hydride source, see: (*a*) Richards, A. F.; Phillips, A. D.; Olmstead, M. M.; Power, P. P. *J. Am. Chem. Soc.* **2003**, *125*, 3204; (*b*) Lummis, P. A.; Momeni, M. R.; Lui, M. W.; McDonald, R.; Ferguson, M. J.; Miskolzie, M.; Brown, A.; Rivard, E. *Angew. Chem. Int. Ed.* **2014**, *53*, 9347.

21. Duchateau, R.; Lancaster, S. J.; Thornton-Pett, M.; Bochmann, M. *Organometallics* **1997**, *16*, 4995.

22. Otsuka, S.; Yoshida, T.; Matsumoto, M.; Nakatsu, K. *J. Am. Chem. Soc.* **1976**, *98*, 5850.

23. (*a*) Charmant, J. P. H.; Fan, C.; Norman, N. C.; Pringle, P. G. *Dalton Trans.* **2007**, 114; (*b*) Braunschweig, H.; Brenner, P.; Müller, A.; Radacki, K.; Rais, D.; Uttinger, K. *Chem. Eur. J.* **2007**, *13*, 7171; (*c*) Braunschweig, H.; Radacki, K.; Uttinger, K. *Inorg. Chem.* **2007**, *46*, 8796.

24. Braunschweig, H.; Gruss, K.; Radacki, K. *Inorg. Chem.* **2008**, *47*, 8595.

25. Braunschweig, H.; Brenner, P.; Cogswell, P.; Kraft, K.; Schwab, K. *Chem. Commun.* **2010**, *46*, 7894.

26. Pangborn, A. B.; Giardello, M. A.; Grubbs, R. H.; Rosen, R. K.; Timmers, F. J. *Organometallics* **1996**, *15*, 1518.

27. Balch, A. L.; Oram, D. E. *Organometallics* **1988**, *7*, 155.

28. Kolychev, E. L.; Bannenberg, T.; Freytag, M.; Daniliuc, C. G.; Jones, P. G.; Tamm, M. *Chem. Eur. J.* **2012**, *18*, 16938.

29. Hope, H. *Prog. Inorg. Chem.* **1994**, *41*, 1.

30. Blessing, R. H. *Acta Crystallogr.* **1995**, *A51*, 33.

31. Sheldrick, G. M. *Acta Crystallogr*. **2008**, *A64*, 112.

32. Beurskens, P. T.; Beurskens, G.; de Gelder, R.; Smits, J. M. M.; Garcia-Garcia, S.; Gould, R. O. *DIRDIF-2008*; Crystallography Laboratory, Radboud University: Nijmegen, The Netherlands **2008**.

33. Zaidlewicz, M.; Krzeminski, M. *Sci. Synth.* **2004**, *6*, 1097.

Chapter 4

1. (*a*) Paetzold, P. *Adv. Inorg. Chem.* **1987**, *31*, 123; (*b*) Nöth, H. *Angew. Chem. Int. Ed. Engl.* **1988**, *27*, 1603; (*c*) Paetzold, P. *Pure Appl. Chem.* **1991**, *63*, 345; (*d*) Fischer, R. C.; Power, P. P. *Chem. Rev.* **2010**, *110*, 3877; For related M-B≡NR chemistry, see: (*e*) Braunschweig, H.; Dewhurst, R. D.; Schneider, A. *Chem. Rev.* **2010**, *110*, 3924; **(*f*)** Paetzold, P.; Plotho, C. V. *Chem. Ber.* **1982**, *115*, 2819.

2. (*a*) Paetzold, P.; Richter, A.; Thijssen, T.; Wurtenberg, S. *Chem. Ber.* **1979**, *112*, 3811; (*b*) Balak, E.; Herberich, G. E.; Manners, I.; Mayer, H.; Paetzold, P. *Angew. Chem. Int. Ed. Engl.* **1988**, *27*, 958.

3. (*a*) Dahcheh, F.; Martin, D.; Stephan, D. W.; Bertrand, G. *Angew. Chem. Int. Ed.* **2014**, *53*, 13159; (*b*) Dahcheh, F.; Stephan, D. W.; Bertrand, G. *Chem. Eur. J.* **2015**, *21*, 199; (*c*) Braunschweig, H.; Ewing, W. C.; Geetharani, K.; Schaefer, M. *Angew. Chem. Int. Ed.* **2015**, *54*, 1662.

4. (*a*) Lory, E. R.; Porter, R. F. *J. Am. Chem. Soc.* **1973**, *95*, 1766; (*b*) Kawashima, Y.; Kawaguchi, K.; Hirota. E. *J. Chem. Phys*. **1987**, *87*, 6331; (*c*) Thompson, C. A.;

Andrews, L. *J. Am. Chem. Soc.* **1995**, *117*, 10125; (*d*) Zhang, F.; Maksyutenko, P.; Kaiser, R. I.; Mebel, A. M.; Gregusova, A.; Perera, S. A.; Bartlett, R. J. *J. Phys. Chem. A* **2010**, *114*, 12148.

5. For selected computational studies on HBNH, see: (*a*) Baird, N. C.; Datta, R. K. *Inorg. Chem.* **1972**, *11*, 17; (*b*) Matus, M. H.; Grant, D. J.; Nguyen, M. T.; Dixon, D. A. *J. Phys. Chem. C* **2009**, *113*, 16553; (*c*) Sundaram, R.; Scheiner, S.; Roy, A. K.; Kar, T. *J. Phys. Chem. C* **2015**, *119*, 3253.

6. Liu, H.; Jin, P.; Xue, Y.-M.; Dong, C.; Li, X.; Tang, C.-C.; Du, X.-W. *Angew. Chem. Int. Ed.* **2015**, *54*, 7051.

7. (*a*) Paine, R. T.; Narula, C. K. *Chem. Rev.* **1990**, *90*, 73; (*b*) Geim, A. K.; Grigorieva, I. V. *Nature* **2013**, *499*, 419; c) Liu, L.; Park, J.; Siegel, D. A.;. McCarty, K. F.; Clark, K. W.; Deng, W.; Basile, L.; Idrobo, J. C.; Li, A. P.; Gu, G.; *Science* **2014**, *343*, 16.

8. (*a*) Vogel, U.; Timonshkin, A. Y.; Scheer, M. *Angew. Chem. Int. Ed.* **2001**, *40*, 4409; (*b*) Rupar, P. A.; Jennings, M. C.; Ragogna, P. J.; Baines, K. M. *Organometallics* **2007**, *26*, 4109; (*c*) Al-Rafia, S. M. I.; Malcolm, A. C.; Liew, S. K.; Ferguson, M. J.; Rivard, E. *J. Am. Chem. Soc*. **2011**, *133*, 777; (*d*) Al-Rafia, S. M. I.; Malcolm, A. C.; McDonald, R.; Ferguson, M. J.; Rivard, E. *Angew. Chem. Int. Ed.* **2011**, *50*, 8354; (*e*) Yamaguchi, T.; Sekiguchi, A.; Driess, M. *J. Am. Chem. Soc.* **2010**, *132*, 14061; (*f*) Ghadwal, R. S.; Roesky, H. W. *Acc. Chem. Res.* **2013**, *46*, 444; (*g*) Filippou, A. C.; Baars, B.; Chernov, O.; Lebedev, Y. N.; Schnakenburg, G. *Angew. Chem. Int. Ed.* **2014**, *53*, 565; (*h*) Rivard, E. *Dalton Trans.* **2014**, *43*, 8577.

9. Stephan, D. W. *Acc. Chem. Res.* **2015**, *48*, 306.

10. (*a*) Hamilton, C. W.; Baker, R. T.; Staubitz, A.; Manners, I. *Chem. Soc. Rev.* **2009**, *38*, 279; (*b*) Leitao, E. M.; Titel, J.; Manners, I. *Nature Chem.* **2013**, *5*, 817; (*c*) Krieg, M.; Reicherter, F.; Haiss, P.; Ströbele, M.; Eichele, K.; Treanor, M.-J.; Schaub, R.; Bettinger, H. F. *Angew. Chem. Int. Ed.* **2015**, *54*, 8284.

11. For related rearrangements involving organic azides, see: (*a*) Rokade, B. V.; Prabhu, J. R. *J. Org. Chem.* **2012**, *77*, 5364; (*b*) Albertin, G.; Antoniutti, S.; Baldan, D.; Castro, J.; García-Fontán, S. *Inorg. Chem.* **2008**, *47*, 742.

12. For recent computational study on LB•BN•LA species, see: Momeni, M. R.; Shulman, L.; Rivard, E.; Brown, A. *Phys. Chem. Chem. Phys.* **2015**, *17*, 16525.

13. A related H/OTf exchange process is known within zinc(II) hydride chemistry: Lummis, P. A.; Momeni, M. R.; Lui, M. W.; McDonald, R.; Ferguson, M. J.; Miskolzie, M.; Brown, A.; Rivard, E. *Angew. Chem. Int. Ed.* **2014**, *53*, 9347.

14. Solovyev, A.; Chu, Q.; Geib, S. J.; Fensterbank, L.; Malacria, M.; Lacôte, E.; Curran, D. P. *J. Am. Chem. Soc.* **2010**, *132*, 15072.

15. (*a*) Al-Rafia, S. M. I.; McDonald, R.; Ferguson, M. J.; Rivard, E. *Chem. Eur. J.* **2012**, *18*, 13810; (*b*) Stubbs, N. E.; Jurca, T.; Leitao, E. M.; Woodall, C. H.; Manners, I. *Chem. Commun.* **2013**, *49*, 9098.

16. Kolychev, E. L.; Bannenberg, T.; Freytag, M.; Daniliuc, C. G.; Jones, P. G.; Tamm, M. *Chem. Eur. J.* **2012**, *18*, 16938.

17. Schulz, A.; Villinger, A. *Chem. Eur. J.* **2010**, *16*, 7276.

18. Photolysis of **3** (Hg lamp, 200 W) for 3 hrs in toluene or CH_2Cl_2 gave the new product, **4**, along with unknown by-products.

19. Pyykkö, P.; Atsumi, M. *Chem. Eur. J.* **2009**, *15*, 12770.

20. Malcolm, A. C.; Sabourin, K. J.; McDonald, R.; Ferguson, M. J.; Rivard, E. *Inorg. Chem.* **2012**, *51*, 12905.

21. For a related study on boranitrenes, see: Filthaus, M.; Schwertmann, L.; Neuhaus, P.; Seidel, R. W.; Oppel, I.; Bettinger, H. F. *Organometallics* **2012**, *31*, 3894.

22. Fox, A. R.; Cummins, C. C. *J. Am. Chem. Soc.* **2009**, *131*, 5716.

23. Axenrod, T.; Pregosin, P. S.; Wieder, M. J.; Becker, E. D.; Bradley, R. B.; Milne, G. W. A. *J. Am. Chem. Soc.* **1971**, *93*, 6536.

24. Wrackmeyer, B.; Tok, O. L. *Z. Naturforsch. B* **2007**, *62b*, 220.

25. To estimate the activation barrier, the N3-N4 bond length in **3** was scanned. The extrusion of N_2 is accompanied by a 1,2-H-shift and formation of **4**.

26. Kuhn, N.; Kratz, T. *Synthesis* **1993**, 561.

27. Kuhn, N.; Henkel, G.; Kratz, T.; Kreutzberg, J.; Boese, R.; Maulitz, A. M. *Chem. Ber.* **1993**, *126*, 2041.

28. Ge, F.; Kehr, G.; Daniliuc, C. G.; Mück-Lichtenfeld, C.; Erker, G.; *Organometallics* **2015**, *34*, 4205.

29. (*a*) Laubengayer, A. W.; Beachley Jr., O. T.; Porter, R. F. *Inorg. Chem.* **1965**, *4*, 578; (*b*) Beachley Jr., O. T.; Washburn, B. *Inorg. Chem*. **1975**, *14*, 120.

30. Malcolm, A. C.; Sabourin, K. J.; McDonald, R.; Ferguson, M. J.; Rivard, E. *Inorg. Chem.* **2012**, *51*, 12905.

31. (*a*) Sumerin, V.; Schulz, F.; Atsumi, M.; Wang, C.; Nieger, M.; Leskelä, M.; Repo, T.; Pyykkö, P.; Rieger, B. *J. Am. Chem. Soc.* **2008**, *130*, 14117; (*b*) Legare, M.-A.; Courtemanche, M. –A.; Rochette, E.; Fontaine, F.-G. *Science* **2015**, *349*, 513; (*c*) Wang, T.; Kehr, G.; Liu, L.; Grimme, S.; Daniliuc, C. G.; Erker, G. *J. Am. Chem. Soc*.

2016, *138*, 4302; (*d*) Mo, Z.; Rit, A.; Campos, J.; Kolychev, E. L.; Aldridge, S. *J. Am. Chem. Soc.* **2016**, *138*, 3306; (*e*) Stephan, D. W. *Acc. Chem. Res.* **2015**, *48*, 306.

32. For related examples of transfer hydrogenation between amine-boranes and unsaturated B-N compounds, see: (*a*) Robertson, A. P. M.; Leitao, E. M.; Manners, I. *J. Am. Chem. Soc.* **2011**, *133*, 19322; (*b*) Lui, M. W.; Paisley, N. R.; McDonald, R.; Ferguson, M. J.; Rivard, E. *Chem. Eur. J.* **2016**, *22*, 2134; (*c*) Leitao, E. M.; Stubbs, N. E.; Robertson, A. P. M.; Helten, H.; Cox, R. J.; Lloyd-Jones, G. C.; Manners, I. *J. Am. Chem. Soc*. **2012**, *134*, 16805.

33. We also explored the possible Lewis basic nature of **7**. When **7** was combined with CuI and $BAr^F{}_3$, no reaction was found; treatment of **7** with $Me_2S{\bullet}BH_3$ (as a source of BH_3) gave a complicated product mixture.

34. Ruiz, D. A.; Melaimi, M.; Bertrand, G. *Chem. Commun*. **2014**, *50*, 7837.

35. (*a*) Benson, S. W. *J. Chem. Educ.* **1965,** *42*, 502; (*b*) Walsh, R. *Acc. Chem. Res*. **1981**, *14*, 246.

36. For the synthesis of BN by treating $[XBNH]_3$ (X = Cl or Br) with molten alkali metals, see: (*a*) Hamilton, E. J. M.; Dolan, S. E.; Mann, C. M.; Colijn, H. O.; McDonald, C. E.; Shore, S. G. *Science* **1993**, *260*, 659; (*b*) Hamilton, E. J. M.; Dolan, S. E.; Mann, C. M.; Colijn, H. O.; Shore, S. G. *Chem. Mater.* **1995**, *7*, 111.

37. (*a*) Dewar, M. J. S.; Kubba, V. P.; Pettit, R. *J. Chem. Soc.* **1958**, 3073; (*b*) Emslie, D. J. H.; Piers, W. E.; Parvez, M. *Angew. Chem. Int. Ed.* **2003**, *42*, 1252; (*c*) Campbell, P. G.; Marwitz, A. J. V.; Liu, S.-Y. *Angew. Chem. Int. Ed.* **2012**, *51*, 6074; (*d*) Edel, K.; Brough, S. A.; Lamm, A. N.; Liu, S.-Y.; Bettinger, H. F. *Angew. Chem. Int. Ed.* **2015**, *54*, 7819.

38. Pangborn, A. B.; Giardello, M. A.; Grubbs, R. H.; Rosen, R. K.; Timmers, F. J. *Organometallics.* **1996**, *15*, 1518.

39. Jafarpour, L.; Stevens, E. D.; Nolan, S. P. *J. Organomet. Chem*. **2000**, *606*, 49.

40. Al-Rafia, S. M. I.; Lummis, P. A.; Swarnakar, A. K.; Deutsch, K. C.; Ferguson, M. J.; McDonald, R.; Rivard, E. *Aust. J. Chem.* **2013**, *66*, 1235.

41. Sloan, M. E.; Staubitz, A.; Clark, T. J.; Russell, C. A.; Lloyd-Jones, G. C.; Manners, I. *J. Am. Chem. Soc.* **2010**, *132*, 3831.

42. Straus, D. A.; Zhang, C.; Tilley, T. D. *J. Organomet. Chem*. **1989**, *369*, C13.

43. Asadi, A.; Avent, A. G.; Hill, M. S.; Hitchcock, P. B.; Meehan, M. M.; Smith, J. D. *Organometallics* **2002**, *21*, 2183.

44. Savoia, D.; Trombini, C.; Umani-Ronchi, A. *J. Org. Chem.* **1978**, *43*, 2907.

45. Hope, H. *Prog. Inorg. Chem.* **1994**, *41*, 1.

46. Blessing, R. H. *Acta Crystallogr.* **1995**, *A51*, 33.

47. Sheldrick, G. M. *Acta Crystallogr*. **2008**, *A64*, 112.

48. Beurskens, P. T.; Beurskens, G.; de Gelder, R.; Smits, J. M. M.; Garcia-Garcia, S.; Gould, R. O. DIRDIF-2008; Crystallography Laboratory, Radboud University: Nijmegen, The Netherlands, **2008**.

49. Wang, Y.; Quillian, B.; Wei, P.; Wannere, C. S.; Xie, Y.; King, R. B.; Schaefer, H. F.; Schleyer, P. v: R.; Robinson, G. H. *J. Am Chem. Soc*. **2007**, *129*, 12412.

50. (*a*) Jaska, C. A.; Temple, K.; Lough, A. J.; Manners, I. *J. Am. Chem. Soc.* **2003**, *125*, 9424; (*b*) Robertson, A. P. M.; Leitao, E. M.; Manners, I. *J. Am. Chem. Soc.* **2011**, *133*, 19322; (*c*) Nöth, H.; Thomas, S. *Eur. J. Inorg. Chem*. **1999**, 1373.

51. Kuhn, A.; Sander, W. *Organometallics* **1998**, *17*, 4776.

Chapter 5

1. (a) Jones, C. *Chem. Commun.* **2001**, 2293; (*b*) Kuhn, N.; Al-Sheikh, A. *Coord. Chem. Rev.* **2005**, *249*, 829; (*c*) Wang, Y.; Robinson, G. H. *Dalton Trans.* **2012**, *41*, 337; (*d*) Ghadwal, R. S.; Azhakar, R.; Roesky, H. W. *Acc. Chem. Res.* **2013**, *46*, 444; (*e*) Murphy, L. K.; Robertson, K. N.; Masuda, J. D.; Clyburne, J. A. C. in *N-Heterocyclic Carbenes*, S. P. Nolan (ed.), Wiley-VCH, Weinheim, **2014**, pp-427-497; (*f*) Rivard, E. *Dalton Trans.* **2014**, *43*, 8577; (*g*) Prabusankar, G.; Sathyanarayana, A.; Suresh, P.; Babu, C. N.; Srinivas, K.; Metla, B. P. R. *Coord. Chem. Rev.* **2014**, *269*, 96; (*h*) Präsang, C.; Scheschkewitz, D. *Chem. Soc. Rev.* **2016**, *45,* 900; (*i*) Würtemberger-Pietsch, S.; Radius, U.; Marder, T. B. *Dalton Trans.* **2016**, *45*, 5880.

2. (*a*) Martin, D.; Melaimi, M.; Soleilhavoup, M.; Bertrand, G. *Organometallics* **2011**, *30*, 5304; (*b*) Mondal, K. C.; Roy, S.; Roesky, H. W. *Chem. Soc. Rev.* **2016**, *45*, 1080; (*c*) Soleilhavoup, M.; Bertrand, G. *Acc. Chem. Res.* **2015**, *48*, 256.

3. (*a*) Kuhn, N.; Bohnen, H.; Kreutzberg, J.; Bläser, D.; Boese, R. *J. Chem. Soc., Chem. Commun.* **1993**, 1136; (*b*) Al-Rafia, S. M. I.; Malcolm, A. C.; Liew, S. K.; Ferguson, M. J.; McDonald, R.; Rivard, E. *Chem. Commun.* **2011**, *47*, 6987; (*c*) Y. Wang, Y.; Abraham, M. Y.; Gilliard Jr., R. J.; Sexton, D. R.; Wei, P.; Robinson, G. H. *Organometallics* **2013**, *32*, 6639; (*d*) Ghadwal, R. S. *Dalton Trans.* **2016**, *45*, 16081; (*e*) Powers, K.; Hering-Junghans, C.; McDonald, R.; Ferguson, M. J.; Rivard, E. *Polyhedron* **2016**, *108*, 8; (*f*) Huang, J. -S.; Lee, W. -H.; Shen, C. -T.; Lin, Y. -F.; Liu, Y. -H.; Peng, S. -M.; Chiu, C. -W. *Inorg. Chem.* **2016**, *55*, 12427.

4. (*a*) Braunschweig, H.; Dewhurst, R. D.; Hammond, K.; Mies, J.; Radacki, K.; Vargas, A. *Science* **2012**, *336*, 1420; (*b*) Böhnke, J.; Braunschweig, H.; Ewing, W. C.; Hörl, C.;

Kramer, T.; Krummenacher, I.; Mies, J.; Vargas, A. *Angew. Chem. Int. Ed.* **2014**, *53*, 9082.

5. (*a*) Swarnakar, A. K.; Hering-Junghans, C.; Nagata, K.; Ferguson, M. J.; McDonald, R.; Tokitoh, N.; Rivard, E. *Angew. Chem. Int. Ed.* **2015**, *54*, 10666; (*b*) Swarnakar, A. K.; Hering-Junghans, C.; Ferguson, M. J.; McDonald, R.; Rivard, E. *Chem. Sci*. **2017**, *8,* 2337.
6. Solovyev, A.; Chu, Q.; Geib, S. J.; Fensterbank, L.; Malacria, M.; Lacôte, E.; Curran, D. P. *J. Am. Chem. Soc.* **2010**, *132*, 15072.
7. For related donor-acceptor chemistry in the main group, see: (*a*) Marks, T. J. *J. Am. Chem. Soc.* **1971**, *93*, 7090; (*b*) Vogel, U.; Timoshkin, A. Y.; Scheer, M. *Angew. Chem. Int. Ed.* **2001**, *40*, 4409; (*c*) Al-Rafia, S. M. I.; Malcolm, A. C.; McDonald, R.; Ferguson, M. J.; Rivard, E. *Angew. Chem. Int. Ed.* **2011**, *50*, 8354; (*d*) Filippou, A. C.; Baars, B.; Chernov, O.; Lebedev, Y. N.; Schnakenburg, G. *Angew. Chem. Int. Ed.* **2014**, *53*, 565; (*e*) Dielmann, F.; Peresypkina, E. V.; Krämer, B.; Hastreiter, F.; Johnson, B. P.; Zabel, M.; Heindl, C.; Scheer, M. *Angew. Chem. Int. Ed.* **2016**, *55*, 14833; (*f*) Zhou, Y. –P.; Karni, M.; Yao, S.; Apeloig, Y.; Driess, M. *Angew. Chem. Int. Ed.* **2016**, *55*, 15096.
8. (*a*) Amano, H.; Sawaki, N.; Akasaki, I.; Toyoda, Y. *Appl. Phys. Lett.* **1986**, *48*, 353; (*b*) Nakamura, S.; Harada, Y.; Seno, M. *Appl. Phys. Lett.* **1991**, *58*, 2021; (*c*) Morkoc, H.; Mohammad, S. N. *Science* **1995**, *267*, 51.
9. (*a*) Neumayer, D. A.; Cowley, A. H.; Decken, A.; Jones, R. A.; Lakhotia, V.; Ekerdt, J. G. *J. Am. Chem. Soc.* **1995**, *117*, 5893; (*b*) Kouvetakis, J.; McMurran, J.; Matsunaga, P.; O'Keeffe, M.; Hubbard, J. L. *Inorg. Chem.* **1997**, *36*, 1792; (*c*) Dingman, S. D.;

Rath, N. P.; Buhro, W. E. *Dalton Trans.* **2003**, 3675; (*d*) Beachley Jr., O. T.; Pazik, J. C.; Noble, M. J. *Organometallics* **1998**, *17*, 2121.

10. Cole, M. L.; Furfari, S. K.; Kloth, M. *J. Organomet. Chem.* **2009**, *694*, 2934; (*b*) Abernethy, C. D.; Cole, M. L.; Jones, C. *Organometallics* **2000**, *19*, 4852; (*c*) Baker, R. J.; Jones, C. *Appl. Organomet. Chem.* **2003**, *17*, 807; (*d*) Francis, M.D.; Hibbs, D. E.; Hursthouse, M. B.; Jones, C.; Smithies, N. A. *J. Chem. Soc., Dalton Trans*. **1998**, 3249.
11. Shirk, A. E.; Shriver, D. F.; Dilts, J. A.; Nutt, R. W. *Inorg. Synth.* **1977**, *17*, 45.
12. (*a*) Ball, G. E.; Cole, M. L.; McKay, A. I. *Dalton Trans.* **2012**, *41*, 946; (*b*) Marion, N.; Escudero-Adán, E. C.; Benet-Buchholz, J.; Stevens, E. D.; Fensterbank, L.; Malacria, M.; Nolan, S. P. *Organometallics* **2007**, *26*, 3256.
13. Haiges, R.; Boatz, J. A.; Williams, J. M.; Christe, K. O. *Angew. Chem. Int. Ed.* **2011**, *50*, 8828.
14. (*a*) Herrington, T. J.; Thom, A. J. W.; White, A. J. P.; Ashley, A. E. *Dalton Trans.* **2012**, *41*, 9019; (*b*) Blagg, R. J.; Lawrence, E. J.; Resner, K.; Oganesyan, V. S.; Herrington, T. J.; Ashley, A. E.; Wildgoose, G. G. *Dalton Trans*. **2016**, *45*, 6023.
15. (*a*) Burns, M. E.; Smith Jr, R. H. *Chem. Eng. News* **1984**, *62*, 2; (*b*) Hassner, A.; Stern, M.; Gottlieb, H. E.; Frolow, F. *J. Org. Chem.* **1990**, *55*, 2304.
16. Jancik, V.; Pineda, L. W.; Stückl, A. C.; Roesky, H. W.; Herbst-Irmer, R. *Organometallics* **2005**, *24*, 1511.
17. Hild, F.; Dagorne, S. *Organometallics* **2012**, *31*, 1189.
18. For related work on using main group species as hydrosilylation/borylation catalysts, see: (*a*) Lummis, P. A.; Momeni, M. R.; Lui, M. W.; McDonald, R.; Ferguson, M. J.;

Misklozie, M.; Brown, A.; Rivard, E. *Angew. Chem. Int. Ed.* **2014**, *53*, 9347; (*b*) Revunova, K.; Nikonov, G. I. *Dalton Trans.* **2015**, *44*, 840; (*c*) Chong, C. C.; Kinjo, R. *ACS Catal.* **2015**, *5*, 3238; (*d*) Wiegand, A.-K.; Rit, A. Okuda, J. *Coord. Chem. Rev.* **2016**, *314*, 71; (*e*) Roy, M. M. D.; Ferguson, M. J.; McDonald, R.; Rivard, E. *Chem. Eur. J.* **2016**, *22*, 18236; (*f*) Hadlington, T. J.; Hermann, M.; Frenking, G.; Jones, C. *J. Am. Chem. Soc.* **2014**, *136*, 3028; (*g*) Bismuto, A.; Thomas, S. P.; Cowley, M. J. *Angew. Chem. Int. Ed.* **2016**, *55*, 15356. Initial studies show that **2** is a competent catalyst for the hydrosilylation of benzophenone at room temperature.

19. Pangborn, A. B.; Giardello, M. A.; Grubbs, R. H.; Rosen, R. K.; Timmers, F. J. *Organometallics* **1996**, *15*, 1518.
20. Tang, S.; Monot, J.; El-Hellani, A.; Michelet, B.; Guillot, R.; Bour, C.; Gandon, V. *Chem. Eur. J.* **2012**, *18*, 10239.
21. Kolychev, E. L.; Bannenberg, T.; Freytag, M.; Daniliuc, C. G.; Jones, P. G.; Tamm, M. *Chem. Eur. J.* **2012**, *18*, 16938.
22. Hope, H. *Prog. Inorg. Chem.* **1994**, *41*, 1.
23. Blessing, R. H. *Acta Crystallogr. Sect. A* **1995**, *51*, 33.
24. Sheldrick, G. M. *Acta Crystallogr. Sect. A* **2007**, *64*, 112.

Chapter 6

1. (*a*) Coté, A. P.; Benin, A. I.; Ockwig, N. W.; O'Keeffe, M.; Matzger, A. J.; Yaghi, O. M. *Science* **2005**, *310*, 1166; (*b*) El-Kaderi, H. M.; Hunt, J. R.; Mendoza-Cortes, J. L.; Cote, A. P.; Taylor, R. E.; O'Keeffe, M.; Yaghi, O. M. *Science* **2007**, *316*, 268; (*c*) De, P.; Gondi, S. R.; Roy, D.; Sumerlin, B. S. *Macromolecules* **2009**, *42*, 5614; (*d*) Perttu,

E. K.; Arnold, M.; Iovine, P. M. *Tetrahedron Lett.* **2005**, *46*, 8753; (*e*) Hawkins, R. T.; Lennarz, W. J.; Snyder, H. R. *J. Am. Chem. Soc.* **1960**, *82*, 3053; (*f*) Li, Y.; Ding, J.; Day, M.; Tao, Y.; Lu, J.; D'iorio, M. *Chem. Mater.* **2003**, *15,* 4936.

2. (*a*) Kirk, R. W.; Timms, P. L. *Chem. Commun.* **1967**, 18; (*b*) Kroto, H. W. *Chem. Soc. Rev*. **1982**, *11*, 435; (*c*) Groteklaes, M.; Paetzold, P. *Chem. Ber.* **1988**, *121*, 809; (*d*) Burkholder T. R.; Andrews, L. *J. Chem. Phys*. **1991**, *95*, 8697; (*e*) Page, M. *J. Phys. Chem*. **1989**, *93*, 3639; (*f*) Paetzold, P.; Neyses, S.; Géret, L.; *Z. Anorg. Allg. Chem.* **1995**, *621*, 732; (*g*) Osiac, M.; Röpcke, J.; Davies, P. B. *Chem. Phys. Lett.* **2001**, *344*, 92; (*h*) Bettinger, H. *Organometallics* **2007**, *26*, 6263.

3. Pachaly, B.; West, R. *J. Am. Chem. Soc.* **1985**, *107*, 2987.

4. For related studies on isolating reactive LBO species (L = supporting ligand(s)), see: (*a*) Nöth, H. *Angew. Chem. Int. Ed. Engl.* **1988**, *27*, 1603; (*b*) Ito, M.; Tokitoh, N.; Okazaki, R. *Tet. Lett.* **1997**, *38*, 4451; (*c*) Vidovic, D.; Moore, J. A.; Jones, J. N.; Cowley, A. H. *J. Am. Chem. Soc*. **2005**, *127*, 4566; (*d*) Wang, Y.; Hu, H.; Zhang, J.; Cui, C. *Angew. Chem. Int. Ed*. **2011**, *50*, 2816; (*e*) Del Grosso, A.; Clark, E. R.; Montoute, N.; Ingleson, M. J. *Chem. Commun*. **2012**, *48*, 7589; (*f*) Loh, Y. K.; Chong, C. C.; Ganguly, R.; Li, Y.; Vidovic, D.; Kinjo, R. *Chem. Commun*. **2014**, *50*, 8561.

5. Braunschweig, H.; Radacki, K.; Schneider, A. *Science* **2010**, *328*, 345.

6. (*a*) Paetzold, P. *Adv. Inorg. Chem.* **1987**, *31*, 123; (*b*) Fischer, R. C.; Power, P. P. *Chem. Rev.* **2010**, *110*, 3877; (*c*) Wang, Y.; Robinson, G. H. *Dalton Trans*. **2012**, *41*, 337; (*d*) Mizuhata, Y.; Sasamori, T.; Tokitoh, N. *Chem. Rev.* **2009**, *109*, 3479; (*e*) Asay, M.; Jones, C.; Driess, M. *Chem. Rev.* **2011**, *111*, 354; (*f*) He, G.; Shynkaruk, O.; Lui, M. W.; Rivard, E. *Chem. Rev.* **2014**, *114*, 7815; (*g*) Brand, J.; Braunschweig, H.;

Sen, S. S. *Acc. Chem. Res.* **2014**, *47*, 180; (*h*) Präsang. C.; Scheschkewitz, D. *Chem. Soc. Rev.* **2016**, *45*, 900.

7. (*a*) Parker, D. S. N.; Dangi, B. B.; Balucani, N.; Stranges, D.; Mebel, A. M.; Kaiser, R. I. *J. Org. Chem.* **2013**, *78*, 11896; (*b*) Liu, H.; Jin, P.; Xue, Y.-M.; Dong, C.; Li, X.; Tang, C.-C.; Du, X.-W. *Angew. Chem. Int. Ed.* **2015**, *54*, 7051; (*c*) Purkait; Swarnakar, A. K.; De Los Reyes, G. B.; Hegmann, F. A.; Rivard, E.; Veinot, J. G. C. *Nanoscale* **2015**, *7*, 2241; (*d*) Velian, A.; Cummins, C. C. *Science* **2015**, *348*, 1001.
8. (*a*) Power, P. P. *Nature* **2010**, *463*, 171; (*b*) Hadlington, T. J.; Hermann, M.; Frenking, G.; Jones, C. *J. Am. Chem. Soc.* **2014**, *136*, 3028.
9. (*a*) Rivard, E. *Chem. Soc. Rev.* **2016**, *45*, 989; FLP can also be viewed as donor-acceptor complexes: (*b*) Stephan, D. W.; Erker, G. *Angew. Chem. Int. Ed.* **2010**, *49*, 46.
10. The related dihalosilylether species $Br_2BOSiMe_3$ was prepared previously (see ref. 5).
11. Kolychev, E. L.; Bannenberg, T.; Freytag, M.; Daniliuc, C. G.; Jones, P. G.; Tamm, M. *Chem. Eur. J.* **2012**, *18*, 16938.
12. For the use of $BAr^F{}_3$ to intercept main group species, see: (*a*) Swarnakar, A. K.; Hering-Junghans, C.; Nagata, K.; Ferguson, M. J.; McDonald, R.; Tokitoh, N; Rivard, E. *Angew. Chem. Int. Ed.* **2015**, *54*, 10666; (*b*) Swarnakar, A. K.; Hering-Junghans, C.; Ferguson, M. J.; McDonald, R.; Rivard, E. *Chem. Sci.* **2017**, *8*, 2337.
13. Brahmia, M. M.; Malacria, M.; Curran, D. P.; Fensterbank, L.; Lacôte, E. *Synlett.* **2013**, *24*, 1260.
14. Caputo, C. B.; Hounjet, L. J.; Dobrovetsky, R.; Stephan, D. W. *Science* **2013**, *341*, 1374.

15. Wang, Y.; Xie, Y.; Abraham, M. Y.; Wei, P.; Schaefer III, P. H. F.; Schleyer, P. v. R.; Robinson, G. H. *J. Am. Chem. Soc.* **2010**, *132*, 14370.

16. (*a*) Stahl, T.; Klare, H. F. T.; Oestreich, M. *ACS Catal*. **2013**, *3*, 1578; (*b*) Douvris, C.; Ozerov, O. V. *Science* **2008**, *321*, 1188; (*c*) Caputo, C. B.; Stephan, D. W. *Organometallics* **2012**, *31*, 27; (*d*) Alcarazo, M.; Gomez, C.; Holle, S.; Goddard, R. *Angew. Chem. Int. Ed.* **2010**, *49*, 5788; (*e*) Ahrens, M.; Scholz, G.; Braun, T.; Kemnitz, E. *Angew. Chem. Int. Ed*. **2013**, *52*, 5328.

17. Pangborn, A. B.; Giardello, M. A.; Grubbs, R. H.; Rosen, R. K.; Timmers, F. J. *Organometallics* **1996**, *15*, 1518.

18. Jafarpour, L.; Stevens, E. D.; Nolan, S. P. *J. Organomet. Chem*. **2000**, *606*, 49.

19. (*a*) Kuprat, M.; Lehmann, M.; Schulz, A.; Villinger, A. *Organometallics* **2010**, *29*, 1421; (*b*) Massey, A. G.; Park, A. J. *J. Organomet. Chem.* **1964**, *2*, 245.

20. Hope, H. *Prog. Inorg. Chem.* **1994**, *41*, 1.

21. Blessing, R. H. *Acta Crystallogr.* **1995**, *A51*, 33.

22. Sheldrick, G. M. *Acta Crystallogr*. **2008**, *A64*, 112.

23. Beurskens, P. T.; Beurskens, G.; de Gelder, R.; Smits, J. M. M.; Garcia-Garcia, S.; Gould, R. O. DIRDIF-2008; Crystallography Laboratory, Radboud University: Nijmegen, The Netherlands **2008**.

24. Candish, L.; Standley, E. A.; Gómez-Suμrez, A.; Mukherjee, S.; Glorius, F. *Chem. Eur. J.* **2016**, *22*, 9971.

Chapter 7

1. (*a*) Al-Rafia, S. M. I.; Malcolm, A. C.; Liew, S. K.; Ferguson, M. J.; Rivard, E. *J. Am. Chem. Soc.* **2011**, *133*, 777; (*b*) Swarnakar, A. K.; McDonald, S. M.; Deutsch, K. C.; Choi, P.; Ferguson, M. J.; McDonald, R.; Rivard, E. *Inorg. Chem*. **2014**, *53*, 8662.

2. Fox, A. R.; Cummins, C. C. *J. Am. Chem. Soc.* **2009**, *131*, 5716.

3. (*a*) Lummis, P. A.; Momeni, M. R.; Lui, M. W.; McDonald, R.; Ferguson, M. J.; Misklozie, M.; Brown, A.; Rivard, E. *Angew. Chem. Int. Ed.* **2014**, *53*, 9347; (*b*) Revunova, K.; Nikonov, G. I. *Dalton Trans.* **2015**, *44*, 840; (*c*) Chong, C. C.; Kinjo, R. *ACS Catal.* **2015**, *5*, 3238; (*d*) Wiegand, A.-K.; Rit, A. Okuda, J. *Coord. Chem. Rev.* **2016**, *314*, 71; (*e*) Roy, M. M. D.; Ferguson, M. J.; McDonald, R.; Rivard, E. *Chem. Eur. J.* **2016**, *22*, 18236; (*f*) Hadlington, T. J.; Hermann, M.; Frenking, G.; Jones, C. *J. Am. Chem. Soc.* **2014**, *136*, 3028; (*g*) Bismuto, A.; Thomas, S. P.; Cowley, M. J. *Angew. Chem. Int. Ed.* **2016**, *55*, 15356.